DECIPHERING THE SIGNALING NETWORKS UNDERLYING SIMVASTATIN-INDUCED APOPTOSIS IN HUMAN CANCER CELLS

ZHU YAN

(BSc. (Hons.), NUS)

A THESIS SUBMITTED

FOR THE DEGREE OF DOCTOR OF PHILOSOPHY

NUS GRADUATE SCHOOL FOR INTEGRATIVE SCIENCES AND ENGINEERING

NATIONAL UNIVERSITY OF SINGAPORE

2012

DECLARATION

I hereby declare that this thesis is my original work and it has been written by me in its entirety. I have duly acknowledged all the sources of information, which have been used in the thesis.

This thesis has also not been submitted for any degree in any university previously.

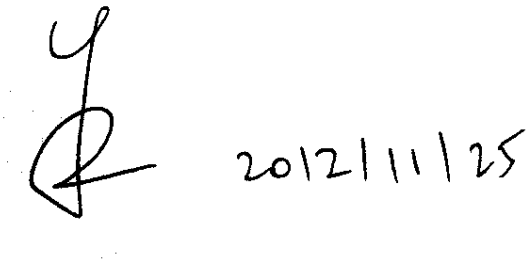

2012/11/25

Zhu Yan

ACKNOWLEDGEMENTS

Firstly to my supervisor, Prof. Shazib Pervaiz, thank you for giving me the opportunity to embark on this journey. Thank you for your continuous support, encouragement and guidance along the way. I appreciate you for being "tough" at times, from which I have learnt to become a true scientist. You have left a lasting impact on my academic life.

To Dr. Alan Prem Kumar, thanks for guiding and supervising me when I was working in the Numi lab the first two years. I will always remember you as someone who never says "No" to students, always caring and giving.

To my TAC members, Prof Patrick Casey and Assoc. Prof Edward Manser, the time you spent with me is a true reflection of the phrase "quality over quantity". Despite your busy schedules, you have continually provided constructive and impactful feedback throughout this journey. I am especially grateful to Prof Casey for providing invaluable inputs during the drafting of this thesis.

As a PhD student, failure is a commonplace; but one thing that gives me joy is the friendship that has blossomed over the years. I would like to thank all the friends from ROS biology lab and Numi lab for your constant support and encouragements, not forgetting all the fun and laughter out of the workplace. Special mentions to Carolyn and Zhou Ting - I am really glad that we have shared this part of our life journey together and look forward to many more good years ahead.

Lastly, to my most-loved people in the world: Yujun, thanks for your unconditional love and the constant support from your family. And to my parents, I love you!

TABLE OF CONTENTS

DECLARATION ..... **i**

ACKNOWLEDGEMENTS ..... **ii**

TABLE OF CONTENTS ..... **iii**

SUMMARY ..... **viii**

LIST OF TABLES ..... **x**

LIST OF FIGURES ..... **xi**

LIST OF ABBREVIATIONS ..... **xv**

INTRODUCTION **1**

1. Statins overview **1**

1.1 Types of statins 1

1.2 Pleiotropic effects of statins 3

1.3 Anti-tumor effects of statins: bench to bedside 5

1.4 Statin effects in colorectal cancer 8

2 Programmed cell death **9**

2.1 Apoptosis 9

2.1.1 Characteristics and physiological role of apoptosis 9

2.1.2 Molecular mechanisms of apoptosis 10

2.1.2.1 Caspases 12

2.1.2.2 Bcl-2 family member 13

2.1.2.3 Intrinsic pathway 17

2.1.2.4 Extrinsic pathway 18

2.2 Autophagy 19

2.3 Necrosis 20

3. Rho GTPase family **22**

3.1 Regulation of Rho GTPases: GDP/GTP cycling 22

3.2 Lipid modification of Rho GTPases 25

3.3 Rho GTPases: their effectors and functions 26

3.4 Rho GTPases in cancer 28

3.5 Rho GTPases in regulating apoptosis 29

4. Reactive oxygen species **31**

4.1 ROS overview: types and their physiological roles 31

4.2 Sources of ROS 32

4.2.1 Mitochondrial electron transport chain 32

4.2.2 NADPH oxidase complex 33

4.2.3 Other sources 34

4.3 ROS: role in oncogenesis and cell death 35

5. Signaling Pathways: AKT and MAPKs **37**

5.1 AKT 37

5.1.2 AKT in cancer 38
5.2 ERK 39
5.2.1 ERK signaling cascade 39
5.2.2 ERK in cancer and cell death 40
5.3 JNK 41
5.3.1 JNK signaling cascade 41
5.3.2 JNK and cell death 42
5.3.3 JNK in cancer 43

MATERIALS AND METHODS 45
1 Cell lines and cell culture 45
2 Reagents and chemicals 45
3 Plasmids and siRNAs 46
4 Transfection of plasmids and siRNAs 47
5 Determination of cell viability by crystal violet assay 47
6 Determination of cell viability by MTT assay 48
7 Colony forming assay 49
8 DNA fragmentation assay by propidium iodide staining 49
9 Caspase activity assay 50
10 Western blot analysis 50
11 Coimmunoprecipitation (Co-IP) 53
12 Isolation of GTP-loaded RhoA, Rac1 and Cdc42 GTPases 53
13 Mitochondrial-cytoplasmic fractionation 54
14 Isolation of membrane lipid rafts by sucrose gradient ultracentrifugation 55
15 Triton X-114 phase separation 56
16 Measurement of superoxide by Lucigenin chemiluminescence assay 57
17 Measurement of superoxide by DHE dye 57
18 Statistical analysis 58

RESULTS 59

1. Simvastatin activates the mitochondrial apoptotic pathway in HCT116 cells 59
1.1 Simvastatin effectively reduces cell viability in a dose-dependent manner 59
1.2 Simvastatin inhibits long-term colony formation of HCT116 cells 61
1.3 Simvastatin-triggered cell death bears apoptotic hallmarks 63
1.3.1 Cell death is accompanied by cell shrinkage and DNA fragmentation 63
1.3.2 Simvastatin induces effective proteolytic processing and activation of caspases 65
1.4 Simvastatin activates the mitochondrial apoptotic pathway 70
1.4.1 Simvastatin induces mitochondrial Bax translocation and release of pro-apoptogenic factor cytochrome c into the cytosol 70
1.4.2 MMP modulator protein Bax is essential for simvastatin-induced cell death 72
1.5 Simvastatin-induced apoptosis is independent of p53 status 74

2 Simvastatin induces apoptosis by activating RhoA and Rac1 in HCT116 cells 75

2.1 Protein geranylgeranylation is essential in simvastatin-mediated apoptosis ... 75
2.1.1 Simvastatin induces apoptosis via depletion of isoprenoid precursor GGPP 75
2.1.2 Inhibitor of GGTase-I mimics the cytotoxic effects of simvastatin ... 80
2.2 Changes in expression, localization and activities of three geranylgeranylated proteins, namely RhoA, Rac1 and Cdc42, after simvastatin treatment ... 82
2.2.1 Simvastatin dramatically increases protein levels of RhoA and Cdc42 via blocking protein geranylgeranylation ... 82
2.2.2 Simvastatin increases expression of unprenylated RhoA, Rac1 and Cdc42 ... 84
2.2.3 Simvastatin delocalizes RhoA, Rac1 and Cdc42 from the lipid rafts and increases their expression in the cytosol ... 86
2.2.4 Simvastatin increases GTP-loading of RhoA, Rac1 and Cdc42 by downregulation of GGPP synthesis ... 88
2.3 Simvastatin activates RhoA and Rac1 to mediate its apoptotic effects ... 92
2.3.1 Blocking Rac1 by pharmacological inhibitors and expression of dominant negative plasmid rescues cells from simvastatin-induced cell death ... 92
2.3.2 Knockdown of RhoA and Rac1, but not Cdc42, protects cells from simvastatin's cytotoxic effects ... 96
2.3.4 Simvastatin activates RhoA and Rac1 by decreasing their association with the cytosolic inhibitor RhoGDIα ... 98
2.4 Inhibiting newly synthesized RhoA and Rac1 diminishes the increase in active RhoA and Rac1, and protects cells from simvastatin-induced apoptosis .. 101
2.5 Simvastatin increases protein levels of RhoA and Cdc42 via protein synthesis ... 103
2.5.1 Simvastatin upregulates RhoA and Cdc42 protein expression via mRNA and protein synthesis ... 103
2.5.2 Simvastatin does not affect the protein degradation rate of RhoA and Cdc42 ... 105

3. Simvastatin induces superoxide production as an early signal to initiate cell death in HCT116 cells ... 106
3.1 Simvastatin increases superoxide level in a time-dependent manner. ... 106
3.2 Superoxide scavengers confer cells resistance to simvastatin-induced cell death ... 109
3.3 Simvastatin induces superoxide production involving GTP-bound RhoA and Rac1 ... 112
3.3.1 Simvastatin increases superoxide level by blocking protein geranylgeranylation ... 112
3.3.2 Blocking RhoA and Rac1 activities inhibits simvastatin-mediated superoxide production ... 114
3.3.3 Simvastatin-mediated superoxide production does not affect protein levels of Rho proteins ... 116

4. Simvastatin activates stress response JNK pathway to mediate the cell death response in HCT116 cells ... 118

4.1 Simvastatin activates JNK signaling by blocking protein geranylgeranylation 118
4.2 JNK inhibitor SP600125 rescues simvastatin-induced cell death phenotype 122
4.3 Simvastatin-mediated JNK activation is downstream of RhoA and Rac1 activation and superoxide production 124
4.3.1 Blocking RhoA and Rac1 activities prevents simvastatin-induced JNK activation 124
4.3.2 Inhibiting superoxide production prevents simvastatin-mediated JNK activation 126
4.3.3 Inhibiting JNK signaling did not affect simvastatin-induced changes in Rho protein expression and superoxide level 127

5. Simvastatin upregulates the expression of pro-apoptotic Bcl-2 family member Bim-EL to induce apoptosis 129
5.1 Simvastatin upregulates protein level of Bim-EL 129
5.2 Knockdown of Bim-EL protects cells from simvastatin-induced apoptosis.. 131
5.3 Simvastatin increases Bim-EL protein expression downstream of the RhoA/Rac1-Superoxide-JNK signaling cascade 133
5.3.1 Simvastatin upregulates Bim-EL via blocking protein geranylgeranylation 133
5.3.2 Blocking RhoA and Rac1 activites prevents Bim-EL upregulation by simvastatin 135
5.3.3 Blocking superoxide production abrogates simvastatin-mediated Bim-EL upregulation 137
5.3.4 Simvastatin-induced increase in Bim-EL is downstream of JNK activation .138
5.3.5 Bim-EL silencing did not affect Rho protein expression, superoxide level and JNK activation after simvastatin treatment 139
5.4 Simvastatin-induced Bim-EL upregulation is observed in HCT116 Bax-/- cells 141
5.5 Simvastatin increases Bim-EL level via protein synthesis 142
5.5.1 Simvastatin upregulates Bim-EL content via mRNA and protein synthesis.142
5.5.2 Simvastatin does not affect the protein degradation rate of Bim-EL 143

6 Simvastatin's cytotoxic effects is conserved in many cancer types 144
6.1 Simvastatin induces cell death in other cancer cells by inhibiting protein geranylgeranylation 144
6.2 Simvastatin induces apoptosis in SHEP-1 cells via Rac1-Superoxide-JNK signaling cascade 147
6.2.1 Simvastatin induces apoptosis in SHEP-1 cells 147
6.2.2 Simvastatin increases GTP-loading of Rac1, which is responsible for the cell death phenotype 149
6.2.3 Simvastatin increases superoxide production downstream of Rac1 activation to mediate the apoptotic response 151
6.2.4 Simvastatin activates JNK pathway downstream of Rac1-superoxide cascade to relay the cell death signal 153

DISCUSSION 156

1 The cell death mechanism in simvastatin-treated cancer cells 156

2 Identification of novel mechanisms in regulating Rho GTPases and its role in simvastatin-mediated apoptosis.....161
2.1 Geranylgeranylation is the more important form of isoprenylation in the anti-tumor effects of simvastatin..... 161
2.2 Non-canonical regulation of Rho GTPases by simvastatin 163
2.2.1 Inhibiting geranylgeranylation increases GTP-loading of Rho GTPases.....164
2.2.2 Activation of RhoA and Rac1 by simvastatin mediates cell kill 167
2.2.3 Beyond the post-translational modification of Rho GTPases by simvastatin 168
3 The involvement and significance of superoxide production.....172
3.1 Unprenylated RhoA and Rac1 in superoxide production 172
3.2 Statin induces oxidative stress specifically in cancer cells 174
4. The involvement and significance of JNK signaling 177
4.1 JNK is the downstream mediator in simvastatin-induced apoptosis..... 177
4.2 Upstream signals for simvastatin-mediated JNK activation 178
5. The involvement and significance of pro-apoptotic protein BIM.....181
5.1 Increase in Bim-EL content mediates simvastatin's apoptotic effects..... 181
5.2 The mechanism for simvastatin-mediated Bim-EL upregulation 182
CONCLUSION.....185
REFERENCES.....188
APPENDICES 213

SUMMARY

Statins are widely used as cholesterol-lowering drugs that selectively inhibit the enzyme HMG-CoA reductase and block cholesterol biosynthesis. Recent studies show that statins induce apoptotic cell death in several types of cancer cells. However, the underlying molecular mechanisms are still unclear. In this study, we showed that simvastatin activated the mitochondrial death pathway and inhibited colony-forming ability of HCT116 colorectal cancer cells. Exogenously added mevalonate or geranylgeranylpyrophosphate (GGPP), but not farnesylpyrophosphate (FPP), in combination with simvastatin prevented the growth-inhibitory effect of simvastatin. The findings corroborated well with geranylgeranyltransferase I inhibitor GGTI-298 treatment exhibiting similar effects as simvastatin, as opposed to farnesyltransferase inhibitor FTI-277, which had minimal effects on cell viability. These data suggest that simvastatin exerts effects via inhibition of the mevalonate pathway and by modulating the functions of its downstream geranylgeranylated proteins, such as Rho GTPases. Simvastatin treatment led to increased levels of unprenylated RhoA, Rac1 and Cdc42, which were delocalized from the lipid rafts of the plasma membrane and accumulated in the cytosol. Intriguingly however, instead of inhibiting the functions of Rho GTPases as was expected with loss of prenylation, simvastatin caused a paradoxical increase in the GTP-bound form of RhoA, Rac1 and Cdc42 in HCT116 cells. The unprenylated RhoA and Rac1-GTP retained at least part of its functional activities, as evidenced by their ability to mediate production of superoxide and activate JNK pathway in response to simvastatin treatment. Notably, blocking superoxide production attenuated JNK activation as well as cell death elicited by simvastatin treatment. Furthermore, we also discovered that simvastatin induced the expression of extra-long form of Bim (Bim-EL) in a JNK-dependent manner, while

suppression of Bim-EL expression significantly blocked simvastatin-induced apoptosis. Taken together, our study demonstrates that simvastatin-induced apoptosis in HCT116 colorectal cancer cells is mediated via the RhoA/Rac1-superoxide-JNK-Bim signaling cascade. Further studies done in SHEP-1 neuroblastoma cells also implicated multiple aforementioned players in mediating simvastatin's cytotoxic effects. Overall, data from this study not only provides compelling evidence for simvastatin's anti-cancer activities, also suggests the importance of the identified molecular mechanism in other simvastatin-sensitive cancer cell types.

LIST OF TABLES

Table 1: Effectors and functions of Rho GTPases (RhoA, Rac1 and Cdc42) 27

Table 2: Dysregulation of Rho GTPases (RhoA, Rac1 and Cdc42) in human tumors. 28

LIST OF FIGURES

Introduction

Figure A: Chemical structure of simvastatin in its active and carboxylated form..... 2

Figure B: Overview of the mevalonate pathway: important products, enzymes and targets of statins, FTI and GGTI. 4

Figure C: Apoptotic signaling and the molecular players. 11

Figure D: The Rho GTPase switch. 24

Results

Figure 1: Simvastatin effectively reduces cell viability of HCT116 cells. 60

Figure 2: Simvastatin reduces clonogenic ability of HCT116 cells. 62

Figure 3: Simvastatin leads to cell shrinkage and DNA fragmentation in HCT116 cells. 64

Figure 4: Simvastatin induces proteolytic processing and activation of caspases. 67

Figure 5: Pan-caspase inhibitor zVAD-fmk confers full protection to simvastatin-mediated cell death. 69

Figure 6: Simvastatin induces Bax translocation to mitochondria and cytochrome c release into the cytosol. 71

Figure 7: Simvastatin-induced cell death requires Bax. 73

Figure 8: Simvastatin-induced cell death does not require p53. 74

Figure 9: MVA or GGPP preincubation protect cells from simvastatin-mediated cell death. 78

Figure 10: Squalene preincubation did not rescue cells after simvastatin treatment. 79

Figure 11: GGTI-298 mimics the cytotoxic effects of simvastatin. 81

Figure 12: Simvastatin drastically increases protein expression of RhoA and Cdc42 via blocking protein geranylgeranylation. 83

Figure 13: Simvastatin treatment increases Rho proteins in their unprenylated form. 85

Figure 14: Rho proteins decrease from the lipid rafts and accumulate in the cytosol after simvastatin treatment. 87

Figure 15: Simvastatin increases GTP loading of RhoA by blocking protein geranylgeranylation. 89

Figure 16: Simvastatin increases GTP loading of Rac1 by blocking protein geranylgeranylation. 90

Figure 17: Simvastatin increases GTP loading of Cdc42 by blocking protein geranylgeranylation. 91

Figure 18: Pharmacolgical inhibitors of Rac1 rescue cells from simvastatin-induced cell death. 93

Figure 19: Dominant negative Rac1N17 transfection partially protects cells from simvastatin treatment. 95

Figure 20: Knockdown of RhoA and Rac1, but not Cdc42, partially protects the cells from simvastatin's cytotoxic effects. 97

Figure 21: Simvastatin decreases the respective association of RhoA and Rac1 with RhoGDIα by blocking protein geranylgeranylation. 100

Figure 22: Cycloheximide protects cells from simvastatin-induced cell death via blocking the GTP-loading of RhoA and Rac1. 102

Figure 23: Simvastatin-induced upregulation of RhoA and Cdc42 protein expression is blocked by transcription and protein synthesis inhibitors. 104

Figure 24: Simvastatin does not affect the protein degradation rate of RhoA and Cdc42. 105

Figure 25: Simvastatin increases superoxide level in HCT116 cells. 108

Figure 26: Superoxide scavengers protect cells from simvastatin-mediated cell death. 111

Figure 27: Simvastatin induces superoxide production via blockage of GGPP synthesis. 113

Figure 28: Blocking Rac1 and RhoA activation abrogates simvastatin-mediated superoxide production. 115

Figure 29: Superoxide scavengers do not affect Rho protein expressions after simvastatin treatment. 117

Figure 30: Simvastatin dephosphorylates AKT and ERK but induces JNK phosphorylation. 119

Figure 31: Simvastatin activates JNK pathway via blocking protein geranylgeranylation. 121

Figure 32: JNK inhibitor SP600125 partially rescues cells from simvastatin-induced cell death. 123

Figure 33: Blocking RhoA and Rac1 activation downregulates JNK activation after simvastatin treatment. 125

Figure 34: Superoxide scavengers inhibit simvastatin-mediated JNK activation.... 126

Figure 35: JNK inhibitor does not affect simvastatin-mediated upregulation of Rho proteins and superoxide production. 128

Figure 36: Simvastatin increases Bim-EL expression. 130

Figure 37: Knockdown of Bim-EL partially reduces simvastatin-mediated cell death. 132

Figure 38: Simvastatin mediates Bim-EL upregulation via blocking protein geranylgeranlyation. 134

Figure 39: Blocking RhoA and Rac1 activities abrogates simvastatin-induced Bim-EL upregulation. 136

Figure 40: Superoxide scavengers block simvastatin-induced Bim-EL upregulation. 137

Figure 41: JNK inhibitor SP600125 prevents Bim-EL upregulation upon simvastatin treatment. 138

Figure 42: Knockdown of Bim-EL does not affect the protein expression of Rho, superoxide production and JNK activation. 140

Figure 43: Simvastatin-induced Bim-EL upregulation is upstream of Bax signaling. 141

Figure 44: Simvastatin-mediated upregulation of Bim-EL protein level is blocked by transcription and protein synthesis inhibitors. 142

Figure 45: Simvastatin does not affect the protein degradation rate of Bim-EL. 143

Figure 46: Simvastatin effectively reduces cell viability of other cancer cell lines via blocking protein geranylgeranylation. 146

Figure 47: Simvastatin treatment upregulates Bim-EL and activates caspase signaling in SHEP-1 cells via inhibiting protein geranylgeranylation.. 148

Figure 48: Simvastatin-mediated Rac1 activation is responsible for cell death in SHEP-1 cells. 150

Figure 49: Preincubation of superoxide scavenger inhibits simvastatin-induced PARP cleavage in SHEP-1 cells, and simvastatin-mediated superoxide production is downstream of Rac1 activation. 152

Figure 50: JNK inhibitor SP600125 protects simvastatin-treated SHEP-1 cells, and simvastatin-mediated JNK activation is downstream of Rac1 activation and superoxide production. 155

Discussion

Figure 51: Molecular mechanism of simvastatin-mediated apoptosis in HCT116 cells. 185

LIST OF ABBREVIATIONS

ActD	Actinomycin D
AFC	7-Amino-4-trifluoromethylcoumarin
AMC	7-Amino-4-methycoumarin
AML	Acute myeloid leukemia
AP1	Activator protein 1
Apaf-1	Apoptotic protease-activating factor-1
ASK1	Apoptotic signal-regulating kinase-1
Asp	Aspartic acid
ATG	Autophagy related genes
ATP	2-adenosine 5'-triphosphate
Bad	Bcl-2 antagonist of cell death
Bak	Bcl-2 antagonist/killer
Bax	Bcl-2 associated X protein
Bcl-2	B-cell lymphoma protein 2
Bcl-xL	Bcl-2 like protein 1
Bcl-w	Bcl-2 like protein 2
BH	Bcl-2 homology
Bid	BH3 interacting domain death agonist
Bik	Bcl-2 interacting killer
Bim	Bcl-2 interacting mediator
Bim-EL	Bim-extra long
Bim-L	Bim-long
Bim-S	Bim-short
Bmf	Bcl-2 modifying factor
Bok	Bcl-2 related ovarian killer
BPB	Bromophenyl blue
BSA	Bovine serum albumin
CAD	Caspase activated Dnase
CARD	Caspase recruitment domain
Caspase	Cysteine-dependent aspartate-specific protease
CD95	Cluster of differentiation 95
CDK	Cyclin-dependent kinase
Cdc42	Cell division cycle 42
CED	Caenorhabditiselegans genes defective
cFLIP	Cellular FLICE like Inhibitory Protein
CHX	Cyclohexamide
Cys	Cysteine
c-IAP1/2	Cellular inhibitor of apoptosis protein 1/2
DD	Death domain
DED	Death effector domain
DEVD-AFC	N-Acetyl-Asp-Glu-Val-Asp-7-amino-4-trifluoromethylcoumarin
DHE	Dihydroethidium

DIABLO	Direct IAP-binding protein with low pI
DISC	Death-inducing signaling complex
DMEM	Dulbecco's Modified Eagle's Medium
DMSO	Dimethyl sulfoxide
DNA	Deoxyribonucleic Acid
DNA-PK	DNA-dependent protein kinase
DPI	Diphenyleneiodonium
DR	Death receptor
DTT	Dithiothreitol
EDTA	Ethylenediaminetetraacetic acid
EGF	Epidermal growth factor
EGTA	Ethyleneglycotetraacetic acid
Elk-1	E twenty-six (ETS)-like transcription factor 1
eNOS	endothelial nitric oxide synthase
ER	Endoplasmic reticulum
ERK	Extracellular regulated kinase
EtBr	Ethidium Bromide
ETC	Electron transport chain
FACs	Fluorescence activated cell sorter
FADD	Fas-associated death domain-containing protein
FBS	Fetal bovine serum
FOXO3a	Forkhead box protein O3
FPP	Farnesyl pyrophosphate
fmk	Fluoromethylketone
FTI	Farnesyltransferase inhibitor
FTase	Farnesyltransferase
GAP	GTPase-activating protein
GAPDH	Glyceraldehyde-3-phosphate dehydrogenase
GDI	Guanine nucleotide dissociation inhibitors
GDP	Guanosine diphosphate
GEF	Guanine nucleotide exchange factors
GGPP	Geranylgeranyl pyrophosphate
GGTI	Geranylgeranyltransferase inhibitor
GGTase	Geranylgeranyltransferase
GSH	Gluthathione
GTP	Guanosine triphosphate
HCl	hydrochloric acid
H_2O_2	Hydrogen peroxide
HMG-CoA	3-hydroxy-3-methyl-glutaryl-CoA
HtrA2/Omi	high temperature requirement protein 2
IAP	Inhibitor of apoptosis protein
iCAD	Inhibitor of caspase-activated Dnase
IETD-AFC	N-Acetyl-Ile-Glu-Thr-Asp-7-amino-4-trifluoromethylcoumarin
IKK	IkB kinase

JNK	c-Jun N-terminal kinase
KCl	Potassium chloride
LC3	Light Chain 3
LC8	Light Chain 8
LEHD-AFC	N-Acetyl-Leu-Glu-His-Asp-7-amino-4-trifluoromethylcoumarin
LDL	low density lipoprotein
MAPK	Mitogen activated protein kinase
MAPKK	Mitogen activated protein kinase kinase
MAPKKK	Mitogen activated protein kinase kinase kinase
Mcl-1	Myeloid cell leukemia sequence 1
MEK	Meiosis-specific serine/threonine protein kinase
MgCl2	Magnesium chloride
MKK4	Dual specificity mitogen-activated protein kinase kinase 4
MKP	MAPK phosphatase
MMP	Mitochondrial membrane potential
MNK	Map Kinase interacting kinases
MnSOD	Manganese superoxide dismutase
MOMP	Mitochondrial outer membrane permeabilization
MPT	Mitochondrial Permeability Transition
mRNA	messenger RNA
MSK	mitogen and stress-activated protein kinase
mTOR	Mammalian target of rapamycin
MTT	3-(4,5-dimethylthiazol- 2-yl)-2,5 diphenyltetrazolium bromide
myc	v-myc myelocytomatosis viral oncogene homolog (avian)
MVA	Mevalonate
NAC	N-Acetyl cysteine
NaCl	Sodium Chloride
NAD	β-nicotinamide adenine dinucleotide
NADPH	Nicotinamide adenine dinucleotide phosphate
NFκB	Nuclear factor of kappa light
NOXA	Adult T cell leukemia derived PMA responsive
$NO^{\bullet}$	Nitric oxide
NOS	Nitric oxide synthase
NOX	NADPH oxidase
$O_2^{\bullet -}$	Superoxide radical
$OH^{\bullet}$	Hydroxyl radical
PARP	Poly(ADP-ribose) polymerase
PAK	p21-activated kinase
PBS	Phosphate buffered saline
PCD	Programmed cell death
PE	Phycoerythrin
PDGF	Platelet-derived growth factor
PDK1	3-phosphoinositide dependent protein kinase 1

PH	pleckstrin homology
PI	Propidium iodide
PI3K	Phosphatidylinositol-3-kinase
PIDD	p53-induced protein with a death domain
PIDDosome	A protein complex of PIDD
PIP2	Phosphatidylinositol diphosphate
PIP3	Phosphatidylinositol triphosphate
PKB/Akt	Protein kinase B/v-akt murine thymoma viral oncogene homolog 1
PKC	Protein kinase C
PLD	Phospholipase D
PMSF	Phenylmethylsulphonyl fluoride
POSH	plenty of Src Homology 2 (SH2) domains
PTEN	Phosphatase and tensin homolog located on chromosome ten
PTPC	Permeability transition pore complex
PUMA	p53-upregulated mediator of apoptosis
PVDF	Polyvinylidene fluoride
pRB	Retinoblastoma
Rac	Ras-related C3 botulinum toxin substrate
Ras	Rat sarcoma
Rho	Ras homologue GTPase
RhoA	Ras homolog gene family, member A
RhoB	Ras homolog gene family, member B
RhoC	Ras homolog gene family, member C
RhoGDI	Rho GDP-dissociation inhibitor
RIP	Receptor interacting protein
RNA	Ribonucleic acid
RNase	Ribonuclease
RNS	Reactive nitrogen species
ROCK	Rho-associated kinase
ROS	Reactive oxygen species
RPMI 1640	Rosewell Park Memorial Institute 1640
RTK	Receptor tyrosine kinase
SAP	SLAM-Associated Protein 1
SDS	Sodium dodecyl sulphate
SDS-PAGE	SDS-polyacrylamide gel electrophoresis
siRNA	small interfering RNA
Smac	Second Mitochondrail Activator of Caspases
SOD	Superoxide dismutase
SOD1	Copper/zinc superoxide dismutase
Sos	Son of sevenless
SRE	Serum response element
Ser	Serine
tBid	Truncated Bid
TEMED	N,N,N’,N’-tetramethlethylenediamine

Thr	Threonine
TNF	Tumor necrosis factor
TRAIL	TNF-related apoptosis inducing factor
Tyr	Tyrosine
UV	Ultraviolet
VEGF	Vascular endothelial growth factor
VDAC	Voltage dependent anion channel
XIAP	X-linked inhibitor of apoptosis protein
zVAD-fmk	Benzyoxycarbonyl valanyl alanyl-fluoromethylketone

INTRODUCTION

1. Statins overview

Statins are clinically used to treat hyperlipidemia, a disease characterized by the unusual elevation of lipids such as cholesterol and triglycerides in the bloodstream. Statins can effectively control the blood cholesterol level in two ways. On one hand, it reduces the endogenous synthesis of cholesterol by competitively inhibiting 3-hydroxy-3-methylglutaryl-coenzyme A (HMG-CoA) reductase, the rate-limiting enzyme of the mevalonate pathway that is responsible for synthesizing cholesterol in the liver (Weekes 1975). On the other hand, statins also enhance cholesterol clearance from the blood through upregulating low-density-lipoprotein (LDL) receptors in hepatic cells, which is the primary mechanism for removing cholesterol from circulation (Slater, McKinney et al. 1984; Lamon-Fava, Diffenderfer et al. 2007).

1.1 Types of statins

The first known statin was mevastatin (compactin, ML-236B), a natural inhibitor of HMG-CoA reductase isolated from *Penicillium citrinium* in 1976 (Endo, Kuroda et al. 1976). Despite its effectiveness towards cholesterol inhibition, the drug was never marketed because of its unacceptable hepatotoxicity. Subsequently, lovastatin, a more potent fungal metabolite was isolated from a strain of *Aspergillus terreus* in 1979 and became the first statin approved for clinical use. Lovastatin was then chemically modified to form a semi-synthetic derivative, simvastatin (Alberts 1990). In 1986, pravastatin (CS-514) was identified in a bacterium called *Nocardia autotrophica* (Yoshino, Kazumi et al. 1986). The chemical structure of these three statins is closely related. Since then, several synthetic statins have become

commercially available, namely fluvastatin, atorvastatin, cerivastatin, and most recently, pitavastatin and rosuvastatin (Illingworth and Tobert 2001). However, cerivastatin was withdrawn from the market in 2001 due to fetal muscle toxicity (Furberg and Pitt 2001). These drugs differ in potency, key pharmacokinetic and pharmacological properties. Shepherd *et al* has listed the rank of potency in decreasing orders as: rosuvastatin, atorvastatin, simvastatin, lovastatin, pravastatin, and fluvastatin (Shepherd, Hunninghake et al. 2003). The potency of the drugs was orchestrated by a few factors: dose, their active or lactone form and the lipophilicity. Lovastatin and simvastatin are the only statins administered as lactone pro-drugs, which then enzymatically hydrolysed into their active and hydroxy-acid form (Corsini, Maggi et al. 1995); while the other statins are taken directly in their active form. The differences in chemical structure also affect the solubility of statins. Pravastatin is extremely hydrophilic, and fluvastatin has intermediate characteristics, whereas the rest are lipophilic (Blumenthal 2000). The lipophilicity governs the hepatoselectivity of statins and their inhibitory effect on HMG-CoA reductase. Hydrophilic statins enter the hepatocytes by carriers and primarily targeted to the liver; while uptake of lipophilic statins is through passive diffusion and these statins show efficient activities at both hepatic and extrahepatic sites (Hamelin and Turgeon 1998). For example, simvastatin has been shown to enter endothelial cells (Corsini, Bellosta et al. 1999). In this study, we chose the lipophilic simvastatin to study its potential anti-cancer effects, and its chemical structure is shown in Figure A.

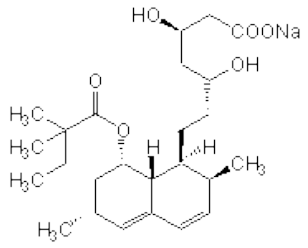

Figure A: Chemical Structure of simvastatin in its active and carboxylated form. Picture is taken from Millipore website.

1.2 Pleiotropic effects of statins

Besides being a huge success as therapeutic agents for hyperlipidemia, statins also display benefits in both primary and secondary prevention of coronary heart diseases by reducing the blood cholesterol level, which is a major risk factor for atherosclerotic diseases (Gordon and Kannel 1971; Sytkowski, Kannel et al. 1990; 1994; Shepherd, Cobbe et al. 1995; Sacks, Pfeffer et al. 1996; 1998; Downs, Clearfield et al. 1998; 2002; Sever, Dahlof et al. 2003). However, recent experimental and clinical evidences suggest that the positive outcome on cardiovascular diseases may also be attributed by the cholesterol-independent "pleiotropic" effects of statins, including improved endothelial function (Anderson, Meredith et al. 1995; Treasure, Klein et al. 1995; O'Driscoll, Green et al. 1997; Laufs, La Fata et al. 1998), inhibition of cardiac hypertrophy (Lefer, Campbell et al. 1999; Scalia, Gooszen et al. 2001; Takemoto, Node et al. 2001; Node, Fujita et al. 2003), decreased oxidative stress and vascular inflammation (Kwak, Mulhaupt et al. 2000; Vaughan, Gotto et al. 2000; Scalia, Gooszen et al. 2001; Stalker, Lefer et al. 2001), inhibition of platelet reactivity and thrombogenic response (Hale, Craver et al. 1998; Huhle, Abletshauser et al. 1999) and stabilization of atherosclerotic plaques (Koh 2000; Crisby, Nordin-Fredriksson et al. 2001). Statin-induced upregulation and activation of endothelial nitric oxide synthase (eNOS) is suggested to be the key mechanism involved in the protection of the cardiovascular system (Balakumar, Kathuria et al. 2012). Furthermore, statins have also shown positive effects on bone formation, the immune and central nerve systems (Yeung and Tsao 2002).

Many of the pleiotropic effects of statins can be traced back to the inhibition of the downstream isoprenoid intermediates of the mevalonate pathway, such as

farnesylpyrophosphate (FPP) and geranylgeranylpyrophosphate (GGPP) (Figure B). These isoprenoids serve as lipid attachments for approximately 1% of all cellular proteins, for example the γ-subunit of heterotrimetic G-proteins, heme-A, nuclear lamins, and small guanosine triphosphate-binding protein Ras superfamily proteins (Liao and Laufs 2005). In particular, many reports have suggested that the observed pleiotropic effects of statins are due to the inhibition of the proper membrane localization and functions of the Ras superfamily proteins (Goldstein and Brown 1990; Liao and Laufs 2005). For examples, it was reported that statin-mediated upregulation of eNOS was due to inhibition of isoprenoids synthesis and the subsequent prevention of prenylation of small GTPase Rho (Laufs and Liao 1998; Rikitake and Liao 2005; Ito, Ito et al. 2010).

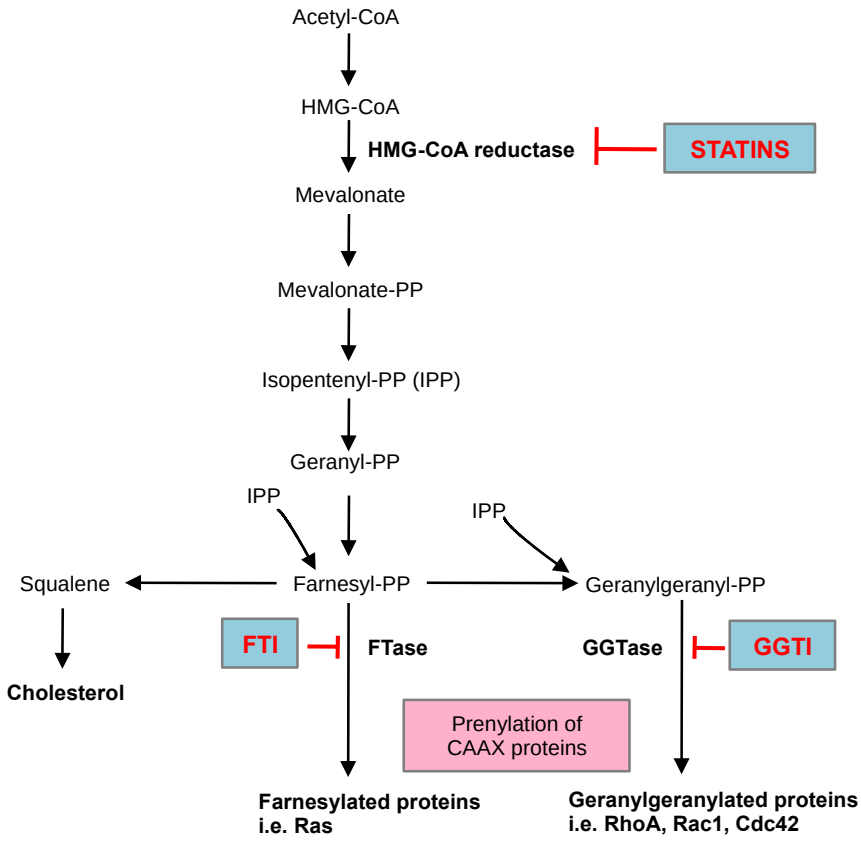

Figure B: Overview of the mevalonate pathway: important products, enzymes and targets of statins, farnesyltransferase inhibitors (FTIs) and geranylgeranyltransferase I inhibitors (GGTIs).

1.3 Anti-tumor effects of statins: bench to bedside

Mounting experimental data has demonstrated that statins exert cytostatic and pro-apoptotic properties in a panel of cancers, including breast carcinoma, prostate carcinoma, colorectal carcinoma, lung carcinoma, glioblastoma, osteosarcoma, acute myeloid leukemia (AML), multiple myeloma and skin carcinoma (Chan, Oza et al. 2003; Ukomadu and Dutta 2003; Jiang, Zheng et al. 2004; Demierre, Higgins et al. 2005; Campbell, Esserman et al. 2006; Fromigue, Hay et al. 2006; Hwang, Na et al. 2011). Statins inhibit cell proliferation by arresting cancer cells in the G1 or S, and occasionally G2/M phases by modulating cell cycle regulatory proteins (Jakobisiak, Bruno et al. 1991; Crick, Andres et al. 1998). For example, it was shown that statins regulate G1/S arrest in colorectal cancer cells by upregulating p21 and p27 expression and downregulating CDK2 activity (Ukomadu and Dutta 2003). Besides the effects of statins on proliferation, they also induce apoptosis in cancer cells. Although the understanding of the functional mechanisms underlying these effects of statins are still limiting, some current work has suggested a few possibilities on how statins tilt the balance of pro-survival and pro-apoptotic signals. For example, lovastatin induces apoptosis in AML cells by downregulating the pro-survival Raf-MEK-ERK pathway (Wu, Wong et al. 2004); in another case, statins trigger apoptosis in osteosarcoma cells by abrogating ERK signaling and Bcl-2 protein expression downstream of RhoA inhibition (Fromigue, Hay et al. 2006). Other reports has also suggested that statins mediate apoptotic response by activating FAS (CD-95) apoptotic signaling downstream of disruption of cholesterol-enriched lipid rafts (Gniadecki 2004). Furthermore, the cytostatic and cytotoxic effects of statins are observed to be more prominent in malignant cells compared to non-malignant cells, which was proposed to be due to the higher expression of HMG-CoA reductase and a

greater need for mevalonate-derived isoprenoids in cancer cells than normal cells (Hentosh, Yuh et al. 2001). Nonetheless, statins are promising treatment options with higher therapeutic index that target cancer cells with better specificity (Wong, Dimitroulakos et al. 2002; Jakobisiak and Golab 2003). Besides being an effective single-agent, various reports also demonstrated that statins could potentiate the effects of commonly used anti-cancer drugs such as cisplatin, doxorubicin and 5-fluorouracil (Feleszko and Jakobisiak 2000; Martirosyan, Clendening et al. 2010; Taylor-Harding, Orsulic et al. 2010). More significantly, statins can also sensitize cells that are previously resistant to chemotherapy and radiation therapy (Wang, Collie-Duguid et al. 2002; Li, Appelbaum et al. 2003). For example, both lovastatin and simvastatin are shown to fully reverse cell adhesion-mediated drug resistance (CAM-DR) in multiple myeloma cells (Schmidmaier, Baumann et al. 2004). These positive *in vitro* observations also highlight that statins may be valuable adjuvant in combinational therapies to treat cancers.

Other than the effects of statins in proliferation and apoptosis, studies in multiple cancer models have also demonstrated their ability to interfere with invasion and metastasis in both *in vitro* and *in vivo* studies. For instance, studies using mouse mammary cancer models showed that both lovastatin and simvastatin reduced tumor formation and metastasis (Alonso, Farina et al. 1998; Farina, Bublik et al. 2002). Similar observations were also established in melanoma cells, where statins inhibited invasion and metastasis by preventing RhoC activities (Collisson, Kleer et al. 2003).

Nonetheless, the clinical efficacy of anti-tumor effects of statins is still controversial. Some epidemiological studies have correlated extended statin use with reduced

cancer risk, while some retrospective studies that monitored cancer risk as a secondary outcome have concluded otherwise (Moorman and Hamilton 2007). It is important to note the drawbacks of retrospective studies, which is the inherent bias of confounding factors such as unhealthy life style that contributes not only to hyperlipidemia and cardiovascular diseases, but also to cancer risk. On the other hand, some prospective observational studies have shown significant statin-mediated reduction in the incidence of a few cancers, including carcinomas of breast, prostate, lung, colorectal and pancreas (Blais, Desgagne et al. 2000; Poynter, Gruber et al. 2005; Shannon, Tewoderos et al. 2005; Boudreau, Yu et al. 2007; Khurana, Bejjanki et al. 2007; Khurana, Sheth et al. 2007). Yet, other studies fail to draw such conclusions (Kaye and Jick 2004). There are multiple factors that may contribute to the discrepancy in those observational studies, such as differences in study methodology and lack of insights in the underlying mechanism of action in *in vitro* systems. It is suggested that large prospective randomized trials will be a better design to determine the preventive and therapeutic effects of statins in cancers. Despite the abovementioned discrepancies, statins are still attractive targets of research in the search of cancer-specific and efficient anti-cancer agents. In addition, statins can be introduced into clinical practice quickly and enjoy a favorable safety profile with uncommon but well-characterized side effects such as myotoxicity (Vamvakopoulos 2005; Moorman and Hamilton 2007). Nevertheless, better understanding of the mechanisms involved will be necessary to identify conditions and molecular features required for statin-mediated anti-cancer effects and to promote conversion of bench observations to reality.

1.4 Statin effects in colorectal cancer

Statins have been found to inhibit colorectal cancer progression in both cell line and animal models. Some mechanistic insights have emerged to explain the observed effects in cancer cell lines. Despite constitutively-active Ras is frequently observed in colorectal cancer and involved in the cancer development, studies have found that the mutational status of Ras might not be of importance in mediating statins' cytostatic and cytotoxic effects in colorectal cancer cell lines. Instead, multiple reports have suggested that the protein geranylgeranylation process and their downstream Rho proteins are important in statin-mediated apoptotic effects (Attoub, Noe et al. 2000; Agarwal, Halmos et al. 2002). Another possible mechanism involves the anti-inflammatory effects of statins, which is found to be effective to prevent colorectal cancer associated with inflammation. Furthermore, all the current *in vivo* mouse-model studies have demonstrated that statin treatment consistently reduced colorectal tumor formation (Demierre, Higgins et al. 2005).

Although the results from observational studies on statin use and colorectal cancer risk are intriguing, quite a number of studies do suggest preventive effects of statins against colorectal cancer (Boudreau, Yu et al. 2010). For instance, a 35–43% reduction in colorectal cancer risk following statin use was observed in two meta-observational studies reported (Poynter, Gruber et al. 2005; Farwell, Scranton et al. 2008). Another large case-control study was conducted to examine the clinical outcomes in colorectal cancer patients, the results showed that long-term statin use correlated with less-advanced cancer, lower incidence of metastases, and a better survival rate compared to non-users (Siddiqui, Nazario et al. 2009).

2 Programmed cell death

Programmed cell death (PCD) is natural physiological process, which involves in morphogenesis, maintenance of tissue homeostasis and removing unwanted cells that may be in excess, damaged or mutated. Hence, when the tight regulation of PCD goes loose, it leads to pathological consequences such as the development of cancer. Accumulating evidence suggests that drugs that can restore functional PCD hold particular importance in the development of cancer therapies. Recently, many studies have divided PCD into three main types: apoptosis (type I), autophagy (type II) and necrosis (type III), based on their differences in morphological appearances, death inducing signals or caspase activation status.

2.1 Apoptosis

2.1.1 Characteristics and physiological role of apoptosis

The term "Apoptosis" was first proposed by Kerr *et al* in 1972; it was described as a novel cell death process distinct from necrosis (Kerr, Wyllie et al. 1972). Apoptotic cells are characterized by morphological hallmarks, such as cell shrinkage, membrane blebbing, nuclear chromatin condensation (pyknosis) and DNA fragmentation (karyorrhexis) (Wyllie, Kerr et al. 1980). At the early stage of apoptosis, changes like externalization of phosphatidylserine happens without compromising cell membrane integrity (Fadok, Voelker et al. 1992). Eventually, cells break and form apoptotic bodies, which are membrane-bound cellular fragments. Apoptotic bodies contain intact organelles enclosed by membranes, which are rapidly engulfed by surrounding phagocytic cells without triggering any inflammatory responses (Kurosaka, Takahashi et al. 2003).

Apoptosis is involved in various physiological processes. During embryogenesis, apoptosis mediates the formation of inter-digit spaces allowing for proper separation of fingers (Jacobson, Weil et al. 1997). Apoptosis also takes part in eliminating pathogen-invaded cells in order to facilitate wound-healing (Greenhalgh 1998), or removing lymphocytes that synthesize inactive or autoimmune antibodies (Opferman and Korsmeyer 2003). Clearly, deregulation of the apoptotic pathways can potentially result in various diseases. For example, excessive apoptosis can cause autoimmune diseases and cancer, while neurodegenerative diseases such as Parkinson's and Alzheimer's disease are considered to be due to insufficient apoptosis (Jellinger 2001; Zornig, Hueber et al. 2001; Olanow 2007).

2.1.2 Molecular mechanisms of apoptosis

Apoptosis is a highly regulated and controlled cell death program involving complex interplay of multiple molecular factors. Under different triggers, cells activate different apoptotic signaling pathways, which are broadly characterized as the extrinsic/death receptor pathway and the intrinsic/mitochondrial pathway (Figure C). However, despite the diversity in the initiating stimuli, cells undergo apoptosis display remarkably uniform morphological and biochemical alterations, suggesting the presence of a common execution phase. It was then identified that a particular class of proteases, the caspases, are responsible for the characteristic cellular morphology of apoptosis.

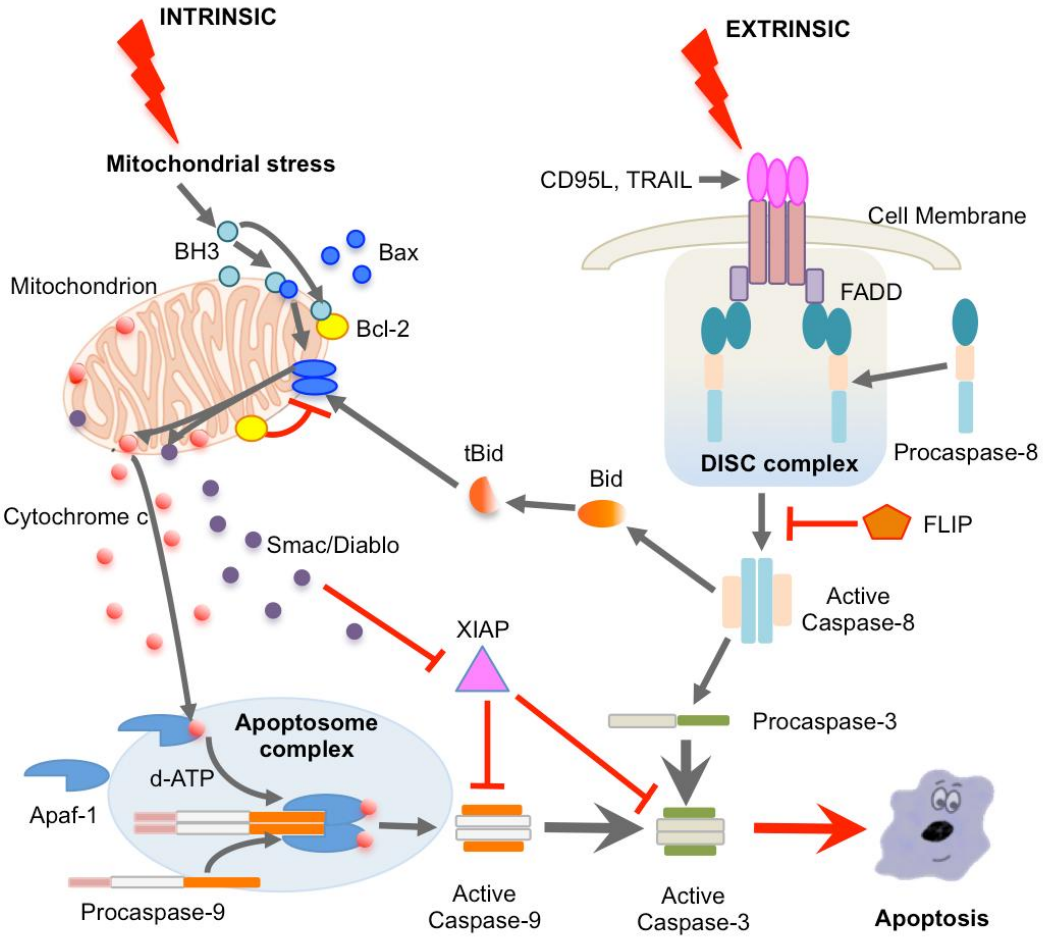

Figure C: Apoptotic signaling and the molecular players.
The extrinsic pathway is exemplified by the activation of death receptor after ligand binding, leading to the recruitment and activation of caspase-8 by the adaptor protein FADD. While the intrinsic pathway is triggered by cellular insults, damage or infection, in response to which BH3-only proteins such as Bax are mobilized to initiate mitochondrial outer membrane permeabilization (MOMP) and release of mitochondria residing factors. Subsequent formation of apoptosome then stimulates activation of caspase-9 and downstream effector caspases. Two pathways are interlinked by caspase-8-mediated cleavage of Bid, which results in translocation of t-Bid to the mitochondria and MOMP (Modified from Macfarlane and Williams, 2004 (MacFarlane and Williams 2004)).

2.1.2.1 Caspases

Caspases (cysteine aspartate-specific protease) was first discovered in the nematode *Caenorhabditis elegans*, where it was known as the cell death gene CED-3 (Yuan, Shaham et al. 1993). The mammalian family members are highly homologus to CED-3. It contains many members, majority of the family members (caspase-2, -3, -6, -7, -8, -9, and -10) participate in the apoptosis signaling (Cohen 1997), whilst caspase-1, 4, 5 and 12 are involved in cytokine processing and inflammation (Martinon and Tschopp 2007), and the functions of caspase-11 and -13 are less established. Despite the differences in their functions, the caspase family members share some common properties, for example, they all have a conservative penta-peptide active site containing a cysteine residue; as their name indicates, they are cysteine proteases that recognize a tetra-peptide site in their substrates and cleave after the Asp residue of the peptide. In addition, they are synthesized in an inactive form (zymogen or proenzyme) and regulated post-translationally to ensure rapid activation upon trigger (Kamens, Paskind et al. 1995; Alnemri, Livingston et al. 1996; Nicholson and Thornberry 1997).

Caspases that participate in apoptosis can be further grouped as initiator caspases (caspase-2, - 8, -9 and -10) and effector caspases (caspase-3, -6 and -7). Unlike the short pro-domains possessed by effector caspases, initiatior caspases possess a long pro-domain containing Death Effector Domain (DED) for caspase-8 and -10, or Caspase Recruitment Domain (CARD) for caspase-2 and -9. Upon pro-apoptotic stimuli trigger, these special domains allow the recruitment of the initiator caspases into complexes such as the death-inducing signaling complex (DISC) for caspase-8 and -10 , the apoptosome for caspase-9, and the PIDDosome for caspase-2 (Peter and

Krammer 2003; Tinel and Tschopp 2004; Shi 2008). The recruitment is followed by the oligomerization and autocatalytic activation of the initiator caspases (Wilson, Black et al. 1994; Kumar and Colussi 1999). On the other hand, activation of the effector caspases is mediated through cleavage of their inactive pro-forms by initiator caspases. Once activated, the effectors caspases in turn cleave a variety of key cellular substrates and accounts for the morphological and biochemical changes occurred during cell death (Nicholson 1999). One of the earliest substrates cleaved by caspase-3 or -7 is poly-ADP-ribose polymerase (PARP) (Casciola-Rosen, Nicholson et al. 1996), a nuclear protein implicated in DNA repair. The effector caspases also mediate the cleaveage of other cellular substrates involved in membrane blebbing (Rho-associated kinase 1 (ROCK1), p-21 activated kinase (PAK), and gelsolin), DNA fragmentation (caspase-activated Dnases), maintenance of cellular structures (cytokeratin-18, fodrin, actin), and nuclear shrinkage (lamin) (Fischer, Janicke et al. 2003).

2.1.2.2 Bcl-2 family member

Besides caspases, apoptosis is also controlled by a highly conserved family of proteins: Bcl-2 proteins. The mammalian Bcl-2 family contains at least 20 members. Despite their full sequences share low levels of homology; all of them contain at least one conserved Bcl-2 homology (BH) domain (BH1 to 4) that is essential for protein-protein interactions (Yin, Oltvai et al. 1994). Bcl-2 family is divided into two groups: the anti-apoptotic and the pro-apoptotic members (Gross, McDonnell et al. 1999). Bcl-2, B-cell lymphoma-extra large (Bcl-XL), Bcl-W and myeloid cell leukemia sequence 1 (Mcl-1) represent the anti-apoptotic members of Bcl-2 family. All of them contain all 4 BH domains (except for Mcl-1 lacking a BH4 domain), also a

hydrophobic COOH-terminal transmembrane domain that allows them to target to the nucleus envelope, the endoplasmic reticulum (ER) or the outer mitochondrial membrane (OMM). Under normal physiological conditions, Bcl-2 locates in the outer mitochondria membrane to maintain the mitochondria membrane integrity and prevent the release of apoptogenic factors from the mitochondria. Sub-fraction of ER-localized Bcl-2 is found to play a role in ER stress-induced apoptosis, whereby it modulates ER calcium homeostasis through enhancing calcium transport across the ER membrane (Foyouzi-Youssefi, Arnaudeau et al. 2000). Compared to Bcl-2, the other anti-apoptotic family members Bcl-xL, Bcl-W and Mcl-1 have not been studied extensively; it is observed that their anti-apoptotic role is restricted to specific tissues. For example, both Mcl-1 and Bcl-xL are found to be highly expressed in the liver and together they mediate the hepatic integrity during liver development. In addition, Mcl-1 is shown to control cortical neurogenesis and mediate neuron survival following DNA damage; while mice with mutant Bcl-W showed progressive and almost complete degeneration of the testes (Ross, Waymire et al. 1998; Ross, Amy et al. 2001; Russell, Warren et al. 2001; Arbour, Vanderluit et al. 2008; Hikita, Takehara et al. 2009).

On the other hand, the pro-apoptotic members can be further sub-divided into two groups: the Bcl-2-associated X (Bax) family proteins and the BH3-only proteins (Cory and Adams 2002). The Bax family proteins include Bax, Bcl-2 homologous antagonist killer (Bak) and Bcl-2-related ovarian killer (Bok). They all contain BH1, BH2 and BH3 domains. Under physiological conditions, Bax normally resides in the cytoplasm while Bak exists as integral mitochondria membrane protein. Upon apoptosis, Bax will translocate and oligomerize in the OMM to form a pore structure,

whereas Bak forms larger aggregates that compromises mitochondrial membrane integrity (Eskes, Desagher et al. 2000; Kroemer, Galluzzi et al. 2007). Oligomerization of Bax/Bak contributes to the mitochondrial outer membrane permeabilization (MOMP), either by forming channels allowing cytochrome c release (Antonsson, Montessuit et al. 2000; Dejean, Martinez-Caballero et al. 2005) and/or by interacting with components of the mitochondrial permeability transition pore complex (PTPC), such as voltage-dependent anion-selective channel protein 1 (VDAC1), which is followed by the opening of the pores allowing the efflux of pro-apoptotic proteins into the cytosol (Shimizu, Narita et al. 1999). Whereas Bax and Bak are widely distributed and interact with all anti-apoptotic proteins, Bok showed restricted tissue distribution in the reproductive tissues (ovary, testis and uterus) and selective heterodimerization with Mcl-1, but not Bcl-2, Bcl-xL, and Bcl-W (Hsu, Kaipia et al. 1997). Scattered studies have suggested that BOK can substitute the function of Bax in DNA damage-triggered intrinsic apoptosis in cancer cells, which might be related to its special ability to translocate into the nucleus (Yakovlev, Di Giovanni et al. 2004; Bartholomeusz, Wu et al. 2006).

Lastly, the pro-apoptotic BH3-only proteins include BH3 interacting domain death agonist (Bid), Bcl-2 interacting mediator (Bim), Bcl-2 antagonist of cell death (Bad), Noxa and p53-upregulated mediator of apoptosis (Puma). As the name suggests, these proteins only contain the BH3 domain. They exhibit pro-apoptotic functions by neutralizng the pro-survival Bcl-2 proteins. In addition, it is found that BH3-only proteins Bid and Bim are also direct activators of Bax/Bak to promote Bax/Bak-mediated membrane permeabilization (Kuwana, Bouchier-Hayes et al. 2005).

2.1.2.3.2 Biology of BIM

The physiological role of Bim was unveiled by deletion studies, where knockout of Bim resulted in accumulation of lymphoid and myeloid cells, disturbed development of immune system and developed autoimmune kidney diseases. These Bim knockout lymphocytes also demonstrated resistance to a certain set of apoptotic signals including cytokine deprivation, calcium ion flux and microtubule perturbation, but showed sensitivity to other insults such as glucocorticoids and DNA damage (Bouillet, Metcalf et al. 1999; Bouillet, Huang et al. 2000; Bouillet, Cory et al. 2001; Bouillet, Purton et al. 2002; Hildeman, Zhu et al. 2002). Three main forms of Bim (Bim-EL, Bim-L and Bim-S) are expressed due to alternative spicing, with Bim-EL being the most prominent form in most cell types (O'Reilly, Cullen et al. 2000). Both transcriptional and post-translational regulations determine the expression level and activity of Bim. Upregulation of Bim protein level to mediate apoptosis has been observed in multiple cell types, such as in neuronal cells upon nerve growth factor deprivation. Past work has also identified transcriptional factors responsible for Bim transcription, such as the activation of the c-Jun, FOXO, and Myb transcription factors (Biswas, Shi et al. 2007). Besides transcriptional control, Bim can also be regulated by phosphorylation. Several kinases such as AKT, ERK and JNK have been shown to phosphorylate Bim to mediate different effects. For examples, ERK-mediated phosphorylation of Bim results in proteosomal degradation and inhibition of its pro-apoptotic effects (Luciano, Jacquel et al. 2003). In contrast, JNK-dependent Bim phosphorylation potentiates apoptosis (Putcha, Le et al. 2003). Lastly, the activity of Bim is also regulated by its interaction with cytoskeletal structures. It is found that both Bim-EL and Bim-L are sequestered by the dynein light chain LC8 under normal conditions. Upon stress or apoptotic trigger, they will be released to

exert its pro-apoptotic effects. Bim-S lacks the interaction motif and does not bind to LC8, which potentially explains why Bim-S possesses the highest killing potency observed among the three members (Puthalakath and Strasser 2002). The tumor suppressor role of Bim has been suggested based on the findings that loss of Bim function promotes oncogenesis (Labi, Erlacher et al. 2006). Hence, drugs that are able to induce or enhance Bim expression may have therapeutic advantage to induce apoptosis in cancer cells.

2.1.2.3 Intrinsic pathway

Intrinsic pathway are induced by a wide range of non-receptor-mediated stimuli such as hypoxia, reactive oxygen species (ROS), UV irradiation, cytotoxic drugs and growth factors withdrawal, which produce intracellular signals that perturbate the integrity of mitochondrial membrane. Mitochondrial membrane permeabilization (MMP) event is the decisive condition for cell death induction in this pathway (Kroemer, Galluzzi et al. 2007). The mechanisms of MOMP induction involve the formation of pores in the mitochondrial membrane discussed in the earlier session. MOMP is frequently associated with the dissipation of the inner mitochondrial membrane potential (Goldstein, Waterhouse et al. 2000; Green and Kroemer 2004) and the release of other sequestered pro-death proteins from the intermembrance space (IMS) into the cytosol. In particular, cytosolic translocation of cytochrome c, which normally functions as an electron shuttle in the mitochondrial respiratory chain, together with the apoptotic protease activating factor-1 (Apaf-1) and procaspase-9, form the “apoptosome” in a nucleotide dATP/ATP dependent manner (Chinnaiyan 1999). Apoptosome formation results in autoactivation of caspase-9 that is responsible for the subsequent activation of executioner caspases (-3, -6 and -7)

and eventually leads to cell demise. Besides cytochrome c, Smac/DIABLO and HtrA2/Omi are also IMS proteins released into the cytosol upon apoptosis; these proteins exert their pro-apoptotic functions by antagonizing the inhibitor of apoptosis (IAP) family of proteins, such as XIAP, c-IAP1, c-IAP2 and survivin (van Loo, van Gurp et al. 2002; Schimmer 2004)

2.1.2.4 Extrinsic pathway

Apoptotic signaling can be initiated by extracellular signals from neighboring or distant cells, which have been identified as cytokines belonging to the tumor necrosis factor (TNFα) superfamily ligands. These ligands bind to the cell surface death receptors that belong to the TNF receptor gene superfamily. Some of the best-characterized death receptors and cognate ligands include FasR/FasL (CD95/APO-1), TNFR1/TNFα, DR3/Apo3L, DR4/TRAIL-R1, and DR5/TRAIL-R2 (Elmore 2007). Ligation of the specific ligand with the death receptors permits trimerization of the receptors and recruitment of the cytoplasmic adapter proteins, such as Fas-associated death domain (FADD) and tumor necrosis factor receptor type 1-associated death domain protein (TRADD) (Hsu, Xiong et al. 1995; Wajant 2002). FADD then allows for the recruitment of procaspase-8 via associations of their death effector domains, the resultant multi-protein complex is referred to as the death-inducing signaling complex (DISC). The close proximity of the recruited procaspase-8 molecules then triggers their autocatalytic activation (Kischkel, Hellbardt et al. 1995).

Following the activation of caspase-8, death signals are conducted in two distinct manners, depending on whether the events are occurring in a type I or type II cell (Ozoren and El-Deiry 2002). In type I cells, activation of caspase-8 alone is sufficient

to activate the downstream effector caspases (caspase-3, -6, -7), which results in cell death. On the other hand, in type II cells, caspase-8 activation is insufficient to directly elicit downstream caspase cascade; instead, it requires amplification via the mitochondrial apoptotic pathway. It has been suggested that Bid, a member of the BH3-only Bcl-2 family protein, mediates the crosstalk between the extrinsic and intrinsic pathway. Bid is proteolytically cleaved by caspase-8, and the cleaved/truncated bid (t-Bid) then translocates to the mitochondria and binds to Bax and Bak, resulting in their oligomerization and MOMP, which is followed by release of pro-apoptic factors such as cytochrome c and subsequent activation of caspase-9 and -3 (Scaffidi, Fulda et al. 1998). In short, type I cells are independent of mitochondria, whereas type II cells are mitochondria-dependent. In accordance with its role in suppressing MOMP, overexpression of the anti-apoptotic protein Bcl-2 is able to block apoptosis in type II cells, but not type I cells (Fulda, Meyer et al. 2002; Ozoren and El-Deiry 2002; Barnhart, Alappat et al. 2003).

2.2 Autophagy

Evolutionarily, autophagy is a process of self-cannibalization, which is highly conserved among eukaryotes. Autophagy is found to be active at a low level in almost all cells, where it maintains tissue homeostasis by replacing old or eradicating damaged cellular components or organelles with new ones. Besides its homeostatic function, autophagy also safeguards cell survival by providing constituents for energy generation under conditions such as starvation or growth factor withdrawal (Klionsky and Emr 2000). However, in some settings, it is considered as a mode of PCD named autophagic cell death, where higher-than-normal autophagy activities are observed (Maiuri, Le Toumelin et al. 2007). Unlike apoptosis, autophagic cell death is

independent of capases (Tsujimoto and Shimizu 2005); in fact, this form of cell death has been shown in cells with defects in apoptotic signaling or in the presence of caspase inhibitors (Shimizu, Kanaseki et al. 2004; Yu, Alva et al. 2004). In terms of morphology, cells undergoing autophagic cell death may present with chromatin condensation or membrane blebbing; however, there is no DNA fragmentation or formation of apoptotic bodies (Codogno and Meijer 2005). Instead, cells are accompanied by massive accumulation of double-membraned autophagic vesicles in the cytoplasm. The double- or multi-membrane–bound structure, called the autophagosome engulfs various cellular constituents, and subsequently fuses with lysosomes to become autolysosomes, where the sequestered cellular components are digested (Klionsky 2004). So far, the most important molecular component of the autophagic machinery consists of the autophagy-related genes (Atg); they encode proteins that are essential for the operation of autophagy. Over 30 ATG genes are identified in yeast with at least 11 orthologs in mammalian systems (ATG1, 3-10, 12 and 16). Notably, ATG8 is called light chain 3 (LC3) in mammals. The conversion of LC3 to LC3-II formation has been used as a reliable marker to assess the autophagosome formation in mammalian cells, where the relative amount of LC3-II formation reflects the abundance of the autophagosomes (Kabeya, Mizushima et al. 2000; Kabeya, Mizushima et al. 2004).

2.3 Necrosis

Necrosis was initially known as a nonregulated and accidental process where cells undergo an energy-independent type of cell death. Necrosis is distinctive from other types of PCD as it lacks the involvement of caspases and lysosomes (Sun and Peng 2009). In terms of morphology, some of the key features of a necrotic cell include

swelling of intracellular organelles (oncosis) like mitochondria, ER and Golgi, which is followed by plasma membrane rupture and subsequent breakdown and release of intracellular contents into the extracellular milieu (Majno and Joris 1995). The release of cytoplasmic contents then results in inflammatory responses, which has been found to promote tumor growth (Vakkila and Lotze 2004). Increasing evidence suggests that necrosis is a programmed course of events, as a result of interplay between several signaling pathways. For example, PARP-1 and apoptosis-inducing factor (AIF) are found to be essential in alkylating DNA damage-induced necrosis, and calpains and Bax are identified as intermediate molecular links (Moubarak, Yuste et al. 2007). Another study identified receptor interacting protein kinase (RIP kinase) as a critical mediator in TNF-induced necrosis; it functions to deplete ATP and impair mitochondrial functions, eventually lead to cell death (Temkin, Huang et al. 2006).

3. Rho GTPase family

The Rho GTPase subfamily of proteins belongs to the Ras superfamily. They mediate various housekeeping functions in the cells, such as cell morphology, polarity, adhesion, motility, membrane trafficking, cytoskeleton organization, proliferation, survival and cell death (Van Aelst and D'Souza-Schorey 1997; Schmitz, Govek et al. 2000; Aznar and Lacal 2001). They act as molecular switches by existing either in an inactive GDP-bound form or an active GTP-bound form. Active GTP-bound Rho proteins would then interact with their respective effectors to exert cellular functions (Jaffe and Hall 2005). Studies done on three classical Rho GTPases: RhoA, Rac1 and Cdc42 have provided insights into linking Rho GTPases with various physiological and pathological processes like embryonic development, immune and inflammation responses, tissue morphogenesis, tumorigenesis and metastasis. In this section of introduction, we will focus on these three Rho GTPases.

3.1 Regulation of Rho GTPases: GDP/GTP cycling

Rho GTPases are guanosine triphosphatases (GTPases), where only GTP-bound form can bind to its effectors to transmit signals. The cycling of GDP to GTP is mediated by guanine nucleotide exchange factors (GEFs) (Figure D). Whitehead *et al.* identified the first mammalian RhoGEF called Dbl in Diffuse B-cell lymphoma, and Dbl was found to be an oncogene (Whitehead, Campbell et al. 1997). Soon more RhoGEFs in the Dbl family were discovered and every member displayed different specificity towards the members of Rho GTPase family. For example, Vav is a GEF for RhoA, Rac1 and Cdc42; while Tiam1 is a Rac-specific GEF (Han, Das et al. 1997; Hordijk, ten Klooster et al. 1997). All the Dbl family members contain a Dbl-homology (DH) domain and a C-terminal pleckstrin homology (PH) domain. On the

contrary, GTPase-activating proteins (GAPs) work in the opposite way of GEFs to inactivate Rho GTPases by facilitating GTP hydrolysis.

Other than GEFs and GAPs, a special set of proteins named guanine nucleotide dissociation inhibitors (GDIs) is also involved in regulation of Rho GTPases. RhoGDIs are expressed in three forms; RhoGDIα is the most ubiquitously-expressed member (Fukumoto, Kaibuchi et al. 1990), while RhoGDIβ exists primarily in haematopoietic cells (Lelias, Adra et al. 1993). The third member RhoGDIγ is found in low abundance and localized to the Golgi apparatus (Zalcman, Closson et al. 1996). RhoGDIs possess dual functions both in the cytosol and at the membrane. On one hand, they form cytosolic complexes with GDP-bound Rho GTPases and prevent exchange of GDP to GTP. On the other hand, they also deliver and extract Rho proteins from membrane interface (Dransart, Olofsson et al. 2005). All three families of proteins work together to modulate the activity of Rho GTPases; deregulation of which would result in inappropriate activation of Rho GTPases and contribute to various pathological disorders such as cancer.

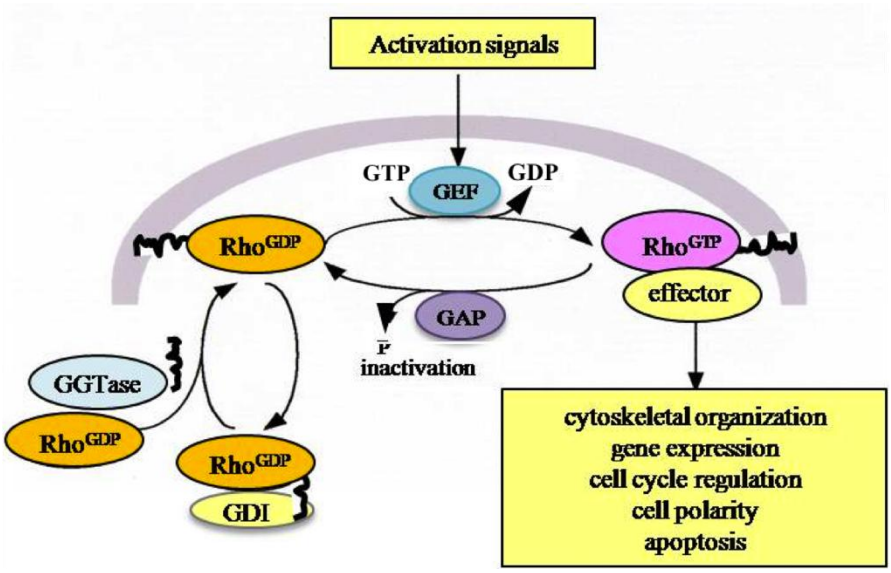

Figure D: The Rho GTPase switch.
Rho GTPases undergo post-modifications such as prenylation by geranylgeranyltransferases (GGTases), which facilitate their membrane-targeting. The GDP-GTP cycling of Rho GTPases are regulated by guanine nucleotide exchange factors (GEFs) and GTPase-activating proteins (GAPs). In addition, guanine-nucleotide dissociation inhibitors (GDIs) negatively regulate the cycling of Rho GTPases at membrane surfaces and in the cytosol. The active and GTP-bound form of Rho GTPases interacts with downstream effector molecules to regulate various cellular responses. (Modified from Anja and Alan Hall, 2002 (Schmidt and Hall 2002)).

3.2 Lipid modification of Rho GTPases

Other than the cycling of GTP/GDP, another important basis for the functionality of Rho GTPases is believed to be their distinct subcellular localization. Most of Rho GTPases undergo a three-step post-translational modification to localize to the plasma membrane or endomembranes. The modifications are signaled by the carboxyl-terminal CAAX motif (C represents cysteine, A represents an aliphatic amino acid, and X is any amino acid), which is present in the majority of identified Rho GTPases (Roberts, Mitin et al. 2008). This CAAX motif is recognized and first modified by prenyltransferases, which add an isoprenoid lipid to the C residue. Depending on the X residue of the CAAX motif, Rho GTPases can be modified by either farnesyltransferase (FTase) or geranylgeranyltransferase I (GGTase-I) to add a 15-carbon farnesyl or 20-carbon geranylgeranyl lipid, respectively (Reid, Terry et al. 2004). For example, RhoA, Rac1 and Cdc42 are geranylgeranylated exclusively, Rnd1-3 are farnesylated, while RhoB can undergo either farnesylation or geranylgeranylation. Following the isoprenylation step, the AAX part of the CAAX motif is cleaved off by the Ras-converting enzyme 1 (Rce1) endoprotease (Boyartchuk, Ashby et al. 1997; Ashby 1998). Lastly, a methyl group is added to the prenylated C residue by isoprenylcysteine-*O*-carboxyl methyltransferase (Icmt) (Hrycyna, Sapperstein et al. 1991; Sebti and Der 2003). Taken together, these modifications make the Rho GTPases more hydrophobic to assist their membrane association. It is generally accepted that drugs that inhibit the modifications of the CAAX motif, such as statins that block prenylation, would affect the localization and functions of Rho GTPases (Winter-Vann and Casey 2005).

3.3 Rho GTPases: their effectors and functions

Following the activation of Rho GTPases, they then interact with their respective downstream effectors to mediate the biochemical and biological functions such as cytoskeletal reorganization, gene transcription, regulation of enzymatic activities, cell cycle progression, cell morphogenesis and cell migration. It is believed that the unique interaction region between each effector and the Rho family member contributes to the diverse downstream responses (Bishop and Hall 2000; Jaffe and Hall 2005). Table 1 shows a list of selected effectors for RhoA, Rac1 and Cdc42 and their respective functions inside the cells. For example, one of the most classical functions of Rho proteins involves the cytoskeleton remodeling, which directly impacts cell migration. RhoA, Rac1 and Cdc42 control specific sets of effectors to mediate actin organization. Rac1 promotes lamellipodia formation via p21-activated kinase (PAK) and WAVE complex, while Cdc42 activation leads to the formation of another structure known as filopodia via its downstream effector PAK and Wiskott–Aldrich syndrome protein (WASP). In addition, RhoA activation results in the detachment of focal adhesions and formation of stress fibers via the effectors mammalian homologue of the *Drosophila* gene *Diaphanous 1* (mDia) and Rho-associated kinases (ROCK) (Frame and Brunton 2002). The coordinated regulation of Rho GTPases to form different structures governs the directional movements of cells. In addition, some of downstream effector proteins can also regulate Rho activities by feedback mechanisms. For example, PAK1 was found to phosphorylate RhoGDI and resulted in dissociation of Rac from RhoGDI, which was proposed to be a mechanism for Cdc42-mediated Rac activation in cells stimulated by platelet-derived growth factor (PDGF) or epidermal growth factor (EGF) (DerMardirossian, Schnelzer et al. 2004).

RHOA, RAC1 and CDC42 Effectors and Functions		
Rho GTPase	**Effectors**	**Function**
RhoA	ROCK I, II	Actomyosin contraction, transformation, transcription (SRF)
	mDia	Actin polymerizatioin
	PRK1/PKN	Endocytosis, p38γ MAPK activation, transcription (MEF2C)
	Citron	Cytokinesis
Rac1	PAK1, 2, 3	JNK activation, transformation
	MLK2, 3	JNK activation
	PAR6	Cell polarity, transformation
	p67Phox	NADPH oxidation, transcription (NFκB)
	IQGAP1, 2	Adherens junctions
	POSH	JNK activation, transcription (NFκB)
	IRSp53	Actin polymerization
Cdc42	PAK1, 2, 3	JNK activation, transformation
	MLK2, 3	JNK activation
	PAR6	Cell polarity, transformation
	N-WASP, WASP	Actin polymerization
	MRCK1, 2	Actin organization

Table 1: Effectors and functions of Rho GTPases (RhoA, Rac1 and Cdc42).
Abbreviations: mDia, mammalian homologue of the *Drosophila* gene *Diaphanous 1*; IQGAP, IQ-motif-containing GTPase-activating protein; JNK, JUN N-terminal kinase; MAPK, mitogen-activated protein kinase; MRCK: microtubule affinity regulating kinase; MEF2C, myocyte-enhancer factor 2C; MLK, mixed-lineage kinase; NF-κB, nuclear factor of κB; PAK, p21-activated kinase; PAR, partitioning defective; PIST, PD2 domain protein interacting specifically with TC10; PKN, protein kinase N; POSH, plenty of SH3 domains; ROCK, RHO-associated coiled-coil-forming kinase; SRF, serum response factor; WASP, Wiskott–Aldrich syndrome protein. Table is modified from Sahai and Marshall, 2002 (Sahai and Marshall 2002).

3.4 Rho GTPases in cancer

Rho GTPases are found to be involved in every stage of cancer progression including acquiring unlimited proliferation potential, gaining resistance to apoptosis, angiogenesis, invasion and metastasis. One line of evidence comes from the abundant information showing overexpression or hyperactivity of Rho GTPases in many types of human cancers (Jaffe and Hall 2002; Sahai and Marshall 2002; Gomez del Pulgar, Benitah et al. 2005) (Table 2). In some cases, the expression level of Rho proteins correlates positively with the severity of the cancer (Fritz, Just et al. 1999; Kamai, Arai et al. 2001). Surprisingly, mutations in Rho proteins are rarely observed in human cancers. One exception is the finding of a splice variant of Rac1 called Rac1b in colorectal and breast carcinomas (Singh, Karnoub et al. 2004).

Dysregulation of Rho GTPases in human tumors

Rho GTPase	Regulation	Tumor Types
RhoA	Overexpression	Breast, SCC, Colorectal, Lung (SCLC), Testicular, Ovarian, Gastric, Liver, Bladder
	High signalling activity	Melanoma, Pancreas, Neuroblastoma, Prostate, Leukemia AML, Sarcoma, SCC, Colorectal, Lung (SCLC), Ovarian, Gastric, Liver, Bladder
Rac1	Overexpression	Breast, SCC, Colorectal, Lung (NSCLC), Testicular, Gastric
	High signalling activity	Melanoma, Neuroblastoma, Colorectal, Gastric
	Genetic alteration (Rac1b)	Breast, Colorectal
Cdc42	Overexpression	Breast, SCC, Colorectal, Testicular
	High signalling activity	Melanoma

Table 2: Dysregulation of Rho GTPases (RhoA, Rac1 and Cdc42) in human tumors.
Abbreviations: SSC (squamous cell carcinoma), SCLC (small cell lung cancer), NSCLC (non-small cell lung cancer), AML (acute myeloid leukemia). Table is modified from Gomez del Pulgar, Benitah et al, 2005 (Gomez del Pulgar, Benitah et al. 2005).

The transforming potential of Rho GTPases has been demonstrated utilizing constitutively-active mutants of RhoA, Rac1 and Cdc42. Conversely, inactivating mutants of these Rho proteins abrogated Ras-mediated transformation of fibroblasts, suggesting that oncogenesis is coordinated by both Ras and Rho signaling networks (Khosravi-Far, Solski et al. 1995; Qiu, Chen et al. 1995; Qiu, Chen et al. 1995; Qiu, Abo et al. 1997; Roux, Gauthier-Rouviere et al. 1997). Multiple effectors of Rho GTPases are identified to contribute to the transformation process. For instance, PAK family proteins, which are downstream effectors of Rac and Cdc42, are reported to mediate Rac- and Ras-mediated transformation (Osada, Izawa et al. 1997). It is proposed that the underlying mechanism involves the PAK-dependent activation of c-Jun N-terminal kinase (JNK) and p38 pathways (Bagrodia, Derijard et al. 1995; Zhang, Han et al. 1995; Brown, Stowers et al. 1996). Further exploration also suggests PAK-independent activation of JNK and p38 activity downstream of Rac and Cdc42 activation via other effectors, such as Plenty of SH2 domain (POSH) (Tapon, Nagata et al. 1998). Transcription regulation is another mode to mediate the transforming activity of Rho GTPases. For example, activation of transcription factor nuclear factor kappa B (NF-kB) is found to mediate RhoA, Rac1 and Cdc42's oncogenic potential (Sulciner, Irani et al. 1996; Finco, Westwick et al. 1997).

3.5 Rho GTPases in regulating apoptosis

As opposed to the observation of the transforming activity of Rho GTPases, their role in inducing apoptosis has also been reported both *in vitro* and *in vivo*. Several key players have since been identified in mediating Rho-induced apoptotic responses. For instance, Rac1 induces apoptosis in fibroblasts by upregulating ceramide and Fas-L level upon serum starvation, and the increase of Fas-L is mediated by transcription control involving JNK and NF-kB (Embade, Valeron et al. 2000). As mentioned

earlier that both JNK and NF-kB are positive regulators of Rho-mediated transformation process, the discrepancy suggests that both factors have dual functions in both transformation and apoptosis depending on the cellular contexts and stimuli. In addition, some evidence has also suggested that the caspase-mediated cleavage of effector PAK2 and protein kinase N (PKN) regulates the morphological changes and signal transduction in apoptotic cells respectively (Lee, MacDonald et al. 1997; Rudel and Bokoch 1997; Takahashi, Mukai et al. 1998). Another factor POSH is also identified to be a strong inducer of apoptosis by regulating JNK and NF-kB pathway (Tapon, Nagata et al. 1998). Similar to Rac1, RhoA overexpression also induces apoptosis in multiple cell lines by increasing ceramide levels depending on Bcl-2 level (Esteve, Embade et al. 1998); however, the effectors remain to be identified. Furthermore, Cdc42-mediated apoptosis in Jurket T-lymphocytes is suggested to be due to activation of JNK signaling pathway (Chuang, Hahn et al. 1997). Future studies are required to understand the roles of specific effectors in Rho-mediated transformation and apoptosis, the identification of which could allow specific pharmacological manipulations to tilt the equilibrium towards apoptosis.

4. Reactive oxygen species

4.1 ROS overview: types and their physiological roles

Oxygen is required for normal aerobic metabolism of cells. It can travel freely across cellular membranes and form a variety of oxygen-derive free radicals and non-radicals, which are termed as Reactive oxygen species (ROS). ROS are generated when the unpaired electrons of oxygen go through electron transfers and form partially reduced oxygen derivatives. Oxygen-derived free radicals are defined as chemical species that are capable of existence on their own and contain one or more unpaired electrons, such as superoxide anion (O_2^-), singlet oxygen, peroxy radical, nitric oxide (NO) and hydroxyl radical (OH.). On the other hand, examples for non-radical ROS include hydrogen peroxide (H_2O_2) and peroxynitrite ($ONOO^-$).

Every type of ROS requires different reactions and shows different reactivity. Superoxide is not very reactive and it is highly compartmentalized to the site of production. Superoxide can be converted to hydrogen peroxide under the catalysis of superoxide dismutases (SODs). Instead, hydrogen peroxide can move freely across membranes (Fridovich 1978). Hydrogen peroxide is an important intermediate to produce more reactive ROS such as hydroxyl radical through the Fenton reaction which involves reductive homolytic cleavage in an iron-dependent manner (Andreyev, Kushnareva et al. 2005). When high concentrations of nitric oxide and superoxide are present in the cells, they can react to produce another powerful oxidant, peroxynitrite. Nitric oxide-derived oxidants are also called Reactive nitrogen species (RNS), which are found to induce nitrosative stress in the cells (Beckman and Koppenol 1996). However, this thesis will be focused on ROS. Physiologically, ROS-mediated oxidative stress can contribute to aging, neurodegeneration,

inflammation, atherosclerosis and chemotherapeutic effects etc. Recent research has also suggested its role in oncogenesis (Waris and Ahsan 2006).

4.2 Sources of ROS

4.2.1 Mitochondrial electron transport chain

One of the major sources of ROS comes from the mitochondria electron transport chain (ETC). The ETC consists of multiple components (Complex I-IV), from which electrons are passed through to oxygen followed by reduction reaction to produce water (Kakkar and Singh 2007). However, a small amount of electrons directly leaks to oxygen and leads to superoxide formation as a byproduct. It is estimated that 1-4% of oxygen might be incompletely reduced to superoxide (Betteridge 2000; Orrenius 2007). Studies have been devoted to identify specific sites of the ETC involved in ROS production. It has been observed that Complex I (NADH Hydrogenase) is the main site responsible for mitochondrial superoxide production via a single electron transfer to oxygen under normal physiological conditions (Cadenas, Boveris et al. 1977; Han, Williams et al. 2001). Besides that, Complex III (Ubiquinol/cytochrome c oxidio-reductase) are reported to produce superoxide especially under ischemic or apoptotic conditions (St-Pierre, Buckingham et al. 2002; Tahara, Navarete et al. 2009; Kang and Pervaiz 2012). Superoxide generated is then quickly converted to hydrogen peroxide by mitochondrial-localized manganese superoxide dismutase (MnSOD) (Buettner, Ng et al. 2006). Subsequently, hydrogen peroxide goes through the Fenton reaction and forms hydroxyl radical, a highly reactive and cytotoxic radical (Andreyev, Kushnareva et al. 2005). Other than the ETC, a few other mitochondrial enzymes are also reported to be able to generate superoxide (Chan and Bielski 1974; Chan and Bielski 1980; Andreyev, Kushnareva et al. 2005), such as the Krebs cycle

enzymes α-ketoglutarate dehydrogenase and pyruvate dehydrogenase (Starkov, Fiskum et al. 2004; Tretter and Adam-Vizi 2004). However, the precise mechanism involved in superoxide formation is still unclear. To keep the intracellular ROS level in check, mitochondria also possess a few anti-oxidant mechanisms such as MnSOD, glutathione peroxidase (Gpx1) and peroxiredoxin (PrxIII) (Droge 2002).

4.2.2 NADPH oxidase complex

Another main mechanism for ROS production involves the nicotinamide adenine dinucleotide phosphate oxidases (NADPH oxidases or NOX), which are flavoenzymes responsible for transferring electrons across biological membranes. The earliest observation was made in phagocytes in 1933. The phagocyte respiratory burst was later identified as a function of NADPH oxidase to generate superoxide. It is also the first example of an enzyme system to generate ROS as the primary function (Rossi and Zatti 1964; Babior, Kipnes et al. 1973). Subsequently, the phagocyte NADPH oxidase NOX2, transmembrane protein p22phox, cytosolic subunits p47phox, p40phox and p67phox, together with small GTP-binding protein Rac were identified to be the components responsible for ROS production in phagocytes (Royer-Pokora, Kunkel et al. 1986; Teahan, Rowe et al. 1987; Abo, Pick et al. 1991; Wientjes, Hsuan et al. 1993). In addition, ROS production using similar oxidase system is present in many other cell types, such as fibroblasts, vascular smooth muscle, endothelial cells and various tumor cells (Meier, Cross et al. 1991; Szatrowski and Nathan 1991; Griendling, Minieri et al. 1994; Li and Shah 2003). The current NOX family includes seven NOX isoforms (NOX1-5, DUOX1-2). They all share conserved structures such as NADPH-binding and flavin adenine dinucleotide (FAD)-binding domains and six conserved transmembrane domain (Bedard and

Krause 2007). However, the members differ in their tissue distribution, mechanism of action, and types of ROS produced. For example, it is understood that the activation of NOX5 and DUOX1-2 requires Ca^{2+} and no other subunits, while NOX1 and NOX2 activation requires Rac and other subunits (Cheng, Diebold et al. 2006). In contrast to superoxide-generating NOX1 and NOX2, NOX4 produces hydrogen peroxide (Takac, Schroder et al. 2011). The assembly of functional NOX complex is mostly on the plasma membrane (Bayraktutan, Blayney et al. 2000); however, some recent studies have reported functional NOX in other cellular compartments. NOX4 was recently found to localize to the mitochondria in rat mesangial cells and kidney cortex (Block, Gorin et al. 2009), mouse cardiac myocytes (Kuroda, Ago et al. 2010), and chronic myeloid leukemia cells overexpressed with Bcl-2 (Velaithan, Kang et al. 2011). Localization of NOX4 in the nucleus has been reported as well (Kuroda, Nakagawa et al. 2005).

4.2.3 Other sources

Other than the membrane-associated oxidases, soluble xanthine oxidase, aldehyde oxidase, dihydroorotate dehydrogenase, flavoprotein dehydrogenase and tryptophan dioxygenase can also produce ROS during catalytic cycling (Freeman and Crapo 1982). However, their physiological roles are not well studied. Besides the mitochondria and plasma membrane, ER is another site for ROS production. The ER-residing enzymes such as NADPH-cytochrome P450 reductase (CPR) catalyze reactions to detoxify lipid-soluble drugs and harmful metabolites (Aust, Roerig et al. 1972; Capdevila, Chacos et al. 1981). However, the intermediates in the catalytic cycle can sometimes reduce oxygen rather than its appropriate substrates, which results in superoxide generation. Apart from that, superoxide can also be generated

from direct leakage of electrons from CPR to oxygen (Santos, Tanaka et al. 2009). To counter the increase in intracellular ROS, cells also employ a few extra-mitochondrial anti-oxidant enzymes to maintain the original redox status, such as Cu/Zn SOD, catalase, gluthathione (GSH) peroxidase, GSH reductase and non-enzymatic activities of α-tocopherol, β-carotene, ascorbate and glutathione (Droge 2002).

4.3 ROS: role in oncogenesis and cell death

The cellular effects of ROS depend on its type and intensity present in the intracellular milieu (Mates, Segura et al. 2008). A pro-oxidant environment in cancer cells was first observed in 1985, where it was shown that presence of SOD1 (Cu/ZnSOD), a superoxide scavenging cytosolic enzyme, reversed the clastogenic process induced by patients' serum; in reverse, high oxygen tensions increased transformation frequency in irradiated mouse embryonic cells (Emerit and Cerutti 1981). Another piece of evidence supporting the role of ROS in oncogenesis comes from the observations on SOD2 (MnSOD). The expression of MnSOD expression is lower in tumor cells compared to their normal counterparts and the reduction in MnSOD level enhances the invasiveness of tumor cells (Weydert, Roling et al. 2003). On the contrary, increased expression of this protein inhibited the tumor malignancy (Zhao, Xue et al. 2001). In addition, ROS acts as important second messengers to promote cell growth and survival by regulating mitogen-activated protein kinases (MAPKs) and redox-regulated transcription factors such as NF-kB and activator protein-1 (AP1) (Bubici, Papa et al. 2006; Clerkin, Naughton et al. 2008). Our lab has also provided some convincing evidence by establishing that dominant negative form of Rac1 (Rac1N17) reduced superoxide production from NOX complex and

increased sensitivity of NIH3T3 fibroblast cells to apoptotic triggers (Pervaiz, Cao et al. 2001).

Despite mounting experimental evidence suggesting the role of ROS in oncogenesis and cell survival, its role in regulating cell death is also well established. The mode of cell death is dependent on the type and concentrations of ROS present inside the cells. Generally, excessive amount of ROS leads to necrosis as a result of modifications of essential intracellular proteins and DNA damage (Takeda, Shirato et al. 1999; Teramoto, Tomita et al. 1999; Saito, Nishio et al. 2006). On the other hand, moderate amount of ROS is found to induce apoptosis through depletion of anti-oxidant defenses and selective oxidation or activation of molecules regulating cell death responses (Takeda, Shirato et al. 1999; Teramoto, Tomita et al. 1999; Saito, Nishio et al. 2006). One such example is hydrogen peroxide, where intermediate concentrations (< 500 μM in most systems) triggers apoptosis and doses higher than 500 μM induces necrosis (Burdon, Alliangana et al. 1995). A few mechanisms have been proposed for hydrogen peroxide-mediated apoptosis. Previous work in the lab has demonstrated that cytosolic acidification is accompanied by exogenous or endogenous increase in hydrogen peroxide level to create a permissive intracellular milieu for apoptosis to occur (Pervaiz and Clement 2002). Other groups have reported that hydrogen peroxide promotes dimerization of apoptosis signal-regulating kinase 1 (ASK1) or activation of JNK, which is followed by engaging the intrinsic apoptotic machinery (Gotoh and Cooper 1998; Inoshita, Takeda et al. 2002; Schroeter, Boyd et al. 2003).

5. Signaling Pathways: AKT and MAPKs

The ability for cells to respond to extracellular stimuli is largely attributed to the interplays of intercellular signaling networks. These signaling pathways serve to relay, amplify and integrate signals to mount an appropriate response of a cell. Here, we focus on two groups of intracellular signaling pathways: AKT and mitogen-activated protein kinases (MAPK), and discuss their roles in cancer progression and cell death.

5.1 AKT

5.1.1 AKT signaling cascade

AKT is also known as protein kinase B (PKB). This serine/threonine kinase plays an important role in various cellular processes, for example insulin response, glucose metabolism, cell proliferation and survival (Lawlor and Alessi 2001). The AKT family is made of three widely expressed isoforms (AKT1, 2 and 3). They all contain an N-terminal PtdIns(3,4,5)P3- (PIP3) and PtdIns(3,4)P2 (PIP2)-binding pleckstrin homology (PH) domain and a C-terminal kinase catalytic domain. Following stimulations from cytokines, growth factors, insulin and attachment to extracellular matrix, AKT binds to PIP3 or PIP2 generated by upstream class 1 phosphoinositide 3-kinases (PI3K). Then AKT is recruited to the peripheral membrane that allows for AKT activation by phosphorylation at two residues (Cantrell 2001). Phosphorylation at Thr308 is mediated by 3-phosphoinositide dependent protein kinase 1 (PDK1) and the second phosphoylation happens at Ser473 by multiple kinases such as mammalian target of rapamycin (mTORC2) or DNA-dependent protein kinase (DNA-PK) (Alessi, Deak et al. 1997; Alessi 2001; Sarbassov, Guertin et al. 2005; Lu, Huang et al. 2006). In the later stage, active AKT then translocates to the nucleus to

activate the downstream substrates. Other than kinases, phosphatases also play an important role in regulating AKT activity. One of them is PtdIns(3,4,5)P3 3-phosphatase (PTEN), loss of which leads to AKT hyperactivation and is observed in many cancers (Maehama, Taylor et al. 2001). Currently, around fifty AKT substrates have been identified to be involved in the regulation of AKT-mediated cellular processes (Hers, Vincent et al. 2011).

5.1.2 AKT in cancer

The importance of AKT in oncogenesis is demonstrated by the frequent mutations of multiple signaling components of the PI3K/AKT pathway in human cancers, such as loss of PTEN and amplification of PI3K, which happen in over 30% of human cancers (Fresno Vara, Casado et al. 2004). Other than the gene alterations of this pathway in cancer, AKT also promotes tumor development via its downstream targets. For example, AKT inhibits apoptosis by inactivating the pro-apoptotic BAD and pro-caspase-9 (Cardone, Roy et al. 1998; Downward 1999); it also activates NF-kB signalling by phosphorylating IkB kinase (IKK) to induce transcription of anti-apoptotic genes (Ozes, Mayo et al. 1999). In addition, AKT promotes proliferation by allowing cell cycle progression through downregulation of p21 and p27 and stabilizing cyclin D1 (Diehl, Cheng et al. 1998; Sun, Lesche et al. 1999). AKT signalling also promotes angiogenesis, invasion and metastasis to allow tumor progression (Lawlor and Alessi 2001; Fresno Vara, Casado et al. 2004). Due to its important roles in tumorigenesis, drugs that are able to downregulate the PI3K/AKT pathway are promising anti-tumor agents, for example PI3K inhibitors wortmannin and LY294002 are found to have anti-tumor properties *in vitro* and *in vivo* (Powis, Bonjouklian et al. 1994; Schultz, Merriman et al. 1995; Casagrande, Bacqueville et al.

1998).

5.2 ERK

5.2.1 ERK signaling cascade

ERK is one of the major MAPKs. It is involved in multiple cellular and physiological processes, such as cell cycle control, cell differentiation, proliferation, survival, migration and senescence (Rubinfeld and Seger 2005). Two genes, ERK1 and ERK2, encode ERK protein and they are expressed as p44 and p42 (Boulton, Nye et al. 1991). Both proteins share 84% amino acid sequence homology and are functionally redundant (Lloyd 2006). The activation of ERK happens through the classical three-tier kinase signaling module for all MAPKs, which consists of mitogen activated protein kinase kinase kinase (MAPKKK), mitogen activated protein kinase kinase (MAPKK) and MAPK (Johnson and Lapadat 2002). In a typical ERK signaling cascade, following exposure of extracellular factors such as various cytokines, growth factors and neurotransmitters, MAPKKK, such as Raf-1 will be recruited to the plasma membrane and mediate the phosphorylation and activation of MAPKK such as MEKs. Subsequently, MEKs lead to the activation of ERK through a dual phosphorylation at Thr and Tyr residues within a Thr-Glu-Tyr motif (Chang, Steelman et al. 2003).

In general, ERK recognizes the consensus sequence Pro-Leu-Ser/Thr-Pro and phosphorylates Ser/Thr residues on its substrates (Gonzalez, Raden et al. 1991). The classical substrates of ERK are nuclear transcription factors, for example the ternary complex factors (TCFs) that include E twenty-six (ETS)-like transcription factors such as Elk-1, SAP-1 and SAP-2 and the activator protein-1 (AP-1) family members

c-Jun, c-Fos and activating transcription factor 2 (ATF2). Other than transcriptional factors, ERK also phosphorylates multiple cytosolic proteins such as the ribosomal S6 kinase, mitogen and stress-activated protein kinase (MSK) and MAPK interacting kinase (MNK). In addition, feedback inhibition is also an important regulatory mechanism for ERK signaling, where ERK can phosphorylate its upstream activators such as Raf, MEKs, GEFs and son of sevenless (SOS) (Langlois, Sasaoka et al. 1995; Eblen, Slack-Davis et al. 2004; Dougherty, Muller et al. 2005).

5.2.2 ERK in cancer and cell death

Conventionally, ERK activation is associated with cell proliferation and oncogenic transformation. Tumor development following activation of ERK signaling has been demonstrated in both *in vitro* and *in vivo* models (Kyriakis, App et al. 1992; Sobczak, Galabova-Kovacs et al. 2008). On the contrary, tumor progression can be blocked with inhibition of the ERK cascade (Murphy, Makonnen et al. 2006; Ouyang, Knauf et al. 2006). In addition, MEK1, the upstream activator of ERK, is also found to be implicated in malignant transformation. Constitutive activation of MEK1 induced oncogenesis whereas dominant negative form of MEK1 reversed tumor formation (Cowley, Paterson et al. 1994; Manser, Leung et al. 1994; Seger, Seger et al. 1994). More importantly, ERK activation promotes oncogenesis by integrating mitogenic signals. For example, ERK-mediated activation of Elk-1 could continue to induce activation of c-Fos, which is predominantly involved in cell cycle progression and growth (Marais, Wynne et al. 1993; Whitmarsh, Shore et al. 1995).

Despite its established role in pro-survival effects, ERK activation has recently been shown to be involved in cell death in certain cellular contexts. One example is in

DNA damage-induced cell death, abrogation of ERK activity reduced apoptosis (Lee, Fang et al. 2000; Wang, Martindale et al. 2000; Tang, Wu et al. 2002). Our lab has also reported that ERK activation mediates autophagy and apoptosis in cancer cells upon exposure to a novel compound (Wong, Iskandar et al. 2010).

5.3 JNK

5.3.1 JNK signaling cascade

Another important MAPK family member is the c-Jun NH2-terminal kinase (JNK), also known as the stress-activated protein kinase (SAPK). JNK is implicated in the regulation of multiple cellular processes, for example diabetes, metabolism, lifespan, autophagy and apoptosis (Weston and Davis 2007). JNKs family consist of ten isoforms derived from three different genes, *Jnk1* (MAPK8, four isoforms), *Jnk2* (MAPK9, four isoforms) and *Jnk3* (MAPK10, two isoforms). JNK1 and JNK2 are ubiquitously expressed, while JNK3 expression is specific to tissues such as brain, heart and testis (Kyriakis, Banerjee et al. 1994; Gupta, Barrett et al. 1996; Yang, Kuan et al. 1997; Weston, Lambright et al. 2002). Every isoform has a different substrate recognition and activation profile. However, they are all expressed as either 46kDa or 54kDa, with the difference of a COOH terminal extension (Pulverer, Kyriakis et al. 1991). The activation of JNK happens through a dual phosphorylation of Thr and Tyr residues within a Thr-Pro-Tyr motif, which is a common response to assaults from various cytokines, UV radiation, oxidative stress and osmotic shock (Davis 2000; Weston and Davis 2002; Weston, Lambright et al. 2002). The precise biological outcome from JNK activation varies from different stimuli and cellular contexts, but most of the cellular effects are attributed to the activation of AP-1 proteins. It is found that JNK specifically phosphorylates AP-1 transcription factor

family member c-Jun on Ser-63 and Ser-73 residues by binding to its N-terminus activation domain (Pulverer, Kyriakis et al. 1991; Hibi, Lin et al. 1993). Other than activating c-Jun, JNK is also observed to phosphorylate other AP-1 family members such as JunB, JunD and ATF-2 (Ip and Davis 1998).

5.3.2 JNK and cell death

Activation of JNK signaling in apoptosis is quite well observed and the underlying mechanism is context-dependent. One important discovery to address this issue is the temporal control of JNK activation that determines the biological responses. Multiple reports have showed that early and transient JNK activation contributes to cell survival, while prolonged and sustained JNK activation promotes apoptosis (Chang, Kamata et al. 2006; Lin 2006; Ventura, Hubner et al. 2006). The identification of downstream substrates of JNK activation provides great insight into the mechanisms in JNK-mediated apoptosis. One of them is H_2AX, a histone H_2A variant; it is shown that H_2AX phosphorylation by JNK is required for caspase-activated DNase (CAD)-mediated DNA fragmentation in UV-triggered cells (Lu, Zhu et al. 2006). Fas-L is another important downstream target of JNK (Le-Niculescu, Bonfoco et al. 1999). Other than that, multiple components of the mitochondrial death pathway are proposed to be regulated by JNK signaling. Depends on the cellular contexts, Bcl-2 family members Bax, Bcl-2, Bcl-xL, Mcl-1, Bad, Bmf and Bim can be phosphorylated by JNK to promote apoptotic responses (Lei and Davis 2003; Putcha, Le et al. 2003; Becker, Howell et al. 2004; Liu and Lin 2005; Kim, Ryu et al. 2006). In addition, Bim expression can also be transcriptionally-upregulated following activation of its transcription factors c-Jun and FOXO3a downstream of JNK activation (Harris and Johnson 2001; Putcha, Moulder et al. 2001; Whitfield, Neame

et al. 2001; Gilley, Coffer et al. 2003; Essers, Weijzen et al. 2004). Besides that, the production of a novel cleaved form of Bid (jBid) in a JNK-dependent manner also contributes to the activation of intrinsic pathway (Deng, Ren et al. 2003).

Some recent evidence has also suggested that JNK is involved in other forms of cell death such as necrosis and autophagy. One paper has reported that JNK plays a role in TNF-mediated necrosis through ROS production under the condition of NF-κB inhibition (Ventura, Cogswell et al. 2004). Another example linking JNK to autophagy regulation comes from the observation that targeted deletion of *Jnk3* protected damaged neurons that underwent autophagic cell death following cerebral ischemia-hypoxia (Kuan, Whitmarsh et al. 2003; Adhami, Liao et al. 2006). Collectively, JNK has shown to play important roles in multiple forms of cell death.

5.3.3 JNK in cancer

The role of JNK in tumorigenesis is quite controversial. Both tumor-promoting and tumor-suppressing activities of JNK have been demonstrated, which is probably due to the fact that JNK can be pro-survival or pro-apoptotic depending on the stimulus or cellular context. Several lines of evidence support the role of JNK in tumor development. One of them is that Ras-mediated oncogenic transformation can be effectively blocked by ablation of the *c-jun* gene or mutations at the JNK phosphorylation sites (Nateri, Spencer-Dene et al. 2005). In addition, another study has reported that JNK promoted hepatocarcinogenesis induced by chemical carcionogens (Sakurai, Maeda et al. 2006). It has been proposed that the pro-oncogenic role of JNK may be associated to its link with cell survival.

On the contrary, other studies have demonstrated the tumor suppressor role of JNK. It is proposed that the tumor suppression effects may be mediated by JNK's association with apoptosis (Kennedy and Davis 2003). One possible mechanism is through MKK4, an upstream activator of both JNK, which has been suggested as a potential tumor suppressor. Loss of function mutations of MKK4 is present in ~5% of human cancers (Whitmarsh and Davis 2007). In addition, suppression of MKK4 exhibited increased metastasis in lung, ovarian and prostate carcinomas (Yamada, Hickson et al. 2002; Xin, Yun et al. 2004; Vander Griend, Kocherginsky et al. 2005).

MATERIALS AND METHODS

1 Cell lines and cell culture

HCT116 WT (p53+/-), p53-/- and Bax-/- colorectal carcinoma cells were generously provided by Dr. Bert Vogelstein (The Johns Hopkins University School of Medicine, Baltimore, MD, USA) and maintained in McCoy 5A (Gibco Invitrogen Corporation, Carlsbad, CA, USA) supplemented with 10% fetal bovine serum (FBS, Hyclone, Irvine, CA, USA), 1% L-glutamine, and 1% penicillin/streptomycin (Hyclone, ThermoScientific, Waltham, MA, USA). SHEP-1 neuroblastoma cell line and A549 non-small cell lung carcinoma cell line were purchased from American Type Culture Collection (ATCC, Rockville, MD, USA), and were cultured in Dulbecco's Modified Eagle's Medium (DMEM, Hyclone, Logan, Utah, USA) supplemented with 10% fetal bovine serum and 1% penicillin/streptomycin. M14 melanoma cells stably transfected with an empty pIREShyg (M14 pIRES) or the same vector encoding the myc-RacV12 protein (M14 RacV12) were generated from our lab and maintained in DMEM supplemented with 10% fetal bovine serum and 1% penicillin/streptomycin. In addition, the culture medium for M14RacV12 cells was supplemented with 250 μg/ml selection antibiotic hygromycine. RKO colorectal carcinoma cell line, MDA-MB-231 breast cancer cell lines was purchased from ATCC and maintained in Roswell Park Memorial Institute 1640 medium (RPMI, Hyclone, Logan, Utah, USA) supplemented with 1% L-glutamine, 1% penicillin/streptomycin and 10% FBS. All cell lines were maintained in a humidified incubator at 37°C with 5% CO_2.

2 Reagents and chemicals

Simvastatin, GGTI-298, FTI-277, NSC23766 and PAK1-PBD beads were purchased from Merck Millipore (Billerica, MA, USA). Mevalonate, GGPP, FPP, SP600125,

Tiron, Tempol, DPI, MTT, Lucigenin, crystal violet, bromophenol blue, Tween 20, Triton X-114, EDTA, DTT, glycine, BSA, DMSO, Squalene, ATP releasing buffer, cycloheximide and actinomycin D were purchased from Sigma Aldrich Co (St Louis, MO). EHT1864 was purchased from Tocris biosciences (Bristol, UK). Rhotekin-RBD beads were brought from Cytoskeleton, Inc (Denver, CO, USA). Pan-caspase inhibitor zVAD-fmk was purchased from Alexis Biochemicals (Lausane, Switzerland). Fluorogenic substrates of caspase-3, -8 and -9 were purchased from Biomol (Plymouth Meeting, PA, USA). Protein A agarose beads and glutathione beads were purchased from Santa Cruz Biotechnology (Santa Cruz, CA, USA). Coomassie Blue was purchased from Pierce Biotechnology (Rockford, IL, USA). 10x PBS, 10x SDS, Tris-HCl buffer (pH7.4) were purchased from NUMI Media Preparation Facility (NUS, Singapore).

3 Plasmids and siRNAs

Plasmids: pIRES1hyg vector and pIRESRacN17 plasmids were generously provided by Dr. Marie-Véronique Clément (NUS, Singapore).

siRNAs: ON-TARGET*plus* SMARTpool siRNAs (a mixture of 4 siRNAs in a single reagent) targeting RhoA, Rac1, Cdc42 as well as siRNA negative control (non-homologous to any known gene sequence) were purchased from Dharmacon Technologies (ThermoFisher Scientific, Lafeyette, CO). One single siRNA sequence targeting Bim was purchased from Qiagen (Duesseldorf, Germany). Three unique 26mer siRNA duplexes targeting Bim and siRNA negative control were purchased from Origene (Rockville, MD, USA).

4 Transfection of plasmids and siRNAs

The Calcium Phosphate Mammalian Transfection Kit (Clonetech Laboratories Inc., Palo Alto, CA) was used for transfection of plasmids or siRNAs into HCT116 cells. Cells to be transfected were grown to 40% confluency in 24-well tissue culture plates (for crystal violet assay, seeded at 0.12 x 10^6 cells/well) or 12-well plates (for Western blot analysis and Lucigenin assay, seeded at 0.2 x 10^6 cells/well). Before performing transfection, the cell culture medium was changed to fresh DMEM supplemented with 10% FBS, 1% L-glutamine and 1% penicillin/streptomycin. On 12-well plates, 1 μg of plasmids were used per well for all expression plasmids. For siRNAs, 10 nM was used per sample for siRNAs targeting Bim (three independent sequences: Bim#1, #2 and #3); 35 nM was used for siRNA targeting RhoA and Cdc42, while 100 nM was used for siRNA targeting Bim (another sequence: Bim#0) and Rac1. Transfection mixture contained calculated amounts of DNA or siRNAs, sterile dH_2O and 6.2 μl of 2.5 mM $CaCl_2$, which summed up to a total amount of 50 μl per 12 well. For a 24-well, the calculation was halved. The DNA-$CaCl_2$ or siRNA-$CaCl_2$-containing solution was then mixed with an equal volume of the DNA precipitation buffer (2x HEPES-buffered saline) in a drop-wise manner with gentle vortexing. The mixture was then incubated for 20 mins at room temperature followed by adding drop-wise into the cells (50 μl per 24-well, 100 μl per 12-well). After 14-18 h of incubation, cell were washed with 1x phosphate buffered saline (PBS) and recovered in cell culture medium used for maintenance. Downstream procedures were carried out at least 30 h from the time of adding transfection reagents.

5 Determination of cell viability by crystal violet assay

HCT116 cells are seeded in 24-well tissue culture plates (0.12 x 10^6 cells/well) or 12-

well plates (0.2 x 10^6 cells/well) for two days prior to any treatments and cytotoxicity caused was determined by crystal violet assay. After drug treatment, cells were washed once with 1x PBS followed by addition of 0.2 ml of crystal violet solution to each well and incubated for 10 mins. Crystal violet stain was retained inside cells that were attached to the plates, while the excess crystal violet solution was washed away using distilled water. The remaining crystals were then dissolved in a 1% SDS in 1x PBS solution and absorbance was determined by reading at wavelength 595nm using a TECAN spectrophotometer (Tecan Trading AG, Switzerland). The optical density (OD) obtained is proportional to the number of viable cells. Cell viability is calculated as percentage relative to the untreated control cells. Same protocol was used for other types of cancer cells such as RKO, A549, MDA-MB-231 and SHEP-1 cells.

Crystal violet solution: 0.75% crystal violet in 50% (v/v) ethanol with 1.75% formaldehyde and 0.25% NaCl. Stored at room temperature.

6 Determination of cell viability by MTT assay

Cell viability was also determined by the 3-(4,5-dimethyl-2- thiazolyl)-2,5-diphenyltetrazolium bromide (MTT) assay. HCT116 were seeded in 24-well plates (0.12 x 10^6 cells/well) and cultured for two days before drug treatment. At the end of drug treatment, all cells in the same well were collected and re-plated in a 96-well plate (100 µl of medium per well) and incubated with 100 µl MTT (3 mg/ml) per 96-well at 37°C for 2 h. Following that, the formazan crystals formed were spun down at 3,000 rpm by centrifugation for 15 mins. The resultant supernatant was aspirated off and the crystals formed were dissolved with 250 µl dimethyl sulfoxide (DMSO). Absorbance was measured with a TECAN sprectrophotometer (Tecan Trading AG,

Switzerland) at 570nm. Cell viability is calculated as percentage relative to the untreated control cells.

7 Colony forming assay

After 30 h of drug treatment, cells were washed with 1x PBS and trypsinized. 10,000 cells per treatment were replated in a 6-well plate or a 100mm dish in complete tissue culture medium. Cells were then left to form colonies over a period of 7 days (for 6-well plates) or 14 days (for 100mm dishes). Colonies formed were stained with crystal violet. The number of colonies formed was counted manually.

8 DNA fragmentation assay by propidium iodide staining

HCT116 were plated in 12-well tissue culture plates (0.2 x 10^6 cells/well) for two days before drug treatment. Following treatment, the DNA content of the cells was analyzed using propidium iodide (PI) staining. Cells were harvested on ice and pelleted down by centrifugation at 1,500 rpm for 5 mins. After washing once with ice-cold 1x PBS, cells were immediately fixed with 70% (v/v) ethanol while vortexing, to prevent clumping of cells. The fixed cells were incubated for at least 30 mins at 4°C. Then the cells were washed twice with ice-cold 1x PBS and resuspended in 500 µl of PI/RNase solution (contains 10 µg/ml PI and 250 µg/ml RNase A) for 1 h at 37°C. At least 10,000 events were analyzed for DNA content with flow cytometry (CyAn ADP, Beckman Coulter, USA) with the excitation set at 488nm and emission at 610nm. Data collected were analyzed with the WinMDI software (Windows multiple document interface for flow cytometry, Beckman Coulter Inc., Sunnyvale, CA). In a DNA analysis, the sub-G1 population represents the hypodiploid DNA content which is in the extreme left of histograms.

9 Caspase activity assay

HCT116 were plated in 12-well tissue culture plates (0.2 x 10^6 cells/well) for two days before drug treatment. Fluorogenic substrates were used to determine caspase-3, -8 and -9 activities; they are synthetic oligopeptides containing the caspase cleavage site where the C-terminal aspartic acid is replaced with 7-amino-4-trifluoromethyl coumarin (AFC). Cells were harvested on ice after treatment and lysed with 1x Cell Lysis Buffer (BD Pharmingen, San Diego, CA). Equal volume of cell lysates and 2x Reaction Buffer, together with 1 μl of the respective caspase substrate were added in a 96-well plate. The respective substrates for caspase-3, -8 and -9 are Ac-DEVD-AFC, Ac-IETD-AFC and Ac-LEHD-AFC. The 96-well plate was then incubated at 37°C for 1 h, and the fluorescence was measured with TECAN spectrophotometer (Tecan Trading AG, Switzerland) at excitation 400nm and emission 505nm. The amount of proteins in every sample was quantified by Coomassie Blue reagent and caspase activity was normalized with protein concentration and expressed as relative fluorescence unit (RFU)/μg protein.

2x Reaction Buffer: 10mM HEPES (pH 7.4), 2mM EDTA, 6mM DTT, 10mM and 1.5mM $MgCl_2$, dissolved in distilled water. Stored at 4^oC.

10 Western blot analysis

After drug treatment, whole cell lysates were harvested and lysed on ice using 1x RIPA lysis buffer. Cell lysates prepared from coimmunoprecipitation, isolation of GTP-bound GTPases, sucrose gradient centrifugation, mitochondrial and cytosolic fractionations were described in their respective sections (See section 12-15 respectively). The collected cell lysate were spun down at 1,500 rpm for 5 mins to clear debris and protein concentration of the resultant supernatant was measured

using Coomassie Blue reagent. Briefly, 1.5 µl of the supernatant or protein standards and 200 µl of Coomassie Blue reagent were added in a 96-well plate. Absorbance was measured using TECAN spectrophotometer (Tecan Trading AG, Switzerland) at 595nm. Protein amount ranging from 30 to 70 µg for different purposes were then mixed with 1x Laemmli loading dye and boiled at 100°C for 5 mins. Following that, the samples were subjected to sodium dodecyl sulphate-polyacrylamide gel electrophoresis (SDS-PAGE). Different percentages of gels containing 8, 10, 12 or 15% (v/v) acrylamide were used depending on the molecular weight of target proteins. Subsequently, wet transfer method was used to transfer the resolved proteins onto PVDF membranes (BioRad, CA, USA). The membranes were blocked with 5% (w/v) fat-free milk in Tris-buffered saline containing 0.1% (v/v) Tween 20 (TBST) for 30 mins and washed with TBST for three times to remove excess milk. The membranes were then probed for the target proteins with the respective primary antibodies (refer to list of antibodies below) overnight at 4°C. On the next day, the membranes were washed with TBST for three times to remove unbound primary antibody and probed again using appropriate HRP-conjugated secondary antibody in 5% (w/v) fat-free milk in TBST for 1 h at room temperature. After that, the membranes were washed with TBST for three times to remove any excess unbound secondary antibody, the proteins of interest were detected with Kodak Biomax MR X-ray film (Eastman Kodak Co., Rochestor NY) by enhanced chemiluminescence using the SuperSignal West Pico Chemiluminescent Substrate (Pierce, Rockford, IL, USA). For probing different proteins on the same membrane, the membranes were stripped with Restore Western Blot Stripping Buffer (Pierce, Rockford, IL, USA) and the same procedures were repeated.

(1) Buffers used in western blot analysis

RIPA lysis buffer: 50 mM Tris-HCl (pH 7.5), 150 mM NaCl, 1% (v/v) Nonidet P40, 0.25% deoxycholic acid, 1 mM EDTA supplemented with fresh protease inhibitors (5 μg/ml leupeptin, 1 mM PMSF, 10 μg/ml aprotinine, 20 μg/ml pepstatin A) and a phosphatase inhibitor (1 mM Na_3VO_4). Stored at 4^oC.

5x Laemmli Loading Buffer: 3.1 ml Tris-HCL (pH 6.8), 1 g SDS, 2 ml glycerol, 2.5 ml β-Mercaptoethanol, 0.01 g Bromophenol Blue, topped up to 10 ml with 2.4 ml of dH_2O. Stored at room temperature.

10x Running Buffer for SDS-Page gel: 60 g Tris-base, 288 g glycine, 20 g SDS, topped up to 2 L with dH_2O. Stored at room temperature.

Transfer Buffer for western blot: 2.42 g Tris-base, 11.57 g glycine, 200 ml methanol, topped up to 1L with dH_2O. Keep cold before use.

TBS: 500 ml of 1 M Tris-HCl (pH 7.4) with 87.6 g of NaCl in 10 L of dH_2O and stored at room temperature.

TBST: 2 L TBS with 2 ml of Tween-20 and stored at room temperature.

(2) Primary antibodies for western blot analysis

Primary antibodies specific for RhoA, Cdc42, RhoGDIα, Bax, cytochrome c, VDAC, p53, Bcl-xL, β-actin and GAPDH were purchased from Santa Cruz Biotechnology (Santa Cruz, CA, USA). Primary antibodies probing for Bim, Bid, phosphorylated-AKT, AKT, phosphorylated-Erk, Erk, JNK, SOD1, PARP, myc-tag, caspase-3, caspase-8 and caspase-9 were purchased from Cell Signaling Technology (Danvers, MA). Primary antibody for Rac1 and phosphorylated-JNK were purchased from Merck Millipore (Billerica, MA). Primary antibody for Flotilin was purchased from Abcam (Cambridge, UK).

11 Coimmunoprecipitation (Co-IP)

HCT116 were plated in 100mm tissue culture dishes (1.2 x 10^6 cells/dish) for two days prior to drug treatment. Cells from two dishes receiving same treatments were pooled together for one sample. Cells were harvested on ice and washed once with ice-cold 1x PBS followed by lysing in Co-IP buffer on ice for 15 mins. The lysates were spun at 1,500 rpm for 5 mins to clear debris. The resultant supernatant was collected and pre-cleared with 25 µl protein A agarose beads on a rotator for 4 h at 4^oC. The beads were cleared away by centrifugation at 12,000 rpm for 5 mins at 4°C. Protein concentration of the supernatant (cell lysate) was determined using Coomassie Blue reagent. 1 mg of the cell lysate was incubated with 4 ug of rabbit polyclonal anti-RhoGDIα antibody for overnight on a rotator at 4°C. On the next day, 30 µl protein A agarose beads were added to every sample and rotated for another 2 h at 4°C. The complexes were then washed with 0.5 ml ice-cold Co-IP buffer for three times. The resultant bead-protein complexes were mixed with 1x Laemmli loading dye and boiled at 100°C for 20 mins. The samples were then subjected to Western blot analysis as described above.

Co-IP buffer: 50 mM Tris-HCl (pH 7.5), 150 mM NaCl, 0.5% v/v Nonidet P40, 1 mM EDTA with supplements of fresh protease inhibitors (5 µg/ml leupeptin, 1 mM PMSF, 10 µg/ml aprotinine, 20 µg/ml pepstatin A) and a phosphatase inhibitor (1 mM Na_3VO_4). Stored at 4°C.

12 Isolation of GTP-loaded RhoA, Rac1 and Cdc42 GTPases

HCT116 were plated in 100mm tissue culture dishes (1.2 x 10^6 cells/dish) for two days before drug treatment. Cells from two dishes were pooled together as one sample. Then cells were washed with 1x PBS and lysed in MLB buffer for 20 mins

on ice. Cell lysates were cleared by centrifugation at 1,500 rpm for 5 mins at 4°C. The resultant supernatant was collected and pre-cleared with 20 µl glutathione beads on a rotator for 20 mins at 4°C. The beads were cleared away by centrifugation at 12,000 rpm for 5 mins at 4°C. Protein concentrations of the supernatants were determined by Coomassie Blue reagent and 800 µg of protein from each sample was used. The GTP-bound form of GTPases was isolated by their ability to interact with their specific effector protein binding domains. Hence, GTP-bound RhoA, Rac1 and Cdc42 were isolated by incubating the protein sample with 20 µg of GST-Rhotekin beads (for RhoA) or 10 µg GST-PAK beads (for Rac1 and Cdc42) on a rotator for 1 h at 4°C. The bead-protein complexes were washed with 0.5 ml ice-cold MLB buffer for three times. The resultant bead-protein complexes were mixed with 1x Laemmli loading dye and boiled at 100°C for 20 mins. The samples were then subjected to Western blot analysis as described above. Same protocol was used to assess GTP-bound form of Rac1 in SHEP-1 cells.

MLB buffer: 25 mM HEPES (pH 7.5), 10 mM $MgCl_2$, 150 mM NaCl, 10% v/v glycerol, 1mM EDTA, 25 mM NaF, 1 mM Na_3VO_4, 10 µg/ml leupeptin and 10 µg/ml aprotinine. Stored at 4°C.

13 Mitochondrial-cytoplasmic fractionation

HCT116 were plated in 100mm tissue culture dishes (1.2 x 10^6 cells/dish) for two days before drug treatment. Cells from at least three dishes were pooled together for one sample. Cells were harvested and washed once with ice-cold 1x PBS before incubation on ice for 7 mins with extraction buffer A. After incubation, cells were homogenized using a dounce homogenizer and passaged for 7 strokes before being centrifuged at 300 g for 5 mins at 4°C. The resultant supernatant was subjected to

another two rounds of centrifugation at 1,000 g for 10 mins. The remaining supernatant was transferred into a new microcentrifuge tube and centrifuged again at 12,000 g for 15 mins at 4°C. The resultant pellet enriched with mitochondria was washed with Buffer A for another 15 mins at 12,000 g, followed by lysing with standard 1xRIPA lysis buffer supplemented with protease inhibitors. The supernatant was collected as the cytosolic fraction. Both fractions obtained were then subjected to protein concentration quantification and Western blot analysis.

In this particular project, in order to assess the amount of Rho protein in the cytosol, we performed further purification from the above mitochondria-cytosol preparations to isolate cytosolic fractions without any contamination from light membranes. After isolating the mitochondrial fractions as stated above, the supernatant was subjected to ultracentrifugation at 100,000 g for 1 h at 4°C. The pellet obtained was enriched with light membrane fractions while the supernatant of our interest contained mainly cytosolic proteins. The cytosolic fraction obtained was then subjected to protein concentration quantification and Western blot analysis.

Extraction buffer A (pH 7.4): 50 mM PIPES-KOH, 200 mM mannitol, 68 mM sucrose, 50 mM KCl, 5 mM EGTA, 2 mM $MgCl_2$, 1 mM DTT supplemented with fresh protease inhibitors (5 μg/ml leupeptin, 1mM PMSF, 10 μg/ml aprotinine, 20 μg/ml pepstatin A) and a phosphatase inhibitor (1 mM Na_3VO_4). Stored at 4°C.

14 Isolation of membrane lipid rafts by sucrose gradient ultracentrifugation

HCT116 cells were seeded in 100mm tissue culture dishes (1.2 x 10^6 cells/dish) for two days before drug treatment. Cells from at least five dishes were pooled together for one sample. Cells were then harvested and washed with ice-cold 1x PBS before

incubating in 500 µl HEPES buffer containing 1% Triton X-100 for 10 mins. Lysates were then frozen in -80°C and freeze-thawed on ice, followed by homogenizing for 20 strokes with a dounce homogeniser. The homogenised lysates were centrifuged at 400 g for 10 mins at 4°C to remove debris. The supernatant were then subjected to 20 passes through a 27G syringe, which was followed by three times sonication (10sec pulses at 40V). Protein concentration was quantified and equal amount of proteins was used for subsequent ultracentrifugation. The lysates were transferred to a special 5ml centrifuge tube and mixed with an equal volume of 80% sucrose (w/v) in HEPES buffer, followed by overlaying with 1.5 ml of 30% sucrose and 1.5 ml of 5% sucrose solutions. The sucrose gradient was centrifuged for 21 h at 4°C in a Beckman rotor at 32,000 rpm and eight 0.5 ml fractions were harvested separately. 30 µl from fraction number 2-6 were used for subsequent Western blot analysis.

HEPES Buffer: 25 mM HEPES (pH 7.4), 150 mM NaCl, 1% Triton X-100 and 1 mM PMSF, 10 µg/ml aprotinin, 20 µg/ml pepstatin A and 10 µg/ml leupeptin. Stored at 4°C.

15 Triton X-114 phase separation

HCT116 cells were seeded in 100mm tissue culture dishes (1.2 x 10^6 cells/dish) for two days before drug treatment. Cells from at least two dishes were pooled together for one sample. Cells were then harvested and washed with ice-cold 1x PBS before incubating in 500 µl lysis buffer containing 1% Triton X-114 followed by centrifugation at 13,000 g for 15 mins. The resultant supernatant was put inside 37°C incubator for 10 min, and micelles formed were pelleted by centrifugation at 13,000 g for 2 mins at room temperature. The aqueous supernatant was cooled to 4°C and the detergent pellet was topped up to the same volume as the aqueous fraction using lysis

buffer without Triton X-114. Equal volumes of lysates from both fractions were assessed by Western blot analysis.

Lysis Buffer: 20 mM Tris, 150 mM NaCl.

16 Measurement of superoxide by Lucigenin chemiluminescence assay

HCT116 were seeded at 0.2 x 10^6 cells/well in 12-well tissue culture plates for two days before drug treatments for specified durations. Cells were washed once with ice cold 1x PBS and trypsinized. Cell pellets were collected after spinning at 1,500 rpm for 5 mins. The pellet was quickly lysed with 450µl somatic ATP releasing buffer, 400 µl of which was placed into the Sirius LB 9505 luminometer (Berthold) for quantification of chemiluminescence with 100 µl of 10 mM lucigenin solution. The remaining 50 µl was kept for protein quantification. The luminescence reading is normalized with the protein concentration and presented as relative light units (RLU) per µg protein. Same protocol was used to assess superoxide level in SHEP-1 cells.

17 Measurement of superoxide by DHE dye

HCT116 cells were seeded at 0.2 x 10^6cells/well in 12-well tissue culture plates for two days before drug treatments for specified durations. Cells were then harvested on ice and washed once with ice cold 1x PBS. Subsequently, cell pellets were resuspended in 100 µl ice cold 1x PBS containing 10 µM Dihydroethidine (DHE) dye (Molecular Probes, Invitrogen corporation, CA) and incubated at 37°C for 20 mins in the dark. After that, cells were pelleted at 1,500 rpm for 5 mins and resuspended in 1x PBS. At least 10,000 events were analyzed by flow cytometry with the excitation set at 590nm and emission at 619nm. Data collected were analyzed with the DAKO software (Beckman Coulter Inc., Sunnyvale, CA). Final fluorescence values obtained

were normalized against the untreated control and plotted as x fold increase in fluorescence over the untreated control.

18 Statistical analysis

All statistical analysis was based on at least three independent experiments, and the results were expressed as mean ± s.e.m unless otherwise stated. The paired Student's t-test was performed and the statistical significance was set at $p < 0.05$.

RESULTS

1. Simvastatin activates the mitochondrial apoptotic pathway in HCT116 cells

1.1 Simvastatin effectively reduces cell viability in a dose-dependent manner

Significant clinical evidence has emerged to implicate statins as anti-tumor agents, showing activity in carcinomas of the prostate, colon and rectum, breast, lung, AML, multiple myeloma and skin (Chan, Oza et al. 2003; Demierre, Higgins et al. 2005; Hwang, Na et al. 2011). In this project, we aimed to explore the underlying mechanisms for simvastatin's anti-tumor effects in human cancer cells. Firstly, we investigated if simvastatin possessed anti-cancer properties as described. HCT116 colorectal cancer cells were treated with increasing doses of simvastatin (0-30 μM) for 24 and 48 h, and the resultant loss of cell viability was assessed by both crystal violet assay (Figure 1A) and MTT assay (Figure 1B). Crystal violet is able to stain the DNA, and upon solubilization it quantifies the relative density of cells still adhering to the culture dishes; while the reduction of MTT dye by active mitochondrial enzymes to formazan crystals is proportional to the amount of viable cells. Cell viability was determined by comparing to untreated control cells. Both assays demonstrated that 24 h simvastatin treatment has no profound effects on cell viability; however, incubation up to 48 h elicited effective loss in HCT116 cell viability (10 μM simvastatin: 65.72 ± 1.26% cell loss obtained by crystal violet assay and 58.69 ± 2.47% obtained by MTT assay). This inhibitory effect was also shown to be dose-dependent; at low dose of 3 μM simvastatin, there was about 25% cell viability loss while at 5 μM and 10 μM simvastatin, about 40% and 65% cells were not viable measured by crystal violet assay respectively. For subsequent experiments,

we selected simvastatin 3 or 10 μM as the main effective working concentrations to explore the mechanisms underlying the cytotoxic effects.

A

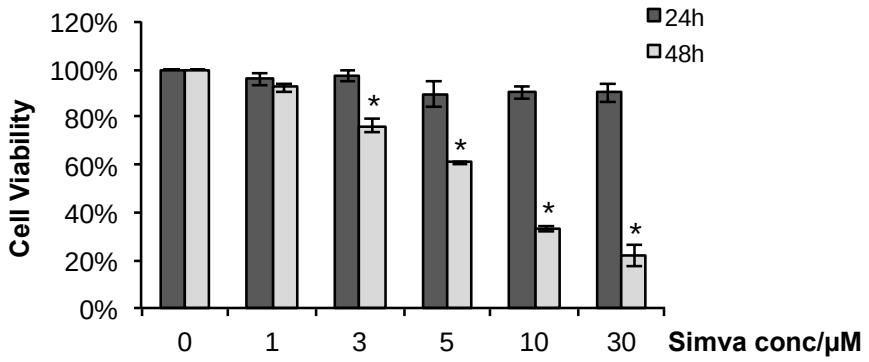

B

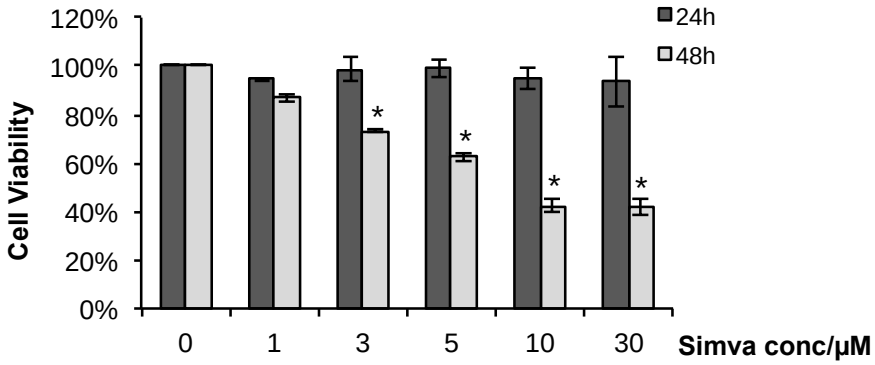

Figure 1: Simvastatin effectively reduces cell viability of HCT116 cells.
HCT116 cells were treated with various concentrations of simvastatin (0-30 μM) for 24 and 48 h. Cell viability was measured by (A) crystal violet assay and (B) MTT assay as described in Materials and Methods. In both panels, cell viability was expressed as % of untreated control. Data are shown as means ± s.e.m of three independent experiments. *, $p < 0.05$ compared with untreated control cells.

1.2 Simvastatin inhibits long-term colony formation of HCT116 cells

Following the short-term cell viability assessment, we went on to evaluate if the short-term cytotoxic effects of simvastatin translated into long-term suppression of their clonogenic abilities. HCT116 cells were treated with increasing doses of simvastatin (0-30 μM) for 30 h, and 10000 cells from each condition was replated onto a 6-well plate and allowed to form colonies for seven days. A dose-dependent reduction in colonies was observed after simvastatin treatment (Figure 2) (45.58 ± 1.44% reduction after 3 μM simvastatin, 73.11 ± 4.43% reduction after 10 μM simvastatin compared to untreated control, $p < 0.05$). Moreover, a greater extent of reduction in long-term colony-formation was observed compared to the short-term viability loss at corresponding doses. As the colony forming assay detects cells that retained progeny-producing ability after chemotherapy treatment (Franken, Rodermond et al. 2006), out results indicate that simvastatin triggers reproducible and extensive cell death in HCT116 cells.

A

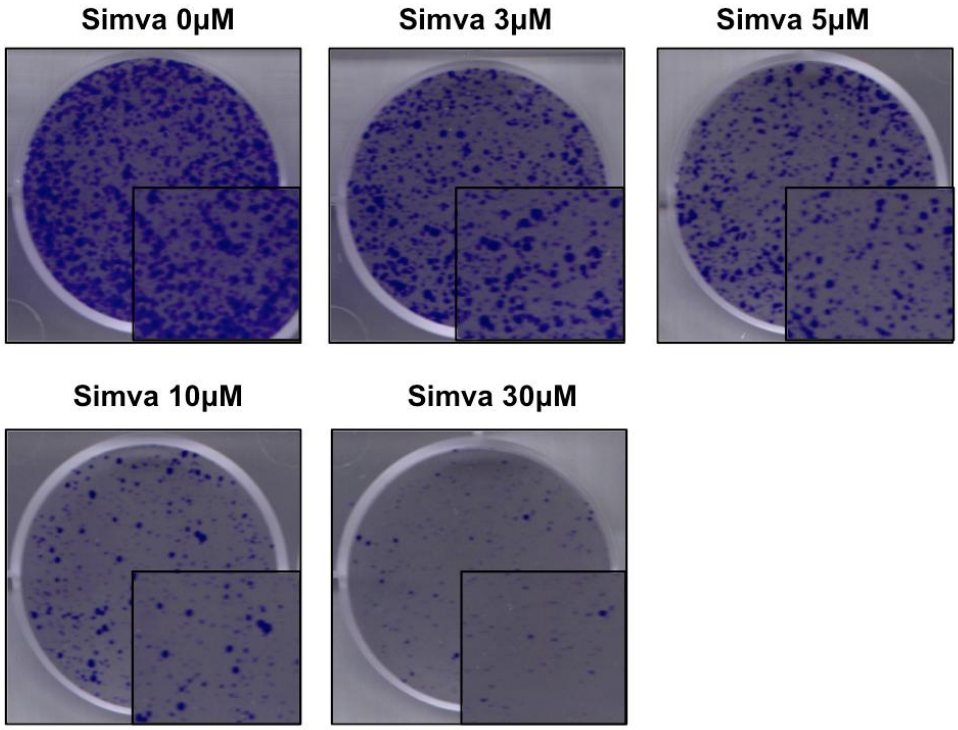

B

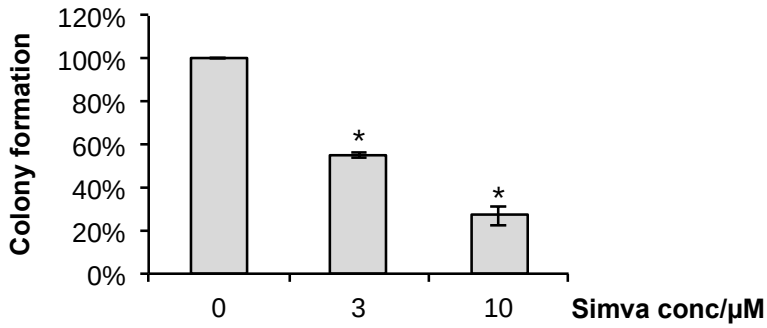

Figure 2: Simvastatin reduces clonogenic ability of HCT116 cells.
HCT116 cells were treated with various concentrations of simvastatin (0-30 μM) for 30 h before being replated onto a 6-well plate (10000 cells/well) and allowed to form colonies over 7 days. Colonies formed were then stained with crystal violet. (A) Representative photos of colonies formed from one set of experiment are shown here. (B) Colonies formed were scored and expressed as % number of colonies formed by untreated control. The bars represent means ± s.e.m from three independent experiments. *, $p < 0.05$ compared with untreated control cells.

1.3 Simvastatin-triggered cell death bears apoptotic hallmarks

1.3.1 Cell death is accompanied by cell shrinkage and DNA fragmentation

Having ascertained that simvastatin reduces cell viability effectively in HCT116 cells, we proceded to assess if the observed anti-viability effect was a consequence of cell death or a mere cytostatic effect. Firstly, cells were observed under phase contrast microscope. Unlike control cells, simvastatin-treated cells were seen shrinking in size and rounding up (Figure 3A). Subsequently, we analyzed the DNA content of simvastatin-treated HCT116 cells using propidium iodide (PI) staining (Figure 3B). The intensity of fluorescence emitted is proportional to the amount of PI dye being incorporated into the DNA and can be detected by flow cytometry analysis (Suzuki, Fujikura et al. 1997). We observed that the sub-G1 population, which represented cells with fragmented DNA, was dose-dependently increased after simvastatin treatment (Figure 3C) (7.87 ± 0.84% sub-G1 population in control cells *vs.* 25.14 ± 1.17% with 3 μM simvastatin and 60.58 ± 2.64% with 10 μM simvastatin treatment, $p < 0.05$). This observation is consistent with the extent of loss of cell viability seen in Figure 1. Given that cell shrinkage and DNA fragmentation are known hallmarks of apoptosis, our data suggests the occurrence of apoptotic cell death.

A

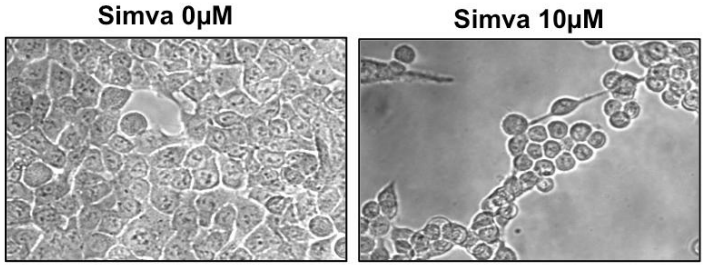

B

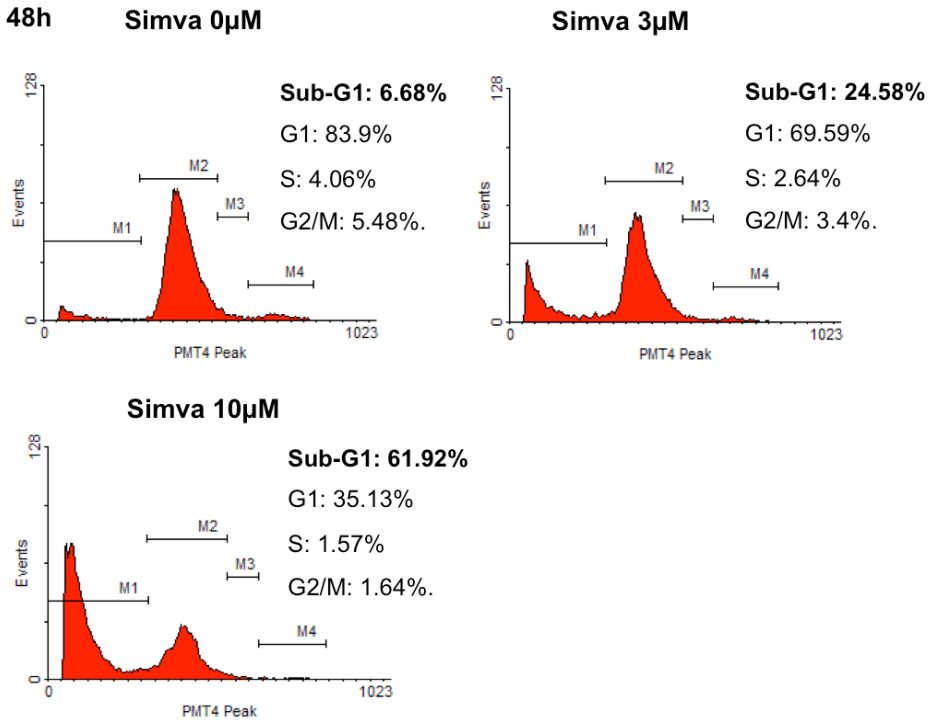

C

Cell Cycle	Control	Simva 3μM	Simva 10μM
Sub G1	**7.87 ± 0.84**	**25.14 ± 1.17 ***	**60.58 ± 2.64 ***
G1	81.28 ± 1.28	67.84 ± 1.76	35.15 ± 1.79
S	2.56 ± 0.3	3.56 ± 0.45	2.01 ± 0.44
G2/M	7.87 ± 0.92	3.93 ± 0.04	2.20 ± 1.10

Figure 3: Simvastatin leads to cell shrinkage and DNA fragmentation in HCT116 cells.
(A) HCT116 cells were treated with 10 μM simvastatin for 28 h and morphology of the cells was photographed under phase contrast microscope (Magnification: 200X). (B) Cells were treated with 3 or 10 μM simvastatin for 48 h, DNA content was analyzed by flow cytometry after staining with propidium iodide (PI) as described in Materials and Methods. Cell cycle profiles obtained from one set of experiment are shown here. (C) The average percentages of cells in different cell-cycle phases are summarized in this table. Data are presented as means ± s.e.m from three independent experiments. *, $p < 0.05$ compared with untreated control cells.

1.3.2 Simvastatin induces effective proteolytic processing and activation of caspases

The aforementioned observations of apoptotic hallmarks such as cell shrinkage and DNA fragmentation upon simvastatin treatment prompted us to investigate the involvement of caspases in simvastatin-triggered cell death. Caspases act as the main 'executioners' of apoptosis by cleaving specific cellular substrates involved in cellular demise (Cohen 1997). We investigated the activities of three key caspases, namely caspase-9 and -8, which are initiator caspases involved in intrinsic or extrinsic apoptotic pathway respectively; and their downstream effector caspase-3. Western blot analysis revealed time-dependent proteolytic conversion of pro-caspase-8 and -9 into catalytically active subunits as early as 28 h, and followed by processing of caspase-3 into 17- or 19 kDa fragments that peaked at 36 h post-treatment (Figure 4A). Proteolytic processing of caspase-3 then resulted in cleavage of its downstream targets, evidenced by cleavage of poly-ADP-ribose polymerase (PARP) from 116 kDa to the 86 kDa fragment observed at 36 h (Figure 4B).

To verify the western blot results, we also studied the activities of caspase-3, -8 and -9 using their respective fluorescence-conjugated caspase substrates (DEVD-AFC, IETD-AFC and LEHD-AFC). This sensitive measurement method showed detectable activation of all three caspases after 36 h simvastatin treatment (Figure 4C) (5.67 ± 0.73 fold increase for caspase-3, 3.75 ± 0.41 fold increase for caspase-8, 3.82 ± 0.38 fold increase for caspase-9 after 10 μM simvastatin compared to untreated control, $p < 0.05$), which is consistent with the robust proteolytic processing of caspases observed in Figure 4A.

A

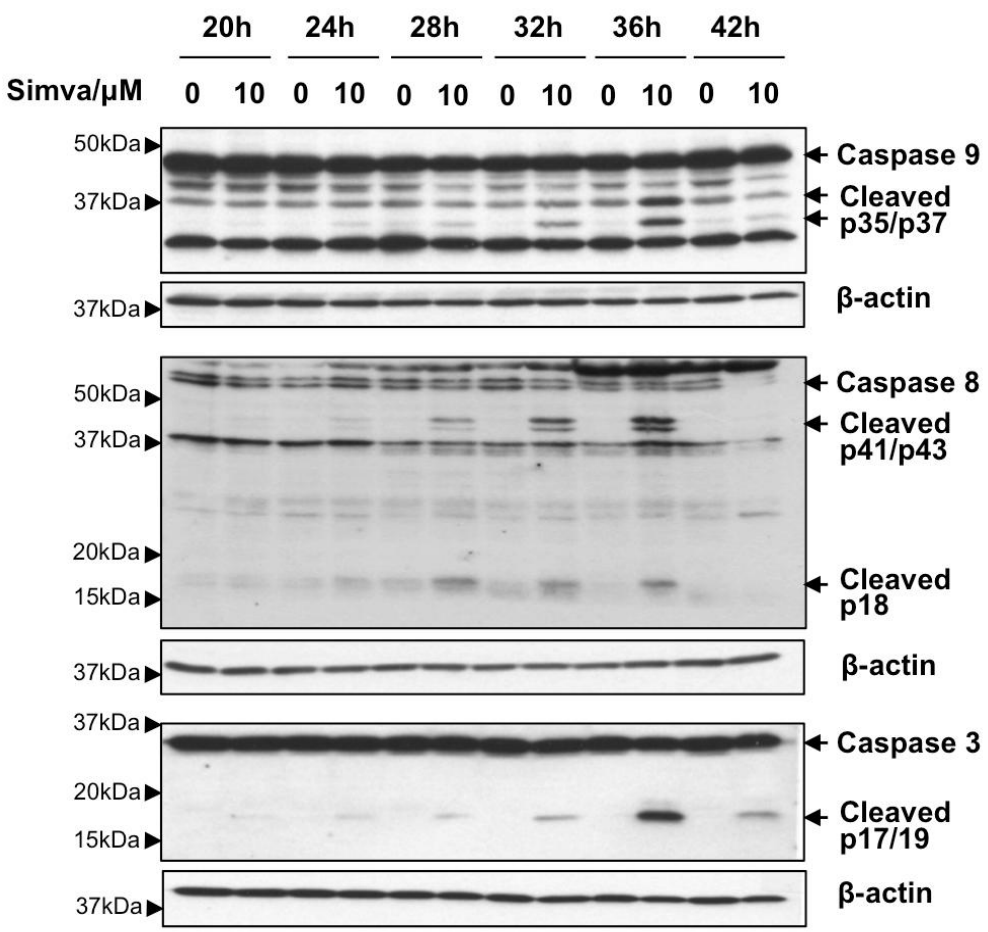
20h
24h
28h
32h
36h
42h
Simva/μM
0 10 0 10 0 10 0 10 0 10 0 10
50kDa
37kDa
Caspase 9
Cleaved p35/p37
37kDa
β-actin
50kDa
37kDa
Caspase 8
Cleaved p41/p43
20kDa
15kDa
Cleaved p18
37kDa
β-actin
37kDa
Caspase 3
20kDa
15kDa
Cleaved p17/19
37kDa
β-actin

B

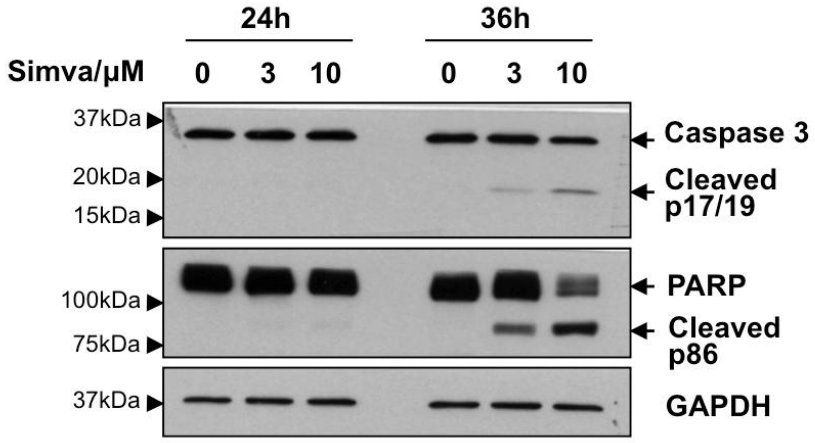
24h
36h
Simva/μM
0 3 10 0 3 10
37kDa
Caspase 3
20kDa
Cleaved p17/19
15kDa
100kDa
PARP
75kDa
Cleaved p86
37kDa
GAPDH

C

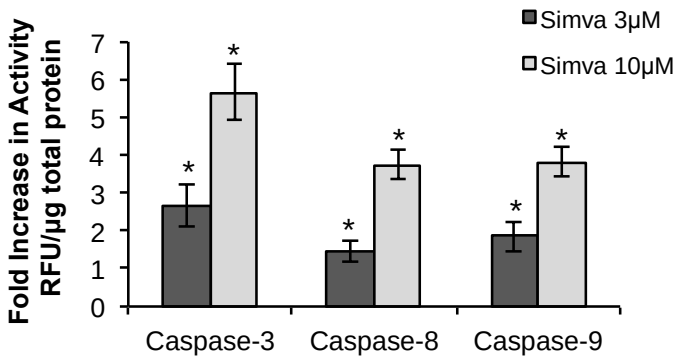

Figure 4: Simvastatin induces proteolytic processing and activation of caspases.
HCT116 cells were treated with 3 or 10 μM simvastatin for the indicated duration before whole cell lysates were harvested for Western blot analysis. (A) Caspase-3, -8 and -9 and (B) PARP were immunoblotted using antibodies that recognize both the pro- and cleaved forms of the respective proteins. In both panels, β-actin or GAPDH was included as a loading control. (C) At 36 h post-treatment, total cell lysates were used to assess caspase-3, -8, and -9 activation levels using fluorescence-conjugated substrates. Caspase activity was normalized to total protein and expressed as fold increase over untreated cells. The bars represent means ± s.e.m of three independent experiments. *, $p < 0.05$ compared with untreated control cells.

In agreement with the observed activation of caspases, preincubation of cells with the pan-caspase inhibitor zVAD-fmk for 2 h almost fully recovered viability of simvastatin treated-cells assessed by crystal violet assay (Figure 5A) (87.84 ± 5.43% cell viability with zVAD-fmk preincubation *vs.* 30.08 ± 6.51% cell viability with 10 μM simvastatin alone, $p < 0.05$). This was supported by the ability of zVAD-fmk to completely inhibit caspase activity as evidenced by successful abrogation of simvastatin-induced PARP cleavage (Figure 5B). Taken together, these results (Figure 3-5) demonstrate that simvastatin induces apoptosis in HCT116 cells in a caspase-dependent manner, exemplified by caspase activation, PARP cleavage and DNA fragmentation.

A

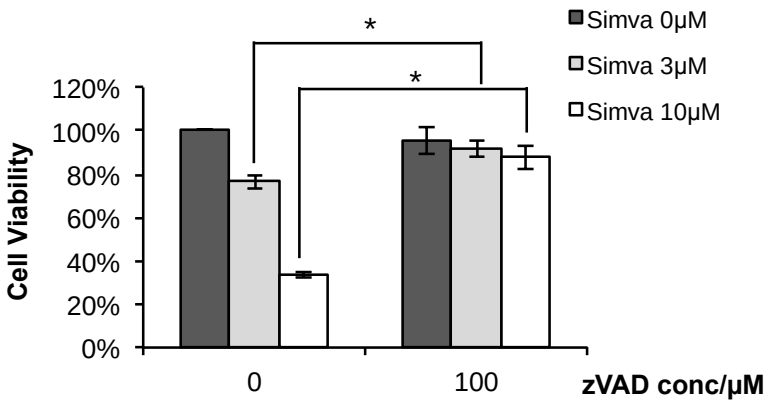

B

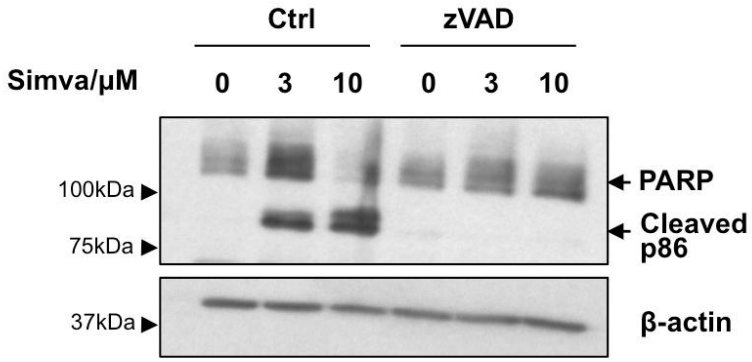

Figure 5: Pan-caspase inhibitor zVAD-fmk confers full protection to simvastatin-mediated cell death.
HCT116 cells were preincubated with or without 100 μM zVAD-fmk for 2 h before treatment with 3 or 10 μM simvastatin. (A) Cell viability after 48 h simvastatin treatment was measured by crystal violet assay. The bars represent means ± s.e.m of three independent experiments. *, $p < 0.05$ compared with simvastatin treatment alone. (B) PARP cleavage was assessed by Western blot analysis.

1.4 Simvastatin activates the mitochondrial apoptotic pathway

1.4.1 Simvastatin induces mitochondrial Bax translocation and release of pro-apoptogenic factor cytochrome c into the cytosol

Several reports have suggested the role of mitochondria in statin-mediated apoptosis in breast tumor cells (Herrero-Martin and Lopez-Rivas 2008), lymphoblasts and myeloma cells (Cafforio, Dammacco et al. 2005). Hence, to understand the apoptotic signaling in simvastatin-treated HCT116 cells, we tested the involvement of the mitochondrial/intrinsic apoptotic pathway. The rate-limiting step in the intrinsic pathway is considered to be the mitochondrial membrane permeabilization (MMP) upon trigger. The phenomenon involves the mitochondrial outer membrane permeabilization (MOMP), which is indicated by release of proteins that are normally confined to the intermembrane space (IMS), such as cytochrome c. The MOMP can be manifested by pro-apoptotic second messengers. For example, upon apoptotic trigger, mitochondrial translocation of Bcl-2 family member Bax has been reported as a common mechanism for the induction of MMP, where the full insertion of Bax oligomers forms mitochondrial permeability pores into the outer membrane that allows for subsequent release of the aforementioned IMS proteins (Kroemer and Reed 2000).

Hence, we studied the subcellular translocation of cytochrome c and Bax after exposure to simvastatin. After 24 h simvastatin treatment, HCT116 cells were lysed and the cytosolic- and mitochondrial-enriched heavy membrane fractions were prepared. Simvastatin triggered MOMP in these cells, as evidenced by the release of IMS protein cytochrome c to the cytosol and, reciprocally, the translocation of cytosolic Bax to the mitochondria. VDAC and SOD1 were used as mitochondrial and

cytosolic markers respectively to ensure the clean isolation of both fractions (Figure 6). Surprisingly, we also detected a small amount of cytochrome c in the cytosol without any apoptotic triggers. Similar observations have been made by others, and it has been speculated that the observed basal cytosolic cytochrome c is maintained in a reduced form, thereby unable to elicit an effective caspase activation cascade (Hancock, Desikan et al. 2001; Suto, Sato et al. 2005; Borutaite and Brown 2007).

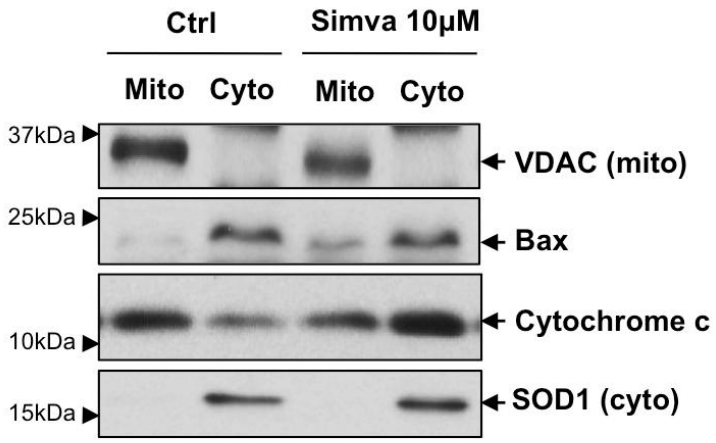

Figure 6: Simvastatin induces Bax translocation to mitochondria and cytochrome c release into the cytosol.
HCT116 cells were treated with 10 μM simvastatin for 24 h, after which cells were harvested and fractioned to obtain mitochondrial and cytosolic fractions as described in Materials and Methods. Levels of cytochrome c and Bax were assessed by Western blot analysis. VDAC and SOD1 were used as mitochondrial and cytosolic marker, respectively.

1.4.2 MMP modulator protein Bax is essential for simvastatin-induced cell death

To further validate the functional relevance of Bax in our cell death model, we compared the effect of simvastatin on HCT116 wildtype (HCT116 WT) and its counterpart in which Bax has been knocked out (HCT116 Bax-/-). Genetic invalidation of Bax protected cells to a large extent upon simvastatin treatment (Figure 7A) (33.28 ± 1.26% cell viability in WT cells *vs.* 72.12 ± 3.72% cell viability in Bax-/- cells after 10 μM simvastatin treatment, $p < 0.05$). This observation was also supported by abolished activation of caspase-3, -8 and -9 (Figure 7B) in Bax-/- cells compared to WT cells. In addition, PARP cleavage as a downstream event of caspase-3 activation was no longer observed in Bax-/- cells (Figure 7C). Taken together with the data on the translocation of cytochrome c and Bax, our findings indicate that the mitochondrial apoptotic pathway is the main death mechanism activated by simvastatin to induce cancer cell death.

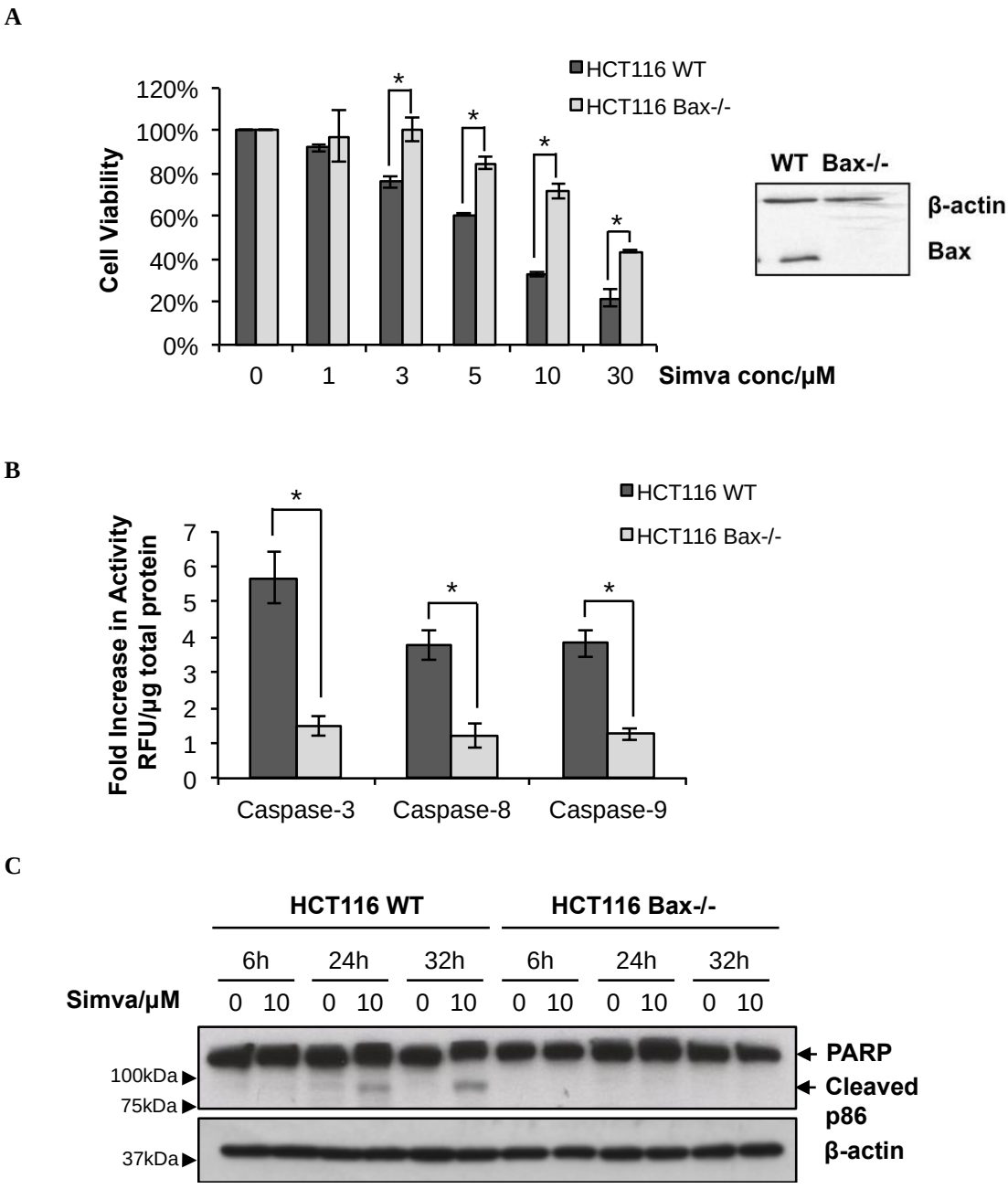

Figure 7: Simvastatin-induced cell death requires Bax.
(A) Absence or presence of Bax expression was confirmed in HCT116 WT and Bax-/- cell lines by Western blot analysis of basal cell lysates (right). Both cell lines were treated with various doses of simvastatin (0-30 μM) for 48 h and cell viability was measured by crystal violet assay (left). (B) Both cell lines were treated with 10 μM simvastatin for 36 h, and caspase-3, -8, and -9 activation levels were assessed using fluorescence-conjugated substrates. (C) PARP cleavage after treating with 10 μM simvastatin for the indicated duration was detected by Western blot analysis. β-actin was included as a loading control. In (A) and (B), data shown represents means ± s.e.m of three independent experiments. *, $p < 0.05$ as compared with untreated control.

1.5 Simvastatin-induced apoptosis is independent of p53 status

The tumor suppressor protein p53 executes complex control over apoptosis by regulating transcription and cytosolic function of Bcl-2 family members including Bax and BH3-only members, PUMA and NOXA (Chipuk, Kuwana et al. 2004; Maddika, Ande et al. 2007). Hence, to assess the dependency of p53 in simvastatin-mediated apoptosis, we compared the response of p53-null HCT116 cells (HCT116 p53-/-) to its p53 wildtype counterpart (HCT116 WT) towards simvastatin treatment. The expression status of p53 in both cell lines was confirmed by Western blot analysis in Figure 8 (right). As illustrated by crystal violet results, both p53-/- and WT cells exhibited similar extent of decrease in cell viability after simvastatin treatment (Figure 8, Left). Even though we have to rule out the importance of this key molecule in our model, the observed sensitivity of HCT116 p53-/- cell line nonetheless highlights the therapeutic potential of simvastatin in cancers with p53 deficiency.

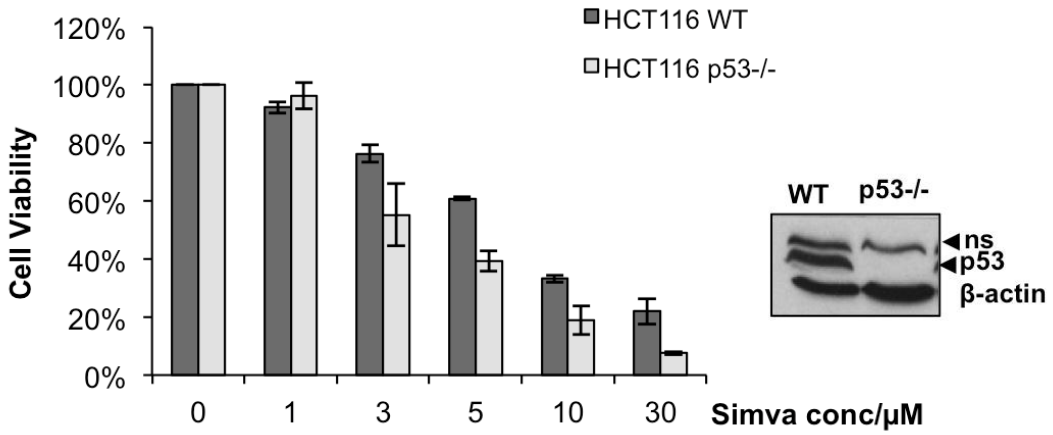

Figure 8: Simvastatin-induced cell death does not require p53.
Absence or presence of p53 expression was confirmed in HCT116 WT and HCT116 p53-/- cell lines by Western blot analysis of basal cell lysates (right). Both cell lines were treated with various doses of simvastatin (0-30 μM) for 48 h and cell viability was measured by crystal violet assay (left). Data shown represents means ± s.e.m of three independent experiments. (n.s. is non-specific band).

2 Simvastatin induces apoptosis by activating RhoA and Rac1 in HCT116 cells

2.1 Protein geranylgeranylation is essential in simvastatin-mediated apoptosis

2.1.1 Simvastatin induces apoptosis via depletion of isoprenoid precursor GGPP

Simvastatin is designed to selectively inhibit HMG-CoA reductase, the rate-limiting enzyme involved in the mevalonate pathway (Figure B in Introduction). Mevalonate is the precursor for cholesterol and some other biologically significant compounds such as the isoprenoids, which are reported to be responsible for the observed pleiotropic effects of statins (Werner, Nickenig et al. 2002). Hence, to examine the signaling mechanism for simvastatin-induced apoptosis in HCT116 cells, we felt it was important to first determine if the effect was through the inhibition of the mevalonate pathway. Cells were incubated with simvastatin in the presence or absence of mevalonate (MVA, 100 μM), geranylgeranylpyrophosphate (GGPP, 10 μM) and farnesylpyrophosphate (FPP, 10 μM). Consistent with the observations in other cell types (Xia, Tan et al. 2001; Dimitroulakos, Marhin et al. 2002; van de Donk, Kamphuis et al. 2003; Zhong, Wang et al. 2003), pretreatment with MVA or GGPP, but not FPP, almost completely reversed cell death phenotype induced by simvastatin in HCT116 cells (Figure 9A) (Crystal violet assay: 92.01 ± 4.37% cell viability with MVA preincubation, 84.37 ± 5.19% with GGPP preincubation *vs.* 33.28 + 1.26% with 10 μM simvastatin alone, $p < 0.05$; MTT assay: 94.98 ± 2.25% cell viability with MVA preincubation, 85.74 ± 5.46% with GGPP preincubation *vs.* 42.31 ± 2.47% with 10 μM simvastatin alone, $p < 0.05$). In addition, morphological examination revealed that MVA or GGPP preincubation restored normal morphology to cells akin to untreated control (Figure 9B). The involvement of the isoprenoid GGPP in the cell death elicited by simvastatin was confirmed by two additional

assays that assessed the DNA fragmentation and caspase activation status. Here, the sub-G1 population, caspase-3 and PARP cleavage following simvastatin treatment was significantly reduced with MVA or GGPP preincubation (Figure 9C, 9D). These observations were further supported by long-term clonogenic assay (Figure 9E), where MVA or GGPP preincubation exerted cytoprotective effect in simvastatin-treated cells.

Considering that FPP is an upstream isoprenoid precursor for cholesterol, the inability of FPP preincubation to protect cells from simvastatin treatment indirectly suggests that simvastatin's cytotoxic effect is cholesterol-independent. To confirm this notion, we pretreated cells with different concentrations of squalene, the immediate precursor of cholesterol, which has been used commonly to reverse cholesterol-mediated effects of statins (Michikawa and Yanagisawa 1999). Crystal violet data showed that squalene preincubation was unable to exert any protective effects in simvastatin-treated cells, similarly as FPP preincubation (Figure 10). The results confirm that the cytotoxic effects are cholesterol-independent.

In summary, simvastatin effects were selectively reversed by incubating cells with either mevalonate or its metabolite GGPP but not by squalene or FPP. These results suggest that simvastatin's apoptotic effects were mainly derived from depletion of intracellular pools of GGPP, the substrate required for protein geranylgeranylation.

A-I

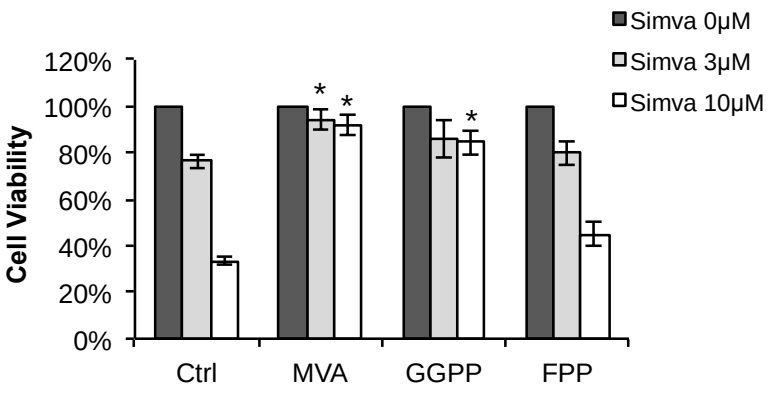
Simva 0μM
Simva 3μM
Simva 10μM
Cell Viability
120%
100%
80%
60%
40%
20%
0%
Ctrl
MVA
GGPP
FPP
*
*
*
*

A-II

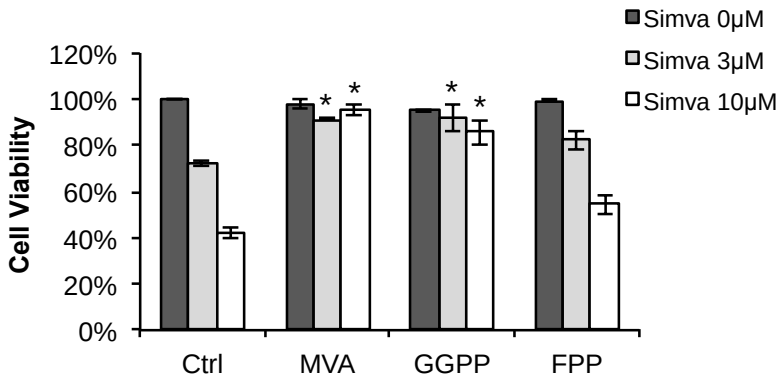
Simva 0μM
Simva 3μM
Simva 10μM
Cell Viability
120%
100%
80%
60%
40%
20%
0%
Ctrl
MVA
GGPP
FPP
*
*
*
*

B

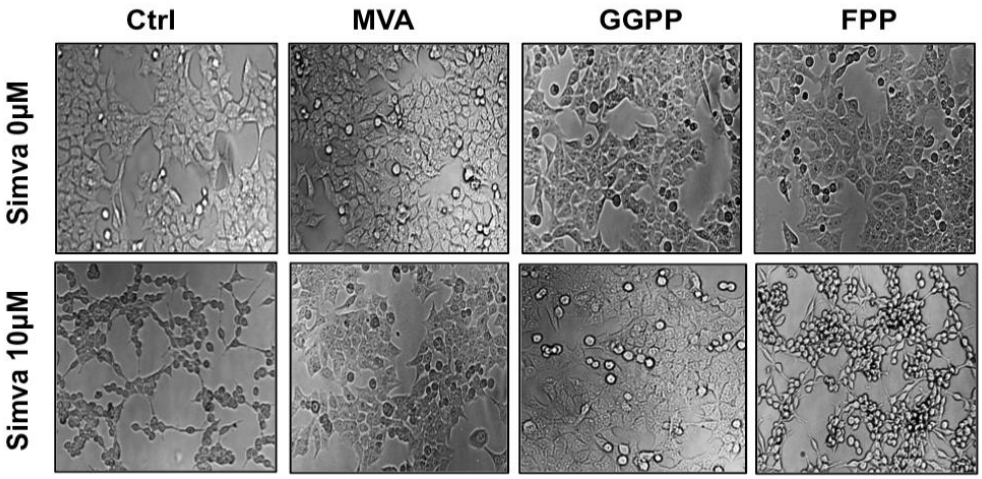
Ctrl
MVA
GGPP
FPP
Simva 0μM
Simva 10μM

C

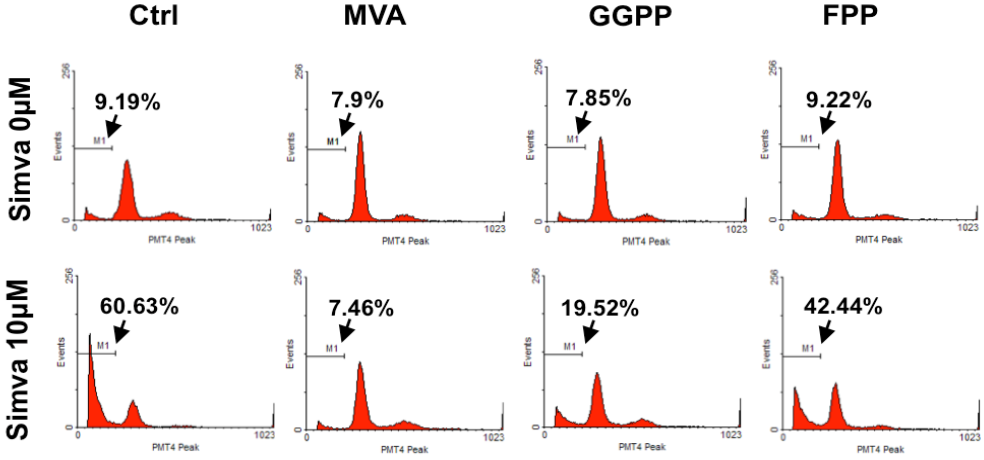
Ctrl
MVA
GGPP
FPP
Simva 0μM
Simva 10μM
9.19%
7.9%
7.85%
9.22%
60.63%
7.46%
19.52%
42.44%
M1
PMT4 Peak
Events

D

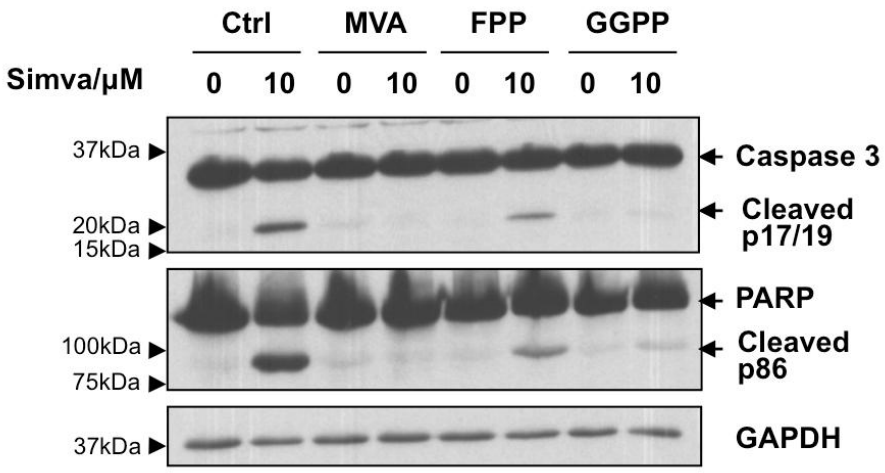

E

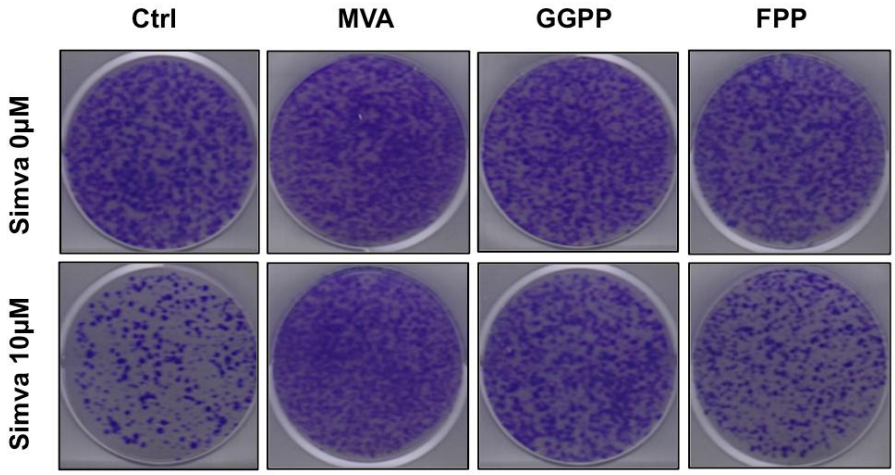

Figure 9: MVA or GGPP preincubation protect cells from simvastatin-mediated cell death.
In all panels, HCT116 cells were preincubated with or without 100 μM MVA, 10 μM GGPP or 10 μM FPP for 2 h before treatment with 3 or 10 μM simvastatin. (A) Cell viability of treated cells was measured by (I) crystal violet assay or (II) MTT assay. The bars represent means ± s.e.m of three independent experiments. *, $p < 0.05$ compared with simvastatin treatment alone. (B) Cell morphology after 28 h treatment was photographed using phase contrast microscope (Magnification: 100X). (C) DNA content was analyzed after 48 h treatment by PI staining; percentage of cells in sub-G1 is indicated in the graph. (D) Caspase-3 and PARP cleavage was assessed after 36 h simvastatin treatment by Western blot analysis. (E) Photos of colonies formed after 30 h simvastatin treatment in the presence or absence of 2h MVA, GGPP or FPP pretreatment.

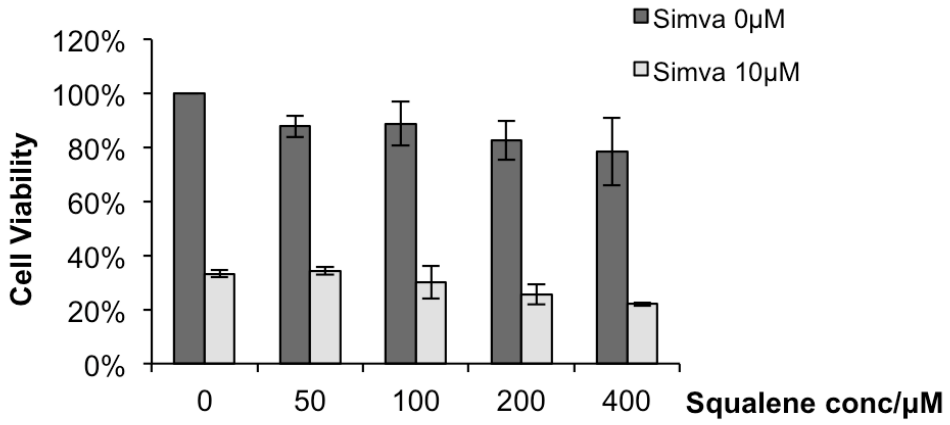

Figure 10: Squalene preincubation did not rescue cells after simvastatin treatment.
HCT116 cells were preincubated with or without various doses of squalene (0-400 μM) for 2 h before treatment with 10 μM simvastatin for 48 h. Cell viability of treated cells was measured by crystal violet assay. The bars represent means ± s.e.m of three independent experiments.

2.1.2 Inhibitor of GGTase-I mimics the cytotoxic effects of simvastatin

As detailed in the previous section, the impact of simvastatin treatment in cells seemed to be due to the depletion of cellular GGPP and subsequent inhibition of protein geranylgeranylation, as restoration of this isoprenoid could protect from simvastatin's toxicity. Hence, we proposed that direct inhibition of the enzyme responsible for the transfer of geranylgeranyl-group to proteins ought to show similar cytotoxic effects. We tested the hypothesis with two inhibitors: geranylgeranyltransferase-I (GGTase-I) inhibitor GGTI-298 and farnesyltransferase (FTase) inhibitor FTI-277. Both inhibitors specifically block the transfer of the geranylgeranyl-group and farnesyl-group to their downstream targets, respectively. Cells were treated with 20 μM and 40 μM of GGTI-298 or FTI-277, and the cytotoxic effects of these two inhibitors were compared with 10 μM simvastatin alone. The cell viability data showed that GGTI-298 was able to illicit cell loss; while FTI-277 showed no significant cell death effects in HCT116 cells (Figure 11A) (Crystal violet assay: 61.76 ± 4.13% cell viability with 40 μM GGTI-298, 85.72 ± 0.04% with 40 μM FTI-277 *vs.* 33.28 ± 1.26% with 10 μM simvastatin alone; MTT assay: 56.93 ± 9.02% cell viability with 40 μM GGTI-298, 86.22 ± 0.36% with 40 μM FTI-277 *vs.* 42.31 ± 2.47% with 10 μM simvastatin alone). Morphological examination as well as proteolytic processing of caspase-3 (Figure 11B, 11C) also supported the notion that GGTI-298-treated cells exhibited apoptotic hallmarks comparable to simvastatin treatment. These observations corroborated well with the findings that GGPP preincubation, but not FPP, largely protected cells from simvastatin treatment, confirming that protein geranylgeranylation is more important than farnesylation in mediating simvastatin's cytotoxic effects.

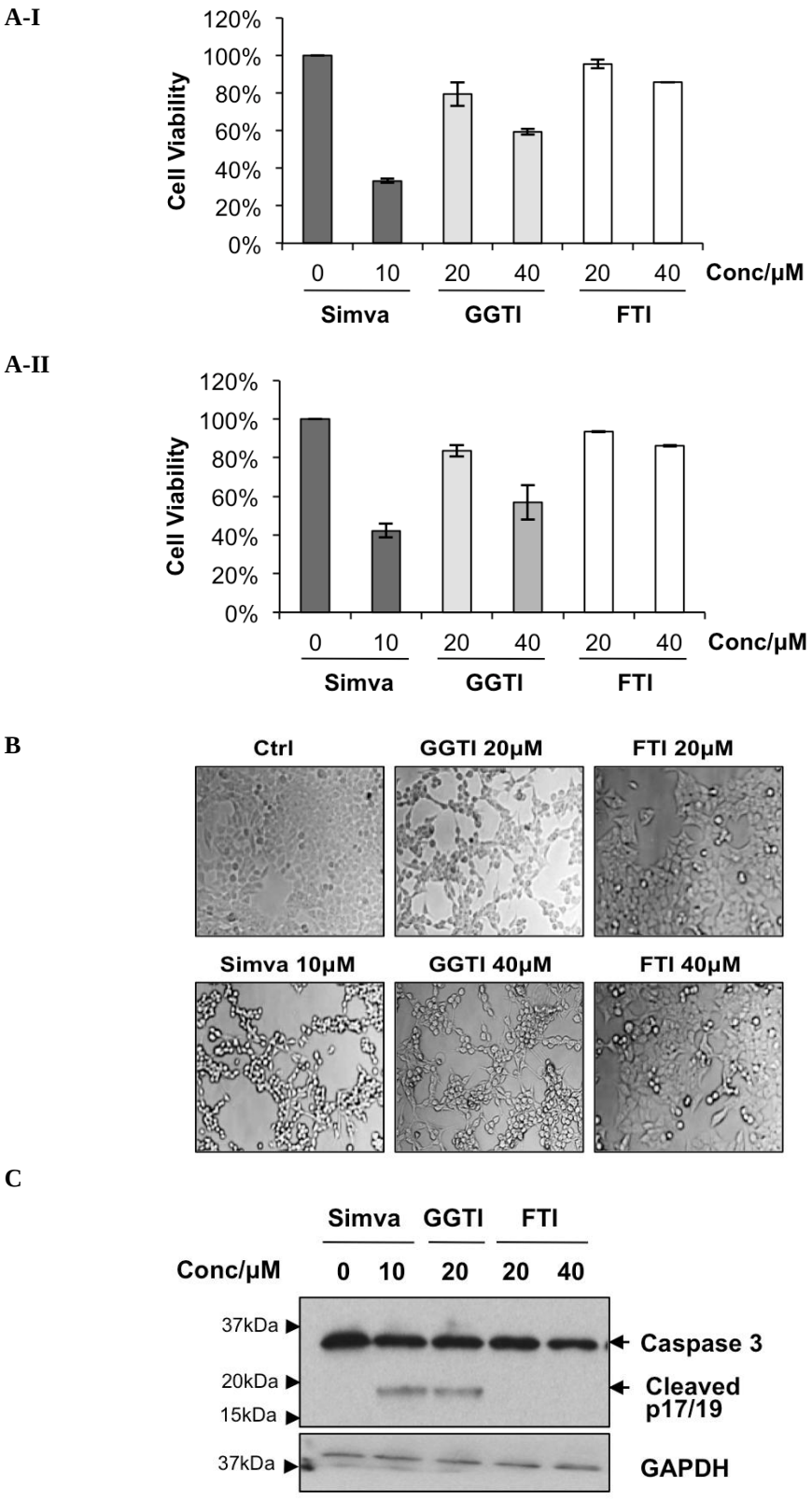

Figure 11: GGTI-298 mimics the cytotoxic effects of simvastatin.
HCT116 cells were treated with simvastatin, GGTI-298 or FTI-277 at indicated doses. (A) Cell viability of treated cells after 48 h was measured by (I) crystal violet assay or (II) MTT assay. The bars represent means ± s.e.m of three independent experiments. (B) Cell morphology after 28 h treatment was photographed using phase contrast microscope (Magnification: 100X). (C) Caspase-3 cleavage after 36 h of treatment was assessed by Western blot analysis. GAPDH was used as loading control.

2.2 Changes in expression, localization and activities of three geranylgeranylated proteins, namely RhoA, Rac1 and Cdc42, after simvastatin treatment

Prenylation is a lipid modification that involves isoprenoids FPP and GGPP to transfer either a farnesyl (15-carbon) or a geranylgeranyl (20-carbon) group to the C-terminus of proteins. This post-modification is essential for membrane localization and participation of proteins in various signaling pathways (Zhang and Casey 1996). Considering the ability of GGPP to prevent simvastatin-induced apoptosis in HCT116 cells, we speculated the possible involvement of geranylgeranylated proteins in mediating the cell death response. We focused on three geranylgeranylated Rho family proteins, RhoA, Rac1 and Cdc42, as their role in cancer progression have been widely studied (Vega and Ridley 2008). Several important properties of these proteins were assessed after simvastatin treatment, namely protein expression, cellular localization and enzymatic activities.

2.2.1 Simvastatin dramatically increases protein levels of RhoA and Cdc42 via blocking protein geranylgeranylation

HCT116 cells were treated with 10 μM simvastatin over the indicated time intervals (2-20 h). Interestingly, we observed a dramatic increase in protein expression of RhoA and Cdc42 after 12 h simvastatin treatment and the levels were sustained till the end of the time course. The expression of Rac1 was increased very mildly by simvastatin treatment (Figure 12A). This increased protein content of Rho proteins after simvastatin treatment was fully blocked when cells were preincubated with MVA and largely prevented with GGPP pretreatment, while FPP-preincubated cells showed comparable levels of Rho proteins with cells treated with simvastatin alone

(Figure 12B). The results suggest that simvastatin affects protein expression of Rho proteins via inhibiting the post-translational geranylgeranylation process.

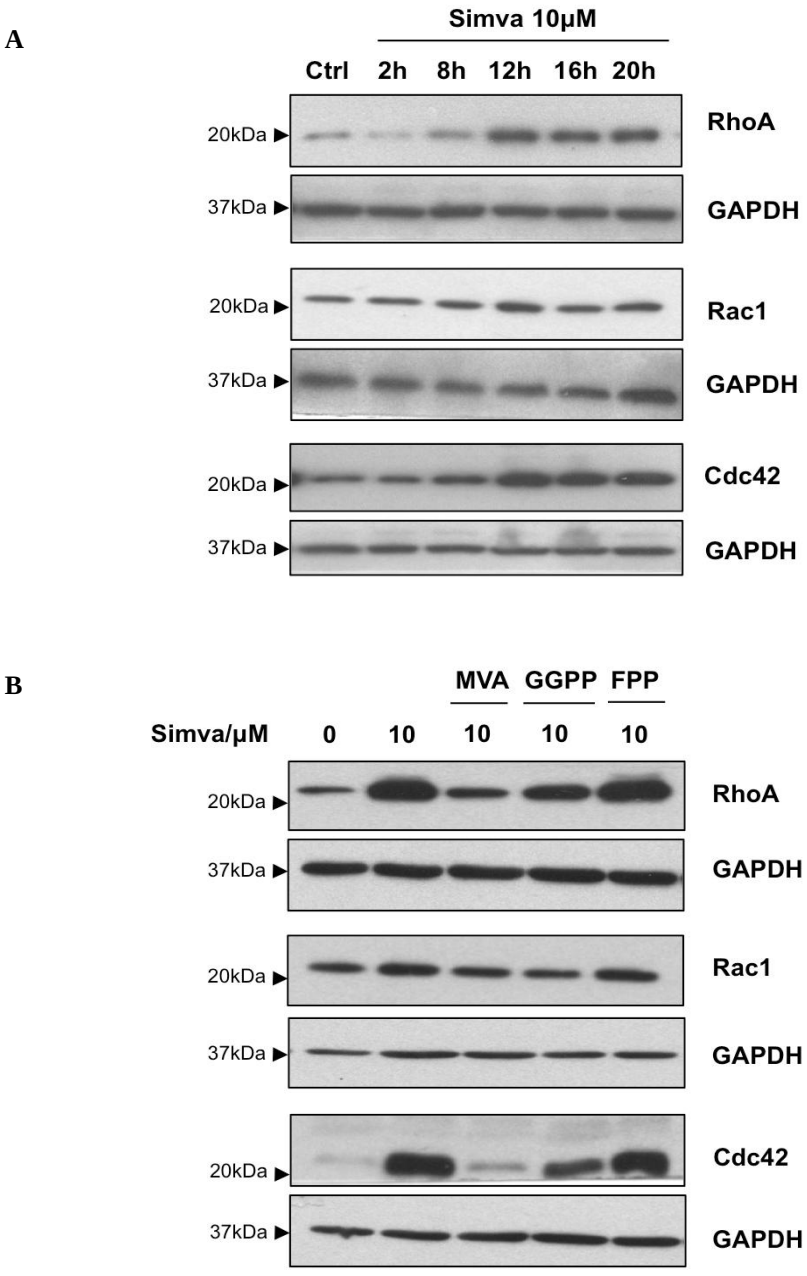

Figure 12: Simvastatin drastically increases protein expression of RhoA and Cdc42 via blocking protein geranylgeranylation.
(A) HCT116 cells were treated with 10 μM simvastatin for the indicated durations. (B) Cells were preincubated with or without 100 μM MVA, 10 μM GGPP or 10 μM FPP for 2 h before treatment with 10 μM simvastatin for 20 h. In both panels, protein level of RhoA, Rac1 and Cdc42 was assessed by Western blot analysis. GAPDH was included as a loading control.

2.2.2 Simvastatin increases expression of unprenylated RhoA, Rac1 and Cdc42

After assessing the levels of RhoA, Rac1 and Cdc42 in total cell lysates, we then studied the amount of Rho proteins in their prenylated and unprenylated forms. We hypothesized that simvastatin would increase Rho proteins in their unprenylated form as the isoprenoids required for this post-modification were deprived. To quantify Rho prenylation, we extracted cells in the low cloud-point detergent Triton X-114 (Brusca and Radolf 1994), which separates cell lysates into an aqueous and detergent phase based on the hydrophobicity of the respective proteins. Previous work has shown that unprenylated Ras and Rho family proteins partition into the aqueous phase, while prenylated proteins partition into the detergent phase (Bordier 1981; Allal, Favre et al. 2000). In the absence of simvastatin, RhoA and Cdc42 were largely in the detergent phase while the majority of Rac1 was found in the aqueous phase. Treating HCT116 cells with 10 μM simvastatin for 12 and 20 h caused a progressive and dramatic increase of RhoA and Cdc42 and to a lesser extent of Rac1, to partition into the aqueous phase, indicating effective inhibition of Rho prenylation (Figure 13). The lack of GAPDH in the detergent phase demonstrated a clear separation of proteins from aqueous phase with the detergent phase. These results demonstrate that simvastatin increases RhoA, Rac1 and Cdc42 in their unprenylated forms.

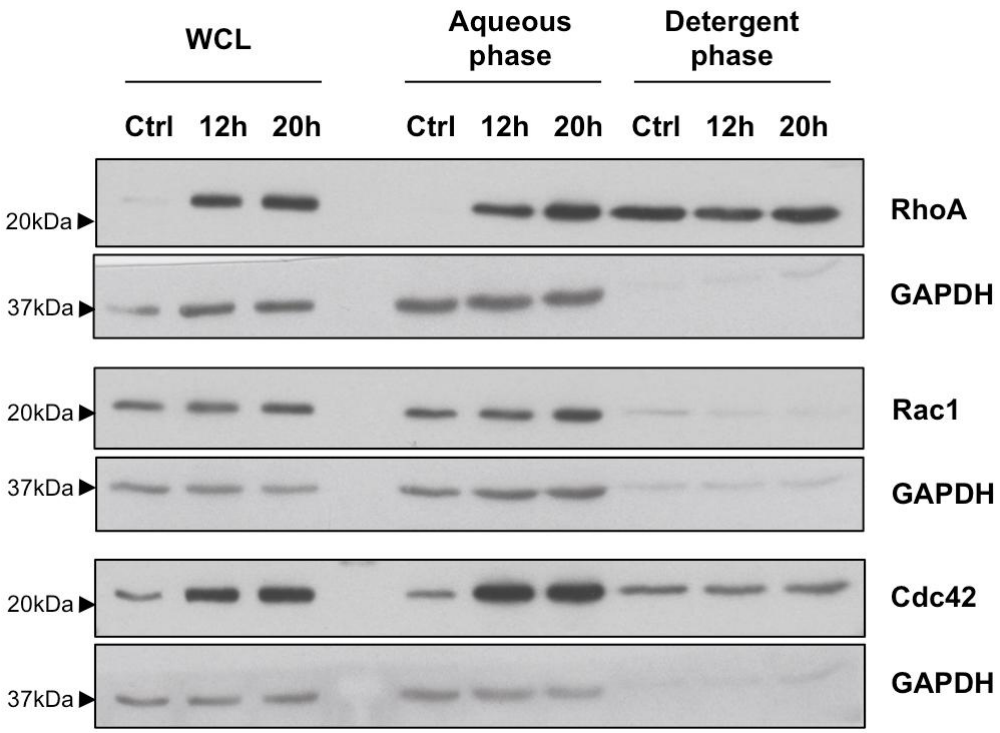

Figure 13: Simvastatin treatment increases Rho proteins in their unprenylated form.
HCT116 cells were treated with 10 μM simvastatin for 12 and 20 h. Cells were extracted in 1% Triton X-114, and total cell lysates were separated into an aqueous supernatant and a detergent-containing pellet. Aliquots of total cell lysate (WCL), aqueous phase (containing unprenylated proteins), and detergent phase (containing prenylated proteins) were assayed by Western blot analysis to check for RhoA, Rac1 and Cdc42 protein expression. GAPDH blot demonstrated no contamination of the detergent pellet with proteins from the aqueous phase.

2.2.3 Simvastatin delocalizes RhoA, Rac1 and Cdc42 from the lipid rafts and increases their expression in the cytosol

Next, we studied the localization of these Rho proteins after simvastatin treatment with focus on two cellular locations: the lipid rafts and the cytosol. The lipid rafts are microdomains within the plasma membrane that are enriched with sphingolipids and cholesterol (Simons and Ikonen 1997; Anderson 1998; Brown and London 1998). Lipid rafts can be isolated by virtue of their detergent insolubility and characterized by the presence of *bona fide* raft-associated proteins, such as flotillin after ultracentrifugation in a sucrose gradient density (Waugh and Hsuan 2009). Studies have shown that Rho GTPases are found to be associated within the lipid rafts of the plasma membrane (Golub, Wacha et al. 2004). Without the post-modification of geranylgeranylation after simvastatin treatment, we would expect unprenylated RhoA, Rac1 and Cdc42 to delocalize from the lipid rafts and accumulate in the cytosol. To test this hypothesis, we assessed the levels of RhoA, Rac1 and Cdc42 in the isolated lipid raft fraction and cytosolic fraction. The lipid raft was separated using sucrose gradient density centrifugation studies as mentioned earlier. As expected, all three Rho proteins decreased from the flotilin-positive raft fractions after 12 and 20 h of simvastatin treatment (Fraction number 3-5). A clear increase of RhoA and Cdc42 were also observed in the non-raft fraction after 20h treatment (Fraction number 6) (Figure 14A). Meanwhile, cytosolic proteins were isolated with high-speed centrifugation; dramatic increase of cytosolic RhoA and Cdc42 and to a lesser extent of cytosolic Rac1 was observed after 12 and 20 h simvastatin treatment. The accumulation was fully reversed with MVA preincubation (Figure 14B). In agreement with literature, simvastatin-induced unprenylated RhoA, Rac1 and Cdc42 decrease from the lipid rafts of the plasma membrane, and accumulate in the cytosol.

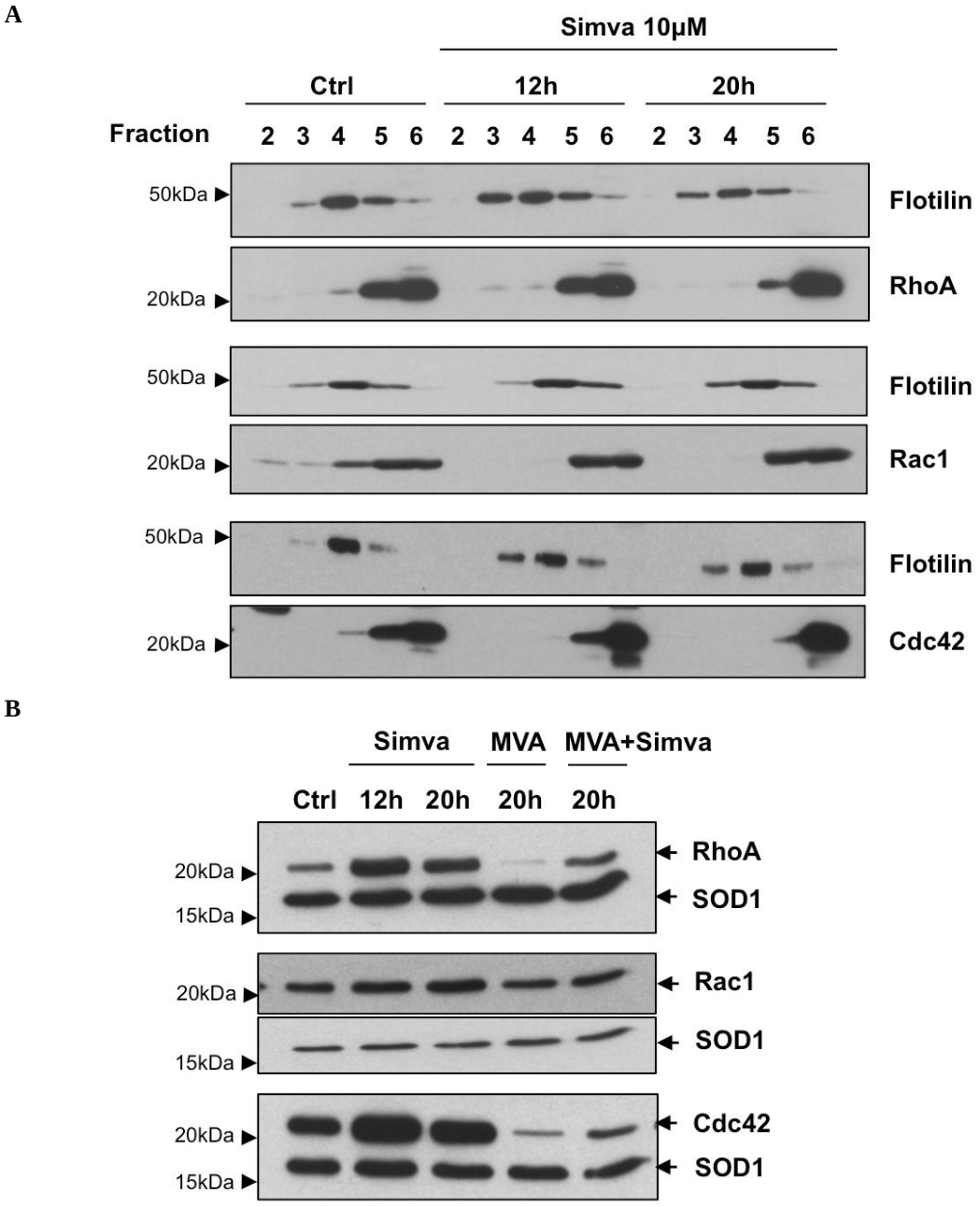

Figure 14: Rho proteins decrease from the lipid rafts and accumulate in the cytosol after simvastatin treatment.

(A) HCT116 cells were treated with 10 μM simvastatin for 12 and 20 h. The lipid raft containing fractions were prepared using sucrose gradient centrifugation as described in Materials and Methods. Equal volume of lysates from Fraction number 2-6 was subjected to Western blot analysis to check for protein levels of RhoA, Rac1 and Cdc42. Flotilin was used as the lipid raft marker. (B) Cells were treated with 10 μM simvastatin alone for 12 and 20 h or preincubated with 100 μM MVA for 2 h prior to simvastatin treatment for 20 h. Cells were then lysed and centrifuged at high speed to obtain supernatant containing cytosolic proteins as described in Materials and Methods. Protein levels of RhoA, Rac1 and Cdc42 were assessed by Western blot analysis. SOD1 was used as cytosolic marker.

2.2.4 Simvastatin increases GTP-loading of RhoA, Rac1 and Cdc42 by downregulation of GGPP synthesis

The post-translational modification of prenylation is also required for Rho proteins to interact with both their activators and inhibitors (Hori, Kikuchi et al. 1991), an increase in unprenylated RhoA, Rac1 and Cdc42 could either increase or decrease the amount of functionally active (GTP-bound) Rho GTPases present in HCT116 cells. Hence, we aimed to measure the amount of RhoA, Rac1 and Cdc42 in GTP-bound form using a pull-down assay. We utilized the protein binding domain (PBD) of p21-activated kinase (PAK), a downstream effector protein of Rac1 and Cdc42, to selectively pull down the active form of Rac1 and Cdc42; while the Rho binding domain (RBD) of Rhotekin protein was used to specifically pull down the active RhoA from cell lysates. Strikingly, the level of GTP-bound RhoA, Rac1 and Cdc42 was significantly increased after 12 and 20 h of simvastatin treatment (Figure 15A, 16A, 17A). Interestingly, the increased GTP-loading of RhoA and Cdc42 following simvastatin treatment was observed together with an increase in the respective protein expression. Moreover, pretreatment of HCT116 cells with GGPP inhibited the increase in RhoA-GTP, Rac1-GTP and Cdc42-GTP; in contrast, FPP-preincubated cells showed comparable level of GTP loading as cells treated with simvastatin alone (Figure 15B, 16B, 17B). The findings suggest that simvastatin-mediated inhibition of geranylgeranylation leads to increase in the GTP-loading of RhoA, Rac1 and Cdc42.

A-I

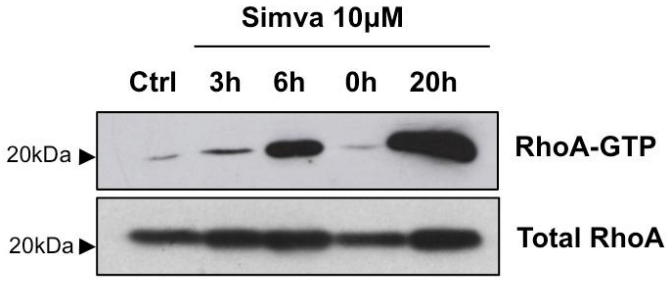

A-II

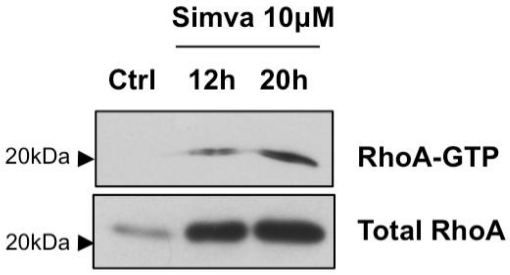

B

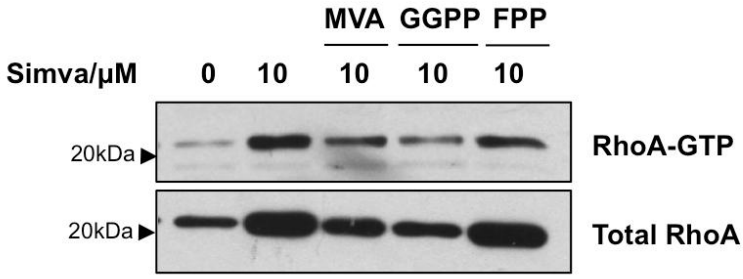

Figure 15: Simvastatin increases GTP loading of RhoA by blocking protein geranylgeranylation. (A) HCT116 cells were treated with 10 μM simvastatin for (I) 3, 6 and 20 h or (II) 12 and 20 h. (B) Cells were preincubated with 100 μM MVA, 10 μM GGPP or 10 μM FPP for 2 h before treated with 10 μM simvastatin for 20 h. In both panels, cells were lysed, and GTP-loaded RhoA was isolated with Rhotekin RBD-agarose beads as described in Materials and Methods. Isolated complexes were separated by Western blot analysis and probed with anti-RhoA antibody. Cell lysates were probed in parallel to monitor total cellular RhoA level.

A-I

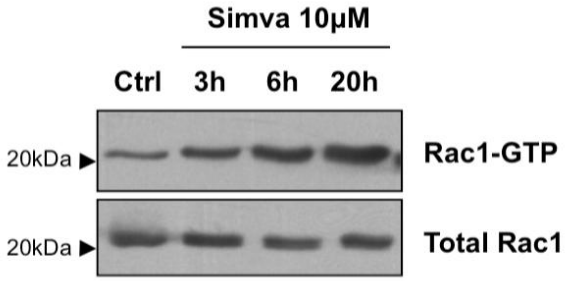

A-II

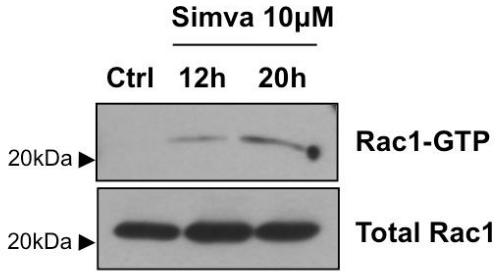

B

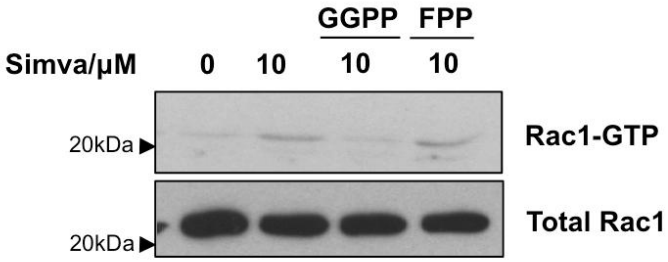

Figure 16: Simvastatin increases GTP loading of Rac1 by blocking protein geranylgeranylation. (A) HCT116 cells were treated with 10 µM simvastatin for (I) 3, 6 and 20 h or (II) 12 and 20 h. (B) Cells were preincubated with 10 µM GGPP or 10 µM FPP for 2 h before treated with 10 µM simvastatin for 20 h. In both panels, cells were lysed, and GTP-loaded Rac1 was isolated with PAK PBD-agarose beads. Isolated complexes were separated by Western blot analysis and probed with anti-Rac1 antibody. Cell lysates were probed in parallel to monitor total cellular Rac1 level.

A

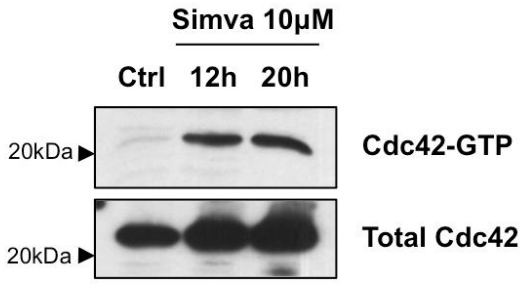

B

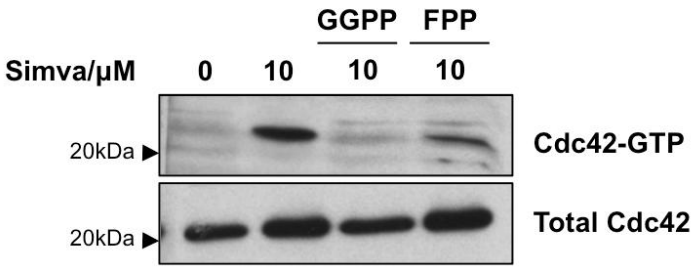

Figure 17: Simvastatin increases GTP loading of Cdc42 by blocking protein geranylgeranylation. (A) HCT116 cells were treated with 10 μM simvastatin for 12 and 20 h. (B) Cells were preincubated with 10 μM GGPP or 10 μM FPP for 2 h before treated with 10 μM simvastatin for 20 h. Cells were lysed, and GTP-loaded Cdc42 was isolated with PAK PBD-agarose bead. Isolated complexes and whole cell lysates were separated by Western blot analysis and probed with anti-Cdc42 antibody.

2.3 Simvastatin activates RhoA and Rac1 to mediate its apoptotic effects

2.3.1 Blocking Rac1 by pharmacological inhibitors and expression of dominant negative plasmid rescues cells from simvastatin-induced cell death

Intrigued by the observation that simvastatin treatment increased GTP-loading of RhoA, Rac1 and Cdc42, we went further to evaluate if the activation of Rho GTPases was important in simvastatin-induced cell kill. We first assessed the involvement of Rac1-GTP, utilizing pharmacological inhibitors and dominant negative plasmid to block Rac1 activity. Two structurally unrelated Rac1 inhibitors NSC23766 and EHT1864 were used. NSC23766 effectively blocks Rac-specific guanine nucleotide exchange factors (GEFs) while EHT1864 directly binds to Rac, both inhibitors then block GTP-loading of Rac1 and impair Rac1-mediated functions (Gao, Dickerson et al. 2004; Onesto, Shutes et al. 2008). HCT116 cells were pretreated with or without 150 μM NSC23766 or 20 μM EHT1864 before treatment with 10 μM simvastatin. Notably, both Rac1 inhibitors significantly protected cells from simvastatin treatment as assessed by crystal violet assay (Figure 18A) (54.06 ± 1.47% cell viability with NSC23766 pretreatment, $p < 0.05$; 70.24 ± 6.93% with EHT1864 pretreatment, $p < 0.05$ *vs.* 33.28 ± 1.26% with 10 μM simvastatin alone). In addition, cells pretreated with both Rac1 inhibitors were visibly healthier and more attached to the culture dish (Figure 18B). Reduced formation of cleaved-PARP was also observed after preincubation with both inhibitors compared to cells treated with simvastatin alone, and more pronounced reduction was seen with EHT1864 compared to NSC23766 pretreatment (Figure 18C).

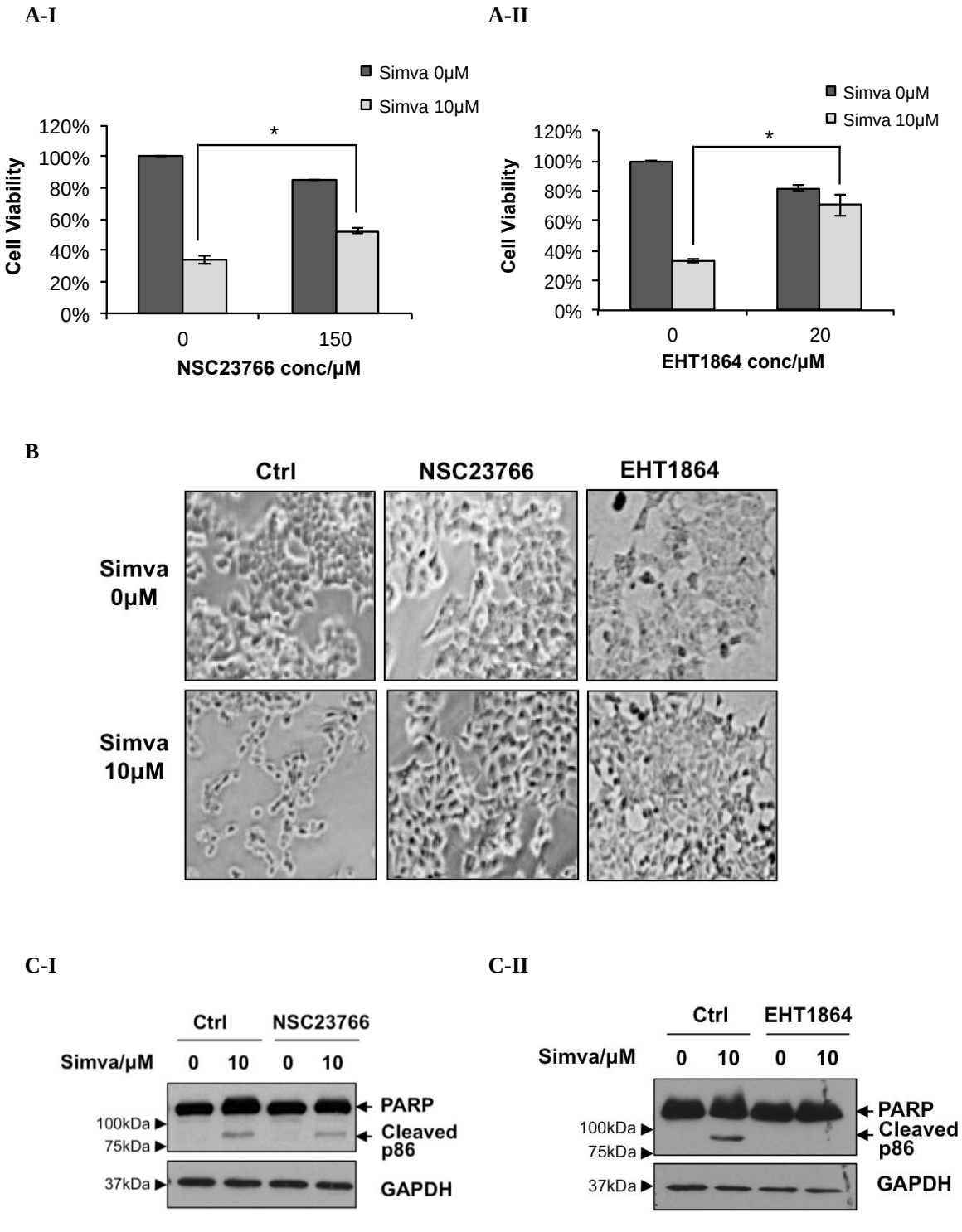

Figure 18: Pharmacological inhibitors of Rac1 rescue cells from simvastatin-induced cell death. HCT116 cells were preincubated with or without 150 μM NSC23766 or 20 μM EHT1864 for 2 h before treated with 10 μM simvastatin. (A) Cell viability of treated cells after 48 h was measured by crystal violet assay. The bars represent means ± s.e.m of three independent experiments. *, $p < 0.05$ compared with simvastatin treatment alone. (B) Cell morphology after 28 h treatment was photographed using phase contrast microscope (Magnification: 100X). (C) PARP cleavage was assessed after 36 h treatment by Western blot analysis. GAPDH was included as a loading control.

To further verify the importance of Rac1-GTP in simvastatin-mediated apoptosis, HCT116 cells were transfected with empty vector (pIRES) or dominant negative Rac1N17 plasmid that does not allow for GDP-GTP exchange before simvastatin treatment. Successful transfection was confirmed by expression of myc-tag that was only expressed in Rac1N17-transfected cells. In addition, the exogenously transfected Rac1 also appeared as a higher band compared to the endogenous Rac1 detected at 21 kDa (Figure 19A). Despite that the proportion of exogenously-introduced Rac1 was much lower than the endogenous level, Rac1N17-transfected cells displayed less sensitivity compared to empty vector-transfected cells upon simvastatin treatment measured by crystal violet assay (Figure 19A) (47.26 ± 5.14% with Rac1N17 transfection *vs.* 29.15 ± 1.51% with empty vector-transfected cells after 10 μM simvastatin treatment, $p < 0.05$). This observation was supported by reduced PARP cleavage in Rac1N17-transfected cells compared to empty vector control (Figure 19B). Furthermore, long-term colony-forming assays confirmed that Rac1N17-transfection endowed cells with pronounce long-term survival advantage against simvastatin-triggered cell death (Figure 19C). Taking together with the observation that Rac1 inhibitor preincubation reduces simvastatin-mediated cell death, we provide evidence that activation of Rac1 is an important event in our cell death model.

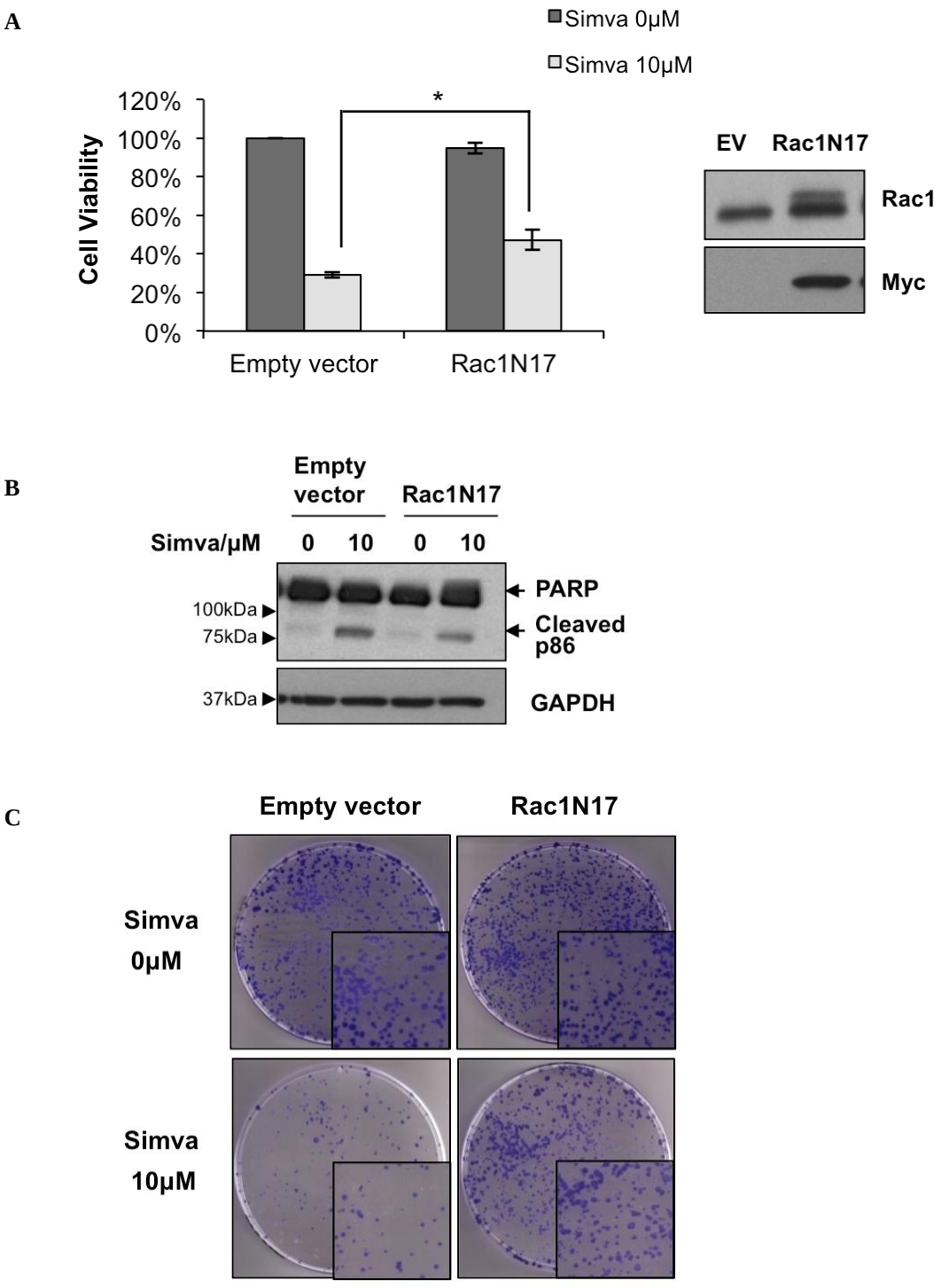

Figure 19: Dominant negative Rac1N17 transfection partially protects cells from simvastatin treatment.

HCT116 cells were transfected with either pIRES empty vector or Rac1N17 plasmid using Calcium phosphate method as described in Materials and Methods. (A) Western blot analysis showed successful expression of Rac1 and Myc-tag 30 h post-transfection (right). Transfected cells were treated with 10 μM simvastatin for 48 h and cell viability was measured by crystal violet assay (left). The bars represent means ± s.e.m of three independent experiments. *, $p < 0.05$ compared with empty vector control cells receiving 10 μM simvastatin. (B) PARP cleavage was assessed 36 h post-treatment by Western blot analysis. GAPDH was included as a loading control. (C) Photos of colonies formed by empty vector- or Rac1N17-transfected cells after simvastatin treatment.

2.3.2 Knockdown of RhoA and Rac1, but not Cdc42, protects cells from simvastatin's cytotoxic effects

After establishing the relevance of Rac1 activation in simvastatin-mediated apoptosis in HCT116 cells, we continued to ascertain the involvement of activation of RhoA and Cdc42 observed after simvastatin treatment. We suppressed the expression of these proteins with targeted RNA interference (RNAi) knockdown. Firstly, we confirmed knockdown of RhoA, Rac1 and Cdc42 with or without simvastatin treatment by Western blot analysis. Simvastatin increased RhoA and Cdc42 protein content and the protein level was fully abrogated by siRNA transfection; while a small amount of Rac1 was still detected after siRNA treatment. Then the effects of these knockdown strategies on cell viability were assessed by crystal violet assay (Figure 20B). Notably, RhoA and Rac1 knockdown significantly reduced simvastatin-induced viability loss, while knockdown of either alone did not appreciably impact cell death (52.77 ± 1.81% cell viability with siRhoA, 50.17 ± 4.04% cell viability with siRac1, $p < 0.05$ *vs.* 31.22 ± 1.11% cell viability with siCtrl after 10 μM simvastatin treatment). Interestingly, we did not observe any protection when Cdc42 was knocked down. The data confirms the involvement of active Rac1 in simvastatin-mediated apoptosis and implicates the possible role of RhoA activation in the cell death model as well.

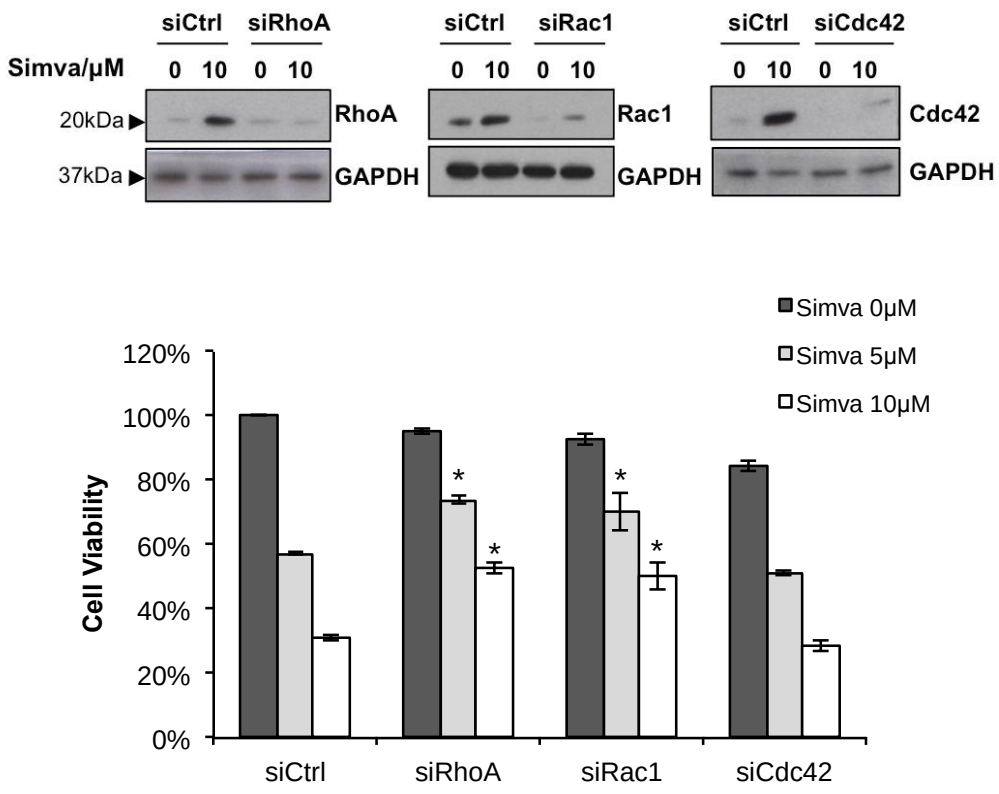

Figure 20: Knockdown of RhoA and Rac1, but not Cdc42, partially protects the cells from simvastatin's cytotoxic effects.
RhoA, Rac1 or Cdc42 were successfully knocked down in HCT116 using Calcium phosphate method as described in Materials and Methods before treatment with 5 or 10 μM simvastatin for 48 h. Cell viability was measured by crystal violet assay. The bars represent means ± s.e.m of three independent experiments. *, $p < 0.05$ compared with siCtrl-transfected cells receiving the same simvastatin treatment.

2.3.4 Simvastatin activates RhoA and Rac1 by decreasing their association with the cytosolic inhibitor RhoGDIα

After identifying that simvastatin-mediated apoptosis was a function of active RhoA and Rac1, we explored further to understand the possible mechanism for the observed increase in GTP-loading. Under basal conditions, GDP-bound Rho proteins are associated primarily with guanine nucleotide dissociation inhibitors (RhoGDIs); after cellular stimulation, they dissociate from RhoGDIs and allow for GDP-GTP exchange (Dovas and Couchman 2005). Hence, we assessed the respective interaction of RhoA and Rac1 with the ubiquitous-expressed RhoGDIα using coimmunoprecipitation studies. The results showed that the RhoA-RhoGDIα and Rac1-RhoGDIα interactions were significantly decreased in simvastatin-treated HCT116 cells compared to untreated control (Figure 21A). This finding was quite striking considering the large increase in total RhoA after simvastatin treatment. Nonetheless, the observations suggest that the decreased interaction of RhoA and Rac1 with their cytosolic inhibitor could be a potential mechanism for the increase in GTP-loading of both proteins.

Furthermore, it has been identified that geranylgeranylation of Rho proteins is required for their interaction with RhoGDIs (Di-Poi, Faure et al. 2001). Hence, we hypothesized that the interaction of RhoA or Rac1 with RhoGDIα would be restored with MVA or GGPP preincubation, but not FPP preincubation. As expected, the interactions were largely restored in MVA- or GGPP-preincubated cells (Figure 21B). The observation corroborated well with the finding that MVA or GGPP preincubation reduced simvastatin-mediated apoptosis (Figure 9). Collectively, these data suggest that simvastatin decreases the respective association of RhoA and Rac1

with RhoGDIα through inhibiting protein geranylgeranylation, which then leads to aberrant activation of RhoA and Rac1 and eventually contributes to cellular demise.

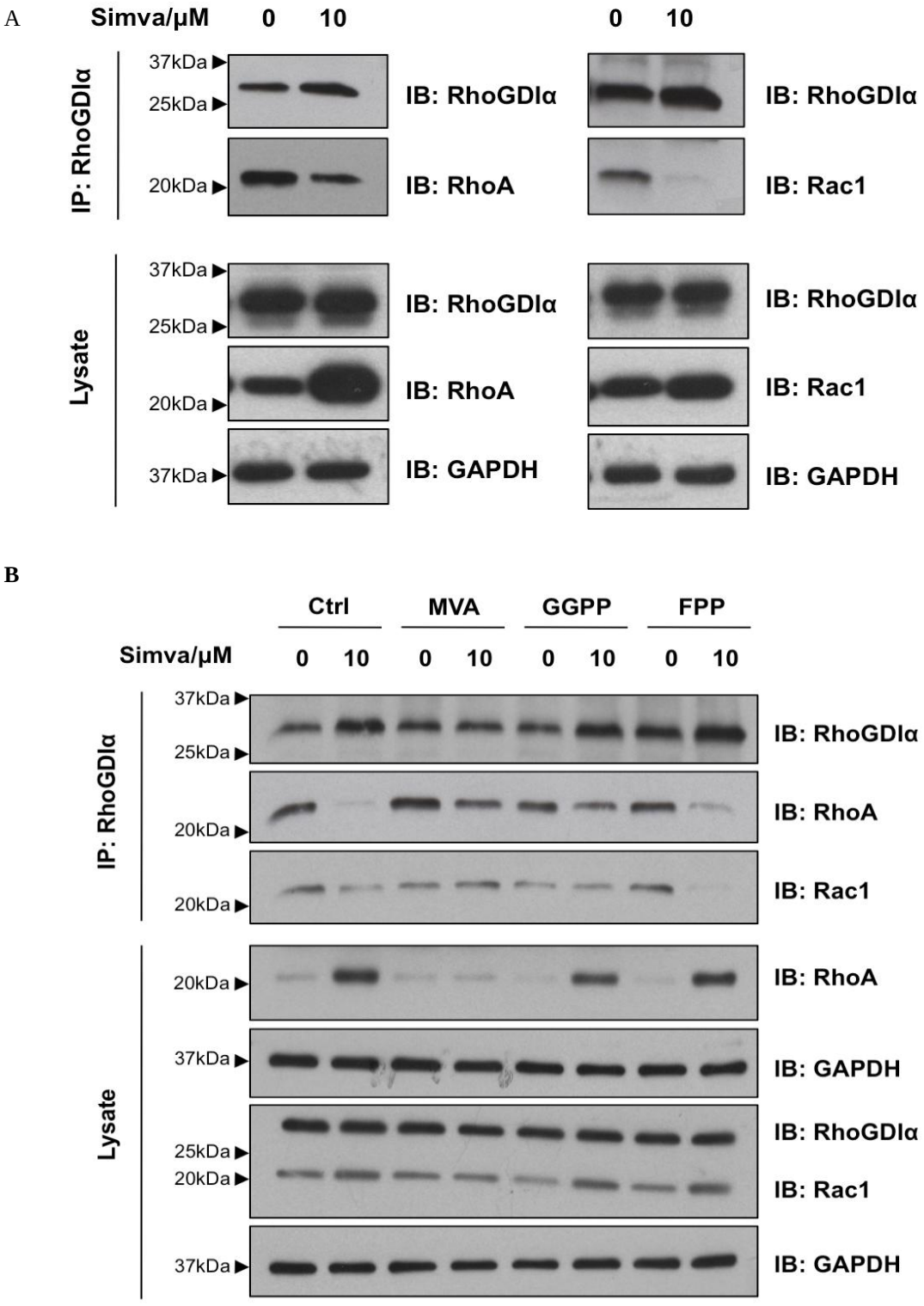

Figure 21: Simvastatin decreases the respective association of RhoA and Rac1 with RhoGDIα by blocking protein geranylgeranylation.
HCT116 cells were treated with (A) simvastatin alone; or (B) preincubated with 100 μM MVA, 10 μM GGPP or 10 μM FPP for 2 h before treated with 10 μM simvastatin for 20 h. In both panels, cells were lysed, and RhoGDIα-RhoA, RhoGDIα-Rac1 complexes were immunoprecipitated with anti-RhoGDIα antibodies. Isolated complexes were separated by Western blot analysis and probed with anti-RhoA and anti-Rac1 antibodies. Protein loading was evaluated by stripping the blots and reprobing with anti-RhoGDIα antibodies. Cell lysates were probed in parallel to monitor total cellular RhoA, Rac1 and RhoGDIα levels. GAPDH was included as a loading control.

2.4 Inhibiting newly synthesized RhoA and Rac1 diminishes the increase in active RhoA and Rac1, and protects cells from simvastatin-induced apoptosis

Because protein prenylation is a post-translational modification, inhibition of protein synthesis should prevent prenylation-dependent apoptosis induced by simvastatin. To test this hypothesis, we assessed the effects of protein synthesis inhibitor cycloheximide on simvastatin-treated HCT116 cells. Interestingly, cells pretreated with all concentrations of cycloheximide were insensitive to simvastatin treatment (Figure 22A). However, high doses of cycloheximide (20 μg/ml) were found to be toxic to cells, while concentrations below 10 μg/ml displayed growth statutory effects. Cells were then pretreated with non-toxic doses of cycloheximide at 1.25 and 5 μg/ml and we observed diminished PARP cleavage in cycloheximide-pretreated cells compared to simvastatin treatment alone (Figure 22B), confirming that simvastatin-mediated apoptosis is dependent on the presence of newly translated proteins.

Previously we have established the essential role of GTP-bound RhoA and Rac1 in simvastatin-induced apoptosis. To confirm that cycloheximide pretreatment protected cells from simvastatin by blocking the synthesis of RhoA and Rac1, we looked at the effects of cycloheximide on RhoA and Rac1 activities. Cells were pretreated with 5 μg/ml cycloheximide before 10 μM simvastatin treatment. The results showed that cycloheximide alone had no effect on the GTP-loading of RhoA or Rac1, but it completely prevented simvastatin-induced accumulation of RhoA-GTP and Rac1-GTP (Figure 22C). These observations provide an explanation for cycloheximide's protective effects, and also suggest that the newly synthesized RhoA and Rac1 are those that have accumulated in the GTP-bound form after simvastatin treatment.

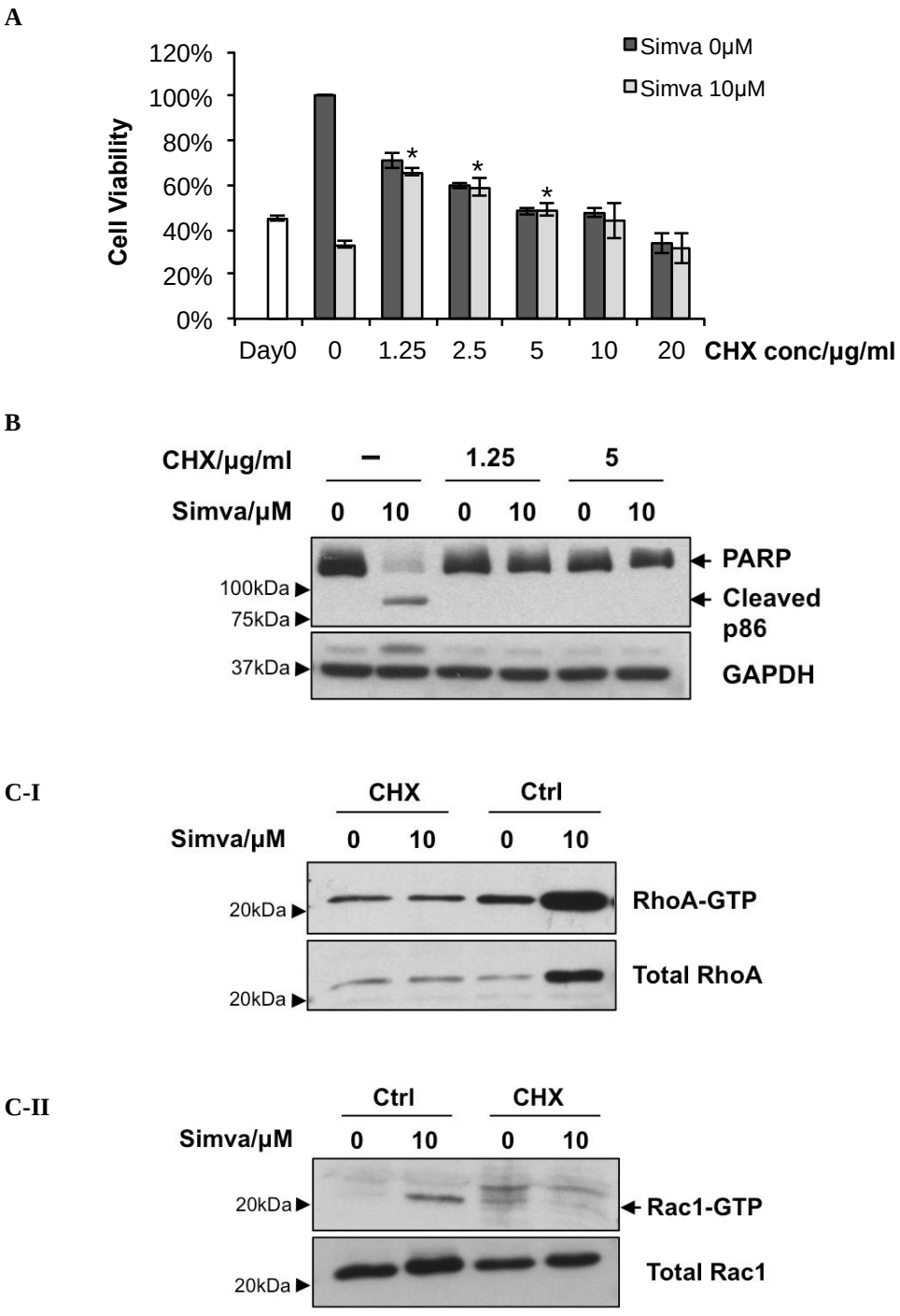

Figure 22: Cycloheximide protects cells from simvastatin-induced cell death via blocking the GTP-loading of RhoA and Rac1.

(A) HCT116 cells were preincubated with or without various concentrations of cycloheximide for 1h before treating with 10 μM simvastatin for 48 h. Cell viability was measured by crystal violet assay. The bars represent means ± s.e.m of three independent experiments. *, $p < 0.05$ compared with simvastatin treatment alone. (B) PARP cleavage was assessed 36 h post-treatment by Western blot analysis. GAPDH was included as a loading control. (C) Cells were pretreated with or without 5 μg/ml cycloheximide for 1h before treating with 10 μM simvastatin for 20 h. The GTP-loading of (I) RhoA and (II) Rac1 were prepared as described in Figure 15 and 16 and assessed by Western blot analysis.

2.5 Simvastatin increases protein levels of RhoA and Cdc42 via protein synthesis

2.5.1 Simvastatin upregulates RhoA and Cdc42 protein expression via mRNA and protein synthesis

Curious about how simvastatin upregulated protein expression of RhoA and Cdc42 in HCT116 cells, we went on to determine the mechanism for the changes in protein levels. We first checked if the accumulation of these proteins is due to *de novo* protein synthesis. Cells were incubated with cycloheximide prior to the addition of simvastatin. Cycloheximide completely prevented the simvastatin-induced increase in Rho protein, also observed in Figure 22C, indicating that the accumulation of RhoA and Cdc42 was due to newly synthesized protein (Figure 23A). Furthermore, treatment with actinomycin D, an inhibitor of gene transcription, dose-dependently ablated simvastatin-mediated increase in RhoA and Cdc42 protein expression (Figure 23B). The results suggest that mRNA and protein synthesis are involved in simvastatin-mediated increase in RhoA and Rac1 protein content.

A

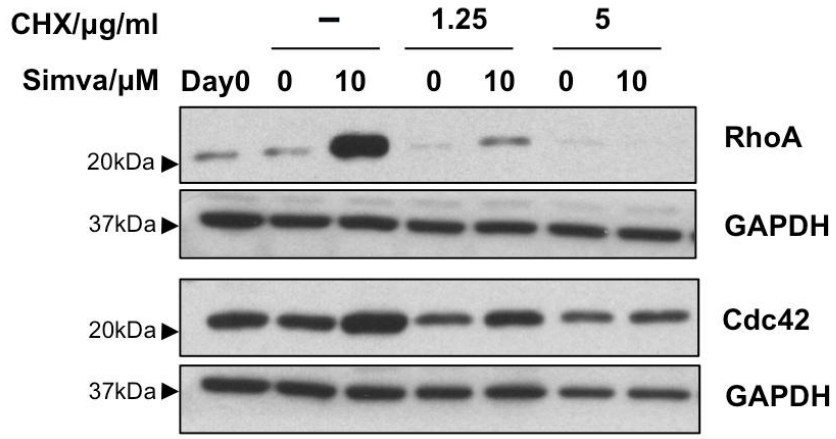

B

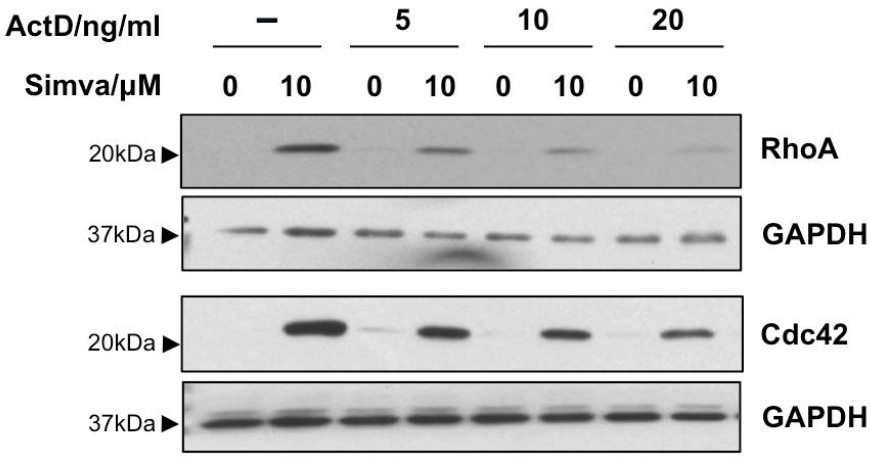

Figure 23: Simvastatin-induced upregulation of RhoA and Cdc42 protein expression is blocked by transcription and protein synthesis inhibitors.
HCT116 cells were pretreated with or without (A) cycloheximide (CHX) or (B) actinomycin D (ActD) at indicated concentrations for 1 h, followed by treatment with 10 μM simvastatin for 20 h. Lysates from Day 0 was collected prior to the above triggers. Protein levels of RhoA and Cdc42 were assessed by Western blot analysis. GAPDH was included as a loading control.

2.5.2 Simvastatin does not affect the protein degradation rate of RhoA and Cdc42

Despite the clear involvement of *de novo* protein synthesis in the regulation of RhoA and Cdc42 protein expression, previous studies have also proposed that prenylation selectively target Rho proteins for proteasomal degradation. Hence, inhibition of prenylation by statins might slow the degradation process and result in the increased protein levels (Von Zee and Stubbs 2011). We therefore explored if simvastatin regulated the protein expression of RhoA and Cdc42 via affecting their degradation rate. HCT116 cells were pretreated with cycloheximide and harvested at different time points. The decrease of both RhoA and Cdc42 protein levels was observed after 16 h in cells treated with or without simvastatin, indicating that protein degradation rate was not likely to be a factor in affecting RhoA and Cdc42 protein level (Figure 24). Taken together, these data indicate that *de novo* protein synthesis is the main contributor to the drastically increased protein expression of RhoA and Cdc42.

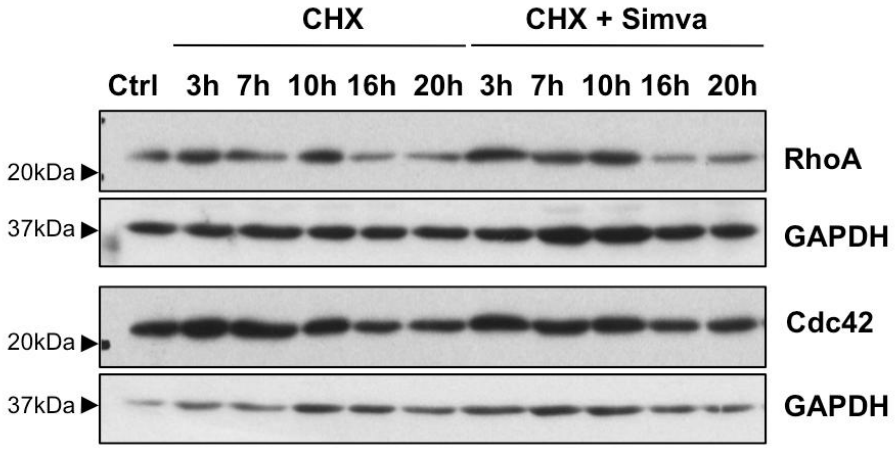

Figure 24: Simvastatin does not affect the protein degradation rate of RhoA and Cdc42.
HCT116 cells were either treated with cycloheximide 5 μg/ml alone or preincubated with cycloheximide for 1 h before addition of 10 μM simvastatin for the indicated durations. The levels of RhoA and Cdc42 were assessed by Western blot analysis. GAPDH was included as a loading control.

3. Simvastatin induces superoxide production as an early signal to initiate cell death in HCT116 cells

After establishing that simvastatin induces active RhoA and Rac1 to mediate the apoptotic process, we set out to identify potential downstream targets involved in our cell death model. Reactive oxygen species (ROS), particularly superoxide came under investigation for a couple of reasons. Firstly, previous reports from our lab and other research groups have provided evidence that intracellular ROS participate in early signaling for apoptotic execution. Secondly, several reports have suggested the role of oxidative stress in statin-induced apoptosis in cancer cells (Laezza, Fiorentino et al. 2008; Sanchez, Rodriguez et al. 2008; Qi, Kim et al. 2010). Most importantly, both active RhoA and Rac1 have been found to be associated with superoxide production by regulating the activation of superoxide generator nicotinamide adenine dinucleotide phosphate-oxidase (NADPH) complex (Babior 1999; Bokoch and Diebold 2002; Kim, Diebold et al. 2004). Hence, we asked if superoxide might play a role in mediating the signal from the activation of RhoA and Rac1 to apoptosis upon simvastatin treatment in HCT116 cells.

3.1 Simvastatin increases superoxide level in a time-dependent manner.

We first monitored intracellular superoxide level using lucigenin chemiluminiscence assay. Lucigenin, bis-N-methylacridiniumdinitrate, has been used extensively as a luminescent indicator of superoxide production. Luminescence occurs via reaction between superoxide and the reduced form of lucigenin (lucigenin cation radical LCU+) to form an unstable dioxetane, whose decomposition yields acridone to emit light (Liochev and Fridovich 1997). HCT116 cells were treated with simvastatin over different duration (3-24 h), and the superoxide level was compared to that in the

untreated cells (Figure 25A). The results showed significant and sustained increment of superoxide production from 4 h up to 24 h post-treatment (1.2 ± 0.14 fold increase after 6 h treatment, 1.51 ± 0.08 fold increase after 24 h treatment compared to untreated cell, $p < 0.05$). The level of superoxide was maintained at around 1.5 fold increase at 8, 16, 20 and 24 h post-treatment.

A second technique was used to confirm the superoxide production after simvastatin treatment, namely the dihydroethidium (DHE) assay. The DHE dye permeates the cell membrane freely and reacts with superoxide anions to form a red fluorescent product that intercalates with DNA. This dye is specific to superoxide as it is less prone to oxidation by other ROS molecules (Robinson, Janes et al. 2006; Zielonka, Vasquez-Vivar et al. 2008). HCT116 cells were treated with simvastatin for 16, 20 and 24 h (Figure 25B). The results showed significant increase in fluorescence at all three times points. Density plot of cells after 24 h simvastatin treatment was displayed as cell size against the florescence detected, and it showed a right shift of cell population, which represented the increase in superoxide production. In addition, both assays showed comparable fold increase in superoxide level after simvastatin treatment, confirming that simvastatin's ability to generate superoxide in this model.

A

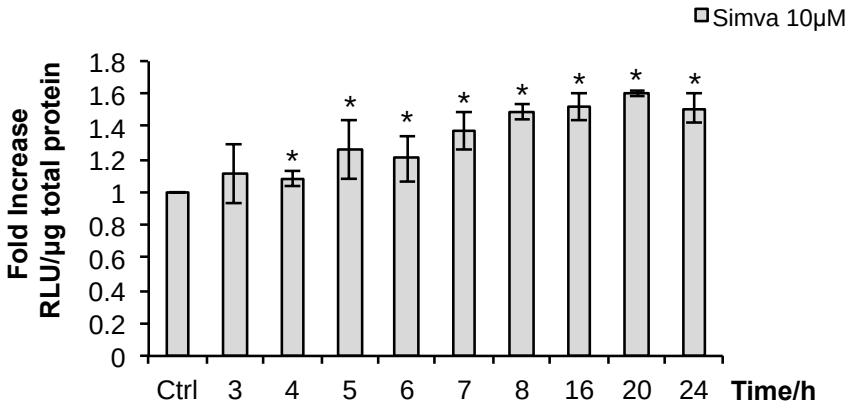

B

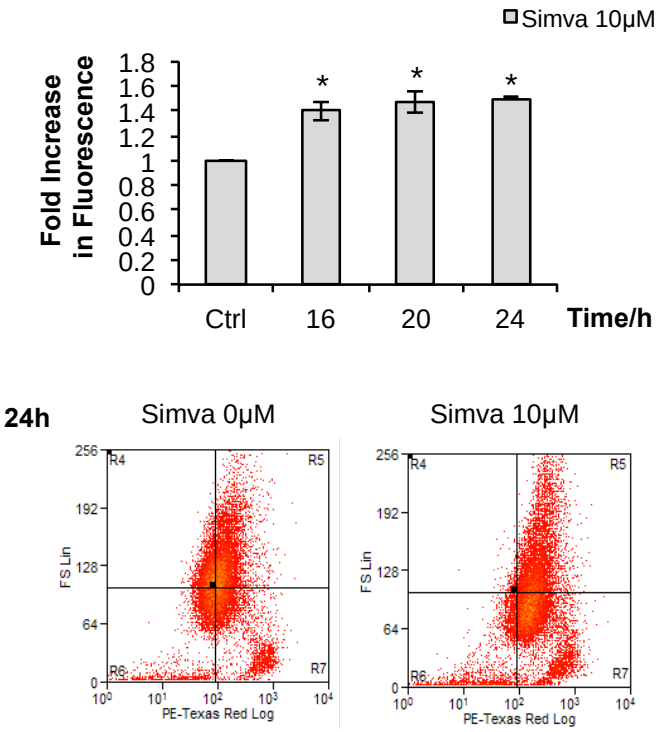

Figure 25: Simvastatin increases superoxide level in HCT116 cells.
HCT116 cells were treated with 10 μM simvastatin for the indicated duration. Intracelluar superoxide level was assessed by (A) lucigenin chemiluminesence assay and (B) DHE assay as described in Materials & Methods. The level of superoxide was expressed as fold increase over untreated cells. Density plots after 24 h simvastatin treatment were displayed as cell size (FS Lin) against DHE fluorescence (PE-Texas Red). The bars represent means ± s.e.m of three independent experiments. *, $p < 0.05$ compared with untreated control cells.

3.2 Superoxide scavengers confer cells resistance to simvastatin-induced cell death

After determining the ability of simvastatin to generate superoxide, the next logical question was whether the production of superoxide was integral in the execution of cell death. To do this, we utilized three superoxide scavengers to reduce superoxide level in the cells. Diphenyleneiodonium (DPI), a known flavoenzyme inhibitor, inhibits the assembly of the superoxide-generator NADPH oxidase complex; while tempol and tiron are mimetics of superoxide dismutase (SOD), the enzyme responsible for clearing superoxide by converting it into hydrogen peroxide. HCT116 cells were preincubated with the scavenger for 2h before treatment with simvastatin. All three scavengers successfully abrogated simvastatin-induced superoxide production (Figure 26A). Remarkably, preincubation with all superoxide scavengers largely reduced simvastatin-induced apoptosis (Figure 26B) (79.12 ± 1.71% cell viability with DPI preincubation, 77.98 ± 5.67% cell viability with tempol preincubation, 78.84 ± 7.02% cell viability with tiron preincubation *vs.* 33.28 + 1.26% with 10 μM simvastatin alone, $p < 0.05$). The rescue effects were also shown by morphological examination, where cell shrinkage observed in simvastatin-treated cells was reversed with preincubation with the scavengers (Figure 26C). In addition, we also observed that proteolytic processing of caspase-3 as well as the activity levels of caspase-3, -8, -9 were significantly reduced in superoxide scavenger-pretreated cells compared to cells treated with simvastatin alone (Figure 26D, E). All the observations support the notion that superoxide plays an essential role in simvastatin-induced cell death in HCT116 cells.

A

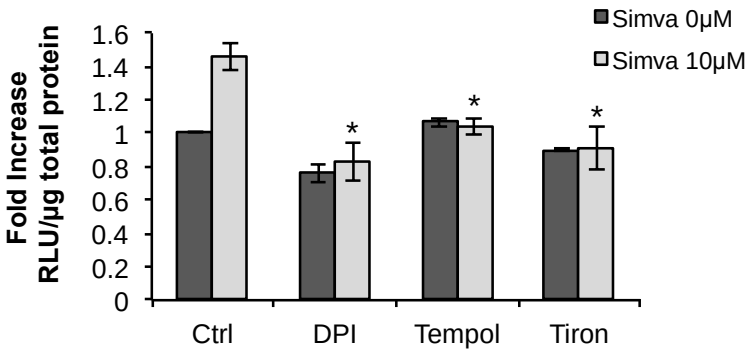
Simva 0μM
Simva 10μM
Fold Increase RLU/μg total protein
1.6
1.4
1.2
1
0.8
0.6
0.4
0.2
0
*
*
*
Ctrl
DPI
Tempol
Tiron

B

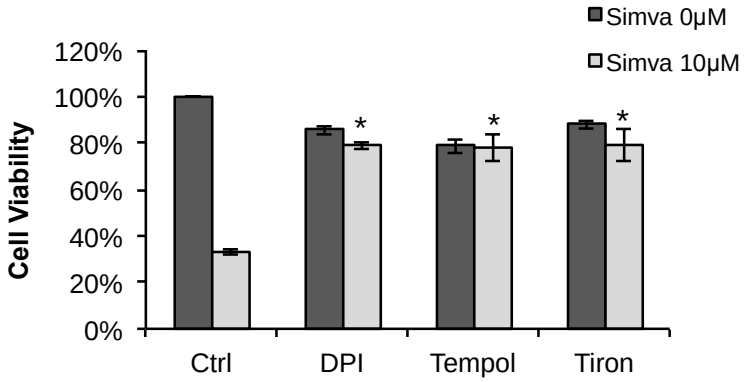
Simva 0μM
Simva 10μM
Cell Viability
120%
100%
80%
60%
40%
20%
0%
*
*
*
Ctrl
DPI
Tempol
Tiron

C

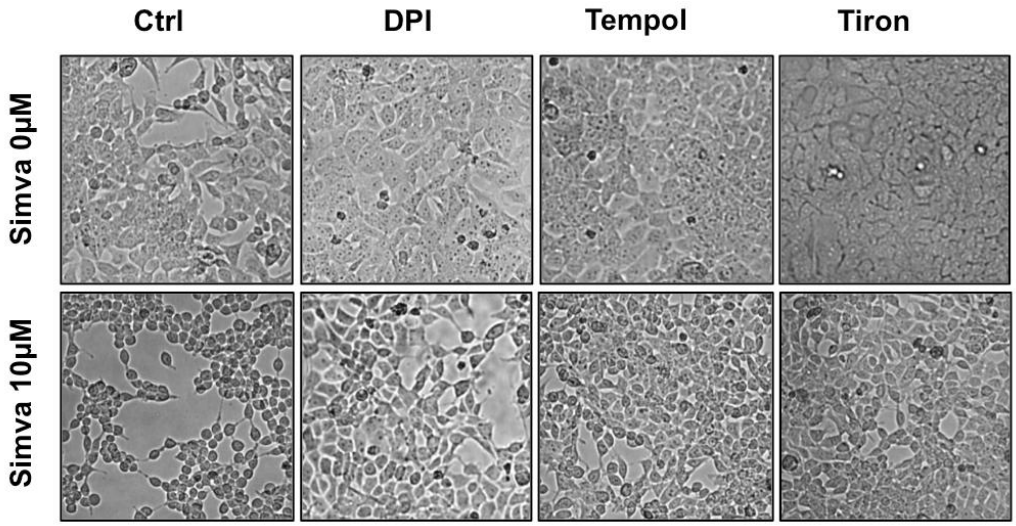
Ctrl
DPI
Tempol
Tiron
Simva 0μM
Simva 10μM

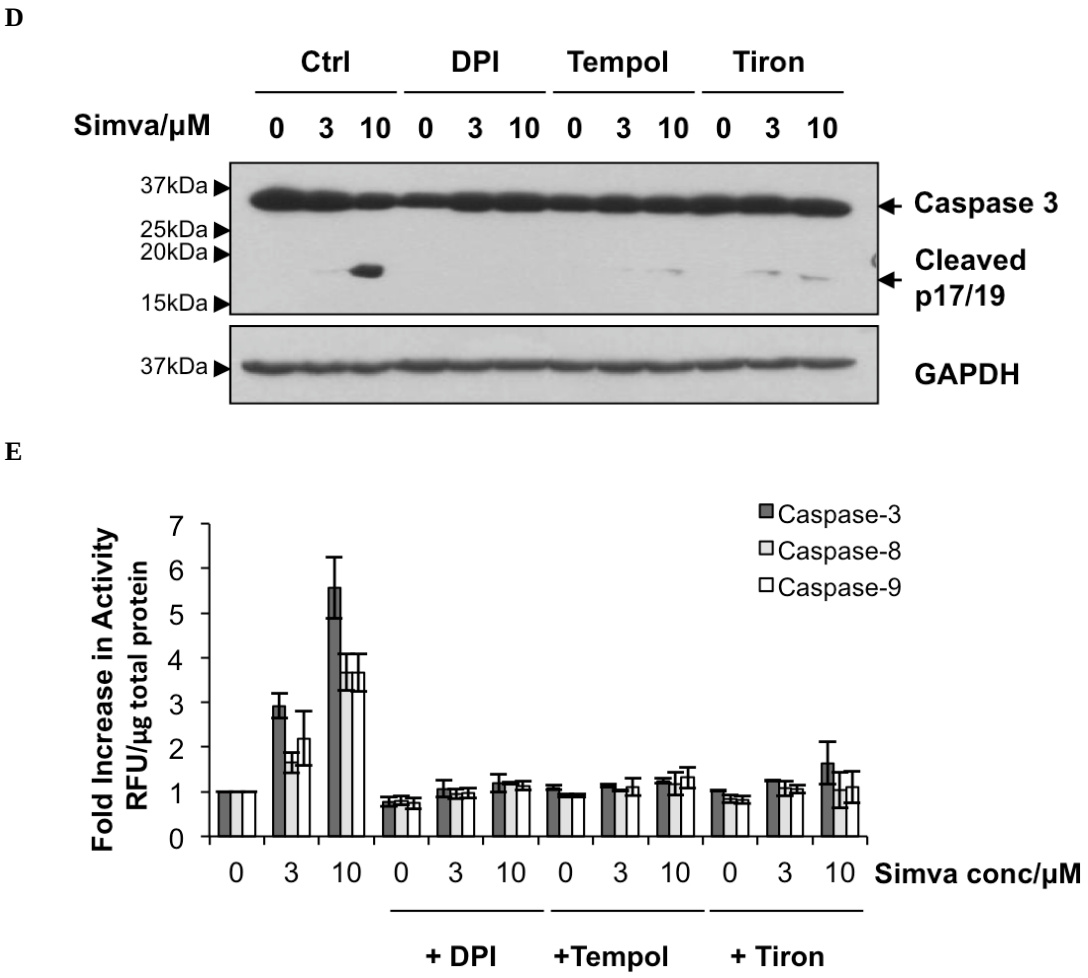

Figure 26: Superoxide scavengers protect cells from simvastatin-mediated cell death.
HCT116 cells were preincubated with or without 5 μM DPI, 2.5 mM tempol or 10 mM tiron for 2 h before treatment with 3 or 10 μM simvastatin. (A) Successful inhibition of superoxide production after 24 h treatment was measured by lucigenin chemiluminesence assay. DPI/tempol/tiron-mediated rescue of cell death was assessed by (B) cell viability measured by crystal violet assay,(C) morphological examination after 28 h treatment with phase-contrast microscopy (Magnification: 100X). (D) (I) Proteolytic processing of caspase-3 and (II) Activities of caspase-3, -8 and -9 were assessed after 36 h of simvastatin treatment. The bars represent means ± s.e.m of three independent experiments. *, $p < 0.05$ compared with simvastatin treatment alone.

3.3 Simvastatin induces superoxide production involving GTP-bound RhoA and Rac1

3.3.1 Simvastatin increases superoxide level by blocking protein geranylgeranylation

In the earlier sessions, we have confirmed that simvastatin-induced apoptosis was dependent on protein geranylgeranylation. Stimulated by the identification of superoxide in the cell death mechanism, we were interested to find out the relationship between superoxide production and the geranylgeranylation process. Cells were preincubated with different isoprenylation precursors: MVA, GGPP or FPP before simvastatin treatment and superoxide level of treated cells were assessed by lucigenin chemiluminescence assay (Figure 27A). It was observed that the increased superoxide production by simvastatin alone was fully blocked in cells preincubated with MVA and GGPP; while FPP preincubation did not reduce superoxide level induced by simvastatin. Of note, preincubation with different compounds alone had no significant changes in superoxide level. To further confirm the involvement of geranylgeranylated proteins in inducing superoxide production after simvastatin treatment, we treated cells with GGTI-298 or FTI-277 (Figure 27B). In agreement with the rescuing effects of GGPP preincubation on superoxide level, GGTI-298 treatment increased superoxide production, but not FTI-277 (1.46 ± 0.21 fold increase after simvastatin treatment, 1.36 ± 0.27 fold increase after GGTI-298 treatment and 1.06 ± 0.01 fold increase after FTI-277 treatment compared to untreated cell). Our findings indicate that simvastatin-mediated superoxide production is a downstream event of protein geranylgeranylation.

A

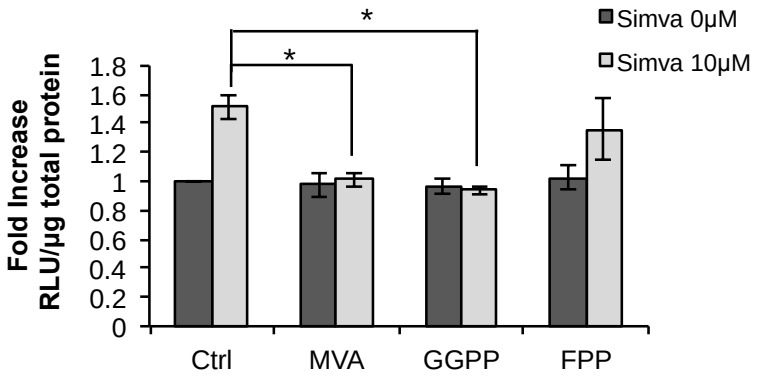

B

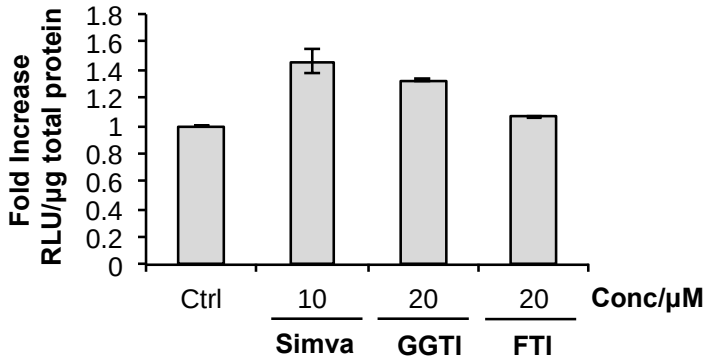

Figure 27: Simvastatin induces superoxide production via blockage of GGPP synthesis.
(A) HCT116 cells were preincubated with or without 100 μM MVA, 10 μM GGPP or 10 μM FPP for 2h before treatment with 10 μM simvastatin for 24 h; (B) Cells were treated with simvastatin, GGTI-298 or FTI-277 at indicated doses for 24 h. In both panels, superoxide level was then assessed by lucigenin chemiluminesence assay. The bars represent means ± s.e.m from three independent experiments. *, $p < 0.05$ compared with untreated control cells.

3.3.2 Blocking RhoA and Rac1 activities inhibits simvastatin-mediated superoxide production

Since our data suggested that simvastatin induced superoxide production via blocking protein geranylgeranylation, we explored whether the earlier-identified RhoA and Rac1 activation was directly involved in superoxide production. To that end, we utilized multiple ways to block the activation of RhoA and Rac1 in HCT116 cells (the same tools used in the experiments of Figure 18-20) and monitored the superoxide level after simvastatin treatment. Pretreatment with Rac1 inhibitor NSC23766 significantly reduced superoxide level compared to cells treated with simvastatin alone (Figure 28A). In addition, introduction of dominant-negative Rac1 plasmid Rac1N17 exerted the same reducing effects on the superoxide level (Figure 28B). Rac1 inhibitor and Rac1N17 plasmid transfection alone reduced 10%-15% superoxide level compared to untreated cells. Transient knockdown of Rac1 or RhoA, but not Cdc42 also attenuated simvastatin-induced superoxide production (Figure 28C). These observations imply that simvastatin-mediated activation of RhoA and Rac1 is the upstream signal for superoxide production.

A

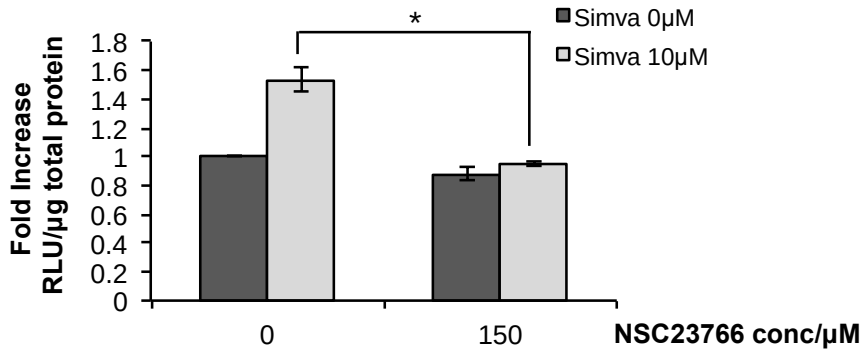

B

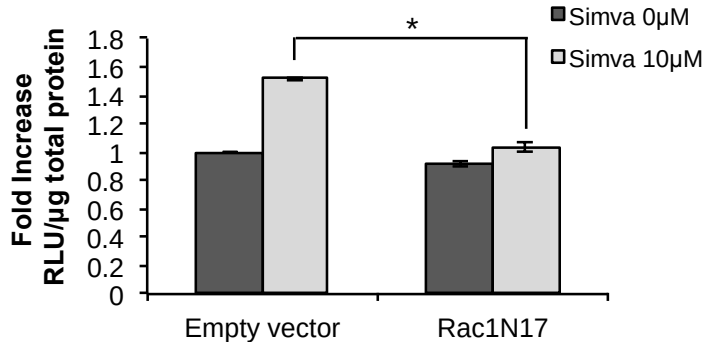

C

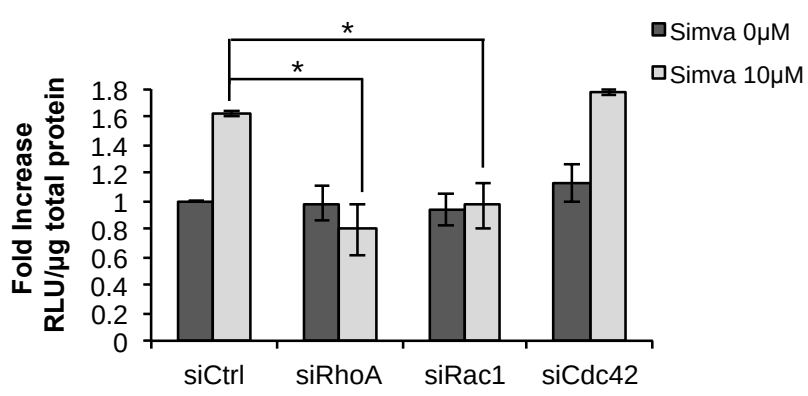

Figure 28: Blocking Rac1 and RhoA activation abrogates simvastatin-mediated superoxide production.
(A) HCT116 cells were preincubated with or without 150 μM NSC23766 for 2 h before treatment with 10 μM simvastatin; (B) Cells were transfected with either pIRES empty vector or Rac1N17 plasmid as previously described and confirmed in Figure 19A. (C) RhoA, Rac1 or Cdc42 were knocked down in HCT116 cells as previously described and confirmed in Figure 20A. In all panels, superoxide level was then assessed after 24 h of simvastatin treatment at 10 μM by lucigenin chemiluminesence assay. The bars represent means ± s.e.m from three independent experiments. *, $p < 0.05$ compared with simvastatin treatment alone.

3.3.3 Simvastatin-mediated superoxide production does not affect protein levels of Rho proteins

The evidence provided so far indicates that simvastatin induces activation of RhoA and Rac1, which then activates the downstream superoxide generation and eventually leads to apoptosis. In this regard, there is evidence from prior studies for redox regulation of Rho GTPases (Mitchell, Hobbs et al. 2012). Hence, we were interested to determine whether simvastatin-induced superoxide production might regulate RhoA, Rac1 and Cdc42 in a feedback manner. Since we have shown that the Rho proteins activated upon simvastatin treatment were newly synthesized (Figure 22), we checked the protein levels of RhoA, Rac1 and Cdc42 after preincubation with superoxide scavenger DPI or tempol followed by simvastatin treatment. The results showed that both DPI and tempol pretreatment did not modulate Rho protein expression after simvastatin treatment (Figure 29). The findings suggest that simvastatin-induced superoxide production is downstream of the activation of Rho GTPases and does not affect Rho GTPases in a feedback fashion.

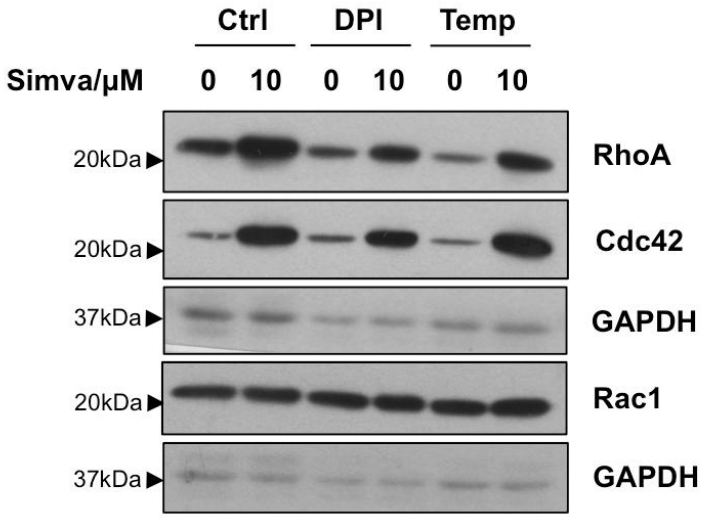

Figure 29: Superoxide scavengers do not affect Rho protein expressions after simvastatin treatment.
HCT116 cells were preincubated with or without 5 μM DPI or 2.5 mM tempol for 2 h before treating with 10 μM simvastatin for 24 h, protein levels of RhoA, Rac1 and Cdc42 were assessed by Western blot analysis. GAPDH was included as a loading control.

4. Simvastatin activates stress response JNK pathway to mediate the cell death response in HCT116 cells

To identify the signaling pathways that hold a role in simvastatin-induced apoptosis, we then evaluated the potential involvement of MAPKs (mitogen-activated protein kinases) and AKT signaling cascades. These signaling pathways are activated through phosphorylation of the kinases on specific residues and they mediate the effects of a wide array of biological processes, such as cellular proliferation, differentiation, cell survival and cell death (Seger and Krebs 1995; Kennedy, Wagner et al. 1997). More importantly, growing evidence is suggesting that both Rho GTPases and ROS are potent regulators of MAPKs and AKT pathways (Hall 2005; Kamata, Honda et al. 2005; Clerkin, Naughton et al. 2008). Hence, we set out to identify if one or more of these signaling pathways were affected and responsible for the apoptotic response following simvastatin treatment.

4.1 Simvastatin activates JNK signaling by blocking protein geranylgeranylation

HCT116 cells were treated with 10 μM simvastatin for the indicated duration. The phosphorylation status of MAPK family members ERK and JNK, as well as survival pathway AKT was assessed by Western blot analysis. Dephosphorylation of AKT and ERK (p42 and p44) started from 6 h and became more obvious and sustained from 9 to 18 h post-treatment. On the contrary, stress-activated JNK signaling was upregulated after simvastatin treatment, which was shown by the increased and sustained phosphorylation of JNK (p54 and p46) at both Thr183 and Tyr185 residues (Figure 30). Of note, simvastatin did not affect the total protein levels of these kinases.

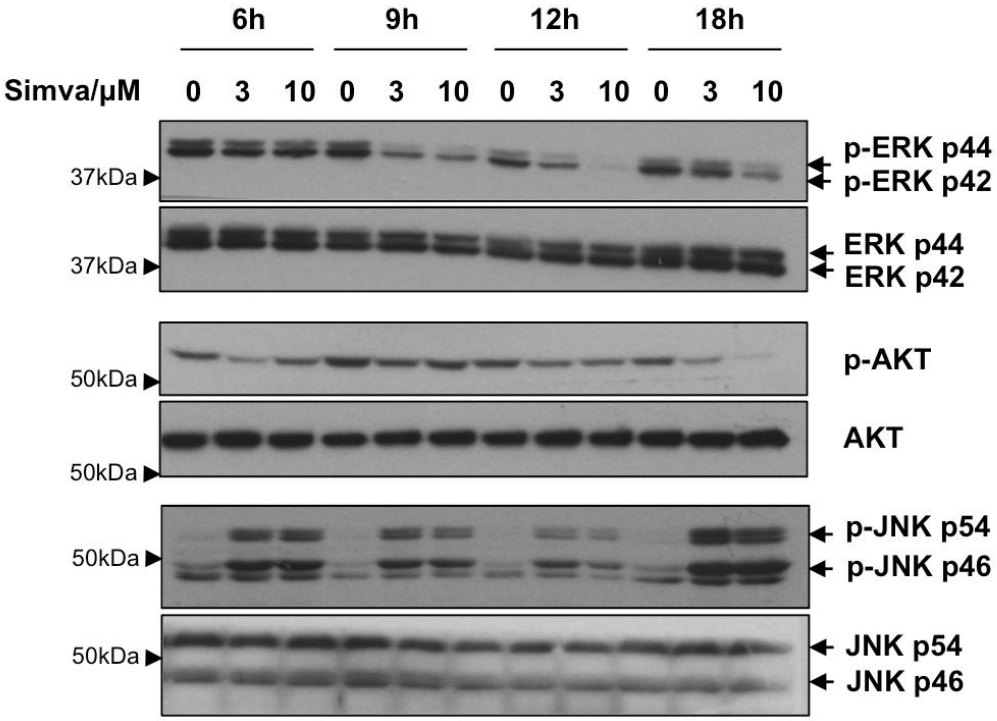

Figure 30: Simvastatin dephosphorylates AKT and ERK but induces JNK phosphorylation. HCT116 cells were treated with 3 or 10 μM simvastatin for the indicated duration. The phosphorylated and total protein levels of AKT, ERK and JNK were assessed by Western blot analysis. GAPDH was included as a loading control.

To assess the involvement of these kinases in our model, we first studied if the phosphorylation or dephosphorylation effects after simvastatin treatment were downstream of the geranylgeranylation process. Cells were incubated with different isoprenylation precursors: MVA, GGPP or FPP, before treatment with simvastatin. Although MVA preincubation fully reversed the dephosphorylation of AKT and ERK upon simvastatin treatment, neither GGPP nor FPP preincubation had any effect on simvastatin-induced dephosphorylation process (Figure 31A), suggesting that simvastatin's effects on AKT or ERK might not be of primary importance in the cell death response that is identified to be dependent on protein geranylgeranylation. Interestingly, JNK pathway stood out as a potential downstream target, where phosphorylation of JNK was fully blocked with MVA preincubation and largely prevented with GGPP pretreatment, while FPP preincubation did not reduce simvastatin-induced JNK phosphorylation (Figure 31B). Furthermore, JNK phosphorylation was also observed in cells treated with GGTI-298, which specifically blocks protein geranylgeranylation, but not in cells with FTI-277 treatment. These observations suggest that JNK signaling pathway might be involved in relaying the cell death response upon simvastatin treatment.

A-I

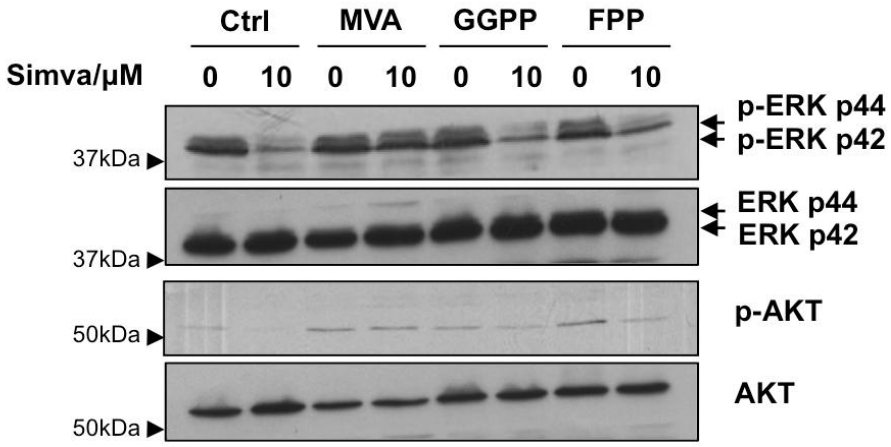

A-II

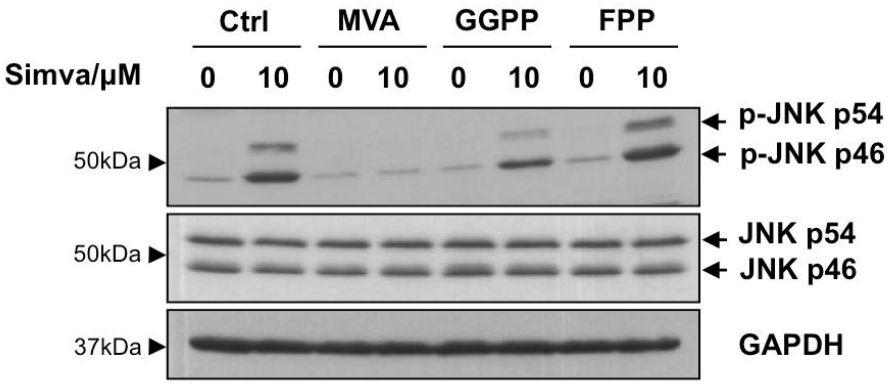

B

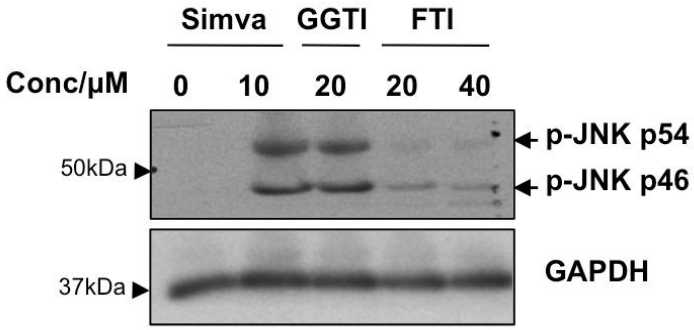

Figure 31: Simvastatin activates JNK pathway via blocking protein geranylgeranylation.
(A) HCT116 cells were preincubated with or without 100 μM MVA, 10 μM GGPP or 10 μM FPP for 2 h before treatment with 10 μM simvastatin for 24 h, phosphorylated and total protein levels of (I) AKT, ERK and (II) JNK were assessed by Western blot analysis. (B) Cells were treated with simvastatin, GGTI-298 or FTI-277 alone at indicated doses for 24 h. Phospho-JNK level was assessed by Western blot analysis. GAPDH was included as a loading control.

4.2 JNK inhibitor SP600125 rescues simvastatin-induced cell death phenotype

To confirm the functional relevance of JNK activation in our model, we performed experiments to effectively block JNK activation with the use of pharmacological inhibitor SP600125, a competitive inhibitor of ATP binding to JNK kinase (Bennett, Sasaki et al. 2001). Successful inhibition of the JNK signaling was shown as the decreased phosphorylation of its downstream effector c-Jun (Figure 32A). Remarkably, pretreatment with SP600125 reversed cell death phenotype induced by simvastatin in HCT116 cells to a large extent measured by crystal violet assay (Figure 32B) (61.23 ± 2.3% cell viability with SP600125 preincubation *vs.* 33.28 ± 1.26% with 10 μM simvastatin alone, $p < 0.05$). In addition, morphological examination also revealed that SP600125 preincubation restored normal morphology to cells akin to untreated control (Figure 32C). The observation was further confirmed in long-term clonogenic assay, where SP600125 pretreatment exerted cytoprotective effect in simvastatin-treated cells (Figure 32D). All these observations indicate the JNK activation is an important mediator in simvastatin-induced apoptosis.

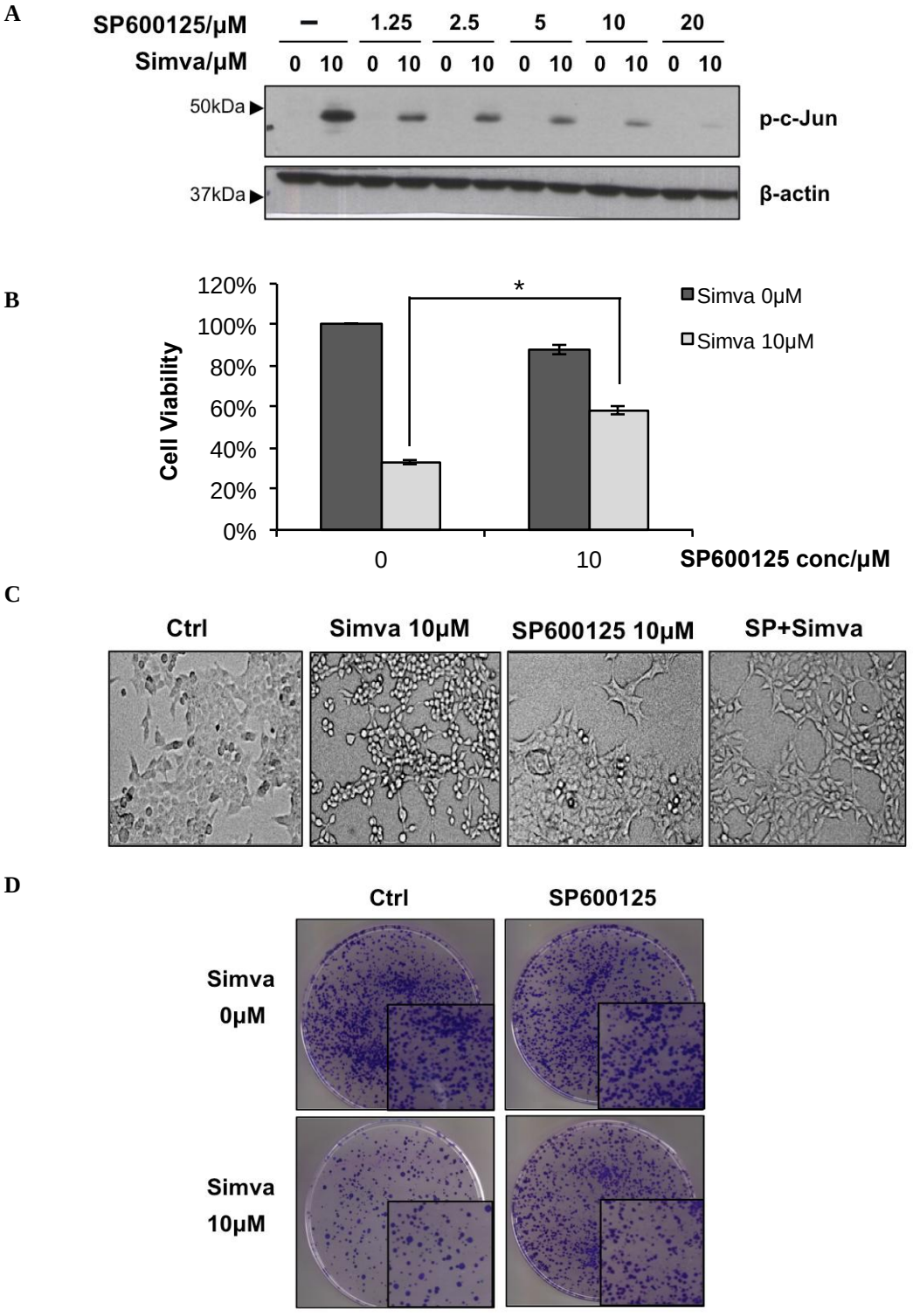

Figure 32: JNK inhibitor SP600125 partially rescues cells from simvastatin-induced cell death. HCT116 cells were preincubated with or without SP600125 at indicated doses for 2 h before treatment with 10 μM simvastatin. (A) Successful inhibition of JNK signaling was confirmed by downregulation of phospho-c-Jun levels shown by Western blot analysis. β-actin was included as a loading control. (B) Cell viability after 48 h simvastatin treatment was measured by crystal violet assay. The bars represent means ± s.e.m from three independent experiments. *, $p < 0.05$ compared with simvastatin treatment alone. (C) Cell morphology aft 28 h treatment was examined with phase-contrast microscopy (Magnification: 100X). (D) Photos of colonies formed by cells after 30 h of simvastatin treatment.

4.3 Simvastatin-mediated JNK activation is downstream of RhoA and Rac1 activation and superoxide production

Having shown earlier that JNK was robustly activated by simvastatin and it was a critical signal for apoptosis, an important question been whether the activation of JNK was linked to simvastatin-induced activation of RhoA and Rac1 and increased superoxide production in any way. Hence, we first checked the status of JNK phosphorylation after blockade of RhoA and Rac1 activities or superoxide production. Then we assessed the impact of inhibiting JNK signaling on the status of Rho GTPases and superoxide production.

4.3.1 Blocking RhoA and Rac1 activities prevents simvastatin-induced JNK activation

To assess the relevance of simvastatin-induced JNK activation to the activation of RhoA and Rac1, we utilized aforementioned ways (pharmacological inhibition of Rac1, expression of dominant negative Rac1N17, and gene silencing of RhoA or Rac1) to inhibit RhoA or Rac1 activity and studied their effects on JNK phosphorylation on both Thr183 and Tyr185 residues. As shown in Figure 33, pretreatment with Rac1 inhibitors NSC23766 and EHT 1864 and silencing of RhoA almost fully inhibited JNK phosphorylation upon simvastatin treatment (Figure 33A, B). Although cells transfected with exogenously-introduced dominant negative Rac1 mutant and Rac1 knockdown did not show as prominent reduction in phosphorylated JNK as compared to other methods, the discrepancy was probably due to the relatively low transfection efficiency seen in Figure 19A and 20. Overall, these findings suggest that JNK signaling is downstream of RhoA and Rac1 activation.

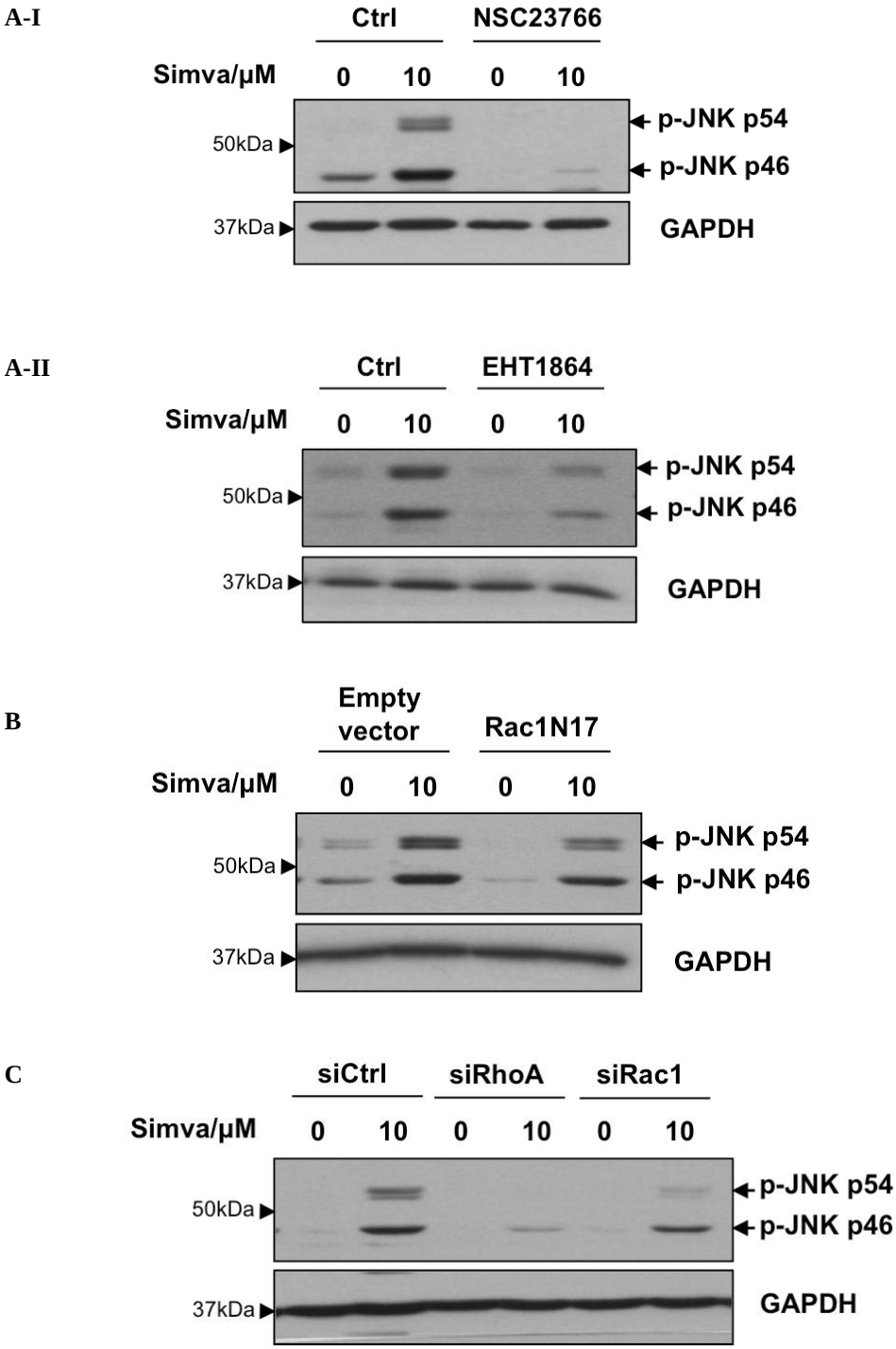

Figure 33: Blocking RhoA and Rac1 activation downregulates JNK activation after simvastatin treatment.

(A) HCT116 cells were preincubated with or without (I) 150 μM NSC23766 or (II) 20 μM EHT1864 for 2 h before simvastatin treatment; (B) Cells were transfected with either pIRES empty vector or Rac1N17 plasmid as previously described and confirmed in Figure 19A. (C) RhoA or Rac1 were knocked down in HCT116 cells as previously described and confirmed in Figure 20A. In all panels, phospho-JNK level after treatment with 10 μM simvastatin for 24 h was assessed by Western blot analysis. GAPDH was included as a loading control.

4.3.2 Inhibiting superoxide production prevents simvastatin-mediated JNK activation

After establishing that simvastatin-induced JNK activation was a downstream target of active RhoA and Rac1, we then set out to study the link between JNK phosphorylation and superoxide production after simvastatin treatment. HCT116 cells were preincubated with superoxide scavengers DPI, tempol or tiron before simvastatin treatment, and the ability of these scavengers to block JNK activation was assessed. Western blot results revealed that all three scavengers significantly reduced JNK phosphorylation on both Thr183 and Tyr185 residues (Figure 34). The observation suggests that JNK activation is likely to be downstream of superoxide production following simvastatin treatment

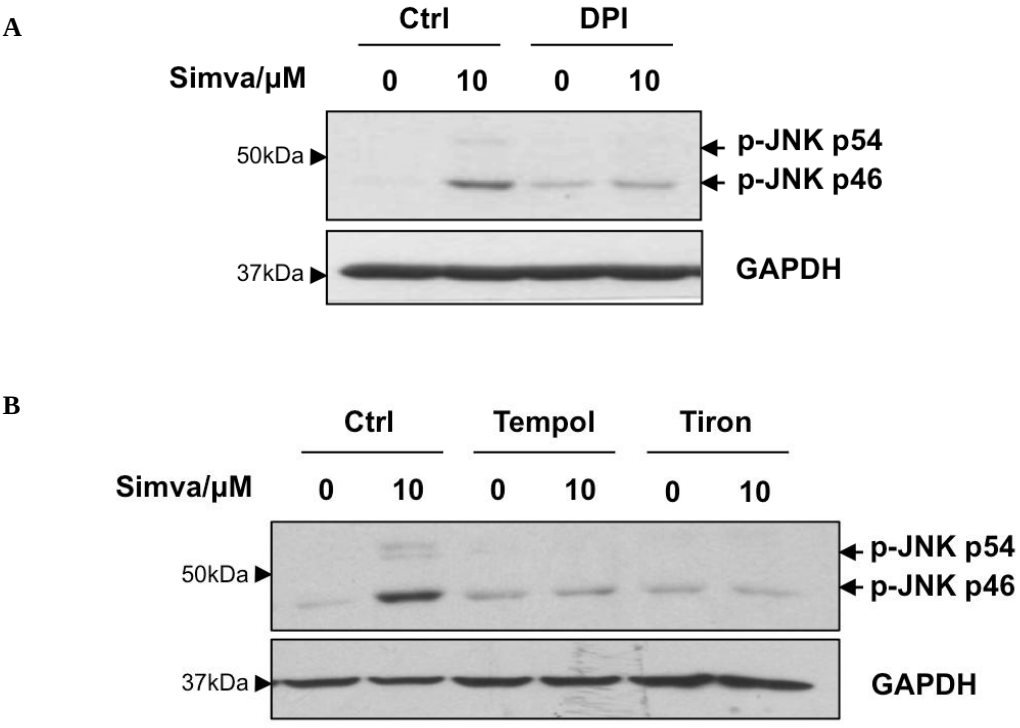

Figure 34: Superoxide scavengers inhibit simvastatin-mediated JNK activation.
HCT116 cells were preincubated with or without (A) 5 μM DPI or (B) 2.5 mM tempol or 10 mM tiron for 2 h before treating with 10 μM simvastatin for 24 h. Phospho-JNK protein expression was assessed by Western blot analysis. GAPDH was included as a loading control.

4.3.3 Inhibiting JNK signaling did not affect simvastatin-induced changes in Rho protein expression and superoxide level

Having demonstrated that simvastatin activated JNK signaling to mediate the apoptotic response, and identified that JNK activation was downstream of RhoA and Rac1 activation and superoxide production, we then checked the effects of JNK signaling on Rho status and superoxide production upon simvastatin treatment. Cells were pretreated with SP600125 to inhibit JNK signaling as previously shown in Figure 32. This pretreatment did not have any impacts on the protein levels of RhoA, Rac1 and Cdc42 upon simvastatin treatment (Figure 35A). In addition, inhibiting JNK signaling did not affect the increase in intracellular superoxide level induced by simvastatin (Figure 35B). In summary, the studies indicate that simvastatin-mediated JNK signaling is a downstream event of RhoA and Rac1 activation and superoxide production, and that no feedback loops are apparent among these players.

A

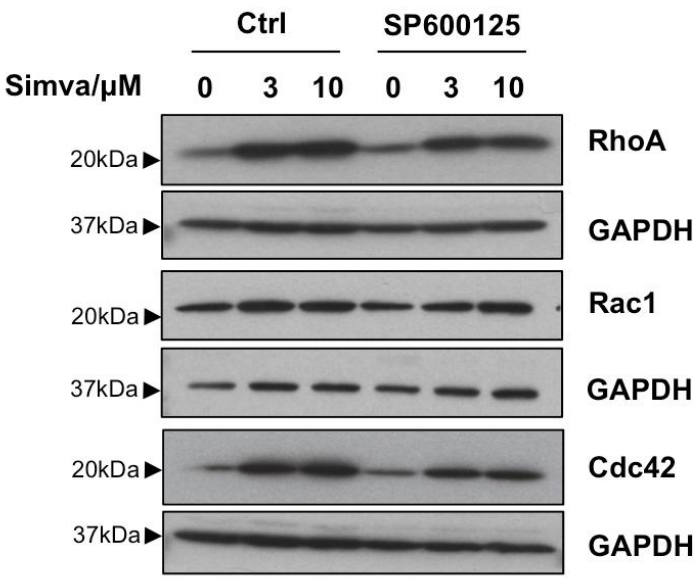

B

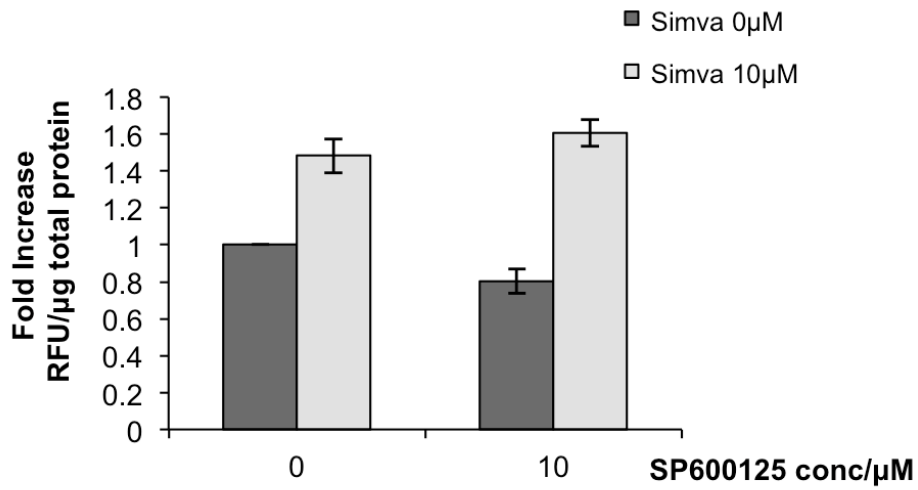

Figure 35: JNK inhibitor does not affect simvastatin-mediated upregulation of Rho proteins and superoxide production.
HCT116 cells were preincubated with or without 10 μM SP600125 for 2 h before treatment with 10 μM simvastatin for 24 h. (A) The levels of RhoA, Rac1 and Cdc42 were assessed by Western blot analysis. GAPDH was included as a loading control. (B) Superoxide level was assessed by lucigenin chemiluminesence assay. The bars represent means ± s.e.m from three independent experiments.

5. Simvastatin upregulates the expression of pro-apoptotic Bcl-2 family member Bim-EL to induce apoptosis

The identification of JNK pathway as a key signaling component in mediating simvastatin's apoptotic response has prompted us to identify its potential downstream effectors in HCT116 cells. JNK has been identified to promote mitochondria-mediated apoptosis by transcriptional upregulation of pro-apoptotic genes or by directly affecting the activities of mitochondrial pro- and anti-apoptotic proteins through distinct phosphorylation events (Dhanasekaran and Reddy 2008). One group of the proteins regulated by JNK is the Bcl-2 family members, whose role in the initiation of mitochondrial apoptotic pathway is well established (Gross, McDonnell et al. 1999). Hence, we continued to explore the potential involvement of Bcl-2 family members in our cell death model.

5.1 Simvastatin upregulates protein level of Bim-EL

The impact of simvastatin treatment on the protein levels of selected Bcl-2 family members, namely, Bcl-xL, an anti-apoptotic protein; and Bim and Bid, BH-3 only members which can directly and indirectly activates Bax (Czabotar, Colman et al. 2009) were assessed. Two other BH-3 only members, PUMA and NOXA, were not studied as we established earlier that the cell death was independent of p53 (Figure 8), and these members are found to be critical mediators of p53-dependent apoptosis (Yu and Zhang 2005). HCT116 cells were treated with 10 μM simvastatin for varying duration. Western blot analysis showed that simvastatin did not affect protein levels of Bcl-xL and Bid. No signs of cleaved-Bid (t-Bid) at 15 kDa were observed after simvastatin treatment. Interestingly, simvastatin increased protein expression of pro-

apoptotic protein Bim, in its extra long form (Bim-EL). This upregulation was observed to be sustained throughout the whole time course (16-32 h) (Figure 36).

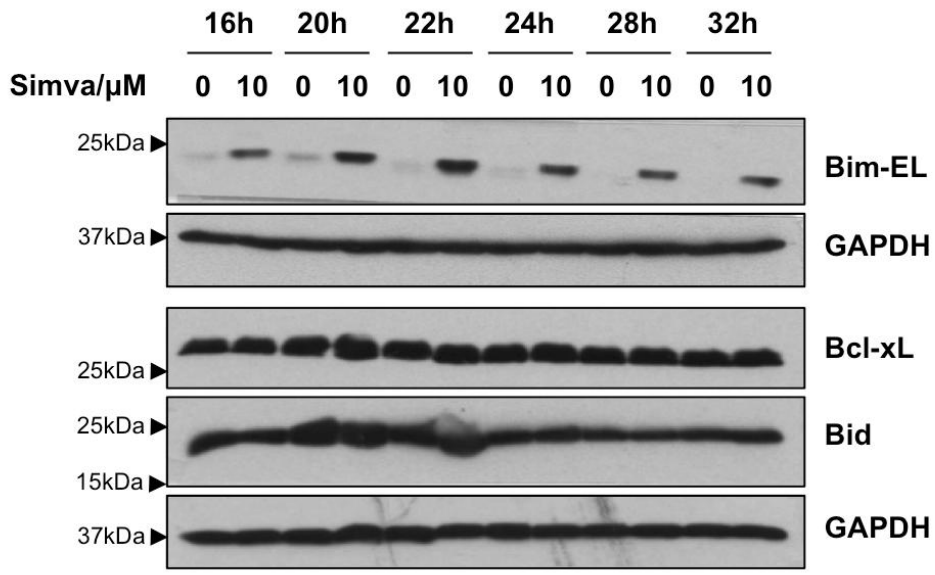

Figure 36: Simvastatin increases Bim-EL expression.
HCT116 cells were treated with 10 μM simvastatin for the indicated duration. Bcl-xL, Bid and extra-long form of Bim (Bim-EL) were assessed by Western blot analysis. GAPDH was included as a loading control.

5.2 Knockdown of Bim-EL protects cells from simvastatin-induced apoptosis

To ascertain if simvastatin-mediated apoptosis was a function of increased Bim-EL protein expression, we suppressed the expression of this protein with RNAi knockdown. Firstly, we confirmed successful knockdown of Bim-EL with one single siRNA sequence (siBim#0) assessed by Western blot analysis. Then the effects on cell viability were illustrated by crystal violet assay (Figure 37A). Notably, Bim-EL knockdown significantly rescued cells from simvastatin-induced viability loss (66.58 ± 6.63% cell viability with siBim#0 *vs.*32.6 ± 1.57% with siCtrl after 10 μM simvastatin treatment, $p < 0.05$). We then extended our study from one single siRNA sequence (siBim#0) to another three independent siBim sequences (siBim#1, #2, #3). All three sequences were able to fully abolish simvastatin-induced increase in Bim-EL protein level. Corroborating well with the cell viability data, the extent of caspase-3 and PARP cleavage was greatly reduced in cells knocked down with Bim-EL compared to cells transfected with scrambled siRNA (siCtrl) after simvastatin treatment (Figure 37B).

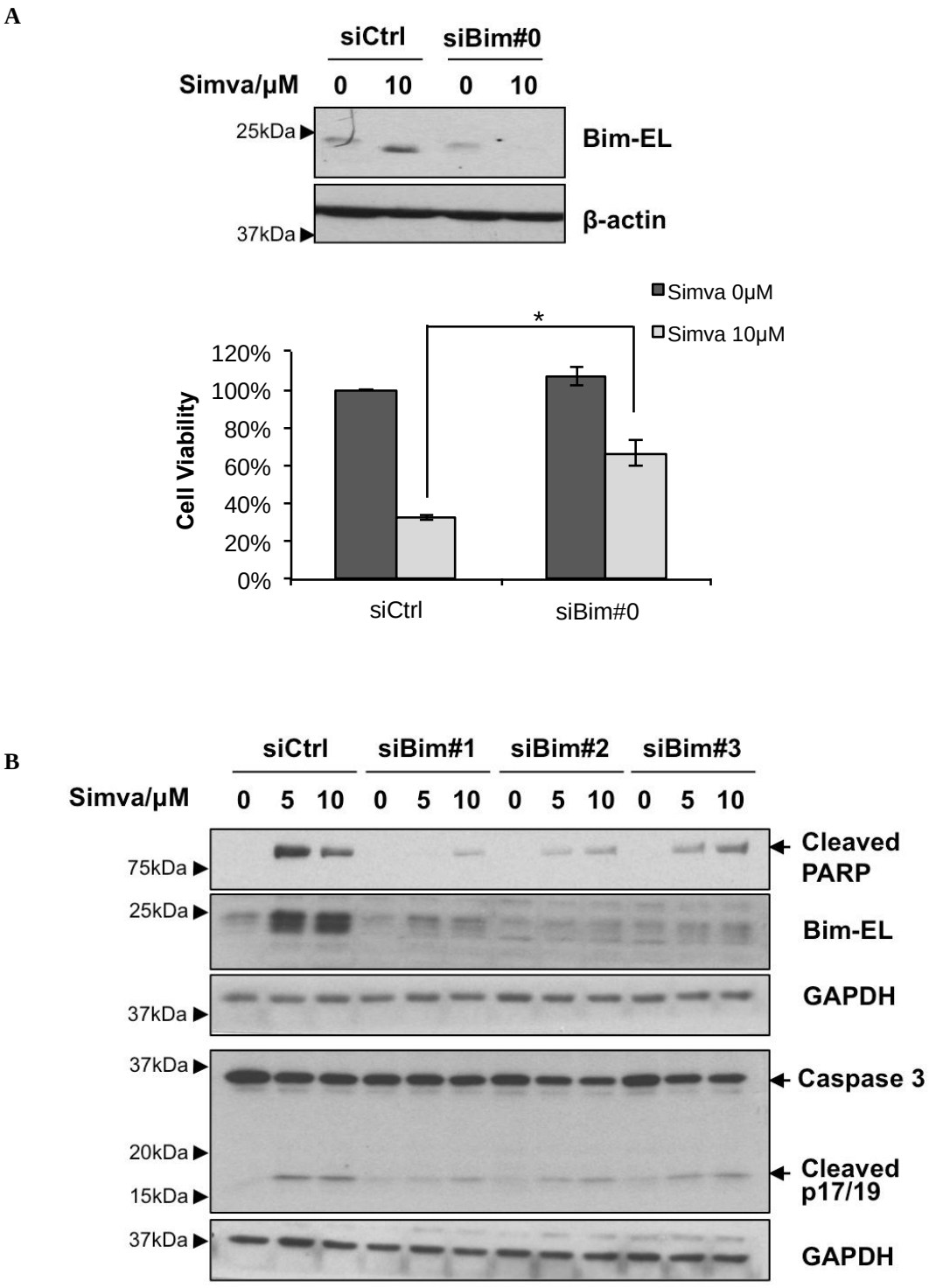

Figure 37: Knockdown of Bim-EL partially reduces simvastatin-mediated cell death.
(A) Bim-EL was successfully knocked down in HCT116 using single siRNA sequence (siBim#0) before treatment with 10 μM simvastatin for 48 h. Cell viability was measured by crystal violet assay. The bars represent means ± s.e.m of three independent experiments. *, $p < 0.05$ compared with siCtrl-transfected control cells receiving simvastatin treatment. (B) Bim-EL was knocked down using another three independent sequences (siBim#1, 2, 3) before simvastatin treatment for 36 h; Caspase-3, PARP and Bim-EL level were assessed by Western blot analysis. In both panels, β-actin or GAPDH was included as a loading control.

5.3 Simvastatin increases Bim-EL protein expression downstream of the RhoA/Rac1-Superoxide-JNK signaling cascade

After confirming that Bim-EL was an important target in simvastatin-mediated apoptosis, we continued to investigate the relationship of Bim-EL upregulation in relevance to the previously identified RhoA/Rac1-superoxide-JNK signaling cascade. We employed a bidirectional approach where we first checked Bim-EL protein level after blockage of RhoA, Rac1, superoxide production or JNK activation; then we studied the effects of Bim-EL gene silencing on the status of Rho, JNK and superoxide production.

5.3.1 Simvastatin upregulates Bim-EL via blocking protein geranylgeranylation

Firstly, we studied the effects of protein geranylgeranylation on simvastatin-induced Bim-EL upregulation. Cells were preincubated with MVA, GGPP or FPP before simvastatin treatment; Western blot analysis revealed that Bim-EL upregulation was fully blocked with MVA and GGPP preincubation, while FPP preincubation had comparable Bim-EL level with cells treated with simvastatin alone (Figure 38A). The finding was further supported by the observation that GGTI-298 alone increased Bim-EL expression, but not FTI-277 treatment (Figure 38B). The results suggest that protein geranylgeranylation is an upstream event of simvastatin-induced Bim-EL upregulation.

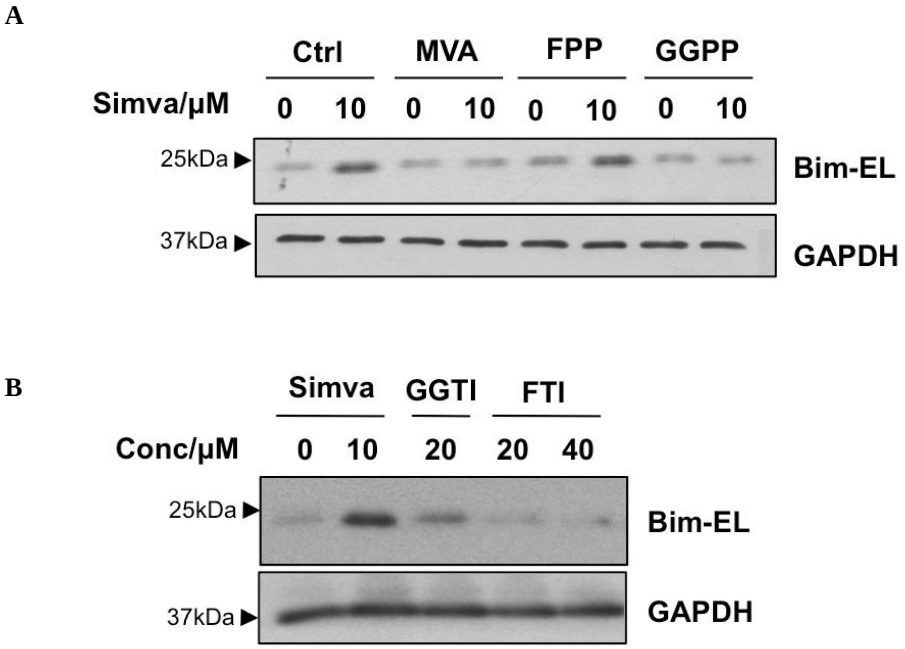

Figure 38: Simvastatin mediates Bim-EL upregulation via blocking protein geranylgeranlyation. HCT116 cells were either (A) preincubated with or without 100 μM MVA, 10 μM GGPP or 10 μM FPP for 2 h before treatment with 10 μM simvastatin for 24 h; (B) Cells were treated with simvastatin, GGTI-298 or FTI-277 alone at indicated doses for 24 h. In both panels, Bim-EL protein expression was assessed by Western blot analysis. GAPDH was included as a loading control.

5.3.2 Blocking RhoA and Rac1 activites prevents Bim-EL upregulation by simvastatin

Subsequently, we looked at the effects of increased GTP-loading of RhoA or Rac1 on the Bim-EL status after simvastatin treatment. As shown in Figure 39, inhibiting Rac1 activity using inhibitor NSC23766 and EHT1864 (Figure 39A), dominant negative mutant transfection (Rac1N17) or gene silencing significantly reduced Bim-EL level upon simvastatin treatment. Similar result was observed in cells knocked down of RhoA (Figure 39C). Our findings support that active RhoA and Rac1 are upstream signals for simvastatin-mediated Bim-EL upregulation. Considering that Bim-EL is a known pro-apoptotic Bcl-2 family member, the ability to reduce Bim-EL level with RhoA and Rac1 inhibition corroborates with the previous finding that activation of RhoA and Rac1 is responsible for simvastatin's apoptotic effects (Figure 18-20).

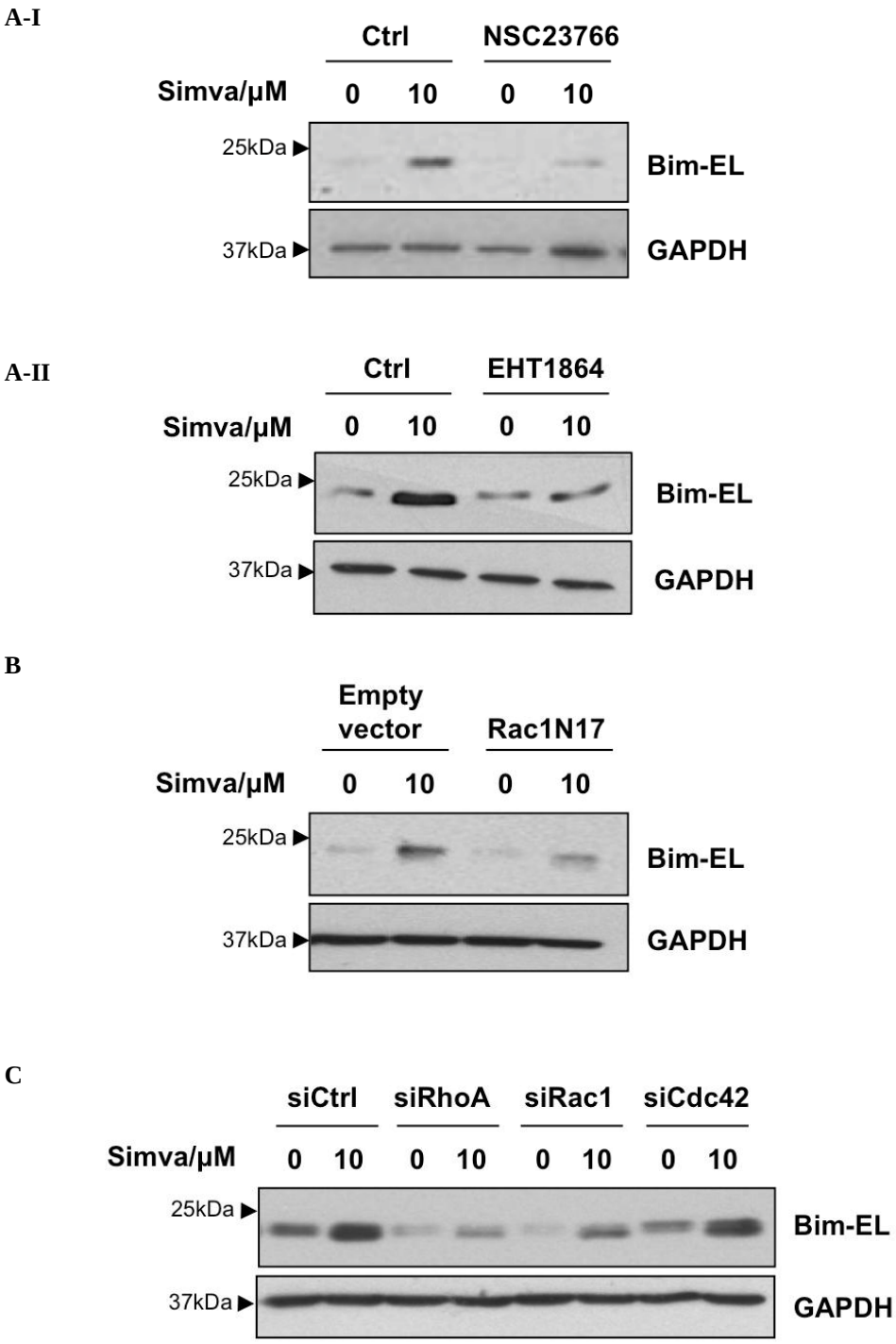

Figure 39: Blocking RhoA and Rac1 activities abrogates simvastatin-induced Bim-EL upregulation.
(A) HCT116 cells were preincubated with or without (I) 150 μM NSC23766 or (II) 20 μM EHT1864 for 2 h before simvastatin treatment; (B) HCT116 cells were transfected with either pIRES empty vector or Rac1N17 plasmid as previously described and confirmed in Figure 19A. (C) RhoA, Rac1 or Cdc42 were knocked down in HCT116 cells as previously described and confirmed in Figure 20A. In all panels, Bim-EL level after treatment with 10 μM simvastatin for 24 h was assessed by Western blot analysis. GAPDH was included as a loading control.

5.3.3 Blocking superoxide production abrogates simvastatin-mediated Bim-EL upregulation

Next, to explore the link between Bim-EL expression and superoxide production in simvastatin-treated HCT116 cells, cells were preincubated with superoxide scavengers: DPI, tempol and tiron before simvastatin treatment. Western blot results showed that the protein level of Bim-EL in cells pretreated with superoxide scavengers was significantly reduced compared to that in cells treated with simvastatin alone (Figure 40). It suggests that superoxide production is likely to be an upstream signal for Bim-EL expression.

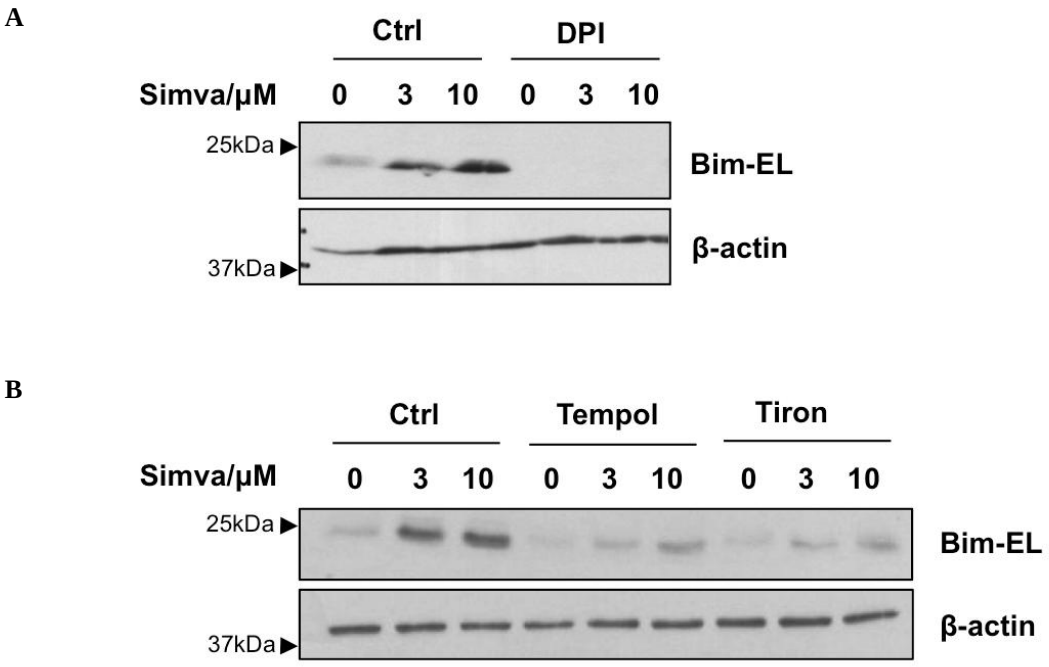

Figure 40: Superoxide scavengers block simvastatin-induced Bim-EL upregulation.
HCT116 cells were preincubated with or without (A) 5 μM DPI or (B) 2.5 mM tempol or 10 mM tiron for 2 h before treatment with 3 or 10 μM simvastatin for 24h. Bim-EL protein expression was assessed by Western blot analysis. β-actin was included as a loading control.

5.3.4 Simvastatin-induced increase in Bim-EL is downstream of JNK activation

Thereafter, we looked at the relationship between JNK activation and Bim-EL upregulation in simvastatin-treated HCT116 cells. Cells were pretreated with SP600125 to block JNK signaling before simvastatin treatment. As shown in Figure 41, SP600125 significantly blocked simvastatin-induced Bim-EL expression, putting JNK activation upstream of Bim-EL upregulation in the signaling events.

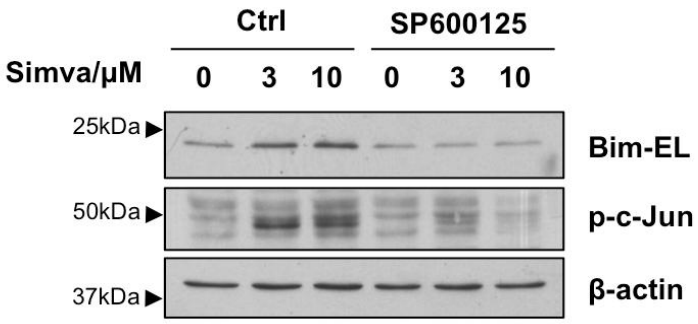

Figure 41: JNK inhibitor SP600125 prevents Bim-EL upregulation upon simvastatin treatment. HCT116 cells were pretreated with 10 μM SP600125 for 2 h before treating with 3 or 10 μM simvastatin for 24 h. Bim-EL protein expression was assessed by Western blot analysis. β-actin was included as a loading control.

5.3.5 Bim-EL silencing did not affect Rho protein expression, superoxide level and JNK activation after simvastatin treatment

Lastly, previous results suggested that simvastatin-mediated Bim-EL was the downstream event of the previously established RhoA/Rac1-superoxide-JNK signaling cascade in HCT116 cells. To elucidate if there was any feedback mechanism from Bim-EL upregulation, we studied the effects of Bim-EL knockdown on Rho proteins, superoxide production and JNK phosphorylation in response to simvastatin treatment. HCT116 cells were transfected with Bim-EL siRNA followed by simvastatin treatment, and the protein expression of RhoA, Rac1, Cdc42 and phospho-JNK were assessed by Western blot analysis, while superoxide level was assessed by lucigenin chemiluminiscence assay. As shown in Figure 42, successful knockdown of Bim-EL did not affect RhoA, Rac1 and Cdc42 protein levels upon simvastatin exposure (Figure 42A). In addition, the increase in superoxide production (Figure 42B) and JNK phosphorylation (Figure 42C) were also observed in cells knocked-down with Bim-EL following simvastatin treatment. These observations demonstrate that Bim-EL is the *bona fide* downstream target of RhoA/Rac1-superoxide-JNK signaling cascade in response to simvastatin treatment, without any feedback loops.

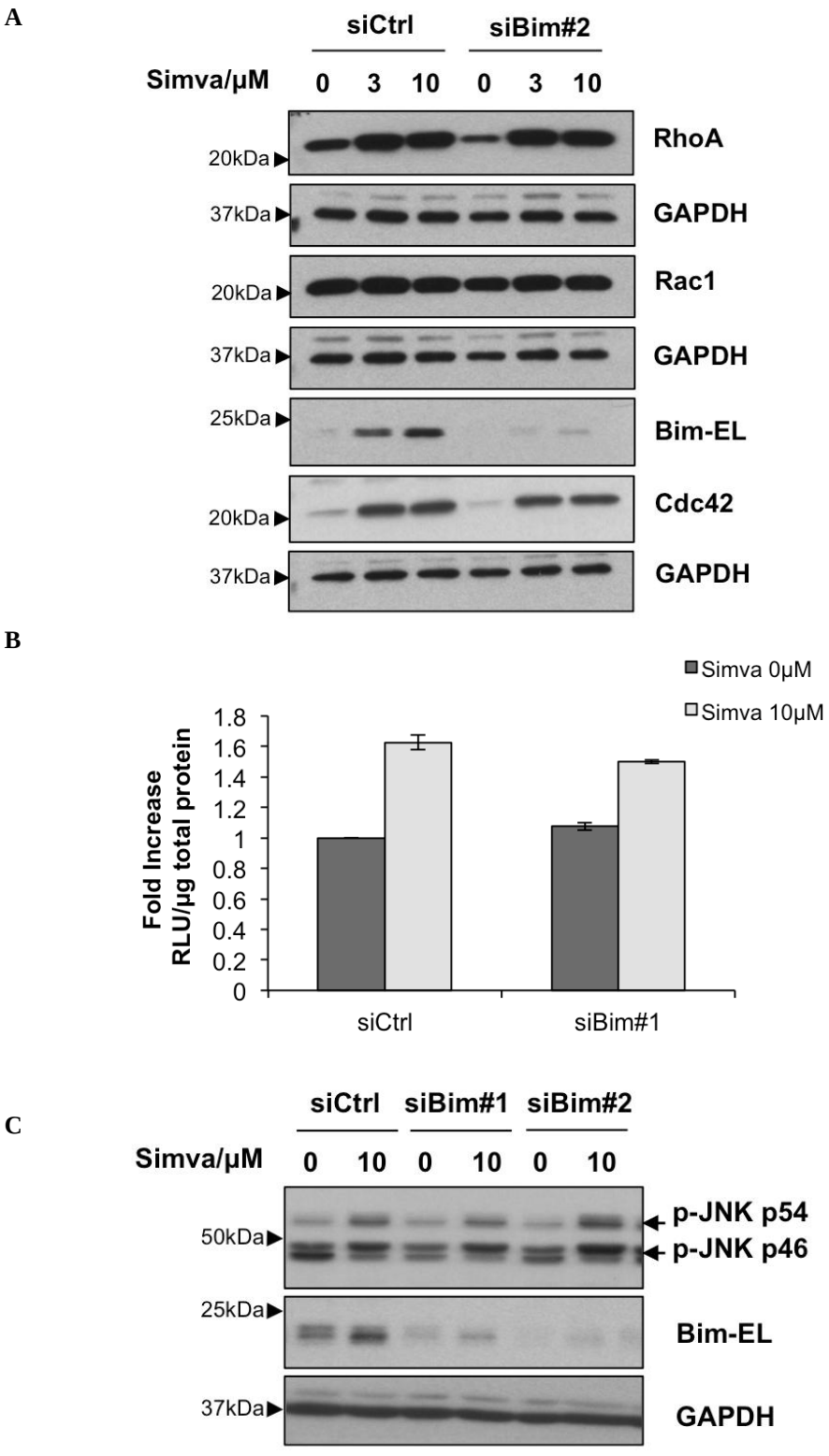

Figure 42: Knockdown of Bim-EL does not affect the protein expression of Rho, superoxide production and JNK activation.

Bim-EL was knocked down in HCT116 cells using different siRNA sequences before treatment with 10 μM simvastatin for 24 h. (A) The levels of RhoA, Rac1, Cdc42 and (C) phospho-JNK level was assessed by Western blot analysis. GAPDH was included as a loading control. (B) Superoxide level was assessed by lucigenin chemiluminesence assay. The bars represent means ± s.e.m of three independent experiments.

5.4 Simvastatin-induced Bim-EL upregulation is observed in HCT116 Bax-/- cells

So far, we established that Bim-EL was the downstream signaling component in our cell death model; however, how Bim-EL led to the activation of the intrinsic pathway remained unanswered. In the literature, Bim was identified to be able to directly activate Bax or act indirectly by antagonizing the pro-survival Bcl-2 proteins, thereby allowing Bax activation to proceed, a key step for apoptosis (Czabotar, Colman et al. 2009). Hence, in our model, we hypothesized that Bim-EL upregulation should be upstream of Bax signaling in response to simvastatin treatment. Both HCT116 WT and Bax-/- cells were treated with 10 μM simvastatin for 6, 24 and 32 h, and we observed comparable level of Bim-EL content in both cell lines after 24 and 32 h of simvastatin treatment (Figure 43). The data suggests that simvastatin-mediated upregulation of Bim-EL is an upstream event of Bax signaling, which eventually leads to cell death.

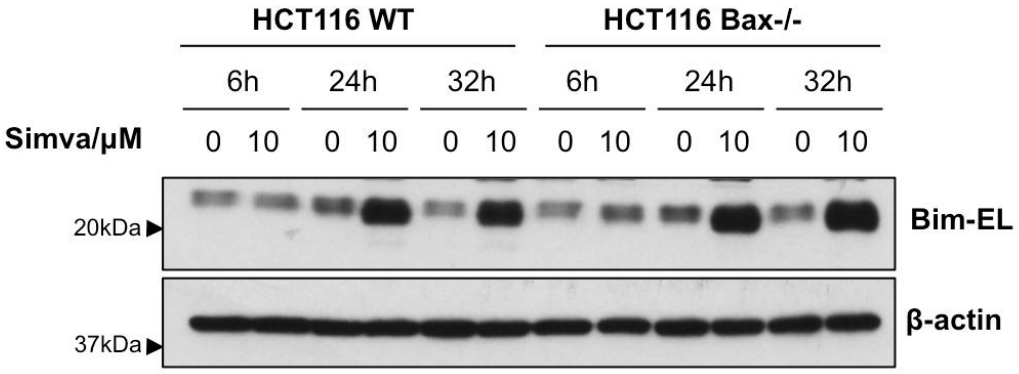

Figure 43: Simvastatin-induced Bim-EL upregulation is upstream of Bax signaling.
Both HCT116 WT and Bax-/- cells were treated with 10 μM simvastatin for the indicated duration. Bim-EL was detected by Western blot analysis. β-actin was included as a loading control.

5.5 Simvastatin increases Bim-EL level via protein synthesis

5.5.1 Simvastatin upregulates Bim-EL content via mRNA and protein synthesis

To understand the biology of how simvastatin upregulated Bim-EL protein expression in HCT116 cells, we first looked at the possible involvement of mRNA and protein synthesis. Inhibiting *de novo* protein synthesis with cycloheximide blocked simvastatin-dependent increase in Bim-EL protein expression (Figure 44A). In addition, treatment with actinomycin D, an inhibitor of gene transcription, ablated simvastatin-dependent increase in Bim-EL expression (Figure 44B). The results suggest that mRNA and protein synthesis are involved in the increased Bim-EL level after simvastatin treatment.

A

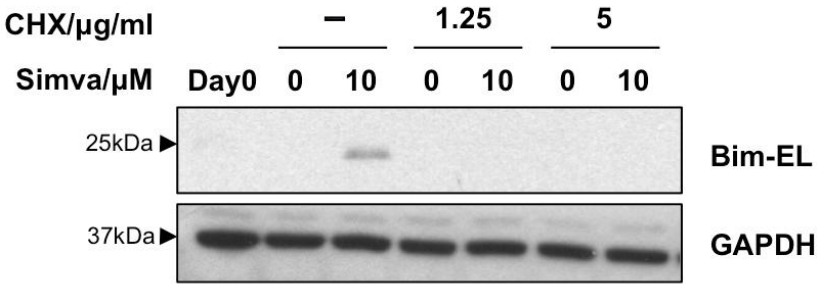

B

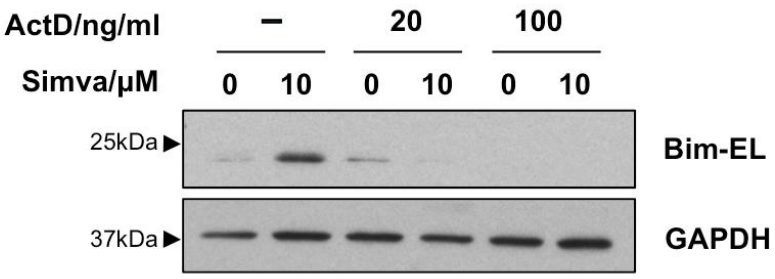

Figure 44: Simvastatin-mediated upregulation of Bim-EL protein level is blocked by transcription and protein synthesis inhibitors.
HCT116 cells were pretreated with or without various doses of (A) cycloheximide or (B) actinomycin D for 1 h, followed by treatment with 10 μM simvastatin for 24 h. Bim-EL protein level was assessed by Western blot analysis. GAPDH was included as a loading control.

5.5.2 Simvastatin does not affect the protein degradation rate of Bim-EL

Besides mRNA and protein synthesis, protein degradation can also impact the changes in protein level. Similar to Figure 24, we conducted half-life studies using cycloheximide to see if simvastatin treatment affected the protein degradation rate of Bim-EL. HCT116 cells were pretreated with cycloheximide alone and cell lysates were collected at different intervals, decrease of Bim-EL protein level was observed after 16 h. In the presence of both cycloheximide and simvastatin, Bim-EL was shown to start decreasing at 16 h as well (Figure 45), suggesting that simvastatin treatment is not likely to affect the stability of Bim-EL, instead the *de novo* protein synthesis demonstrated in Figure 44 is the main mechanism for the increase in Bim-EL content..

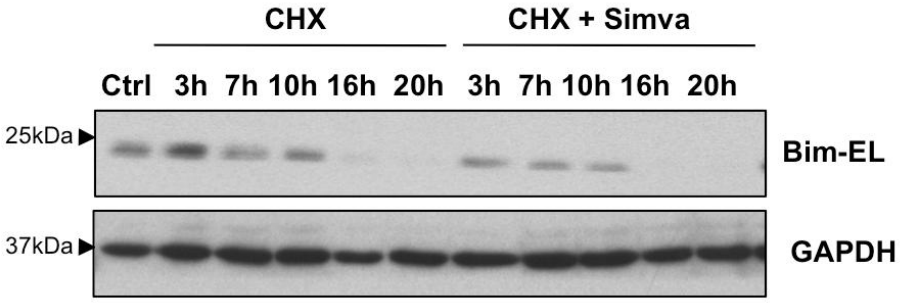

Figure 45: Simvastatin does not affect the protein degradation rate of Bim-EL.
HCT116 cells were either treated with 5μg/ml cycloheximide alone or preincubated with cycloheximide for 1h before addition of 10 μM simvastatin for the indicated durations. The levels of Bim-EL were assessed by Western blot analysis. GAPDH was included as a loading control.

6 Simvastatin's cytotoxic effects is conserved in many cancer types

6.1 Simvastatin induces cell death in other cancer cells by inhibiting protein geranylgeranylation

Not restricting ourselves to only one cancer model, we extended the studies of simvastatin-mediated anti-tumor property in four other cancer cell lines, which include another colorectal cancer cell line RKO, non-small lung cancer cell line A549, neuroblastoma cancer cell line SHEP-1 and breast cancer cell line MDA-MB-231. Cells were treated with increasing doses of simvastatin (0-30 μM) for 24 or 48 h. Resultant loss of cell viability was assessed by crystal violet assay (Figure 46A). Dose-dependent reduction of cell viability was achieved after 24 h treatment for A549, SHEP-1 and MDA-MB-231 cells and 48 h for RKO cells. For all cell lines, 10 μM simvastatin induced about 50% cell loss. The preliminary data suggest that simvastatin's cytotoxic effect is a general phenomenon in different cancer types.

We then went on to determine if simvastatin's cytotoxic effect observed in other cancer cell lines was an effect of inhibition of protein geranylgeranylation. Cells were incubated with simvastatin in the presence or absence of MVA, GGPP or FPP. Remarkably, similar to HCT116 cells, pretreatment with MVA and GGPP, but not FPP, largely reversed cell death phenotype induced by simvastatin in RKO, A549, SHEP-1 and MDA-MB-231 cells (Figure 46B). The observations suggest that protein geranylgeranylation is the more important post-translational modification in mediating simvastatin's cytotoxic effects across different cancer cell lines.

A-I

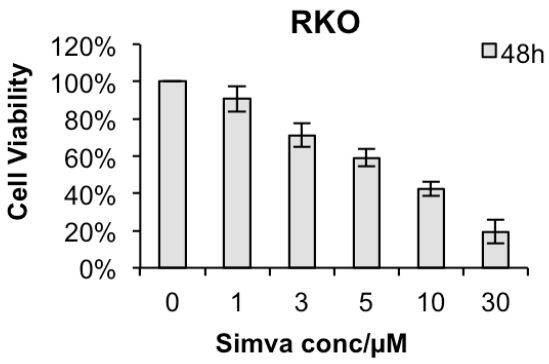

II

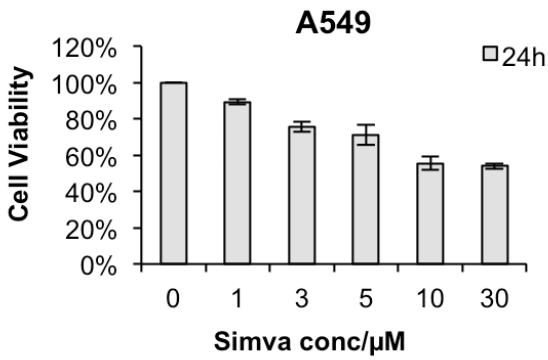

III

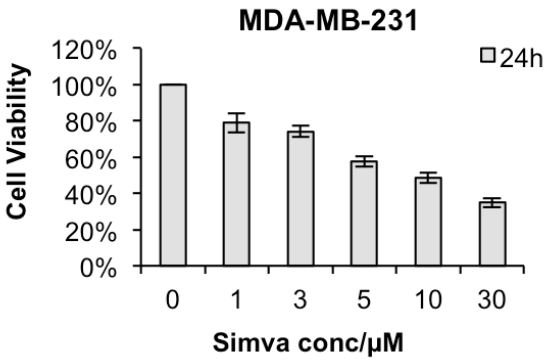

IV

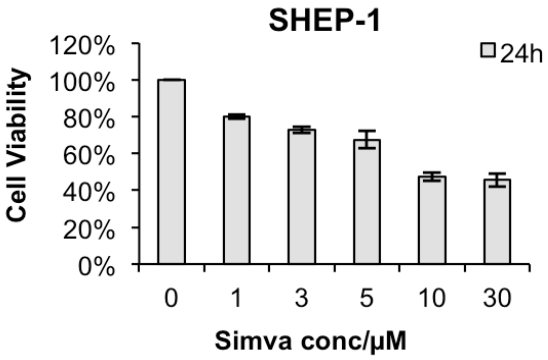

B-I

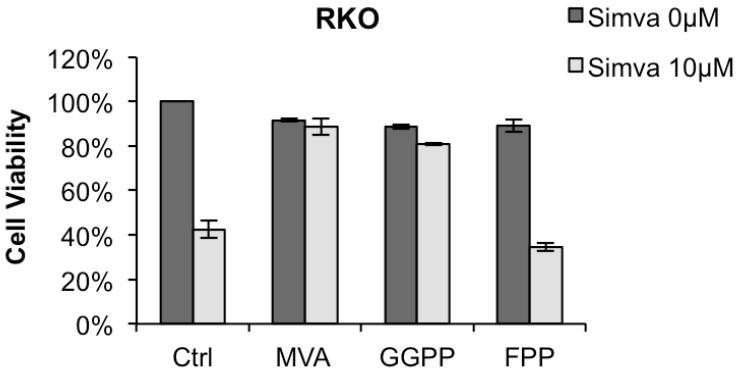

B-II

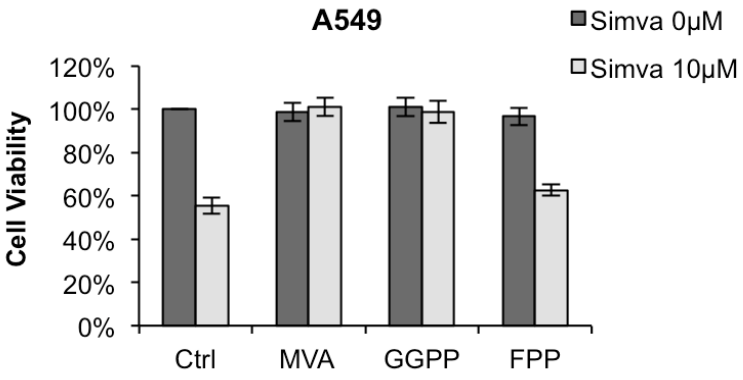

B-III

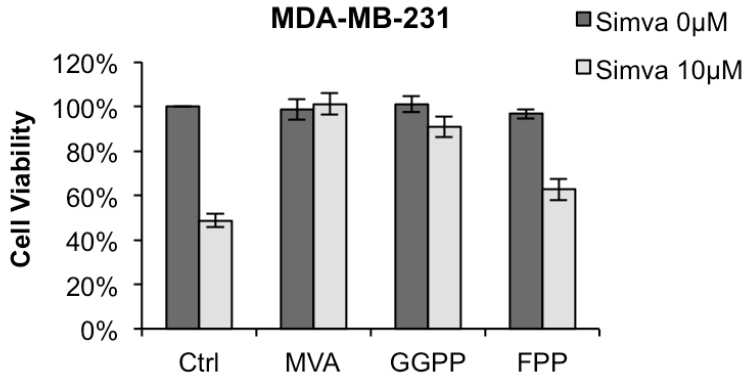

B-IV

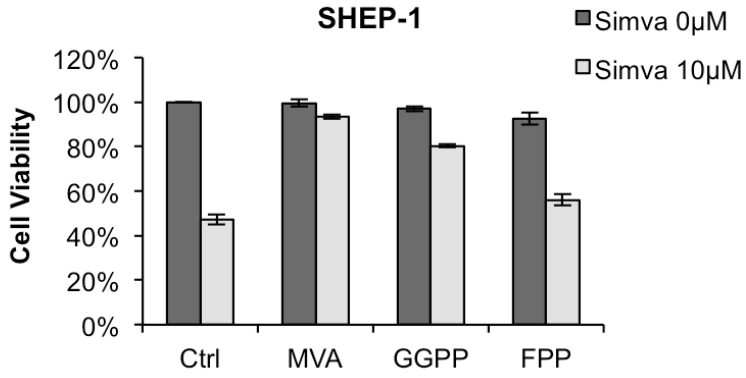

Figure 46: Simvastatin effectively reduces cell viability of other cancer cell lines via blocking protein geranylgeranylation.
Four other cancer cell lines: (I) RKO, (II) A549, (III) MDA-MB-231 and (IV) SHEP-1 cells were (A) treated with various concentrations of simvastatin (0-30 μM) for 24 or 48 h, or preincubated with 100 μM MVA, 10 μM GGPP or 10 μM FPP for 2 h before treatment with 10 μM simvastatin for 24 or 48 h. In all panels, cell viability was measured by crystal violet assay. In all panels, cell viability was expressed as % of untreated control. Data are shown as means ± s.d. of two independent experiments.

6.2 Simvastatin induces apoptosis in SHEP-1 cells via Rac1-Superoxide-JNK signaling cascade

After establishing that simvastatin induced cell death in multiple cancer types via blocking protein geranylgeranylation, we were interested to check if the novel signaling cascade (RhoA/Rac1-Superoxide-JNK-Bim-EL) identified in HCT116 cells could be extended to other cancer cell lines as well. Hence, to provide evidence that this novel mechanism is not a HCT116 cell line-exclusive effect, we continued to study the role of these main players in simvastatin-induced cell death of SHEP-1 neuroblastoma cells.

6.2.1 Simvastatin induces apoptosis in SHEP-1 cells

Firstly, to have a better understanding on the mode of cell death, we checked the status of caspase-3 and PARP cleavage in SHEP-1 cells after simvastatin treatment. Western blot results revealed a clear increase in the cleaved form of caspase-3 as well as its downstream substrate PARP. In addition, the observed cleavage of both proteins was fully inhibited in MVA- and GGPP-, but not FPP-preincubated cells (Figure 47). The protective effects of MVA and GGPP preincubation were consistent with the cell viability data shown in Figure 46 B-III. Furthermore, we also observed upregulation of Bim-EL following simvastatin treatment that was fully reversed by MVA and GGPP pretreatment. The upregulation of caspase signaling and Bim-EL in SHEP-1 cells indicates that apoptosis is likely to be the main mode of cell death activated by simvastatin, same as observed in HCT116 cells.

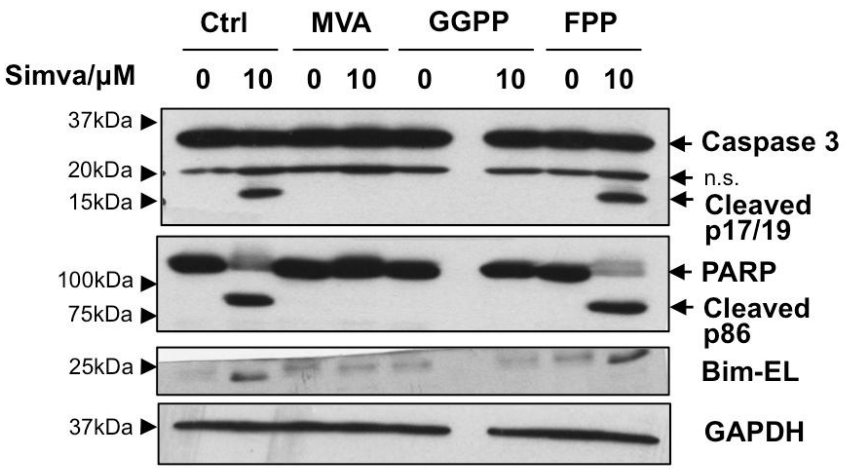

Figure 47: Simvastatin treatment upregulates Bim-EL and activates caspase signaling in SHEP-1 cells via inhibiting protein geranylgeranylation.
SHEP-1 cells were preincubated with or without 100 µM MVA, 10 µM GGPP or 10 µM FPP or 2 h before treatment with 10 µM simvastatin. Protein level of Bim-EL, caspase-3 and PARP cleavage after 20 h treatment was assessed by Western blot analysis. GAPDH was included as a loading control. (n.s. means non-specific band).

6.2.2 Simvastatin increases GTP-loading of Rac1, which is responsible for the cell death phenotype

In HCT116 cells, we identified active Rho GTPases as downstream targets of protein geranylgeranylation to mediate simvastatin's apoptotic effects. Hence, we studied the GTP-loading status of Rac1 and its potential involvement in the cell death signaling in SHEP-1 cells. Using PAK-pulldown assay, we measured GTP-bound Rac1 in the cell lysates. Interestingly, we also observed an increase in GTP-bound Rac1 in SHEP-1 cells. And the increment was observed as early as 3 h post-treatment and lasted even after 20 h simvastatin treatment (Figure 48A).

Then we continued to explore if inhibition of Rac1 activity would have any effects on simvastatin-induced cell death in SHEP-1 cells. Rac1 inhibitor NSC23766 was used to block Rac1 activity. Western blot results showed reduced PARP cleavage in cells pretreated with NSC23766 before addition of simvastatin as compared to cells treated with simvastatin alone (Figure 48B). The findings suggest that activation of Rac1 is involved in mediating the apoptotic effects of simvastatin in SHEP-1 cells; it also provides evidence that simvastatin's ability to activate Rho GTPases is not a HCT116-exclusive effect.

A

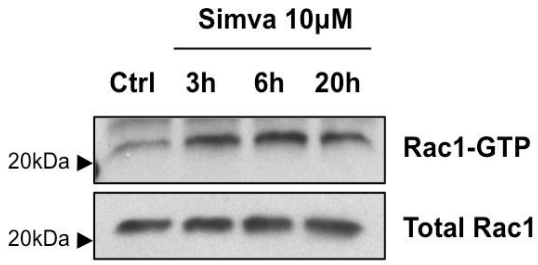

B

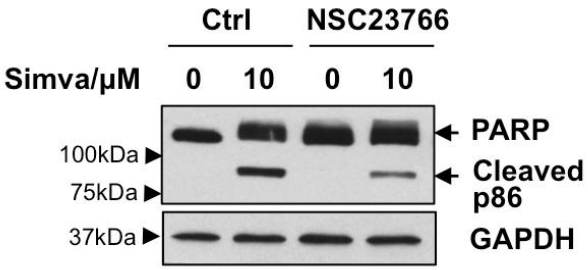

Figure 48: Simvastatin-mediated Rac1 activation is responsible for cell death in SHEP-1 cells.
(A) SHEP-1 cells were treated with 10 µM simvastatin for 3, 6 and 20 h, GTP-loading of Rac1was prepared as described in Figure 15 and 16 and assessed by Western blot analysis. (B) Cells were pretreated with 100 µM NSC23766 for 2 h before treatment with 10 µM simvastatin for 20 h. PARP cleavage was assessed by Western blot analysis. GAPDH was included as a loading control.

6.2.3 Simvastatin increases superoxide production downstream of Rac1 activation to mediate the apoptotic response

After confirming that simvastatin-mediated Rac1 activation was involved in the cell death signaling in both HCT116 and SHEP-1 cells, we continued to study the next molecule of interest, superoxide, which was found to be the downstream target of active Rho-GTPases following simvastatin treatment in HCT116 cells. Hence, we first monitored the superoxide level in SHEP-1 cells using lucigenin chemiluminiscence assay (Figure 49A). The results showed significant and sustained increase in superoxide production from 2 h up to 20 h treatment (1.35 ± 0.1 fold increase after 6 h treatment, 1.4 ± 0.01 fold increase after 20 h treatment compared to untreated cell).

Next, to verify the relevance of superoxide in the cell death process, SHEP-1 cells were preincubated with various doses of superoxide scavenger tiron for 2 h before simvastatin treatment. A dose-dependent reduction of PARP cleavage was observed in tiron-pretreated cells (Figure 49B), indicating that simvastatin-induced superoxide production plays an essential role in mediating the cell demise. Furthermore, preincubation with Rac1 inhibitor NSC23766 not only rescued the cell death phenotype shown in Figure 48, it also reduced the superoxide level akin to untreated cells (Figure 49C), suggesting that Rac1 activation is upstream of superoxide production induced by simvastatin in SHEP-1 cells.

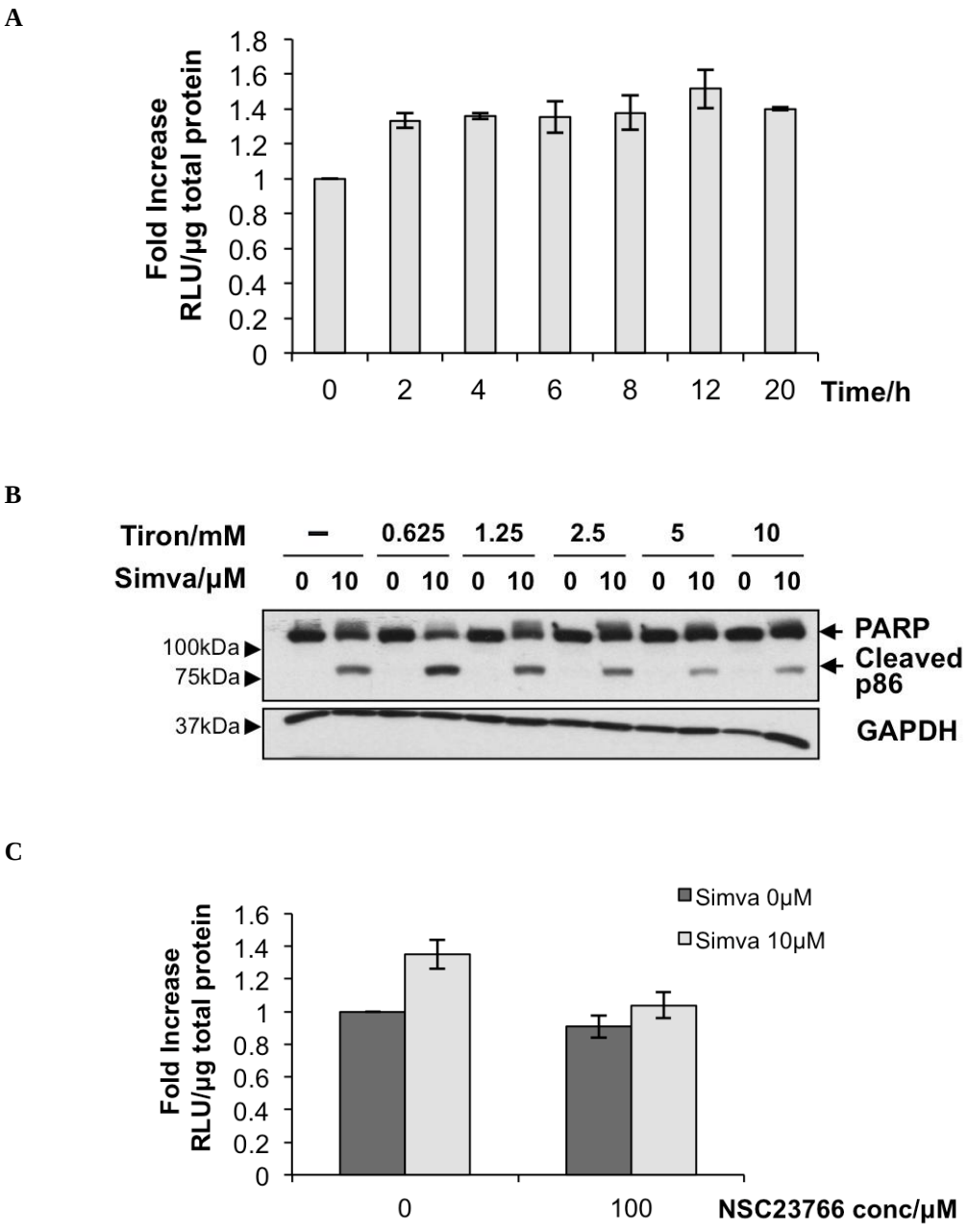

Figure 49: Preincubation of superoxide scavenger inhibits simvastatin-induced PARP cleavage in SHEP-1 cells, and simvastatin-mediated superoxide production is downstream of Rac1 activation.

(A) SHEP-1 cells were treated with 10 µM simvastatin for the indicated durations. Intracellular superoxide level was monitored by lucigenin chemiluminescence assay. (B) Cells were preincubated with various concentrations of tiron for 2 h before treatment with 10 µM simvastatin for 20 h; PARP cleavage was assessed by Western blot analysis. GAPDH was included as a loading control. (C) Cells were pretreated with 100 µM NSC23766 for 2 h before treatment with 10 µM simvastatin for 6 h. Superoxide level was monitored by lucigenin chemiluminescence assay. Data are shown as means ± s.d of two independent experiments.

6.2.4 Simvastatin activates JNK pathway downstream of Rac1-superoxide cascade to relay the cell death signal

Next, we evaluated the involvement of JNK signaling in simvastatin-mediated cell death in SHEP-1 cells, as JNK activation has been found to be the target downstream of Rho GTPases activation and superoxide production in HCT116 cells. Similar to HCT116 cells, simvastatin also upregulated stress-related JNK signaling after in SHEP-1 cells, which was shown by the increased phosphorylation at Thr183 and Tyr185 residues. The effect was fully reversed by MVA and GGPP preincubation, but not FPP, indicating that JNK activation is downstream of protein geranylgeranylation (Figure 50A). To confirm the functional relevance of JNK activation in the SHEP-1 model, we effectively block JNK activation with pharmacological inhibitor SP600125. Successful inhibition of JNK signaling was shown as the decreased phosphorylation of JNK itself (Figure 50B). Remarkably, pretreatment with SP600125 also effectively blocked PARP cleavage (Figure 50B), confirming its role in mediating the cytotoxic effects of simvastatin in SHEP-1 cells.

To understand the link of JNK activation to the observed upregulation of Rac1 activity and superoxide production in SHEP-1 cells, we showed that inhibiting Rac1 activity with Rac1 inhibitor NSC23766 fully blocked JNK phosphorylation (Figure 50C). In addition, reduction of superoxide production by tiron also decreased JNK phosphorylation (Figure 50D). These results imply that JNK activation is downstream of Rac1 activation and superoxide production in SHEP-1 cells.

Collectively, we showed that in SHEP-1 cells, simvastatin unconventionally activates Rac1 and induces downstream superoxide production and JNK activation, which

eventually leads to cell death. This mechanism is very similar to what we have identified in HCT116 cells upon simvastatin treatment, suggesting that simvastatin-mediated activation of Rho GTPases and its downstream signaling cascade might be a common mechanism in simvastatin-sensitive cancer cells.

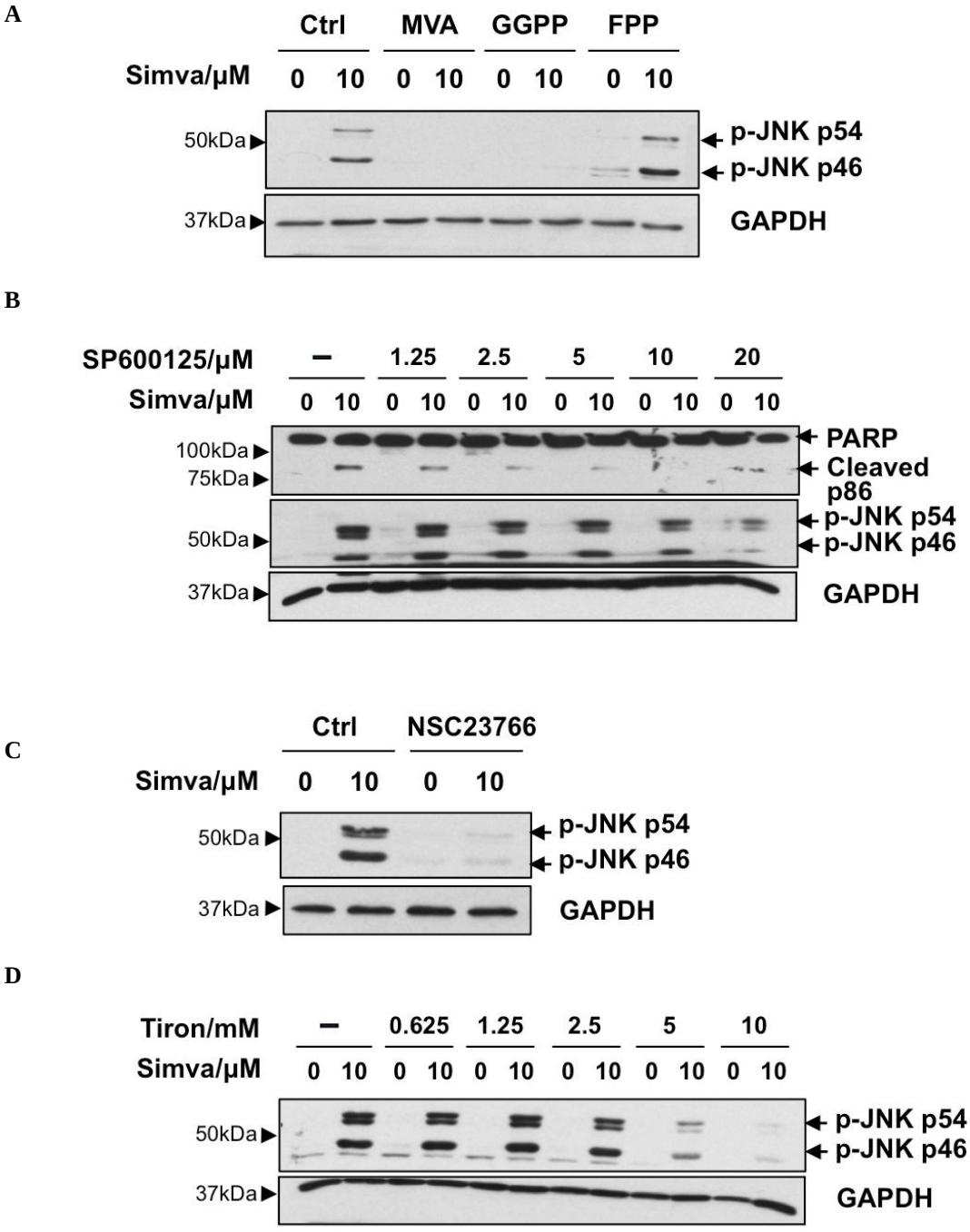

Figure 50: JNK inhibitor SP600125 protects simvastatin-treated SHEP-1 cells, and simvastatin-mediated JNK activation is downstream of Rac1 activation and superoxide production.
(A) SHEP-1 cells were preincubated with or without 100 μM MVA, 10 μM GGPP or 10 μM FPP for 2 h before treatment with 10 μM simvastatin for 6 h. Phospho-JNK level was assessed by Western blot analysis. (B) Cells were preincubated with various concentrations of SP600125 for 2 h before treatment with 10 μM simvastatin for 20 h; PARP cleavage and phospho-JNK level was assessed by Western blot analysis. (C) Cells were pretreated with 100 μM NSC23766 for 2 h before treatment with 10 μM simvastatin for 20 h. Phospho-JNK level was assessed by Western blot analysis.(D) Cells were preincubated with various concentrations of tiron for 2 h before treatment with 10 μM simvastatin for 20 h; Phospho-JNK level was assessed by Western blot analysis. In all panels, GAPDH was included as a loading control.

DISCUSSION

Statins are HMG-CoA reductase inhibitors that have been widely used as cholesterol-lowering agents to treat hyperlipidemia in the clinic. It has been shown to be beneficial in both primary and secondary prevention of cardiovascular diseases, making it one of the most frequently used drugs. In the last decade, increasing experimental data has demonstrated the anti-cancer properties of statins, including activity towards carcinomas of the prostate, colon and rectum, breast, lung, AML, multiple myeloma and skin (Chan, Oza et al. 2003; Ukomadu and Dutta 2003; Jiang, Zheng et al. 2004; Demierre, Higgins et al. 2005; Campbell, Esserman et al. 2006; Fromigue, Hay et al. 2006; Hwang, Na et al. 2011). These positive experimental observations have prompted epidemiological studies and clinical trials to assess the clinical efficacy of statins for treating cancers. However, so far the conclusions are controversial. Some studies have suggested preventive and therapeutic effects of statins against cancers (Blais, Desgagne et al. 2000; Poynter, Gruber et al. 2005; Shannon, Tewoderos et al. 2005; Boudreau, Yu et al. 2007; Khurana, Bejjanki et al. 2007; Khurana, Sheth et al. 2007), while other studies fail to draw such conclusions (Kim, Kim et al. 2001; Kaye and Jick 2004; Lersch, Schmelz et al. 2004). Hence, it is still early to recommend statins for anti-cancer indications in patients until further investigations into their exact mechanisms and overall benefits are undertaken. In this project, we sought to uncover the underlying signaling networks responsible for simvastatin-induced anti-tumor effects in human cancer cells.

1 The cell death mechanism in simvastatin-treated cancer cells

To begin these studies, we first tested the cytotoxic potential of simvastatin in several cancer cell models. As expected, simvastatin caused significant reduction in cell

survival of five cancer cell lines from disparate cancer origins, namely, two colorectal cancer carcinoma HCT116 and RKO, non-small lung carcinoma A549, neuroblastoma SHEP-1 and breast carcinoma MDA-MB-231 (Figure 1 & 46A). Further studies done in HCT116 cells showed both cytostatic and cytotoxic effects of simvastatin (Figure 1). In addition, we observed that the short-term growth inhibitory effects of simvastatin translated into drastically compromised long-term clonogenic ability of cancer cells (Figure 2). Statin-mediated anti-proliferative effects have been well observed in multiple cancer cell lines either by induction of G1 arrest or G2/M arrest (Jakobisiak, Bruno et al. 1991; Crick, Andres et al. 1998; Graaf, Richel et al. 2004). Multiple cell cycle regulators are involved in mediating the cytostatic effects of simvastatin, such as downregulation of cyclin-dependent kinases (Cdk) activities or overexpression of Cdk inhibitors (p27 and p21) (Lee, Ha et al. 1998; Weiss, Ramirez et al. 1999; Ukomadu and Dutta 2003). In some models, the anti-proliferative and pro-cell death effects of statins occur as exclusive events depending on the concentrations of statins used (Denoyelle, Vasse et al. 2001). Here, we observed signs of both events in a time-dependent manner in simvastatin-treated HCT116 cells. Previous studies have suggested potential candidate regulators for modulating both growth arrest and cell death response after statin treatment. For example, statin-induced overexpression of p27 contributes to apoptosis in multiple cancer cell types, while conversely, lovastatin-induced growth arrest and apoptosis in NIH-3T3 cells was postponed after overexpression of cyclin E (Katayose, Kim et al. 1997; Ghosh, Moyer et al. 1999). Although we did not focus on the role of cell cycle regulation in mediating the cytotoxic effects of simvastatin in our study, these cell cycle regulators remain as attractive targets to be explored in future studies.

A variety of studies have indicated that the main mode of statin-mediated cancer cell death is apoptosis, which as noted above is generally preceded by cell cycle arrest (Herrero-Martin and Lopez-Rivas 2008; Kamigaki, Sasaki et al. 2011; Tu, Kang et al. 2011). Very recently, statins have been found to activate autophagy in some cancer cell lines, and there is speculation that this process contributes as well to statin-induced cell death (Parikh, Childress et al. 2010; Asakura, Izumi et al. 2011). In this study, however, our investigations revealed that the molecular events in simvastatin-induced cell death were consistent with classical apoptosis. Firstly, morphological changes such as cell shrinkage during apoptosis were observed in simvastatin-treated cells (Figure 3A). Secondly, simvastatin induced proteolytic cleavage and activation of initiator caspases (caspase-8 and -9), followed by activation of downstream executioner caspase-3, which resulted in PARP cleavage (Figure 4) as well as nuclear DNA fragmentation (Figure 3). The cleaved fragment of PARP also possesses classical apoptotic features to invalidate its DNA repair function (Berger and Petzold 1985). Lastly, the almost complete protection of cells by pretreatment with pan-caspase inhibitor zVAD-fmk confirmed that simvastatin induces cell death via a caspase-dependent pathway (Figure 5).

Further exploration implicated mitochondria in the cell death signaling elicited by simvastatin in HCT116 cells. This was first evidenced by the initiation of mitochondrial membrane permeabilization (MMP) following simvastatin treatment; MMP is commonly regarded as the "point of no return" to cellular demise upon initiation (Kroemer, Galluzzi et al. 2007). Simvastatin induced mitochondrial translocation of Bax as well as release of pro-apoptotic protein cytochrome c to the cytosol, which is responsible for the assembly of apoptosome and downstream

caspase-9, and subsequently caspase-3 activation (Figure 6). Further comparison between HCT116 wildtype and its Bax knockout counterpart showed that Bax-/- cells were much less sensitive to simvastatin treatment, confirming that MMP modulator Bax-mediated mitochondrial apoptotic pathway is the major mechanism responsible for simvastatin's apoptotic effects (Figure 7). In addition, signs of the extrinsic/receptor-mediated apoptotic pathway were also observed after simvastatin treatment as evidenced by caspase-8 activation (Figure 4A). The extrinsic pathway can engage the mitochondria via caspase-8-dependent cleavage of BH-3 only protein Bid in type II cells, where truncated-Bid binds and activates Bax/Bak (Scaffidi, Fulda et al. 1998). However, that was not the case here as we did not observe the formation of t-Bid after simvastatin treatment (Figure 36). Hence, we propose that simvastatin-induced apoptotic signaling in HCT116 cells is primarily executed through the intrinsic pathway, with minor apoptotic effects contributed by the extrinsic signaling. This observation is consistent with several other reports showing the importance of mitochondrial apoptotic pathway in breast tumor cells (Herrero-Martin and Lopez-Rivas 2008), lymphoblasts and myeloma cells (Cafforio, Dammacco et al. 2005) upon exposure of statins. On the other hand, our data indicates that direct involvement of the tumor suppressor p53 in statin-induced apoptosis is likely to be limited. One report showed that lovastatin was able to induce mitochondrial-mediated apoptosis involving cytochrome c release in p53-mutant breast cancer cells (Shibata, Ito et al. 2004). This is consistent with our finding that p53 knockout colorectal cancer cells were equally if not more sensitive to simvastatin treatment compared to its wildtype counterpart (Figure 8). These observations highlight the therapeutic potential of statins in cancers with p53 mutations or deficiency.

Sustained proliferative signaling and resistance to cell death are two important steps during tumor development (Hanahan and Weinberg 2011), and we have demonstrated that simvastatin is able to overcome the resistance to apoptosis and effectively induce cell death in multiple cancer cell types. Taken together with the previous studies that have established the resistance of normal cells to statin treatment (Newman, Clutterbuck et al. 1994; Newman, Clutterbuck et al. 1997; Dimitroulakos, Nohynek et al. 1999), our findings regarding the anti-tumor activities of simvastatin highly suggest its potential as a tumor-selective chemotherapy. To translate the promising anti-tumor effects of simvastatin observed *in vitro* to *in vivo* models, one important factor to address is whether the concentrations at which anti-proliferative and pro-apoptotic effects are observed *in vitro* can be achieved clinically. In our study, we observed that IC50 of simvastatin is around 5-10 μM in all five cancer cell lines tested (Figure 1 and 46A). Moreover, 3 μM simvastatin showed more pronounced effect in long-term, inducing around 50% inhibition in clonogenic ability of HCT116 cells (Figure 2). Clinical trials involving another closely related member of HMG-CoA reductase inhibitors lovastatin showed that administration in doses from 25 mg/kg daily results in peak drug plasma concentration around 3.9 μM in cancer patients (Thibault, Samid et al. 1996). Trials using even higher doses of statins can reach plasma concentration higher than 10 μM, and the occurrence of myopathy (a side effect of high dose statin treatment) can be prevented by ubiquinone supplementation. These findings indicate that the main concentrations of simvastatin used in our study (3 or 10 μM) to induce anti-proliferative and pro-apoptotic effects are within the therapeutically achievable dose ranges, and the downstream signaling networks identified in this project would also be physiologically relevant.

2 Identification of novel mechanisms in regulating Rho GTPases and its role in simvastatin-mediated apoptosis

2.1 Geranylgeranylation is the more important form of isoprenylation in the anti-tumor effects of simvastatin

Statins work by reversibly inhibiting the HMG-CoA reductase, the enzyme catalyzing the conversion of HMG-CoA to mevalonate (Rodwell, Nordstrom et al. 1976). Several downstream metabolites in the mevalonate pathway are suggested to be involved in establishing statins' anti-tumor effects. Cholesterol is one of them as shown by a handful studies that linked cholesterol-regulated lipid raft signaling to the chemopreventive effects of statins. For instance, simvastatin has been shown to induce apoptosis in prostate cancer cells by depleting raft cholesterol level and inhibit AKT signaling both *in vitro* and *in vivo* (Zhuang, Kim et al. 2005). To test the involvement of cholesterol in our model, we preincubated HCT116 cells with cholesterol precursor squalene before simvastatin treatment. However, restoration of sterols with squalene failed to protect simvastatin-induced cell death (Figure 10), indicating that the cytotoxic effects are likely to be independent of cholesterol synthesis. This observation is consistent with several other studies suggesting the importance of other downstream moieties instead of cholesterol. For example, geranylgeranylpyrophosphate (GGPP) and farnesylpyrophosphate (FPP) are responsible for the post-modification of intracellular Ras and Rho GTPases, which in turn regulate its downstream effectors to mediate cell proliferation, differentiation, and apoptosis (Goldstein and Brown 1990; Liao and Laufs 2005). In addition, inhibitors that specifically block the enzymes responsible for protein farnesylation (farnesyltransferase) and geranylgeranylation (geranylgeranyltransferase I), namely FTIs and GGTIs, were developed as anti-cancer drugs primarily because of the

identification of Ras superfamily members' contribution to tumor development (Berndt, Hamilton et al. 2011). In this study, we obtained evidence that simvastatin induced cell death in all five cancer cell lines via depletion of the isoprenoid GGPP. The conclusion came from studies showing that cells preincubated with GGPP exhibited almost full recovery from simvastatin-induced cell death, whereas FPP preincubation had minimal protective effects (Figure 9, 46B). Although FPP lies upstream of GGPP in the mevalonate pathway, the conversion requires another molecule isopentenyl PPi, which is also depleted after statin exposure, providing an explanation as to why the addition of FPP is unable to restore protein geranylgeranylation and show protective effects (Mo and Elson 2004; Demierre, Higgins et al. 2005). Additional experiments in HCT116 cells further demonstrated that a specific inhibitor of GGTase I (GGTI-298), but not of FTase (FTI-277), mimicked the cytotoxic effects of simvastatin (Figure 11), confirming the importance of geranylgeranylation over farnesylation in simvastatin-induced apoptosis.

Our observations, as with previous reports (Xia, Tan et al. 2001; Dimitroulakos, Marhin et al. 2002; van de Donk, Kamphuis et al. 2003; Zhong, Wang et al. 2003), show that statins' cytotoxic effects on cancer cells were mainly attributed to the inhibition of downstream protein geranylgeranylation. Implications of this observation are multi-fold. It directly suggests that the functional consequences after loss of geranylgeranylation are more severe than loss of farnesylation. This could be simply due to the fact that much more proteins undergo geranylgeranylation than farnesylation inside cells (Reid, Terry et al. 2004). Another plausible explanation was proposed by Martin Bergo's group based on their observation that inhibition of GGTIase-I activity reduced K-ras-induced lung tumor formation and promoted

survival of the mice (Sjogren, Andersson et al. 2007). They argued that geranylgeranylated proteins may have higher avidity to the membrane surfaces because of the more hydrophobic nature of the geranylgeranyl lipid compared to the farnesyl lipid. Hence, inhibition of protein geranylgeranylation could have a greater cellular effects compared with loss of protein farnesylation. More significantly, our observations highlight the critical involvement of one or more geranylgeranylated proteins, for example, Rho, Rac, and Cdc42, in the growth and survival of transformed cells (discussed in more detail in the next section). The findings that protein geranylgeranylation is more important than farnesylation in cell survival calls for re-evaluation of the clinical relevance of FTIs as an anti-cancer monotherapy. FTIs were primarily developed to target Ras proteins, the most frequently mutated oncogene identified in cancers. However, the efficacy of the FTI drugs was found to be limited, especially in solid tumors (Konstantinopoulos, Karamouzis et al. 2007; Sousa, Fernandes et al. 2008). Our study also provided evidence that HCT116 cells with oncogenic K-Ras mutation were not responsive to FTI-277 treatment; instead, simvastatin or GGTI-298 alone showed better cell kill (Figure 11). The observation might be explained by the discovery that K- and N-Ras can become geranylgeranylated when treated with FTIs (Rowell, Kowalczyk et al. 1997; Whyte, Kirschmeier et al. 1997). Hence, regimes that target both forms of isoprenylation, such as statins or combination of FTIs and GGTIs, could represent a better strategy to induce cell death in a boarder range of cancers.

2.2 Non-canonical regulation of Rho GTPases by simvastatin

As mentioned previously, farnesylation and geranylgeranylation are post-translational modifications involving the addition of an isoprenoid lipid to the C-

terminus of the proteins. It is generally understood that the post-modification is necessary for the proper localization and function of target proteins (Van Aelst and D'Souza-Schorey 1997). The importance of geranylgeranylation in simvastatin-induced apoptosis prompted us to identify its candidate substrates. We then focused on three widely studied Rho GTPases, namely RhoA, Rac1 and Cdc42, which mediate various housekeeping functions inside the cells, including cytoskeletal rearrangements, cell morphology, polarity, migration, proliferation and survival (Van Aelst and D'Souza-Schorey 1997; Schmitz, Govek et al. 2000; Aznar and Lacal 2001). In addition, mounting evidence is suggesting their role in cancer development, for example overexpression or hyperactivity of Rho GTPases are well observed in multiple types of human tumors (summarized in Table 2 in Introduction) (Jaffe and Hall 2002; Sahai and Marshall 2002; Gomez del Pulgar, Benitah et al. 2005).

2.2.1 Inhibiting geranylgeranylation increases GTP-loading of Rho GTPases

By inhibiting HMG-CoA reductase, statins reduce the endogenous pool of isprenoids required for membrane localization and function of Rho GTPases (Winter-Vann and Casey 2005). Hence, we hypothesize that the Rho proteins would be unprenylated and unable to reside in the plasma membrane following simvastatin treatment. Using detergent Triton X-114, we separated Rho proteins into unprenylated and prenylated forms. As expected, increases in RhoA, Rac1 and Cdc42 levels in their unprenylated form were observed after simvastatin treatment (Figure 13). On top of that, these unprenylated RhoA, Rac1 and Cdc42 delocalized from the lipid raft region of plasma membrane in a time-dependent manner following simvastatin treatment. Correspondingly, increases in soluble RhoA, Rac1 and Cdc42 protein levels were observed in the cytosol compared to untreated controls (Figure 14). Supplementing

cells with mevalonate to restore the prenylation process elicited a detectable decline in the accumulated cytosolic RhoA, Rac1 and Cdc42 content.

Our initial assumption was that cytosolic localized RhoA, Rac1 and Cdc42 should not be GTP-loaded, as membrane localization was thought to be critical for activation of the GTPases. Contrary to our expectations, however, we observed increased GTP-bound forms of RhoA, Rac1 and Cdc42, and also increases in total protein levels of RhoA and Cdc42. Addition of GGPP but not FPP prevented GTP-loading of RhoA, Rac1 and Cdc42 in response to simvastatin treatment (Figure 15-17). These data demonstrate that inhibition of geranylgeranylation paradoxically leads to increased GTP-loading of Rho proteins. To provide a mechanistic basis to these observations, we propose that simvastatin-mediated inhibition of geranylgeranylation prevented Rho proteins from interacting with its negative regulator, Rho GDP-dissociation inhibitor (RhoGDI). RhoGDIs are responsible for sequestering geranylgeranylated GDP-bound Rho proteins in a cytosolic complex and for preventing the guanine nucleotide exchange (Dransart, Olofsson et al. 2005). It has been identified that the essential interaction sites involve the C-terminal geranylgeranyl moiety of Rho proteins and a hydrophobic region on RhoGDIs (Di-Poi, Faure et al. 2001). Hence, it is plausible to hypothesize that lack of geranylgeranylation would prevent this interaction. Indeed, we observed that the respective associations of RhoA and Rac1 with RhoGDIα, the most ubiquitously expressed form of RhoGDIs, were significantly reduced in simvastatin-treated cells. In addition, supplementing cells with MVA or GGPP reversed the interaction (Figure 21). We propose that the decreased association between Rho proteins and their cytosolic inhibitor leads to the accumulation of GTP-bound Rho proteins, possibly due to spontaneous exchange of

GDP to GTP, as the intracellular GTP level is way higher than GDP (Carlucci, Rosi et al. 1997), or it possibly involves the catalytic activities of GEFs (Orita, Kaibuchi et al. 1993).

In addition to geranylgeranylation, we speculate that a second mechanism may exist in regulating Rho-RhoGDI interaction based on previous studies (Mehta, Rahman et al. 2001; Knezevic, Roy et al. 2007), which demonstrated that phosphorylation of RhoGDIα disrupted its association with Rho proteins and resulted in activation of Rho GTPases. Interestingly, several kinases that phosphorylate RhoGDIα are also the downstream effectors of Rho GTPases. For example, p21-activated kinase 1 (PAK1), an effector of both Rac and Cdc42, phosphorylated RhoGDIα at Ser101 and Ser174 to allow for Rac activation upon platelet-derived growth factor or epidermal growth factor stimulation (DerMardirossian, Schnelzer et al. 2004). This study highlighted the possibility that PAK1-mediated disruption of Rac-RhoGDI interaction may be a mechanism for the initiation of Rac activation or a positive feedback response to further amplify the Rac signaling. Hence, future investigation can test if RhoGDIα phosphorylation also plays a role in simvastatin-mediated activation of RhoA and Rac1 by disrupting their interaction with RhoGDIα.

The widely held notion that statins affect Rho GTPases activation by inhibiting their localization via blocking geranylgeranylation is being re-examinered on several fronts. Growing evidence is accumulating that statins are able to increase Rho proteins in their GTP-bound form regardless of their localizations. The observation has not only been seen in the cancer cells used in our studies, but also in BV-2 microglia, THP-1 monocytes, myeloid lineage cells, PC12 pheochromocytoma cells

and N2a mouse neuroblastoma cells, demonstrating a common effect in multiple cell types (Cordle, Koenigsknecht-Talboo et al. 2005).

2.2.2 Activation of RhoA and Rac1 by simvastatin mediates cell kill

Although the Rho proteins in simvastatin-treated cells were unprenylated, we found that the cytosolic GTP-loaded RhoA and Rac1, but not Cdc42, were functional to activate a downstream signaling cascade (involving superoxide production, JNK activation and Bim-EL upregulation, discussed in the later sections), which eventually led to cell death in simvastatin-treated HCT116 cells. This conclusion was supported by the observations that inhibition of RhoA or Rac1 activity using pharmacological inhibitors, gene silencing or expression of dominant negative mutant, substantially restored survival of cancer cells after simvastatin treatment (Figure 18-20). Preliminary data in SHEP-1 cells also showed similar observations, where simvastatin increased GTP-loading of Rac1 and inhibition of which reduced apoptotic hallmarks (Figure 48).

Despite that statins increase GTP-bound Rho proteins in multiple cell types as mentioned in the above section, our study is the first report showing that unprenylated yet GTP-bound Rho proteins are functional to mediate cancer cell death, suggesting that unprenylated Rho can interact with effectors to mediate downstream signaling events. Interestingly, another report complemented our observation by demonstrating that unprenylated RhoA, B and C can partially stimulate the classical serum response element (SRE)-dependent transcription in lovastatin-treated human erythroleukemia cells, albeit significantly less than prenylated Rho proteins (Turner, Zhuang et al. 2008). Functional activity of

unprenylated Rho proteins has been seen in non-cancer models as well. One study showed that mice with GGTase-I deficiency accumulated high levels of GTP-bound RhoA, Rac1 and Cdc42, which then hyperactivate macrophages and induce erosive arthritis (Khan, Ibrahim et al. 2011). Another study demonstrated that N-Bisphosphonates (N-BPs), which prevents prenylation by targeting another enzyme (farnesyl diphosphate synthase, responsible for FPP synthesis) in the mevalonate pathway, inhibited bone resorption by activation of p38 pathway downstream of the unprenylated GTP-loaded Rac (Dunford, Rogers et al. 2006).

Our data provided compelling evidence that the induction of GTP-loaded RhoA and Rac1 is required for simvastatin-mediated cell death. However, inhibiting RhoA or Rac1 activity alone was unable to confer as extensive protection as preincubation with GGPP. We propose that it is possible that inhibition of both RhoA and Rac1 would show an additive or even synergistic protection, or other geranylgeranylated proteins may be contributing to the cell kill by simvastatin treatment. These possibilities can be explored in future investigations.

2.2.3 Beyond the post-translational modification of Rho GTPases by simvastatin

In addition to the intriguing discovery of Rho GTPase activation following simvastatin treatment, we observed that the levels of Rho GTPases were also elevated by such treatment. In our model, simvastatin enhanced protein expression of RhoA and Cdc42 drastically. The effects were shown to be time-dependent; the increment in protein level was obvious from 12 h onwards and lasted throughout the whole time course (Figure 12A). Mevalonate fully reversed the RhoA and Cdc42 overexpression, and GGPP largely prevented the upregulation effects after simvastatin treatment

(Figure 12B). Previous studies have proposed that post-translational geranylgeranylation made Rho proteins more susceptible to proteasomal degradation; hence, inhibition of geranylgeranylation by statins might slow the degradation process and result in the increased protein content (Stamatakis, Cernuda-Morollon et al. 2002; Von Zee and Stubbs 2011). However, we did not observe any changes in protein stability of RhoA and Cdc42 in our model. A chase experiment was performed with protein synthesis inhibitor cycloheximide and the results showed that both proteins decreased at the same time with or without simvastatin treatment, indicating that simvastatin did not change the half-life of these proteins (Figure 24). Instead, *de novo* synthesis of mRNA and protein was more likely to be responsible for the increased protein expression, as pretreatment with transcription inhibitor actinomycin D or cycloheximide dose-dependently reduced protein levels of RhoA and Cdc42 induced by simvastatin (Figure 23).

An impact of statin treatment on transcriptional control of Rho GTPases has been observed in a few recent papers. One study reported that lovastatin treatment increased expression of RhoA and RhoB in human trabecular meshwork cells (Von Zee, Richards et al. 2009); while another study showed that lovastatin and atorvastatin treatment induced Rac and Cdc42 expression in ovarian cancer cells (Liu, Liang et al. 2009). Neither studies reported any functional relevance of the increased Rho proteins; instead they suggested that the upregulation of Rho proteins is merely a feedback response to the induced abrogation of Rho GTPase activities. However, we demonstrate that simvastatin-induced upregulation of Rho proteins is important in mediating the cell death signal. Cells treated with cycloheximide were insensitive to simvastatin treatment, indicating the importance of newly synthesized

proteins in the apoptotic response (Figure 22A, B). Moreover, cycloheximide reduced the GTP-bound form of RhoA and Rac1, the two Rho GTPases responsible for simvastatin-mediated apoptosis (Figure 22C). These observations demonstrated that the newly synthesized unprenylated Rho proteins are those that accumulated in the GTP-bound form. This novel finding of transcriptional control of Rho proteins by a process involves geranylgeranylation and its relevance in mediating the cytotoxic effects of simvastatin could help better understand the cellular consequences due to inhibition of geranylgeranylation. Considering that a large number of proteins undergo geranylgeranylation and the signaling networks are highly complex, it is very likely that one of the affected targets is a component involved in the control of transcription of Rho proteins, such as coactivators, corepressors or transcription factors. However, the understanding of transcription of Rho proteins is very limited. Two mechanisms have been proposed by recent papers: the first is by the action of the small non-coding RNA, or microRNA, miR-31 which suppresses RhoA at post-transcriptional level (Valastyan, Reinhardt et al. 2009). Another recent study provided the first clue of transcription factors involved in RhoA gene regulation; it was shown that RhoA transcription was orchestrated by the Myc-Skp2-Miz1-p300 transcriptional complex in cancer cells (Chan, Lee et al. 2010). Future studies to better understand the transcriptional regulation of Rho GTPases would possibly provide a new angle to interpret statins' anti-tumor effects and understand the molecular basis of Rho overexpression observed in certain tumors.

Collectively, our study is the first to show that post-translational modification by geranylgeranylation can impact Rho GTPases at both transcriptional and post-translational level; the resultant non-canonical activation of Rho GTPases produces

species that are functional in meditating apoptotic effects of simvastatin in cancer cells. Our results along with that presented by other studies challenge the view that inhibiting geranylgeranylation is a means to block the activity of Rho family proteins. On the contrary, inhibiting the process may be stimulating both their expression and activities. Future investigations can be focused on characterizing the status of Rho GTPases in cancer cells that respond to statin treatment in a geranylgeranylation-dependent way, the understanding of which will be fundamental to identify the molecular features required for the non-canonical regulation of Rho GTPases across different cell types and to provide mechanistic insights to statins' anti-cancer effects.

3 The involvement and significance of superoxide production

3.1 Unprenylated RhoA and Rac1 in superoxide production

To further explore the mechanism of how activation of RhoA and Rac1 mediate the cell death response, we identified superoxide production as a downstream event of simvastatin treatment. A time-dependent increase of superoxide production was observed as early as 3 h and sustained from 8 to 24 h following simvastatin treatment (Figure 25). Importantly, abrogation of superoxide production via different types of superoxide-specific scavengers DPI, tempol and tiron invariably protected cancer cells from simvastatin-induced apoptosis, as assessed by morphological rescue and caspases involvement, as well as positive readout from the viability assay (Figure 26). Moreover, simvastatin-mediated superoxide production was downstream of the geranylgeranylation process, based on the observations that GGPP preincubation reversed the superoxide increment accompanying simvastatin treatment, whereas GGTI-298 induced superoxide production (Figure 27).

Inhibition of RhoA and Rac1, but not Cdc42, using the aforementioned tools was also able to abrogate simvastatin-stimulated superoxide production, which was consistent with the cell viability data showing that these manipulations protected cells from simvasstatin-induced cell death (Figure 18-20). In addition, evidence from SHEP-1 cells also suggested that superoxide was a downstream event of Rac1 activation induced by simvastatin (Figure 49). It is not surprising to associate activated Rac1 and RhoA with superoxide production, both of which have been found to activate the superoxide generator NADPH oxidase (NOX). Studies in phagocytic cells have shown that Rac enhances the activity of NOX2 to produce superoxide by assembly of a multimolecular complex at the plasma membrane consisting of membrane

components NOX2 and p22phox, together with cytosolic components p40phox, p47phox, p67phox and Rac. P67phox is proposed to be the Rac effector protein in the NADPH oxidase complex, which directly interacts with GTP-loaded Rac (Diekmann, Abo et al. 1994; Babior 1999; Bokoch and Diebold 2002). Other evidence also supports the role of RhoA in regulating superoxide formation through the NADPH oxidase complex during phagocytosis, most likely via phosphorylation of p47phox (Kim, Diebold et al. 2004). Hence, the current knowledge on Rho GTPases-mediated superoxide production from the NADPH oxidase complex is a promising mechanism to be explored in our model. Indeed, our data suggested that the NADPH oxidase complex is a main source of superoxide production, as evidenced by the protective effect from NOX inhibitor DPI (O'Donnell, Tew et al. 1993) (Figure 26). In addition, our preliminary data showed that gene silencing of NOX2 significantly reduced superoxide level and protected cells from simvastatin-induced cellular insult (Appendix A). Hence, we propose that the unprenylated yet activated RhoA and Rac1 can engage the NADPH oxidase complex to generate superoxide in simvastatin-treated cells, which then leads to cancer cell death. Our finding is supported by another report showing that bacterially-expressed unprenylated Rac can effectively activate the oxidase system in a cell-free assay (Heyworth, Knaus et al. 1993). Together with our report, it directly questioned the necessity for membrane-localized Rac to activate the NADPH oxidase complex.

Currently, one important question that remains to be addressed is the site for the assembly of the functional NADPH oxidase complex in simvastatin-treated cancer cells, other than the plasma membrane. With the expanding of the NOX family from the phagocyte NOX2 to the current seven members identified in non-phagocytic cells (NOX1-5 and DUOX1-2), substantial evidence is suggesting the distribution of NOX

in other cellular compartments (Meier, Cross et al. 1991; Szatrowski and Nathan 1991; Griendling, Minieri et al. 1994; Li and Shah 2003). For example, in smooth muscle cells, NOX2 is found to colocalize with the perinuclear cytoskeleton (Li and Shah 2002). Functional NOX4 was recently found to localize to mitochondria in rat mesangial cells and kidney cortex (Block, Gorin et al. 2009), mouse cardiac myocytes (Kuroda, Ago et al. 2010), and chronic myeloid leukemia cells that overexpress Bcl-2 (Velaithan, Kang et al. 2011). Functional role of NOX4 has also been suggested in the endoplasmic reticulum (ER) and the nucleus from the observations made in vascular smooth muscle and endothelial cells (Hilenski, Clempus et al. 2004; Kuroda, Nakagawa et al. 2005). These pilot studies have provided evidence for activation of NOX in intracellular compartments. The tools and methods used in these studies can be applied to identify the intracellular formation of the NADPH oxidase complex following activation of RhoA and Rac1 upon simvastatin treatment in the future.

3.2 Statin induces oxidative stress specifically in cancer cells

In our model, we established the role of superoxide in simvastatin-mediated killing as various superoxide scavengers were able to abrogate simvastatin-induced apoptosis (Figure 26). Hence, we propose that simvastatin-mediated accumulation of superoxide induces intrinsic oxidative stress and leads to cancer cell death. Earlier publications from the lab have shown that the slight alterations in the intracellular superoxide level lead to a mild “pro-oxidant” state in the cells, which is permissive for cell proliferation as reviewed in (Pervaiz and Clement 2007). However, we argue that an excessive amount of superoxide production would be detrimental to cells via several mechanisms. One possibility is that massive accumulation of superoxide

inside the cells would inactivate critical metabolic enzymes or initiate lipid peroxidation, which results in irreversible cellular injury and ultimately cell death. The same mechanism is used by the anti-cancer agents that target superoxide dismutase (SOD), which also results in superoxide accumulation and selectively kills cancer cells as reviewed in (Huang, Feng et al. 2000). It is also possible that superoxide acts as the initiator ROS, which is then converted into effector ROS/RNS, such as hydrogen peroxide, hydroxyl radical or peroxynitrite, to mediate the apoptotic effects. In addition, NOX-mediated superoxide production has been shown to further amplify the total level of ROS from NOS uncoupling (Verhaar, Westerweel et al. 2004) or the activation of xanthine oxidase (Li and Shah 2004), which may further facilitate the oxidative stress-mediated cellular effects.

Several groups have also demonstrated the involvement of oxidative stress in statin-induced apoptosis in cancer cells, specifically murine CT26 colon cancer (Qi, Kim et al. 2010), K-ras transformed thyroid cells (Laezza, Fiorentino et al. 2008), and MCF-7 breast cancer cells (Sanchez, Rodriguez et al. 2008), suggesting that it might be a common mechanism in statin-sensitive cancer cells. However, the anti-oxidant effects of statins have also been well-established in improving endothelial functions and mediating its cardioprotective effects (Stoll, McCormick et al. 2004). To provide a possible explanation of the opposing observations, it is interesting to notice a pattern whereby statins exert anti-oxidative effects in non-cancerous cells but induce oxidative stress in multiple cancer types. We hypothesize that this oxidative stress response induced by statins might be a possible tumor-selective mechanism that mediates statins' anti-tumor effects. If this hypothesis holds true, then the molecular basis of how statins differentially regulate oxidative stress in different cell types

would be a subject to explore. One possible mechanism may be the non-canonical regulation of the Rho GTPases by statins shown in our study, where unprenylated yet activated Rho proteins can engage its downstream effectors to mediate superoxide production.

4. The involvement and significance of JNK signaling

4.1 JNK is the downstream mediator in simvastatin-induced apoptosis

Our data support the importance of JNK pathway in mediating simvastatin-induced apoptosis in HCT116 cells. Simvastatin elicited JNK activation by fostering phosphorylation at Thr183 and Tyr185 without increasing its expression, and this activation is a sustained and prolonged process which was observed as early as 3 h post-treatment and persisted throughout the time course of analysis (Figure 30).

It has been suggested that the kinetics of JNK activation play a role in determining its biological function. Early and transient activation of JNK mediates cell survival, while sustained JNK activation caused by cytotoxic drugs or cellular insults has been shown to trigger apoptosis (Chang, Kamata et al. 2006; Lin 2006; Ventura, Hubner et al. 2006). It is well documented that transcriptional-dependent or -independent role of JNK can both contribute to apoptosis. For example, activation of c-Jun downstream of JNK signaling can lead to transcription of pro-apoptotic genes such as Fas-L and Bim (Faris, Latinis et al. 1998); on the other hand, JNK can phosphorylate pro- or anti-apoptotic proteins such as p53 and Bcl-2 to exert apoptotic functions (Milne, Campbell et al. 1995; Maundrell, Antonsson et al. 1997). Indeed, in this study, the observed sustained JNK activation was required for cell death as JNK inhibitor SP600125 (Bennett, Sasaki et al. 2001) significantly protected cells from simvastatin-induced apoptosis and reduction in colony formation potential in HCT116 cells (Figure 32); similar responses were also observed in simvastatin-treated SHEP-1 cells (Figure 50).

In accordance with our findings that JNK represents an important mediator in controlling simvastatin-induced apoptotic signaling cascade, several other studies have also highlighted the importance of JNK signaling in mediating statin-induced cell death in human breast cancer cells (Koyuturk, Ersoz et al. 2007), C6 glioma cells (Koyuturk, Ersoz et al. 2004), salivary adenoid cystic cancer cells (Zhang, Wang et al. 2010) and ovarian cancer cells (Liu, Liang et al. 2009). Additionally, we found that JNK activation in response to simvastatin treatment is specifically associated with geranylgeranylation, which was shown by inhibition of JNK phosphorylation by mevalonate and GGPP preincubation but not FPP, as well as induction of JNK phosphorylation by GGTI-298 (Figure 31).

Other than JNK activation, we also observed changes in cell survival signaling pathways ERK and AKT, evidenced by dephosphorylation at Thr202/Tyr204 for ERK and Ser473 for AKT. Dephosphorylation of ERK and AKT by simvastatin was only reversed by mevalonate preincubation, but not affected by either GGPP or FPP (Figure 31A). Since the geranylgeranylation process was found to be essential in mediating the apoptotic response, we conclude that ERK and AKT, unlike JNK, are not the major signaling components to convey the death signal after simvastatin treatment. Indeed some studies have suggested that statin-mediated changes in ERK and AKT were modulated via cholesterol-dependent lipid raft signaling (Roy, Kung et al. 2011).

4.2 Upstream signals for simvastatin-mediated JNK activation

This study highlighted the role of superoxide in activating JNK pathway. JNK phosphorylation was fully abrogated following inhibition of superoxide production

and its upstream activation signal RhoA or Rac1 activity in HCT116 cells (Figure 33, 34). Additional evidence from SHEP-1 cells also showed that inhibiting Rac1 activity or superoxide production reduced JNK activation following simvastatin treatment (Figure 50). Despite this being the first report of superoxide-mediated JNK activation in simvastatin-treated cancer cells, various oxidants and ROS-producing agents have previously been shown to mediate JNK activation, such as hydrogen peroxide, arsenite trioxide, UV radiation and cadmium chloride (Meier, Rouse et al. 1996; Dent, Yacoub et al. 2003; Leonard, Harris et al. 2004; Conde de la Rosa, Schoemaker et al. 2006).

JNK can be activated via two mechanisms, one is from the activation of a MAPKKK-MAPKK-JNK kinase cascade (Lin and Dibling 2002), or it can be regulated by JNK inactivating phosphatases. Here, we propose a few candidate targets which might be modulated by oxidative stress to activate JNK pathway in our model. Apoptosis signal-regulating kinase 1 (ASK1) is a MAPKKK implicated in ROS-mediated JNK activation. The critical role of ASK1 in ROS-mediated apoptosis has been shown both *in vitro* and *in vivo*, and superoxide or hydrogen peroxide production has been identified as the major mechanism for various anti-cancer drugs to regulate ASK1-mediated cell death (Du, Suzuki et al. 2001; Tobiume, Matsuzawa et al. 2001; Machino, Hashimoto et al. 2003; Goldman, Chen et al. 2004). In addition, ASK1 knockout mice are more resistant to oxidative and ER stress-induced apoptosis while exhibiting a significantly lower level of JNK activation as compared to wild type mice (Matsuzawa, Nishitoh et al. 2002). Other than activating kinases, JNK can be regulated by MAPK phosphatase (MKPs) as well. It is worth noting that MKP-1 has been suggested to play an important role in cancer cell survival, downregulation of

which is implicated in cancer prevention and chemosensitization (Liao, Guo et al. 2003; Chen, Huang et al. 2005; Wang, Zhou et al. 2007; Wu 2007). A recent paper showed that superoxide-mediated MKP1 degradation was the main mechanism for JNK-mediated lung cancer cell death induced by a plant-derived flavonoid luteolin (Bai, Xu et al. 2012). Hence, whether simvastatin-mediated oxidative stress affects any kinases or phosphatases, thereby activating JNK, remains an avenue for future investigations.

The significance of superoxide-mediated JNK activation is demonstrated by its ability to modulate cell death response after simvastatin treatment. A large body of evidence in the literature supports the notion that ROS-mediated JNK activation is able to induce apoptosis. For example, our lab has established that the pharmacologic agent LY303511 sensitizes neuroblastoma cells to TRAIL via hydrogen peroxide-mediated JNK activation and upregulation of death receptor (Shenoy, Wu et al. 2009). Another study showed that TNFα induced caspase-dependent ROS accumulation and prolonged JNK activation, which was followed by apoptotic and necrotic cell death in various tumor cells (Nakajima, Kojima et al. 2008). Together with our observations, we propose that ROS-mediated JNK activation may be a common mechanism utilized by other types of statins or ROS producing-agents to induce cancer cell death.

5. The involvement and significance of pro-apoptotic protein BIM

5.1 Increase in Bim-EL content mediates simvastatin's apoptotic effects

Initiation of mitochondrial apoptotic pathway is always orchestrated by the interplays between pro-survival and pro-apoptotic Bcl-2 family proteins (Gross, McDonnell et al. 1999). In our study, when HCT116 cells were treated with simvastatin over a period from 16 to 32 h, we did not observe any changes in pro-survival protein Bcl-xL and cleavage of pro-apoptotic protein Bid. However, the level of pro-apoptotic BH3-only protein Bim was markedly elevated after simvastatin treatment (Figure 36). Moreover, reduction of Bim-EL expression with four individual siRNA sequences significantly protected cells from simvastatin-induced apoptosis, as shown by an increase in cell viability and reduced caspase-3 and PARP cleavage (Figure 37). Considering that complete inhibition of Bim-EL by siRNA transfection did not completely protected the cells, it seems that other factors other than Bim-EL may contribute to simvastatin-induced apoptosis. Nonetheless, it does appear that the increased Bim-EL level accounts for the major component in mediating the apoptotic effects of simvastatin in HCT116 cells. The results also support the hypothesis that chemotherapy which tilts the balance of Bcl-2 family proteins to the pro-apoptotic side may confer cells susceptible to apoptosis. Previous studies have demonstrated that Bim is a unique BH3 protein that is able to directly induce the conformational changes of Bax and Bak, or indirectly activates Bax and Bak by neutralizing the anti-apoptotic Bcl-2 proteins, which precedes apoptosis (Czabotar, Colman et al. 2009). We also showed that simvastatin increased Bim-EL content in Bax knockout HCT116 cells comparable to that in the wildtype cells, suggesting that Bim-EL acts upstream of the Bax signaling to assist apoptosis (Figure 43). Our findings are among the first few to demonstrate the importance of Bim-EL upregulation in statin-

mediated cancer cell death, together with the report of Jang *et al* showing that Bim-EL upregulation is essential in lovastatin-induced glioblastoma cell death (Jiang, Zheng et al. 2004). There is a third report that also showed induction of Bim in ovarian cancer by lovastatin. However, that study did not further address the relevance of Bim in the cell death mechanism (Liu, Liang et al. 2009).

5.2 The mechanism for simvastatin-mediated Bim-EL upregulation

Previously, we have established that simvastatin triggers apoptosis via depletion of GGPP. Here, we observed that cells preincubated with GGPP, but not FPP, fully prevented accumulation of Bim-EL after simvastatin treatment (Figure 38), suggesting that the increase in Bim-EL content was regulated primarily by geranylgeranylation, but not farnesylation. We then identified that RhoA/Rac1-Superoxide-JNK signaling cascade contributes to the induction of Bim-EL expression in response to simvastatin treatment. Separate inhibition of RhoA or Rac1 activation (Figure 39), superoxide production (Figure 40) and JNK activation (Figure 41) successfully abrogated Bim-EL expression after simvastatin treatment. The observation of JNK-mediated Bim-EL upregulation was also made in lovastatin-treated ovarian cancer cells (Liu, Liang et al. 2009).

The role of JNK-Bim-EL signaling pathway in apoptosis has been very well characterized in the nervous system upon withdrawal of nerve growth factor (NGF), where JNK regulates the apoptotic activity of Bim-EL via increasing Bim-EL expression or JNK-mediated phosphorylation of Bim-EL at Ser65 (Harris and Johnson 2001; Putcha, Moulder et al. 2001; Becker, Howell et al. 2004). Transcriptional factors that drive Bim transcription, such as c-Jun and Forkhead box

3a (FOXO3a), are identified to be downstream targets of JNK activation, providing possible mechanisms for JNK-mediated transcriptional control of Bim upregulation (Whitfield, Neame et al. 2001; Wang, Chen et al. 2012). On the other hand, the phosphorylation status of Bim-EL has been found to affect its protein expression by modulating its stability. Phosphorylation by ERK facilitated proteosomal degradation of Bim-EL and promoted cell survival (Ley, Balmanno et al. 2003). However, the role of JNK-mediated Bim-EL phosphorylation in its degradation has been controversial. To further understand whether Bim-EL upregulation is due to transcriptional or post-translational control, we showed that both actinomycin D and cycloheximide attenuated the increased Bim-EL protein content, in support of the role of *de novo* Bim-EL protein synthesis (Figure 44). Moreover, we did not observe any changes in the degradation rate of Bim-EL with or without simvastatin treatment, indicating that the stability of Bim-EL remained intact (Figure 45). This observation also indirectly excludes the possibility of phosphorylation-mediated changes in Bim-EL protein expression. In summary, we propose that JNK-mediated transcriptional control of Bim-EL is the main mechanism responsible for simvastatin-induced apoptosis in HCT116 cells, possibly involving the transcriptional factors c-Jun and FOXO3a. In line with the hypothesis, our preliminary data showed phosphorylation of c-Jun and upregulation of FOXO3a, following JNK activation upon simvastatin treatment (Appendix B). Due to the unsuccessful attempts to detect endogenous Bim-EL phosphorylation at Ser65 in our experiments, we did not explore the possible role of phosphorylated Bim-EL in mediating simvastatin's apoptotic effects. Future studies are required to address this aspect of Bim regulation by JNK.

Our study is the first to explore the mechanisms responsible for Bim upregulation induced by statins. Preliminary studies in M14 melanoma cells stably transfected with constitutively-active Rac1 also showed that simvastatin activated a more pronounced Rac1-JNK-Bim signaling cascade, corresponding to more efficient PARP cleavage, compared to M14 cells stably transfected with empty vector. Together with the signaling cascade we have established in simvastatin-treated HCT116 cells, our data in M14 cells further supports the notion that the JNK-Bim cascade may be a common mechanism activated by Rac1 signaling to mediate cell death (Appendix C). To support this proposal, a recent study also demonstrated a role of Rac-JNK-Bim axis in c-Myc-induced apoptosis in mammary epithelial cells MCF 10A (Zhan, Rosenberg et al. 2008).

CONCLUSION

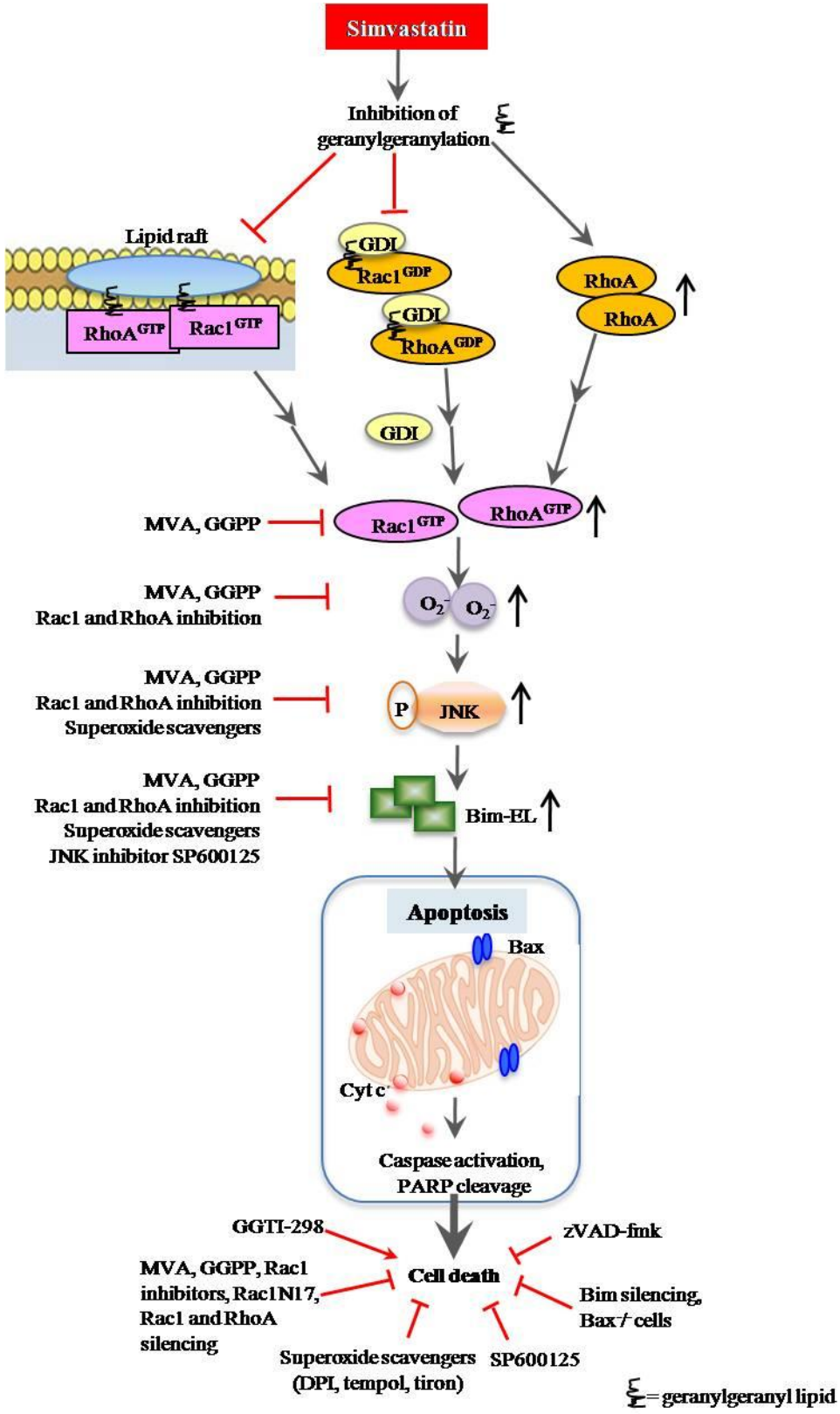

Figure 51: Molecular mechanism of simvastatin-mediated apoptosis in HCT116 cells.

This is a novel report providing mechanistic insights for simvastatin's anti-tumor effects in human cancer cells. Our findings from a combination of breast carcinoma, colorectal carcinoma, lung carcinoma, melanoma and neuroblastoma models confirm that the potent tumorcidal activity of simvastatin treatment is not restricted to one but multiple cancer types. Our data in colorectal cancer cells demonstrate that apoptosis is the main mechanism mediated by simvastatin, which is further identified as Bax- and caspase-dependent. This study also reinforces that simvastatin exerts effects via inhibiting the mevalonate pathway, and highlights the importance of the downstream protein geranylgeranylation over farnesylation in mediating the cytotoxic effects, as exogenously-added GGPP prevents cell death while GGTI-298 exhibits similar effects as simvastatin. Further investigations on the potential involvement of geranylgeranylated proteins show that active RhoA and Rac1 are required and responsible for cellular demise in the wake of simvastatin treatment. Suppression of RhoA and Rac1 activity largely abolished the apoptotic hallmarks. This is most intriguing in view of the fact that inhibition of geranylgeranylation is normally associated with inhibition of Rho GTPases functions. We provide a possible explanation that simvastatin-mediated increase in GTP-loaded RhoA and Rac1 are due to decreased association with their cytosolic sequester RhoGDIα by inhibiting geranylgeranylation. The functionality of RhoA and Rac1 were further evidenced by their ability to mediate production of superoxide and activation of JNK pathway in response to simvastatin treatment. Superoxide represents a central initiator of the simvastatin-elicited cellular signaling pathway, which kick-starts the apoptotic process by activating the MAPK family member JNK. The function of JNK in apoptosis has been well established and in this study we identify that simvastatin induces the expression of extra-long form of Bim (Bim-EL) in a JNK-dependent

manner. Suppression of Bim-EL expression significantly prevents simvastatin-induced apoptosis. In summary, our results unveil a novel signaling cascade consisting of players such as RhoA, Rac1, superoxide, JNK and Bim-EL that is responsible for simvastatin's cytotoxicity in colorectal cancer cells. We also establish that most of the players are critically involved in simvastatin-mediated neuroblastoma cell death, suggesting that this molecular mechanism might be activated in other cancer cells sensitive to simvastatin treatment.

Taken together, our data demonstrates the tremendous potential of simvastatin to induce cancer cell death. Together with the advantages that statins can be introduced into clinical practice quickly and enjoy a favorable safety profile with uncommon but well-characterized side effects, they represent attractive targets in the search of tumor-specific and efficient anti-cancer agents. Further, the molecular players identified in this project not only provide novel potential targets for therapeutic manipulation, also lays the foundation to explore the role of statins as an adjuvant in combinational therapies to treat cancer.

REFERENCES

(1994). "Randomised trial of cholesterol lowering in 4444 patients with coronary heart disease: the Scandinavian Simvastatin Survival Study (4S)." Lancet **344**(8934): 1383-1389.

(1998). "Prevention of cardiovascular events and death with pravastatin in patients with coronary heart disease and a broad range of initial cholesterol levels. The Long-Term Intervention with Pravastatin in Ischaemic Disease (LIPID) Study Group." N Engl J Med **339**(19): 1349-1357.

(2002). "MRC/BHF Heart Protection Study of cholesterol lowering with simvastatin in 20,536 high-risk individuals: a randomised placebo-controlled trial." Lancet **360**(9326): 7-22.

Abo, A., E. Pick, et al. (1991). "Activation of the NADPH oxidase involves the small GTP-binding protein p21rac1." Nature **353**(6345): 668-670.

Adhami, F., G. Liao, et al. (2006). "Cerebral ischemia-hypoxia induces intravascular coagulation and autophagy." Am J Pathol **169**(2): 566-583.

Agarwal, B., B. Halmos, et al. (2002). "Mechanism of lovastatin-induced apoptosis in intestinal epithelial cells." Carcinogenesis **23**(3): 521-528.

Alberts, A. W. (1990). "Lovastatin and simvastatin--inhibitors of HMG CoA reductase and cholesterol biosynthesis." Cardiology **77 Suppl 4**: 14-21.

Alessi, D. R. (2001). "Discovery of PDK1, one of the missing links in insulin signal transduction. Colworth Medal Lecture." Biochem Soc Trans **29**(Pt 2): 1-14.

Alessi, D. R., M. Deak, et al. (1997). "3-Phosphoinositide-dependent protein kinase-1 (PDK1): structural and functional homology with the Drosophila DSTPK61 kinase." Curr Biol **7**(10): 776-789.

Allal, C., G. Favre, et al. (2000). "RhoA prenylation is required for promotion of cell growth and transformation and cytoskeleton organization but not for induction of serum response element transcription." J Biol Chem **275**(40): 31001-31008.

Alnemri, E. S., D. J. Livingston, et al. (1996). "Human ICE/CED-3 protease nomenclature." Cell **87**(2): 171.

Alonso, D. F., H. G. Farina, et al. (1998). "Reduction of mouse mammary tumor formation and metastasis by lovastatin, an inhibitor of the mevalonate pathway of cholesterol synthesis." Breast Cancer Res Treat **50**(1): 83-93.

Anderson, R. G. (1998). "The caveolae membrane system." Annu Rev Biochem **67**: 199-225.

Anderson, T. J., I. T. Meredith, et al. (1995). "The effect of cholesterol-lowering and antioxidant therapy on endothelium-dependent coronary vasomotion." N Engl J Med **332**(8): 488-493.

Andreyev, A. Y., Y. E. Kushnareva, et al. (2005). "Mitochondrial metabolism of reactive oxygen species." Biochemistry (Moscow) **70**(2): 200-214.

Andreyev, A. Y., Y. E. Kushnareva, et al. (2005). "Mitochondrial metabolism of reactive oxygen species." Biochemistry (Mosc) **70**(2): 200-214.

Antonsson, B., S. Montessuit, et al. (2000). "Bax oligomerization is required for channel-forming activity in liposomes and to trigger cytochrome c release from mitochondria." Biochem J **345 Pt 2**: 271-278.

Arbour, N., J. L. Vanderluit, et al. (2008). "Mcl-1 is a key regulator of apoptosis during CNS development and after DNA damage." J Neurosci **28**(24): 6068-6078.

Asakura, K., Y. Izumi, et al. (2011). "The cytostatic effects of lovastatin on ACC-MESO-1 cells." J Surg Res **170**(2): e197-209.
Ashby, M. N. (1998). "CaaX converting enzymes." Curr Opin Lipidol **9**(2): 99-102.
Attoub, S., V. Noe, et al. (2000). "Leptin promotes invasiveness of kidney and colonic epithelial cells via phosphoinositide 3-kinase-, rho-, and rac-dependent signaling pathways." FASEB J **14**(14): 2329-2338.
Aust, S. D., D. L. Roerig, et al. (1972). "Evidence for superoxide generation by NADPH-cytochrome c reductase of rat liver microsomes." Biochem Biophys Res Commun **47**(5): 1133-1137.
Aznar, S. and J. C. Lacal (2001). "Rho signals to cell growth and apoptosis." Cancer Lett **165**(1): 1-10.
Babior, B. M. (1999). "NADPH oxidase: an update." Blood **93**(5): 1464-1476.
Babior, B. M., R. S. Kipnes, et al. (1973). "Biological defense mechanisms. The production by leukocytes of superoxide, a potential bactericidal agent." J Clin Invest **52**(3): 741-744.
Bagrodia, S., B. Derijard, et al. (1995). "Cdc42 and PAK-mediated signaling leads to Jun kinase and p38 mitogen-activated protein kinase activation." J Biol Chem **270**(47): 27995-27998.
Bai, L., X. Xu, et al. (2012). "A superoxide-mediated mitogen-activated protein kinase phosphatase-1 degradation and c-Jun NH(2)-terminal kinase activation pathway for luteolin-induced lung cancer cytotoxicity." Mol Pharmacol **81**(4): 549-555.
Balakumar, P., S. Kathuria, et al. (2012). "Is targeting eNOS a key mechanistic insight of cardiovascular defensive potentials of statins?" J Mol Cell Cardiol **52**(1): 83-92.
Barnhart, B. C., E. C. Alappat, et al. (2003). "The CD95 type I/type II model." Semin Immunol **15**(3): 185-193.
Bartholomeusz, G., Y. Wu, et al. (2006). "Nuclear translocation of the pro-apoptotic Bcl-2 family member Bok induces apoptosis." Mol Carcinog **45**(2): 73-83.
Bayraktutan, U., L. Blayney, et al. (2000). "Molecular characterization and localization of the NAD(P)H oxidase components gp91-phox and p22-phox in endothelial cells." Arterioscler Thromb Vasc Biol **20**(8): 1903-1911.
Becker, E. B., J. Howell, et al. (2004). "Characterization of the c-Jun N-terminal kinase-BimEL signaling pathway in neuronal apoptosis." J Neurosci **24**(40): 8762-8770.
Beckman, J. S. and W. H. Koppenol (1996). "Nitric oxide, superoxide, and peroxynitrite: the good, the bad, and ugly." Am J Physiol **271**(5 Pt 1): C1424-1437.
Bedard, K. and K. H. Krause (2007). "The NOX family of ROS-generating NADPH oxidases: physiology and pathophysiology." Physiol Rev **87**(1): 245-313.
Bennett, B. L., D. T. Sasaki, et al. (2001). "SP600125, an anthrapyrazolone inhibitor of Jun N-terminal kinase." Proc Natl Acad Sci U S A **98**(24): 13681-13686.
Berger, N. A. and S. J. Petzold (1985). "Identification of minimal size requirements of DNA for activation of poly(ADP-ribose) polymerase." Biochemistry **24**(16): 4352-4355.
Berndt, N., A. D. Hamilton, et al. (2011). "Targeting protein prenylation for cancer therapy." Nat Rev Cancer **11**(11): 775-791.
Betteridge, D. J. (2000). "What is oxidative stress?" Metabolism **49**(2 Suppl 1): 3-8.
Bishop, A. L. and A. Hall (2000). "Rho GTPases and their effector proteins." Biochem J **348 Pt 2**: 241-255.

Biswas, S. C., Y. Shi, et al. (2007). "Pro-apoptotic Bim induction in response to nerve growth factor deprivation requires simultaneous activation of three different death signaling pathways." J Biol Chem **282**(40): 29368-29374.
Blais, L., A. Desgagne, et al. (2000). "3-Hydroxy-3-methylglutaryl coenzyme A reductase inhibitors and the risk of cancer: a nested case-control study." Arch Intern Med **160**(15): 2363-2368.
Block, K., Y. Gorin, et al. (2009). "Subcellular localization of Nox4 and regulation in diabetes." Proc Natl Acad Sci U S A **106**(34): 14385-14390.
Blumenthal, R. S. (2000). "Statins: effective antiatherosclerotic therapy." Am Heart J **139**(4): 577-583.
Bokoch, G. M. and B. A. Diebold (2002). "Current molecular models for NADPH oxidase regulation by Rac GTPase." Blood **100**(8): 2692-2696.
Bordier, C. (1981). "Phase separation of integral membrane proteins in Triton X-114 solution." J Biol Chem **256**(4): 1604-1607.
Borutaite, V. and G. C. Brown (2007). "Mitochondrial regulation of caspase activation by cytochrome oxidase and tetramethylphenylenediamine via cytosolic cytochrome c redox state." J Biol Chem **282**(43): 31124-31130.
Boudreau, D. M., O. Yu, et al. (2010). "Statin use and cancer risk: a comprehensive review." Expert Opin Drug Saf **9**(4): 603-621.
Boudreau, D. M., O. Yu, et al. (2007). "Statin use and breast cancer risk in a large population-based setting." Cancer Epidemiol Biomarkers Prev **16**(3): 416-421.
Bouillet, P., S. Cory, et al. (2001). "Degenerative disorders caused by Bcl-2 deficiency prevented by loss of its BH3-only antagonist Bim." Dev Cell **1**(5): 645-653.
Bouillet, P., D. C. Huang, et al. (2000). "The role of the pro-apoptotic Bcl-2 family member bim in physiological cell death." Ann N Y Acad Sci **926**: 83-89.
Bouillet, P., D. Metcalf, et al. (1999). "Proapoptotic Bcl-2 relative Bim required for certain apoptotic responses, leukocyte homeostasis, and to preclude autoimmunity." Science **286**(5445): 1735-1738.
Bouillet, P., J. F. Purton, et al. (2002). "BH3-only Bcl-2 family member Bim is required for apoptosis of autoreactive thymocytes." Nature **415**(6874): 922-926.
Boulton, T. G., S. H. Nye, et al. (1991). "ERKs: a family of protein-serine/threonine kinases that are activated and tyrosine phosphorylated in response to insulin and NGF." Cell **65**(4): 663-675.
Boyartchuk, V. L., M. N. Ashby, et al. (1997). "Modulation of Ras and a-factor function by carboxyl-terminal proteolysis." Science **275**(5307): 1796-1800.
Brown, D. A. and E. London (1998). "Functions of lipid rafts in biological membranes." Annu Rev Cell Dev Biol **14**: 111-136.
Brown, J. L., L. Stowers, et al. (1996). "Human Ste20 homologue hPAK1 links GTPases to the JNK MAP kinase pathway." Curr Biol **6**(5): 598-605.
Brusca, J. S. and J. D. Radolf (1994). "Isolation of integral membrane proteins by phase partitioning with Triton X-114." Methods Enzymol **228**: 182-193.
Bubici, C., S. Papa, et al. (2006). "Mutual cross-talk between reactive oxygen species and nuclear factor-kappa B: molecular basis and biological significance." Oncogene **25**(51): 6731-6748.
Buettner, G. R., C. F. Ng, et al. (2006). "A new paradigm: manganese superoxide dismutase influences the production of H2O2 in cells and thereby their biological state." Free Radic Biol Med **41**(8): 1338-1350.

Burdon, R. H., D. Alliangana, et al. (1995). "Hydrogen peroxide and the proliferation of BHK-21 cells." Free Radic Res **23**(5): 471-486.
Cadenas, E., A. Boveris, et al. (1977). "Production of superoxide radicals and hydrogen peroxide by NADH-ubiquinone reductase and ubiquinol-cytochrome c reductase from beef-heart mitochondria." Arch Biochem Biophys **180**(2): 248-257.
Cafforio, P., F. Dammacco, et al. (2005). "Statins activate the mitochondrial pathway of apoptosis in human lymphoblasts and myeloma cells." Carcinogenesis **26**(5): 883-891.
Campbell, M. J., L. J. Esserman, et al. (2006). "Breast cancer growth prevention by statins." Cancer Res **66**(17): 8707-8714.
Cantrell, D. A. (2001). "Phosphoinositide 3-kinase signalling pathways." J Cell Sci **114**(Pt 8): 1439-1445.
Capdevila, J., N. Chacos, et al. (1981). "Liver microsomal cytochrome P-450 and the oxidative metabolism of arachidonic acid." Proc Natl Acad Sci U S A **78**(9): 5362-5366.
Cardone, M. H., N. Roy, et al. (1998). "Regulation of cell death protease caspase-9 by phosphorylation." Science **282**(5392): 1318-1321.
Carlucci, F., F. Rosi, et al. (1997). "Purine nucleotide metabolism: specific aspects in chronic lymphocytic leukemia lymphocytes." Biochim Biophys Acta **1360**(3): 203-210.
Casagrande, F., D. Bacqueville, et al. (1998). "G1 phase arrest by the phosphatidylinositol 3-kinase inhibitor LY 294002 is correlated to up-regulation of p27Kip1 and inhibition of G1 CDKs in choroidal melanoma cells." FEBS Lett **422**(3): 385-390.
Casciola-Rosen, L., D. W. Nicholson, et al. (1996). "Apopain/CPP32 cleaves proteins that are essential for cellular repair: a fundamental principle of apoptotic death." J Exp Med **183**(5): 1957-1964.
Chan, C. H., S. W. Lee, et al. (2010). "Deciphering the transcriptional complex critical for RhoA gene expression and cancer metastasis." Nat Cell Biol **12**(5): 457-467.
Chan, K. K., A. M. Oza, et al. (2003). "The statins as anticancer agents." Clin Cancer Res **9**(1): 10-19.
Chan, P. C. and B. H. Bielski (1980). "Glyceraldehyde-3-phosphate dehydrogenase-catalyzed chain oxidation of reduced nicotinamide adenine dinucleotide by perhydroxyl radicals." Journal of Biological Chemistry **255**(3): 874-876.
Chan, P. C. and H. J. Bielski (1974). "Enzyme-catalyzed Free Radical Reactions with Nicotinamide Adenine Nucleotides." Journal of Biological Chemistry **249**(4): 1317-1319.
Chang, F., L. S. Steelman, et al. (2003). "Regulation of cell cycle progression and apoptosis by the Ras/Raf/MEK/ERK pathway (Review)." Int J Oncol **22**(3): 469-480.
Chang, L., H. Kamata, et al. (2006). "The E3 ubiquitin ligase itch couples JNK activation to TNFalpha-induced cell death by inducing c-FLIP(L) turnover." Cell **124**(3): 601-613.
Chen, Y. W., S. C. Huang, et al. (2005). "Bowman-Birk inhibitor abates proteasome function and suppresses the proliferation of MCF7 breast cancer cells through accumulation of MAP kinase phosphatase-1." Carcinogenesis **26**(7): 1296-1306.

Cheng, G., B. A. Diebold, et al. (2006). "Nox1-dependent reactive oxygen generation is regulated by Rac1." J Biol Chem **281**(26): 17718-17726.
Chinnaiyan, A. M. (1999). "The apoptosome: heart and soul of the cell death machine." Neoplasia **1**(1): 5-15.
Chipuk, J. E., T. Kuwana, et al. (2004). "Direct activation of Bax by p53 mediates mitochondrial membrane permeabilization and apoptosis." Science **303**(5660): 1010-1014.
Chuang, T. H., K. M. Hahn, et al. (1997). "The small GTPase Cdc42 initiates an apoptotic signaling pathway in Jurkat T lymphocytes." Mol Biol Cell **8**(9): 1687-1698.
Clerkin, J. S., R. Naughton, et al. (2008). "Mechanisms of ROS modulated cell survival during carcinogenesis." Cancer Lett **266**(1): 30-36.
Codogno, P. and A. J. Meijer (2005). "Autophagy and signaling: their role in cell survival and cell death." Cell Death Differ **12 Suppl 2**: 1509-1518.
Cohen, G. M. (1997). "Caspases: the executioners of apoptosis." Biochem J **326 (Pt 1)**: 1-16.
Collisson, E. A., C. Kleer, et al. (2003). "Atorvastatin prevents RhoC isoprenylation, invasion, and metastasis in human melanoma cells." Mol Cancer Ther **2**(10): 941-948.
Conde de la Rosa, L., M. H. Schoemaker, et al. (2006). "Superoxide anions and hydrogen peroxide induce hepatocyte death by different mechanisms: involvement of JNK and ERK MAP kinases." J Hepatol **44**(5): 918-929.
Cordle, A., J. Koenigsknecht-Talboo, et al. (2005). "Mechanisms of statin-mediated inhibition of small G-protein function." J Biol Chem **280**(40): 34202-34209.
Corsini, A., S. Bellosta, et al. (1999). "New insights into the pharmacodynamic and pharmacokinetic properties of statins." Pharmacol Ther **84**(3): 413-428.
Corsini, A., F. M. Maggi, et al. (1995). "Pharmacology of competitive inhibitors of HMG-CoA reductase." Pharmacol Res **31**(1): 9-27.
Cory, S. and J. M. Adams (2002). "The Bcl2 family: regulators of the cellular life-or-death switch." Nat Rev Cancer **2**(9): 647-656.
Cowley, S., H. Paterson, et al. (1994). "Activation of MAP kinase kinase is necessary and sufficient for PC12 differentiation and for transformation of NIH 3T3 cells." Cell **77**(6): 841-852.
Crick, D. C., D. A. Andres, et al. (1998). "Geranylgeraniol overcomes the block of cell proliferation by lovastatin in C6 glioma cells." J Neurochem **70**(6): 2397-2405.
Crisby, M., G. Nordin-Fredriksson, et al. (2001). "Pravastatin treatment increases collagen content and decreases lipid content, inflammation, metalloproteinases, and cell death in human carotid plaques: implications for plaque stabilization." Circulation **103**(7): 926-933.
Czabotar, P. E., P. M. Colman, et al. (2009). "Bax activation by Bim?" Cell Death Differ **16**(9): 1187-1191.
Davis, R. J. (2000). "Signal transduction by the JNK group of MAP kinases." Cell **103**(2): 239-252.
Dejean, L. M., S. Martinez-Caballero, et al. (2005). "Oligomeric Bax is a component of the putative cytochrome c release channel MAC, mitochondrial apoptosis-induced channel." Mol Biol Cell **16**(5): 2424-2432.
Demierre, M. F., P. D. Higgins, et al. (2005). "Statins and cancer prevention." Nat Rev Cancer **5**(12): 930-942.

Deng, Y., X. Ren, et al. (2003). "A JNK-dependent pathway is required for TNFalpha-induced apoptosis." Cell **115**(1): 61-70.
Denoyelle, C., M. Vasse, et al. (2001). "Cerivastatin, an inhibitor of HMG-CoA reductase, inhibits the signaling pathways involved in the invasiveness and metastatic properties of highly invasive breast cancer cell lines: an in vitro study." Carcinogenesis **22**(8): 1139-1148.
Dent, P., A. Yacoub, et al. (2003). "MAPK pathways in radiation responses." Oncogene **22**(37): 5885-5896.
DerMardirossian, C., A. Schnelzer, et al. (2004). "Phosphorylation of RhoGDI by Pak1 mediates dissociation of Rac GTPase." Mol Cell **15**(1): 117-127.
Dhanasekaran, D. N. and E. P. Reddy (2008). "JNK signaling in apoptosis." Oncogene **27**(48): 6245-6251.
Di-Poi, N., J. Faure, et al. (2001). "Mechanism of NADPH oxidase activation by the Rac/Rho-GDI complex." Biochemistry **40**(34): 10014-10022.
Diehl, J. A., M. Cheng, et al. (1998). "Glycogen synthase kinase-3beta regulates cyclin D1 proteolysis and subcellular localization." Genes Dev **12**(22): 3499-3511.
Diekmann, D., A. Abo, et al. (1994). "Interaction of Rac with p67phox and regulation of phagocytic NADPH oxidase activity." Science **265**(5171): 531-533.
Dimitroulakos, J., W. H. Marhin, et al. (2002). "Microarray and biochemical analysis of lovastatin-induced apoptosis of squamous cell carcinomas." Neoplasia **4**(4): 337-346.
Dimitroulakos, J., D. Nohynek, et al. (1999). "Increased sensitivity of acute myeloid leukemias to lovastatin-induced apoptosis: A potential therapeutic approach." Blood **93**(4): 1308-1318.
Dougherty, M. K., J. Muller, et al. (2005). "Regulation of Raf-1 by direct feedback phosphorylation." Mol Cell **17**(2): 215-224.
Dovas, A. and J. R. Couchman (2005). "RhoGDI: multiple functions in the regulation of Rho family GTPase activities." Biochem J **390**(Pt 1): 1-9.
Downs, J. R., M. Clearfield, et al. (1998). "Primary prevention of acute coronary events with lovastatin in men and women with average cholesterol levels: results of AFCAPS/TexCAPS. Air Force/Texas Coronary Atherosclerosis Prevention Study." JAMA **279**(20): 1615-1622.
Downward, J. (1999). "How BAD phosphorylation is good for survival." Nat Cell Biol **1**(2): E33-35.
Dransart, E., B. Olofsson, et al. (2005). "RhoGDIs revisited: novel roles in Rho regulation." Traffic **6**(11): 957-966.
Droge, W. (2002). "Free radicals in the physiological control of cell function." Physiol Rev **82**(1): 47-95.
Du, J., H. Suzuki, et al. (2001). "Superoxide-mediated early oxidation and activation of ASK1 are important for initiating methylglyoxal-induced apoptosis process." Free Radic Biol Med **31**(4): 469-478.
Dunford, J. E., M. J. Rogers, et al. (2006). "Inhibition of protein prenylation by bisphosphonates causes sustained activation of Rac, Cdc42, and Rho GTPases." J Bone Miner Res **21**(5): 684-694.
Eblen, S. T., J. K. Slack-Davis, et al. (2004). "Mitogen-activated protein kinase feedback phosphorylation regulates MEK1 complex formation and activation during cellular adhesion." Mol Cell Biol **24**(6): 2308-2317.
Elmore, S. (2007). "Apoptosis: a review of programmed cell death." Toxicol Pathol **35**(4): 495-516.

Embade, N., P. F. Valeron, et al. (2000). "Apoptosis induced by Rac GTPase correlates with induction of FasL and ceramides production." Mol Biol Cell **11**(12): 4347-4358.
Emerit, I. and P. Cerutti (1981). "Clastogenic activity from Bloom syndrome fibroblast cultures." Proc Natl Acad Sci U S A **78**(3): 1868-1872.
Endo, A., M. Kuroda, et al. (1976). "ML-236A, ML-236B, and ML-236C, new inhibitors of cholesterogenesis produced by Penicillium citrinium." J Antibiot (Tokyo) **29**(12): 1346-1348.
Eskes, R., S. Desagher, et al. (2000). "Bid induces the oligomerization and insertion of Bax into the outer mitochondrial membrane." Mol Cell Biol **20**(3): 929-935.
Essers, M. A., S. Weijzen, et al. (2004). "FOXO transcription factor activation by oxidative stress mediated by the small GTPase Ral and JNK." EMBO J **23**(24): 4802-4812.
Esteve, P., N. Embade, et al. (1998). "Rho-regulated signals induce apoptosis in vitro and in vivo by a p53-independent, but Bcl2 dependent pathway." Oncogene **17**(14): 1855-1869.
Fadok, V. A., D. R. Voelker, et al. (1992). "Exposure of phosphatidylserine on the surface of apoptotic lymphocytes triggers specific recognition and removal by macrophages." J Immunol **148**(7): 2207-2216.
Farina, H. G., D. R. Bublik, et al. (2002). "Lovastatin alters cytoskeleton organization and inhibits experimental metastasis of mammary carcinoma cells." Clin Exp Metastasis **19**(6): 551-559.
Faris, M., K. M. Latinis, et al. (1998). "Stress-induced Fas ligand expression in T cells is mediated through a MEK kinase 1-regulated response element in the Fas ligand promoter." Mol Cell Biol **18**(9): 5414-5424.
Farwell, W. R., R. E. Scranton, et al. (2008). "The association between statins and cancer incidence in a veterans population." J Natl Cancer Inst **100**(2): 134-139.
Feleszko, W. and M. Jakobisiak (2000). "Lovastatin augments apoptosis induced by chemotherapeutic agents in colon cancer cells." Clin Cancer Res **6**(3): 1198-1199.
Finco, T. S., J. K. Westwick, et al. (1997). "Oncogenic Ha-Ras-induced signaling activates NF-kappaB transcriptional activity, which is required for cellular transformation." J Biol Chem **272**(39): 24113-24116.
Fischer, U., R. U. Janicke, et al. (2003). "Many cuts to ruin: a comprehensive update of caspase substrates." Cell Death Differ **10**(1): 76-100.
Foyouzi-Youssefi, R., S. Arnaudeau, et al. (2000). "Bcl-2 decreases the free Ca2+ concentration within the endoplasmic reticulum." Proc Natl Acad Sci U S A **97**(11): 5723-5728.
Frame, M. C. and V. G. Brunton (2002). "Advances in Rho-dependent actin regulation and oncogenic transformation." Curr Opin Genet Dev **12**(1): 36-43.
Franken, N. A., H. M. Rodermond, et al. (2006). "Clonogenic assay of cells in vitro." Nat Protoc **1**(5): 2315-2319.
Freeman, B. A. and J. D. Crapo (1982). "Biology of disease: free radicals and tissue injury." Lab Invest **47**(5): 412-426.
Fresno Vara, J. A., E. Casado, et al. (2004). "PI3K/Akt signalling pathway and cancer." Cancer Treat Rev **30**(2): 193-204.
Fridovich, I. (1978). "Superoxide radicals, superoxide dismutases and the aerobic lifestyle." Photochem Photobiol **28**(4-5): 733-741.

Fritz, G., I. Just, et al. (1999). "Rho GTPases are over-expressed in human tumors." Int J Cancer **81**(5): 682-687.
Fromigue, O., E. Hay, et al. (2006). "RhoA GTPase inactivation by statins induces osteosarcoma cell apoptosis by inhibiting p42/p44-MAPKs-Bcl-2 signaling independently of BMP-2 and cell differentiation." Cell Death Differ **13**(11): 1845-1856.
Fukumoto, Y., K. Kaibuchi, et al. (1990). "Molecular cloning and characterization of a novel type of regulatory protein (GDI) for the rho proteins, ras p21-like small GTP-binding proteins." Oncogene **5**(9): 1321-1328.
Fulda, S., E. Meyer, et al. (2002). "Inhibition of TRAIL-induced apoptosis by Bcl-2 overexpression." Oncogene **21**(15): 2283-2294.
Furberg, C. D. and B. Pitt (2001). "Withdrawal of cerivastatin from the world market." Curr Control Trials Cardiovasc Med **2**(5): 205-207.
Gao, Y., J. B. Dickerson, et al. (2004). "Rational design and characterization of a Rac GTPase-specific small molecule inhibitor." Proc Natl Acad Sci U S A **101**(20): 7618-7623.
Ghosh, P. M., M. L. Moyer, et al. (1999). "Effect of cyclin E overexpression on lovastatin-induced G1 arrest and RhoA inactivation in NIH3T3 cells." J Cell Biochem **74**(4): 532-543.
Gilley, J., P. J. Coffer, et al. (2003). "FOXO transcription factors directly activate bim gene expression and promote apoptosis in sympathetic neurons." J Cell Biol **162**(4): 613-622.
Gniadecki, R. (2004). "Depletion of membrane cholesterol causes ligand-independent activation of Fas and apoptosis." Biochem Biophys Res Commun **320**(1): 165-169.
Goldman, E. H., L. Chen, et al. (2004). "Activation of apoptosis signal-regulating kinase 1 by reactive oxygen species through dephosphorylation at serine 967 and 14-3-3 dissociation." J Biol Chem **279**(11): 10442-10449.
Goldstein, J. C., N. J. Waterhouse, et al. (2000). "The coordinate release of cytochrome c during apoptosis is rapid, complete and kinetically invariant." Nat Cell Biol **2**(3): 156-162.
Goldstein, J. L. and M. S. Brown (1990). "Regulation of the mevalonate pathway." Nature **343**(6257): 425-430.
Golub, T., S. Wacha, et al. (2004). "Spatial and temporal control of signaling through lipid rafts." Curr Opin Neurobiol **14**(5): 542-550.
Gomez del Pulgar, T., S. A. Benitah, et al. (2005). "Rho GTPase expression in tumourigenesis: evidence for a significant link." Bioessays **27**(6): 602-613.
Gonzalez, F. A., D. L. Raden, et al. (1991). "Identification of substrate recognition determinants for human ERK1 and ERK2 protein kinases." J Biol Chem **266**(33): 22159-22163.
Gordon, T. and W. B. Kannel (1971). "Premature mortality from coronary heart disease. The Framingham study." JAMA **215**(10): 1617-1625.
Gotoh, Y. and J. A. Cooper (1998). "Reactive oxygen species- and dimerization-induced activation of apoptosis signal-regulating kinase 1 in tumor necrosis factor-alpha signal transduction." J Biol Chem **273**(28): 17477-17482.
Graaf, M. R., D. J. Richel, et al. (2004). "Effects of statins and farnesyltransferase inhibitors on the development and progression of cancer." Cancer Treat Rev **30**(7): 609-641.
Green, D. R. and G. Kroemer (2004). "The pathophysiology of mitochondrial cell death." Science **305**(5684): 626-629.

Greenhalgh, D. G. (1998). "The role of apoptosis in wound healing." Int J Biochem Cell Biol **30**(9): 1019-1030.
Griendling, K. K., C. A. Minieri, et al. (1994). "Angiotensin II stimulates NADH and NADPH oxidase activity in cultured vascular smooth muscle cells." Circ Res **74**(6): 1141-1148.
Gross, A., J. M. McDonnell, et al. (1999). "BCL-2 family members and the mitochondria in apoptosis." Genes Dev **13**(15): 1899-1911.
Gupta, S., T. Barrett, et al. (1996). "Selective interaction of JNK protein kinase isoforms with transcription factors." EMBO J **15**(11): 2760-2770.
Hale, L. P., K. T. Craver, et al. (1998). "Combination of fosinopril and pravastatin decreases platelet response to thrombin receptor agonist in monkeys." Arterioscler Thromb Vasc Biol **18**(10): 1643-1646.
Hall, A. (2005). "Rho GTPases and the control of cell behaviour." Biochem Soc Trans **33**(Pt 5): 891-895.
Hamelin, B. A. and J. Turgeon (1998). "Hydrophilicity/lipophilicity: relevance for the pharmacology and clinical effects of HMG-CoA reductase inhibitors." Trends Pharmacol Sci **19**(1): 26-37.
Han, D., E. Williams, et al. (2001). "Mitochondrial respiratory chain-dependent generation of superoxide anion and its release into the intermembrane space." Biochem J **353**(Pt 2): 411-416.
Han, J., B. Das, et al. (1997). "Lck regulates Vav activation of members of the Rho family of GTPases." Mol Cell Biol **17**(3): 1346-1353.
Hanahan, D. and R. A. Weinberg (2011). "Hallmarks of cancer: the next generation." Cell **144**(5): 646-674.
Hancock, J. T., R. Desikan, et al. (2001). "Does the redox status of cytochrome C act as a fail-safe mechanism in the regulation of programmed cell death?" Free Radic Biol Med **31**(5): 697-703.
Harris, C. A. and E. M. Johnson, Jr. (2001). "BH3-only Bcl-2 family members are coordinately regulated by the JNK pathway and require Bax to induce apoptosis in neurons." J Biol Chem **276**(41): 37754-37760.
Hentosh, P., S. H. Yuh, et al. (2001). "Sterol-independent regulation of 3-hydroxy-3-methylglutaryl coenzyme A reductase in tumor cells." Mol Carcinog **32**(3): 154-166.
Herrero-Martin, G. and A. Lopez-Rivas (2008). "Statins activate a mitochondria-operated pathway of apoptosis in breast tumor cells by a mechanism regulated by ErbB2 and dependent on the prenylation of proteins." FEBS Lett **582**(17): 2589-2594.
Hers, I., E. E. Vincent, et al. (2011). "Akt signalling in health and disease." Cell Signal **23**(10): 1515-1527.
Heyworth, P. G., U. G. Knaus, et al. (1993). "Regulation of NADPH oxidase activity by Rac GTPase activating protein(s)." Mol Biol Cell **4**(11): 1217-1223.
Hibi, M., A. Lin, et al. (1993). "Identification of an oncoprotein- and UV-responsive protein kinase that binds and potentiates the c-Jun activation domain." Genes Dev **7**(11): 2135-2148.
Hikita, H., T. Takehara, et al. (2009). "Mcl-1 and Bcl-xL cooperatively maintain integrity of hepatocytes in developing and adult murine liver." Hepatology **50**(4): 1217-1226.
Hildeman, D. A., Y. Zhu, et al. (2002). "Activated T cell death in vivo mediated by proapoptotic bcl-2 family member bim." Immunity **16**(6): 759-767.

Hilenski, L. L., R. E. Clempus, et al. (2004). "Distinct subcellular localizations of Nox1 and Nox4 in vascular smooth muscle cells." Arterioscler Thromb Vasc Biol **24**(4): 677-683.
Hordijk, P. L., J. P. ten Klooster, et al. (1997). "Inhibition of invasion of epithelial cells by Tiam1-Rac signaling." Science **278**(5342): 1464-1466.
Hori, Y., A. Kikuchi, et al. (1991). "Post-translational modifications of the C-terminal region of the rho protein are important for its interaction with membranes and the stimulatory and inhibitory GDP/GTP exchange proteins." Oncogene **6**(4): 515-522.
Hrycyna, C. A., S. K. Sapperstein, et al. (1991). "The Saccharomyces cerevisiae STE14 gene encodes a methyltransferase that mediates C-terminal methylation of a-factor and RAS proteins." EMBO J **10**(7): 1699-1709.
Hsu, H., J. Xiong, et al. (1995). "The TNF receptor 1-associated protein TRADD signals cell death and NF-kappa B activation." Cell **81**(4): 495-504.
Hsu, S. Y., A. Kaipia, et al. (1997). "Bok is a pro-apoptotic Bcl-2 protein with restricted expression in reproductive tissues and heterodimerizes with selective anti-apoptotic Bcl-2 family members." Proc Natl Acad Sci U S A **94**(23): 12401-12406.
Huang, P., L. Feng, et al. (2000). "Superoxide dismutase as a target for the selective killing of cancer cells." Nature **407**(6802): 390-395.
Huhle, G., C. Abletshauser, et al. (1999). "Reduction of platelet activity markers in type II hypercholesterolemic patients by a HMG-CoA-reductase inhibitor." Thromb Res **95**(5): 229-234.
Hwang, K. E., K. S. Na, et al. (2011). "Apoptotic induction by simvastatin in human lung cancer A549 cells via Akt signaling dependent down-regulation of survivin." Invest New Drugs **29**(5): 945-952.
Illingworth, D. R. and J. A. Tobert (2001). "HMG-CoA reductase inhibitors." Adv Protein Chem **56**: 77-114.
Inoshita, S., K. Takeda, et al. (2002). "Phosphorylation and inactivation of myeloid cell leukemia 1 by JNK in response to oxidative stress." J Biol Chem **277**(46): 43730-43734.
Ip, Y. T. and R. J. Davis (1998). "Signal transduction by the c-Jun N-terminal kinase (JNK)--from inflammation to development." Curr Opin Cell Biol **10**(2): 205-219.
Ito, D., O. Ito, et al. (2010). "Atorvastatin upregulates nitric oxide synthases with Rho-kinase inhibition and Akt activation in the kidney of spontaneously hypertensive rats." J Hypertens **28**(11): 2278-2288.
Jacobson, M. D., M. Weil, et al. (1997). "Programmed cell death in animal development." Cell **88**(3): 347-354.
Jaffe, A. B. and A. Hall (2002). "Rho GTPases in transformation and metastasis." Adv Cancer Res **84**: 57-80.
Jaffe, A. B. and A. Hall (2005). "Rho GTPases: biochemistry and biology." Annu Rev Cell Dev Biol **21**: 247-269.
Jakobisiak, M., S. Bruno, et al. (1991). "Cell cycle-specific effects of lovastatin." Proc Natl Acad Sci U S A **88**(9): 3628-3632.
Jakobisiak, M. and J. Golab (2003). "Potential antitumor effects of statins (Review)." Int J Oncol **23**(4): 1055-1069.
Jellinger, K. A. (2001). "Cell death mechanisms in neurodegeneration." J Cell Mol Med **5**(1): 1-17.

Jiang, Z., X. Zheng, et al. (2004). "Lovastatin-induced up-regulation of the BH3-only protein, Bim, and cell death in glioblastoma cells." J Neurochem **89**(1): 168-178.
Johnson, G. L. and R. Lapadat (2002). "Mitogen-activated protein kinase pathways mediated by ERK, JNK, and p38 protein kinases." Science **298**(5600): 1911-1912.
Kabeya, Y., N. Mizushima, et al. (2000). "LC3, a mammalian homologue of yeast Apg8p, is localized in autophagosome membranes after processing." EMBO J **19**(21): 5720-5728.
Kabeya, Y., N. Mizushima, et al. (2004). "LC3, GABARAP and GATE16 localize to autophagosomal membrane depending on form-II formation." J Cell Sci **117**(Pt 13): 2805-2812.
Kakkar, P. and B. K. Singh (2007). "Mitochondria: a hub of redox activities and cellular distress control." Mol Cell Biochem **305**(1-2): 235-253.
Kamai, T., K. Arai, et al. (2001). "Overexpression of RhoA mRNA is associated with advanced stage in testicular germ cell tumour." BJU Int **87**(3): 227-231.
Kamata, H., S. Honda, et al. (2005). "Reactive oxygen species promote TNFalpha-induced death and sustained JNK activation by inhibiting MAP kinase phosphatases." Cell **120**(5): 649-661.
Kamens, J., M. Paskind, et al. (1995). "Identification and characterization of ICH-2, a novel member of the interleukin-1 beta-converting enzyme family of cysteine proteases." J Biol Chem **270**(25): 15250-15256.
Kamigaki, M., T. Sasaki, et al. (2011). "Statins induce apoptosis and inhibit proliferation in cholangiocarcinoma cells." Int J Oncol **39**(3): 561-568.
Kang, J. and S. Pervaiz (2012). "Mitochondria: redox metabolism and dysfunction." Biochem Res Int **2012**: 896751.
Katayose, Y., M. Kim, et al. (1997). "Promoting apoptosis: a novel activity associated with the cyclin-dependent kinase inhibitor p27." Cancer Res **57**(24): 5441-5445.
Kaye, J. A. and H. Jick (2004). "Statin use and cancer risk in the General Practice Research Database." Br J Cancer **90**(3): 635-637.
Kennedy, N. J. and R. J. Davis (2003). "Role of JNK in tumor development." Cell Cycle **2**(3): 199-201.
Kennedy, S. G., A. J. Wagner, et al. (1997). "The PI 3-kinase/Akt signaling pathway delivers an anti-apoptotic signal." Genes Dev **11**(6): 701-713.
Kerr, J. F., A. H. Wyllie, et al. (1972). "Apoptosis: a basic biological phenomenon with wide-ranging implications in tissue kinetics." Br J Cancer **26**(4): 239-257.
Khan, O. M., M. X. Ibrahim, et al. (2011). "Geranylgeranyltransferase type I (GGTase-I) deficiency hyperactivates macrophages and induces erosive arthritis in mice." J Clin Invest **121**(2): 628-639.
Khosravi-Far, R., P. A. Solski, et al. (1995). "Activation of Rac1, RhoA, and mitogen-activated protein kinases is required for Ras transformation." Mol Cell Biol **15**(11): 6443-6453.
Khurana, V., H. R. Bejjanki, et al. (2007). "Statins reduce the risk of lung cancer in humans: a large case-control study of US veterans." Chest **131**(5): 1282-1288.
Khurana, V., A. Sheth, et al. (2007). "Statins reduce the risk of pancreatic cancer in humans: a case-control study of half a million veterans." Pancreas **34**(2): 260-265.

Kim, B. J., S. W. Ryu, et al. (2006). "JNK- and p38 kinase-mediated phosphorylation of Bax leads to its activation and mitochondrial translocation and to apoptosis of human hepatoma HepG2 cells." J Biol Chem **281**(30): 21256-21265.
Kim, J. S., B. A. Diebold, et al. (2004). "Rho is involved in superoxide formation during phagocytosis of opsonized zymosans." J Biol Chem **279**(20): 21589-21597.
Kim, W. S., M. M. Kim, et al. (2001). "Phase II study of high-dose lovastatin in patients with advanced gastric adenocarcinoma." Invest New Drugs **19**(1): 81-83.
Kischkel, F. C., S. Hellbardt, et al. (1995). "Cytotoxicity-dependent APO-1 (Fas/CD95)-associated proteins form a death-inducing signaling complex (DISC) with the receptor." EMBO J **14**(22): 5579-5588.
Klionsky, D. J. (2004). "Cell biology: regulated self-cannibalism." Nature **431**(7004): 31-32.
Klionsky, D. J. and S. D. Emr (2000). "Autophagy as a regulated pathway of cellular degradation." Science **290**(5497): 1717-1721.
Knezevic, N., A. Roy, et al. (2007). "GDI-1 phosphorylation switch at serine 96 induces RhoA activation and increased endothelial permeability." Mol Cell Biol **27**(18): 6323-6333.
Koh, K. K. (2000). "Effects of statins on vascular wall: vasomotor function, inflammation, and plaque stability." Cardiovasc Res **47**(4): 648-657.
Konstantinopoulos, P. A., M. V. Karamouzis, et al. (2007). "Post-translational modifications and regulation of the RAS superfamily of GTPases as anticancer targets." Nat Rev Drug Discov **6**(7): 541-555.
Koyuturk, M., M. Ersoz, et al. (2004). "Simvastatin induces proliferation inhibition and apoptosis in C6 glioma cells via c-jun N-terminal kinase." Neurosci Lett **370**(2-3): 212-217.
Koyuturk, M., M. Ersoz, et al. (2007). "Simvastatin induces apoptosis in human breast cancer cells: p53 and estrogen receptor independent pathway requiring signalling through JNK." Cancer Lett **250**(2): 220-228.
Kroemer, G., L. Galluzzi, et al. (2007). "Mitochondrial membrane permeabilization in cell death." Physiol Rev **87**(1): 99-163.
Kroemer, G. and J. C. Reed (2000). "Mitochondrial control of cell death." Nat Med **6**(5): 513-519.
Kuan, C. Y., A. J. Whitmarsh, et al. (2003). "A critical role of neural-specific JNK3 for ischemic apoptosis." Proc Natl Acad Sci U S A **100**(25): 15184-15189.
Kumar, S. and P. A. Colussi (1999). "Prodomains--adaptors--oligomerization: the pursuit of caspase activation in apoptosis." Trends Biochem Sci **24**(1): 1-4.
Kuroda, J., T. Ago, et al. (2010). "NADPH oxidase 4 (Nox4) is a major source of oxidative stress in the failing heart." Proc Natl Acad Sci U S A **107**(35): 15565-15570.
Kuroda, J., K. Nakagawa, et al. (2005). "The superoxide-producing NAD(P)H oxidase Nox4 in the nucleus of human vascular endothelial cells." Genes Cells **10**(12): 1139-1151.
Kurosaka, K., M. Takahashi, et al. (2003). "Silent cleanup of very early apoptotic cells by macrophages." J Immunol **171**(9): 4672-4679.
Kuwana, T., L. Bouchier-Hayes, et al. (2005). "BH3 domains of BH3-only proteins differentially regulate Bax-mediated mitochondrial membrane permeabilization both directly and indirectly." Mol Cell **17**(4): 525-535.

Kwak, B., F. Mulhaupt, et al. (2000). "Statins as a newly recognized type of immunomodulator." Nat Med **6**(12): 1399-1402.
Kyriakis, J. M., H. App, et al. (1992). "Raf-1 activates MAP kinase-kinase." Nature **358**(6385): 417-421.
Kyriakis, J. M., P. Banerjee, et al. (1994). "The stress-activated protein kinase subfamily of c-Jun kinases." Nature **369**(6476): 156-160.
Labi, V., M. Erlacher, et al. (2006). "BH3-only proteins in cell death initiation, malignant disease and anticancer therapy." Cell Death Differ **13**(8): 1325-1338.
Laezza, C., L. Fiorentino, et al. (2008). "Lovastatin induces apoptosis of k-ras-transformed thyroid cells via inhibition of ras farnesylation and by modulating redox state." J Mol Med (Berl) **86**(12): 1341-1351.
Lamon-Fava, S., M. R. Diffenderfer, et al. (2007). "Effects of different doses of atorvastatin on human apolipoprotein B-100, B-48, and A-I metabolism." J Lipid Res **48**(8): 1746-1753.
Langlois, W. J., T. Sasaoka, et al. (1995). "Negative feedback regulation and desensitization of insulin- and epidermal growth factor-stimulated p21ras activation." J Biol Chem **270**(43): 25320-25323.
Laufs, U., V. La Fata, et al. (1998). "Upregulation of endothelial nitric oxide synthase by HMG CoA reductase inhibitors." Circulation **97**(12): 1129-1135.
Laufs, U. and J. K. Liao (1998). "Post-transcriptional regulation of endothelial nitric oxide synthase mRNA stability by Rho GTPase." J Biol Chem **273**(37): 24266-24271.
Lawlor, M. A. and D. R. Alessi (2001). "PKB/Akt: a key mediator of cell proliferation, survival and insulin responses?" J Cell Sci **114**(Pt 16): 2903-2910.
Le-Niculescu, H., E. Bonfoco, et al. (1999). "Withdrawal of survival factors results in activation of the JNK pathway in neuronal cells leading to Fas ligand induction and cell death." Mol Cell Biol **19**(1): 751-763.
Lee, N., H. MacDonald, et al. (1997). "Activation of hPAK65 by caspase cleavage induces some of the morphological and biochemical changes of apoptosis." Proc Natl Acad Sci U S A **94**(25): 13642-13647.
Lee, S. J., M. J. Ha, et al. (1998). "Inhibition of the 3-hydroxy-3-methylglutaryl-coenzyme A reductase pathway induces p53-independent transcriptional regulation of p21(WAF1/CIP1) in human prostate carcinoma cells." J Biol Chem **273**(17): 10618-10623.
Lee, S. W., L. Fang, et al. (2000). "Sustained activation of Ras/Raf/mitogen-activated protein kinase cascade by the tumor suppressor p53." Proc Natl Acad Sci U S A **97**(15): 8302-8305.
Lefer, A. M., B. Campbell, et al. (1999). "Simvastatin preserves the ischemic-reperfused myocardium in normocholesterolemic rat hearts." Circulation **100**(2): 178-184.
Lei, K. and R. J. Davis (2003). "JNK phosphorylation of Bim-related members of the Bcl2 family induces Bax-dependent apoptosis." Proc Natl Acad Sci U S A **100**(5): 2432-2437.
Lelias, J. M., C. N. Adra, et al. (1993). "cDNA cloning of a human mRNA preferentially expressed in hematopoietic cells and with homology to a GDP-dissociation inhibitor for the rho GTP-binding proteins." Proc Natl Acad Sci U S A **90**(4): 1479-1483.

Leonard, S. S., G. K. Harris, et al. (2004). "Metal-induced oxidative stress and signal transduction." Free Radic Biol Med **37**(12): 1921-1942.
Lersch, C., R. Schmelz, et al. (2004). "Treatment of HCC with pravastatin, octreotide, or gemcitabine--a critical evaluation." Hepatogastroenterology **51**(58): 1099-1103.
Ley, R., K. Balmanno, et al. (2003). "Activation of the ERK1/2 signaling pathway promotes phosphorylation and proteasome-dependent degradation of the BH3-only protein, Bim." J Biol Chem **278**(21): 18811-18816.
Li, H. Y., F. R. Appelbaum, et al. (2003). "Cholesterol-modulating agents kill acute myeloid leukemia cells and sensitize them to therapeutics by blocking adaptive cholesterol responses." Blood **101**(9): 3628-3634.
Li, J. M. and A. M. Shah (2002). "Intracellular localization and preassembly of the NADPH oxidase complex in cultured endothelial cells." J Biol Chem **277**(22): 19952-19960.
Li, J. M. and A. M. Shah (2003). "ROS generation by nonphagocytic NADPH oxidase: potential relevance in diabetic nephropathy." J Am Soc Nephrol **14**(8 Suppl 3): S221-226.
Li, J. M. and A. M. Shah (2004). "Endothelial cell superoxide generation: regulation and relevance for cardiovascular pathophysiology." Am J Physiol Regul Integr Comp Physiol **287**(5): R1014-1030.
Liao, J. K. and U. Laufs (2005). "Pleiotropic effects of statins." Annu Rev Pharmacol Toxicol **45**: 89-118.
Liao, Q., J. Guo, et al. (2003). "Down-regulation of the dual-specificity phosphatase MKP-1 suppresses tumorigenicity of pancreatic cancer cells." Gastroenterology **124**(7): 1830-1845.
Lin, A. (2006). "A five-year itch in TNF-alpha cytotoxicity: the time factor determines JNK action." Dev Cell **10**(3): 277-278.
Lin, A. and B. Dibling (2002). "The true face of JNK activation in apoptosis." Aging Cell **1**(2): 112-116.
Liochev, S. I. and I. Fridovich (1997). "Lucigenin luminescence as a measure of intracellular superoxide dismutase activity in Escherichia coli." Proc Natl Acad Sci U S A **94**(7): 2891-2896.
Liu, H., S. L. Liang, et al. (2009). "Statins induce apoptosis in ovarian cancer cells through activation of JNK and enhancement of Bim expression." Cancer Chemother Pharmacol **63**(6): 997-1005.
Liu, J. and A. Lin (2005). "Role of JNK activation in apoptosis: a double-edged sword." Cell Res **15**(1): 36-42.
Lloyd, A. C. (2006). "Distinct functions for ERKs?" J Biol **5**(5): 13.
Lu, C., F. Zhu, et al. (2006). "Cell apoptosis: requirement of H2AX in DNA ladder formation, but not for the activation of caspase-3." Mol Cell **23**(1): 121-132.
Lu, D., J. Huang, et al. (2006). "Protein kinase Cepsilon activates protein kinase B/Akt via DNA-PK to protect against tumor necrosis factor-alpha-induced cell death." J Biol Chem **281**(32): 22799-22807.
Luciano, F., A. Jacquel, et al. (2003). "Phosphorylation of Bim-EL by Erk1/2 on serine 69 promotes its degradation via the proteasome pathway and regulates its proapoptotic function." Oncogene **22**(43): 6785-6793.
MacFarlane, M. and A. C. Williams (2004). "Apoptosis and disease: a life or death decision." EMBO Rep **5**(7): 674-678.
Machino, T., S. Hashimoto, et al. (2003). "Apoptosis signal-regulating kinase 1-mediated signaling pathway regulates hydrogen peroxide-induced apoptosis

in human pulmonary vascular endothelial cells." Crit Care Med **31**(12): 2776-2781.
Maddika, S., S. R. Ande, et al. (2007). "Cell survival, cell death and cell cycle pathways are interconnected: implications for cancer therapy." Drug Resist Updat **10**(1-2): 13-29.
Maehama, T., G. S. Taylor, et al. (2001). "PTEN and myotubularin: novel phosphoinositide phosphatases." Annu Rev Biochem **70**: 247-279.
Maiuri, M. C., G. Le Toumelin, et al. (2007). "Functional and physical interaction between Bcl-X(L) and a BH3-like domain in Beclin-1." EMBO J **26**(10): 2527-2539.
Majno, G. and I. Joris (1995). "Apoptosis, oncosis, and necrosis. An overview of cell death." Am J Pathol **146**(1): 3-15.
Manser, E., T. Leung, et al. (1994). "A brain serine/threonine protein kinase activated by Cdc42 and Rac1." Nature **367**(6458): 40-46.
Marais, R., J. Wynne, et al. (1993). "The SRF accessory protein Elk-1 contains a growth factor-regulated transcriptional activation domain." Cell **73**(2): 381-393.
Martinon, F. and J. Tschopp (2007). "Inflammatory caspases and inflammasomes: master switches of inflammation." Cell Death Differ **14**(1): 10-22.
Martirosyan, A., J. W. Clendening, et al. (2010). "Lovastatin induces apoptosis of ovarian cancer cells and synergizes with doxorubicin: potential therapeutic relevance." BMC Cancer **10**: 103.
Mates, J. M., J. A. Segura, et al. (2008). "Intracellular redox status and oxidative stress: implications for cell proliferation, apoptosis, and carcinogenesis." Arch Toxicol **82**(5): 273-299.
Matsuzawa, A., H. Nishitoh, et al. (2002). "Physiological roles of ASK1-mediated signal transduction in oxidative stress- and endoplasmic reticulum stress-induced apoptosis: advanced findings from ASK1 knockout mice." Antioxid Redox Signal **4**(3): 415-425.
Maundrell, K., B. Antonsson, et al. (1997). "Bcl-2 undergoes phosphorylation by c-Jun N-terminal kinase/stress-activated protein kinases in the presence of the constitutively active GTP-binding protein Rac1." J Biol Chem **272**(40): 25238-25242.
Mehta, D., A. Rahman, et al. (2001). "Protein kinase C-alpha signals rho-guanine nucleotide dissociation inhibitor phosphorylation and rho activation and regulates the endothelial cell barrier function." J Biol Chem **276**(25): 22614-22620.
Meier, B., A. R. Cross, et al. (1991). "Identification of a superoxide-generating NADPH oxidase system in human fibroblasts." Biochem J **275 (Pt 1)**: 241-245.
Meier, R., J. Rouse, et al. (1996). "Cellular stresses and cytokines activate multiple mitogen-activated-protein kinase kinase homologues in PC12 and KB cells." Eur J Biochem **236**(3): 796-805.
Michikawa, M. and K. Yanagisawa (1999). "Inhibition of cholesterol production but not of nonsterol isoprenoid products induces neuronal cell death." J Neurochem **72**(6): 2278-2285.
Milne, D. M., L. E. Campbell, et al. (1995). "p53 is phosphorylated in vitro and in vivo by an ultraviolet radiation-induced protein kinase characteristic of the c-Jun kinase, JNK1." J Biol Chem **270**(10): 5511-5518.

Mitchell, L., G. A. Hobbs, et al. (2012). "Redox Regulation of Ras and Rho GTPases: Mechanism and Function." Antioxid Redox Signal.
Mo, H. and C. E. Elson (2004). "Studies of the isoprenoid-mediated inhibition of mevalonate synthesis applied to cancer chemotherapy and chemoprevention." Exp Biol Med (Maywood) **229**(7): 567-585.
Moorman, P. G. and R. J. Hamilton (2007). "Statins and cancer risk: what do we know and where do we go from here?" Epidemiology **18**(2): 194-196.
Moubarak, R. S., V. J. Yuste, et al. (2007). "Sequential activation of poly(ADP-ribose) polymerase 1, calpains, and Bax is essential in apoptosis-inducing factor-mediated programmed necrosis." Mol Cell Biol **27**(13): 4844-4862.
Murphy, D. A., S. Makonnen, et al. (2006). "Inhibition of tumor endothelial ERK activation, angiogenesis, and tumor growth by sorafenib (BAY43-9006)." Am J Pathol **169**(5): 1875-1885.
Nakajima, A., Y. Kojima, et al. (2008). "Downregulation of c-FLIP promotes caspase-dependent JNK activation and reactive oxygen species accumulation in tumor cells." Oncogene **27**(1): 76-84.
Nateri, A. S., B. Spencer-Dene, et al. (2005). "Interaction of phosphorylated c-Jun with TCF4 regulates intestinal cancer development." Nature **437**(7056): 281-285.
Newman, A., R. D. Clutterbuck, et al. (1997). "A comparison of the effect of the 3-hydroxy-3-methylglutaryl coenzyme A (HMG-CoA) reductase inhibitors simvastatin, lovastatin and pravastatin on leukaemic and normal bone marrow progenitors." Leuk Lymphoma **24**(5-6): 533-537.
Newman, A., R. D. Clutterbuck, et al. (1994). "Selective inhibition of primary acute myeloid leukaemia cell growth by simvastatin." Leukemia **8**(11): 2023-2029.
Nicholson, D. W. (1999). "Caspase structure, proteolytic substrates, and function during apoptotic cell death." Cell Death Differ **6**(11): 1028-1042.
Nicholson, D. W. and N. A. Thornberry (1997). "Caspases: killer proteases." Trends Biochem Sci **22**(8): 299-306.
Node, K., M. Fujita, et al. (2003). "Short-term statin therapy improves cardiac function and symptoms in patients with idiopathic dilated cardiomyopathy." Circulation **108**(7): 839-843.
O'Donnell, B. V., D. G. Tew, et al. (1993). "Studies on the inhibitory mechanism of iodonium compounds with special reference to neutrophil NADPH oxidase." Biochem J **290 (Pt 1)**: 41-49.
O'Driscoll, G., D. Green, et al. (1997). "Simvastatin, an HMG-coenzyme A reductase inhibitor, improves endothelial function within 1 month." Circulation **95**(5): 1126-1131.
O'Reilly, L. A., L. Cullen, et al. (2000). "The proapoptotic BH3-only protein bim is expressed in hematopoietic, epithelial, neuronal, and germ cells." Am J Pathol **157**(2): 449-461.
Olanow, C. W. (2007). "The pathogenesis of cell death in Parkinson's disease--2007." Mov Disord **22 Suppl 17**: S335-342.
Onesto, C., A. Shutes, et al. (2008). "Characterization of EHT 1864, a novel small molecule inhibitor of Rac family small GTPases." Methods Enzymol **439**: 111-129.
Opferman, J. T. and S. J. Korsmeyer (2003). "Apoptosis in the development and maintenance of the immune system." Nat Immunol **4**(5): 410-415.
Orita, S., K. Kaibuchi, et al. (1993). "Comparison of kinetic properties between two mammalian ras p21 GDP/GTP exchange proteins, ras guanine nucleotide-

releasing factor and smg GDP dissociation stimulation." J Biol Chem **268**(34): 25542-25546.
Orrenius, S. (2007). "Reactive oxygen species in mitochondria-mediated cell death." Drug Metab Rev **39**(2-3): 443-455.
Osada, S., M. Izawa, et al. (1997). "A domain containing the Cdc42/Rac interactive binding (CRIB) region of p65PAK inhibits transcriptional activation and cell transformation mediated by the Ras-Rac pathway." FEBS Lett **404**(2-3): 227-233.
Ouyang, B., J. A. Knauf, et al. (2006). "Inhibitors of Raf kinase activity block growth of thyroid cancer cells with RET/PTC or BRAF mutations in vitro and in vivo." Clin Cancer Res **12**(6): 1785-1793.
Ozes, O. N., L. D. Mayo, et al. (1999). "NF-kappaB activation by tumour necrosis factor requires the Akt serine-threonine kinase." Nature **401**(6748): 82-85.
Ozoren, N. and W. S. El-Deiry (2002). "Defining characteristics of Types I and II apoptotic cells in response to TRAIL." Neoplasia **4**(6): 551-557.
Parikh, A., C. Childress, et al. (2010). "Statin-induced autophagy by inhibition of geranylgeranyl biosynthesis in prostate cancer PC3 cells." Prostate **70**(9): 971-981.
Pervaiz, S., J. Cao, et al. (2001). "Activation of the RacGTPase inhibits apoptosis in human tumor cells." Oncogene **20**(43): 6263-6268.
Pervaiz, S. and M. V. Clement (2002). "A permissive apoptotic environment: function of a decrease in intracellular superoxide anion and cytosolic acidification." Biochem Biophys Res Commun **290**(4): 1145-1150.
Pervaiz, S. and M. V. Clement (2007). "Superoxide anion: oncogenic reactive oxygen species?" Int J Biochem Cell Biol **39**(7-8): 1297-1304.
Peter, M. E. and P. H. Krammer (2003). "The CD95(APO-1/Fas) DISC and beyond." Cell Death Differ **10**(1): 26-35.
Powis, G., R. Bonjouklian, et al. (1994). "Wortmannin, a potent and selective inhibitor of phosphatidylinositol-3-kinase." Cancer Res **54**(9): 2419-2423.
Poynter, J. N., S. B. Gruber, et al. (2005). "Statins and the risk of colorectal cancer." N Engl J Med **352**(21): 2184-2192.
Pulverer, B. J., J. M. Kyriakis, et al. (1991). "Phosphorylation of c-jun mediated by MAP kinases." Nature **353**(6345): 670-674.
Putcha, G. V., S. Le, et al. (2003). "JNK-mediated BIM phosphorylation potentiates BAX-dependent apoptosis." Neuron **38**(6): 899-914.
Putcha, G. V., K. L. Moulder, et al. (2001). "Induction of BIM, a proapoptotic BH3-only BCL-2 family member, is critical for neuronal apoptosis." Neuron **29**(3): 615-628.
Puthalakath, H. and A. Strasser (2002). "Keeping killers on a tight leash: transcriptional and post-translational control of the pro-apoptotic activity of BH3-only proteins." Cell Death Differ **9**(5): 505-512.
Qi, X. F., D. H. Kim, et al. (2010). "Involvement of oxidative stress in simvastatin-induced apoptosis of murine CT26 colon carcinoma cells." Toxicol Lett **199**(3): 277-287.
Qiu, R. G., A. Abo, et al. (1997). "Cdc42 regulates anchorage-independent growth and is necessary for Ras transformation." Mol Cell Biol **17**(6): 3449-3458.
Qiu, R. G., J. Chen, et al. (1995). "An essential role for Rac in Ras transformation." Nature **374**(6521): 457-459.
Qiu, R. G., J. Chen, et al. (1995). "A role for Rho in Ras transformation." Proc Natl Acad Sci U S A **92**(25): 11781-11785.

Reid, T. S., K. L. Terry, et al. (2004). "Crystallographic analysis of CaaX prenyltransferases complexed with substrates defines rules of protein substrate selectivity." J Mol Biol **343**(2): 417-433.
Rikitake, Y. and J. K. Liao (2005). "Rho GTPases, statins, and nitric oxide." Circ Res **97**(12): 1232-1235.
Roberts, P. J., N. Mitin, et al. (2008). "Rho Family GTPase modification and dependence on CAAX motif-signaled posttranslational modification." J Biol Chem **283**(37): 25150-25163.
Robinson, K. M., M. S. Janes, et al. (2006). "Selective fluorescent imaging of superoxide in vivo using ethidium-based probes." Proc Natl Acad Sci U S A **103**(41): 15038-15043.
Rodwell, V. W., J. L. Nordstrom, et al. (1976). "Regulation of HMG-CoA reductase." Adv Lipid Res **14**: 1-74.
Ross, A. J., S. P. Amy, et al. (2001). "BCLW mediates survival of postmitotic Sertoli cells by regulating BAX activity." Dev Biol **239**(2): 295-308.
Ross, A. J., K. G. Waymire, et al. (1998). "Testicular degeneration in Bclw-deficient mice." Nat Genet **18**(3): 251-256.
Rossi, F. and M. Zatti (1964). "Biochemical aspects of phagocytosis in polymorphonuclear leucocytes. NADH and NADPH oxidation by the granules of resting and phagocytizing cells." Experientia **20**(1): 21-23.
Roux, P., C. Gauthier-Rouviere, et al. (1997). "The small GTPases Cdc42Hs, Rac1 and RhoG delineate Raf-independent pathways that cooperate to transform NIH3T3 cells." Curr Biol **7**(9): 629-637.
Rowell, C. A., J. J. Kowalczyk, et al. (1997). "Direct demonstration of geranylgeranylation and farnesylation of Ki-Ras in vivo." J Biol Chem **272**(22): 14093-14097.
Roy, M., H. J. Kung, et al. (2011). "Statins and prostate cancer: role of cholesterol inhibition vs. prevention of small GTP-binding proteins." Am J Cancer Res **1**(4): 542-561.
Royer-Pokora, B., L. M. Kunkel, et al. (1986). "Cloning the gene for an inherited human disorder--chronic granulomatous disease--on the basis of its chromosomal location." Nature **322**(6074): 32-38.
Rubinfeld, H. and R. Seger (2005). "The ERK cascade: a prototype of MAPK signaling." Mol Biotechnol **31**(2): 151-174.
Rudel, T. and G. M. Bokoch (1997). "Membrane and morphological changes in apoptotic cells regulated by caspase-mediated activation of PAK2." Science **276**(5318): 1571-1574.
Russell, L. D., J. Warren, et al. (2001). "Spermatogenesis in Bclw-deficient mice." Biol Reprod **65**(1): 318-332.
Sacks, F. M., M. A. Pfeffer, et al. (1996). "The effect of pravastatin on coronary events after myocardial infarction in patients with average cholesterol levels. Cholesterol and Recurrent Events Trial investigators." N Engl J Med **335**(14): 1001-1009.
Sahai, E. and C. J. Marshall (2002). "RHO-GTPases and cancer." Nat Rev Cancer **2**(2): 133-142.
Saito, Y., K. Nishio, et al. (2006). "Turning point in apoptosis/necrosis induced by hydrogen peroxide." Free Radic Res **40**(6): 619-630.
Sakurai, T., S. Maeda, et al. (2006). "Loss of hepatic NF-kappa B activity enhances chemical hepatocarcinogenesis through sustained c-Jun N-terminal kinase 1 activation." Proc Natl Acad Sci U S A **103**(28): 10544-10551.

Sanchez, C. A., E. Rodriguez, et al. (2008). "Statin-induced inhibition of MCF-7 breast cancer cell proliferation is related to cell cycle arrest and apoptotic and necrotic cell death mediated by an enhanced oxidative stress." Cancer Invest **26**(7): 698-707.

Santos, C. X., L. Y. Tanaka, et al. (2009). "Mechanisms and implications of reactive oxygen species generation during the unfolded protein response: roles of endoplasmic reticulum oxidoreductases, mitochondrial electron transport, and NADPH oxidase." Antioxid Redox Signal **11**(10): 2409-2427.

Sarbassov, D. D., D. A. Guertin, et al. (2005). "Phosphorylation and regulation of Akt/PKB by the rictor-mTOR complex." Science **307**(5712): 1098-1101.

Scaffidi, C., S. Fulda, et al. (1998). "Two CD95 (APO-1/Fas) signaling pathways." EMBO J **17**(6): 1675-1687.

Scalia, R., M. E. Gooszen, et al. (2001). "Simvastatin exerts both anti-inflammatory and cardioprotective effects in apolipoprotein E-deficient mice." Circulation **103**(21): 2598-2603.

Schimmer, A. D. (2004). "Inhibitor of apoptosis proteins: translating basic knowledge into clinical practice." Cancer Res **64**(20): 7183-7190.

Schmidmaier, R., P. Baumann, et al. (2004). "The HMG-CoA reductase inhibitor simvastatin overcomes cell adhesion-mediated drug resistance in multiple myeloma by geranylgeranylation of Rho protein and activation of Rho kinase." Blood **104**(6): 1825-1832.

Schmidt, A. and A. Hall (2002). "Guanine nucleotide exchange factors for Rho GTPases: turning on the switch." Genes Dev **16**(13): 1587-1609.

Schmitz, A. A., E. E. Govek, et al. (2000). "Rho GTPases: signaling, migration, and invasion." Exp Cell Res **261**(1): 1-12.

Schroeter, H., C. S. Boyd, et al. (2003). "c-Jun N-terminal kinase (JNK)-mediated modulation of brain mitochondria function: New target proteins for JNK signalling in mitochondrion-dependent apoptosis." Biochemical Journal **372**(2): 359-369.

Schultz, R. M., R. L. Merriman, et al. (1995). "In vitro and in vivo antitumor activity of the phosphatidylinositol-3-kinase inhibitor, wortmannin." Anticancer Res **15**(4): 1135-1139.

Sebti, S. M. and C. J. Der (2003). "Opinion: Searching for the elusive targets of farnesyltransferase inhibitors." Nat Rev Cancer **3**(12): 945-951.

Seger, R. and E. G. Krebs (1995). "The MAPK signaling cascade." FASEB J **9**(9): 726-735.

Seger, R., D. Seger, et al. (1994). "Overexpression of mitogen-activated protein kinase kinase (MAPKK) and its mutants in NIH 3T3 cells. Evidence that MAPKK involvement in cellular proliferation is regulated by phosphorylation of serine residues in its kinase subdomains VII and VIII." J Biol Chem **269**(41): 25699-25709.

Sever, P. S., B. Dahlof, et al. (2003). "Prevention of coronary and stroke events with atorvastatin in hypertensive patients who have average or lower-than-average cholesterol concentrations, in the Anglo-Scandinavian Cardiac Outcomes Trial--Lipid Lowering Arm (ASCOT-LLA): a multicentre randomised controlled trial." Lancet **361**(9364): 1149-1158.

Shannon, J., S. Tewoderos, et al. (2005). "Statins and prostate cancer risk: a case-control study." Am J Epidemiol **162**(4): 318-325.

Shenoy, K., Y. Wu, et al. (2009). "LY303511 enhances TRAIL sensitivity of SHEP-1 neuroblastoma cells via hydrogen peroxide-mediated mitogen-activated

protein kinase activation and up-regulation of death receptors." Cancer Res **69**(5): 1941-1950.
Shepherd, J., S. M. Cobbe, et al. (1995). "Prevention of coronary heart disease with pravastatin in men with hypercholesterolemia. West of Scotland Coronary Prevention Study Group." N Engl J Med **333**(20): 1301-1307.
Shepherd, J., D. B. Hunninghake, et al. (2003). "Guidelines for lowering lipids to reduce coronary artery disease risk: a comparison of rosuvastatin with atorvastatin, pravastatin, and simvastatin for achieving lipid-lowering goals." Am J Cardiol **91**(5A): 11C-17C; discussion 17C-19C.
Shi, Y. (2008). "Apoptosome assembly." Methods Enzymol **442**: 141-156.
Shibata, M. A., Y. Ito, et al. (2004). "Lovastatin inhibits tumor growth and lung metastasis in mouse mammary carcinoma model: a p53-independent mitochondrial-mediated apoptotic mechanism." Carcinogenesis **25**(10): 1887-1898.
Shimizu, S., T. Kanaseki, et al. (2004). "Role of Bcl-2 family proteins in a non-apoptotic programmed cell death dependent on autophagy genes." Nat Cell Biol **6**(12): 1221-1228.
Shimizu, S., M. Narita, et al. (1999). "Bcl-2 family proteins regulate the release of apoptogenic cytochrome c by the mitochondrial channel VDAC." Nature **399**(6735): 483-487.
Siddiqui, A. A., H. Nazario, et al. (2009). "For patients with colorectal cancer, the long-term use of statins is associated with better clinical outcomes." Dig Dis Sci **54**(6): 1307-1311.
Simons, K. and E. Ikonen (1997). "Functional rafts in cell membranes." Nature **387**(6633): 569-572.
Singh, A., A. E. Karnoub, et al. (2004). "Rac1b, a tumor associated, constitutively active Rac1 splice variant, promotes cellular transformation." Oncogene **23**(58): 9369-9380.
Sjogren, A. K., K. M. Andersson, et al. (2007). "GGTase-I deficiency reduces tumor formation and improves survival in mice with K-RAS-induced lung cancer." J Clin Invest **117**(5): 1294-1304.
Slater, H. R., L. McKinney, et al. (1984). "Contribution of the receptor pathway to low density lipoprotein catabolism in humans. New methods for quantitation." Arteriosclerosis **4**(6): 604-613.
Sobczak, I., G. Galabova-Kovacs, et al. (2008). "B-Raf is required for ERK activation and tumor progression in a mouse model of pancreatic beta-cell carcinogenesis." Oncogene **27**(35): 4779-4787.
Sousa, S. F., P. A. Fernandes, et al. (2008). "Farnesyltransferase inhibitors: a detailed chemical view on an elusive biological problem." Curr Med Chem **15**(15): 1478-1492.
St-Pierre, J., J. A. Buckingham, et al. (2002). "Topology of superoxide production from different sites in the mitochondrial electron transport chain." J Biol Chem **277**(47): 44784-44790.
Stalker, T. J., A. M. Lefer, et al. (2001). "A new HMG-CoA reductase inhibitor, rosuvastatin, exerts anti-inflammatory effects on the microvascular endothelium: the role of mevalonic acid." Br J Pharmacol **133**(3): 406-412.
Stamatakis, K., E. Cernuda-Morollon, et al. (2002). "Isoprenylation of RhoB is necessary for its degradation. A novel determinant in the complex regulation of RhoB expression by the mevalonate pathway." J Biol Chem **277**(51): 49389-49396.

Starkov, A. A., G. Fiskum, et al. (2004). "Mitochondrial α-ketoglutarate dehydrogenase complex generates reactive oxygen species." Journal of Neuroscience **24**(36): 7779-7788.
Stoll, L. L., M. L. McCormick, et al. (2004). "Antioxidant effects of statins." Drugs Today (Barc) **40**(12): 975-990.
Sulciner, D. J., K. Irani, et al. (1996). "rac1 regulates a cytokine-stimulated, redox-dependent pathway necessary for NF-kappaB activation." Mol Cell Biol **16**(12): 7115-7121.
Sun, H., R. Lesche, et al. (1999). "PTEN modulates cell cycle progression and cell survival by regulating phosphatidylinositol 3,4,5,-trisphosphate and Akt/protein kinase B signaling pathway." Proc Natl Acad Sci U S A **96**(11): 6199-6204.
Sun, Y. and Z. L. Peng (2009). "Programmed cell death and cancer." Postgrad Med J **85**(1001): 134-140.
Suto, D., K. Sato, et al. (2005). "Suppression of the pro-apoptotic function of cytochrome c by singlet oxygen via a haem redox state-independent mechanism." Biochem J **392**(Pt 2): 399-406.
Suzuki, T., K. Fujikura, et al. (1997). "DNA staining for fluorescence and laser confocal microscopy." J Histochem Cytochem **45**(1): 49-53.
Sytkowski, P. A., W. B. Kannel, et al. (1990). "Changes in risk factors and the decline in mortality from cardiovascular disease. The Framingham Heart Study." N Engl J Med **322**(23): 1635-1641.
Szatrowski, T. P. and C. F. Nathan (1991). "Production of large amounts of hydrogen peroxide by human tumor cells." Cancer Res **51**(3): 794-798.
Tahara, E. B., F. D. Navarete, et al. (2009). "Tissue-, substrate-, and site-specific characteristics of mitochondrial reactive oxygen species generation." Free Radic Biol Med **46**(9): 1283-1297.
Takac, I., K. Schroder, et al. (2011). "The E-loop is involved in hydrogen peroxide formation by the NADPH oxidase Nox4." J Biol Chem **286**(15): 13304-13313.
Takahashi, M., H. Mukai, et al. (1998). "Proteolytic activation of PKN by caspase-3 or related protease during apoptosis." Proc Natl Acad Sci U S A **95**(20): 11566-11571.
Takeda, M., I. Shirato, et al. (1999). "Hydrogen peroxide induces necrosis, apoptosis, oncosis and apoptotic oncosis of mouse terminal proximal straight tubule cells." Nephron **81**(2): 234-238.
Takemoto, M., K. Node, et al. (2001). "Statins as antioxidant therapy for preventing cardiac myocyte hypertrophy." J Clin Invest **108**(10): 1429-1437.
Tang, D., D. Wu, et al. (2002). "ERK activation mediates cell cycle arrest and apoptosis after DNA damage independently of p53." J Biol Chem **277**(15): 12710-12717.
Tapon, N., K. Nagata, et al. (1998). "A new rac target POSH is an SH3-containing scaffold protein involved in the JNK and NF-kappaB signalling pathways." EMBO J **17**(5): 1395-1404.
Taylor-Harding, B., S. Orsulic, et al. (2010). "Fluvastatin and cisplatin demonstrate synergistic cytotoxicity in epithelial ovarian cancer cells." Gynecol Oncol **119**(3): 549-556.
Teahan, C., P. Rowe, et al. (1987). "The X-linked chronic granulomatous disease gene codes for the beta-chain of cytochrome b-245." Nature **327**(6124): 720-721.

Temkin, V., Q. Huang, et al. (2006). "Inhibition of ADP/ATP exchange in receptor-interacting protein-mediated necrosis." Mol Cell Biol **26**(6): 2215-2225.
Teramoto, S., T. Tomita, et al. (1999). "Hydrogen peroxide-induced apoptosis and necrosis in human lung fibroblasts: protective roles of glutathione." Jpn J Pharmacol **79**(1): 33-40.
Thibault, A., D. Samid, et al. (1996). "Phase I study of lovastatin, an inhibitor of the mevalonate pathway, in patients with cancer." Clin Cancer Res **2**(3): 483-491.
Tinel, A. and J. Tschopp (2004). "The PIDDosome, a protein complex implicated in activation of caspase-2 in response to genotoxic stress." Science **304**(5672): 843-846.
Tobiume, K., A. Matsuzawa, et al. (2001). "ASK1 is required for sustained activations of JNK/p38 MAP kinases and apoptosis." EMBO Rep **2**(3): 222-228.
Treasure, C. B., J. L. Klein, et al. (1995). "Beneficial effects of cholesterol-lowering therapy on the coronary endothelium in patients with coronary artery disease." N Engl J Med **332**(8): 481-487.
Tretter, L. and V. Adam-Vizi (2004). "Generation of reactive oxygen species in the reaction catalyzed by α-ketoglutarate dehydrogenase." Journal of Neuroscience **24**(36): 7771-7778.
Tsujimoto, Y. and S. Shimizu (2005). "Another way to die: autophagic programmed cell death." Cell Death Differ **12 Suppl 2**: 1528-1534.
Tu, Y. S., X. L. Kang, et al. (2011). "Involvement of Chk1-Cdc25A-cyclin A/CDK2 pathway in simvastatin induced S-phase cell cycle arrest and apoptosis in multiple myeloma cells." Eur J Pharmacol **670**(2-3): 356-364.
Turner, S. J., S. Zhuang, et al. (2008). "Effects of lovastatin on Rho isoform expression, activity, and association with guanine nucleotide dissociation inhibitors." Biochem Pharmacol **75**(2): 405-413.
Ukomadu, C. and A. Dutta (2003). "p21-dependent inhibition of colon cancer cell growth by mevastatin is independent of inhibition of G1 cyclin-dependent kinases." J Biol Chem **278**(44): 43586-43594.
Vakkila, J. and M. T. Lotze (2004). "Inflammation and necrosis promote tumour growth." Nat Rev Immunol **4**(8): 641-648.
Valastyan, S., F. Reinhardt, et al. (2009). "A pleiotropically acting microRNA, miR-31, inhibits breast cancer metastasis." Cell **137**(6): 1032-1046.
Vamvakopoulos, J. E. (2005). "Three's company: regulation of cell fate by statins." Curr Drug Targets Cardiovasc Haematol Disord **5**(2): 145-163.
Van Aelst, L. and C. D'Souza-Schorey (1997). "Rho GTPases and signaling networks." Genes Dev **11**(18): 2295-2322.
van de Donk, N. W., M. M. Kamphuis, et al. (2003). "Inhibition of protein geranylgeranylation induces apoptosis in myeloma plasma cells by reducing Mcl-1 protein levels." Blood **102**(9): 3354-3362.
van Loo, G., M. van Gurp, et al. (2002). "The serine protease Omi/HtrA2 is released from mitochondria during apoptosis. Omi interacts with caspase-inhibitor XIAP and induces enhanced caspase activity." Cell Death Differ **9**(1): 20-26.
Vander Griend, D. J., M. Kocherginsky, et al. (2005). "Suppression of metastatic colonization by the context-dependent activation of the c-Jun NH2-terminal kinase kinases JNKK1/MKK4 and MKK7." Cancer Res **65**(23): 10984-10991.
Vaughan, C. J., A. M. Gotto, Jr., et al. (2000). "The evolving role of statins in the management of atherosclerosis." J Am Coll Cardiol **35**(1): 1-10.

Vega, F. M. and A. J. Ridley (2008). "Rho GTPases in cancer cell biology." FEBS Lett **582**(14): 2093-2101.
Velaithan, R., J. Kang, et al. (2011). "The small GTPase Rac1 is a novel binding partner of Bcl-2 and stabilizes its antiapoptotic activity." Blood **117**(23): 6214-6226.
Ventura, J. J., P. Cogswell, et al. (2004). "JNK potentiates TNF-stimulated necrosis by increasing the production of cytotoxic reactive oxygen species." Genes Dev **18**(23): 2905-2915.
Ventura, J. J., A. Hubner, et al. (2006). "Chemical genetic analysis of the time course of signal transduction by JNK." Mol Cell **21**(5): 701-710.
Verhaar, M. C., P. E. Westerweel, et al. (2004). "Free radical production by dysfunctional eNOS." Heart **90**(5): 494-495.
Von Zee, C. L., M. P. Richards, et al. (2009). "Increased RhoA and RhoB protein accumulation in cultured human trabecular meshwork cells by lovastatin." Invest Ophthalmol Vis Sci **50**(6): 2816-2823.
Von Zee, C. L. and E. B. Stubbs, Jr. (2011). "Geranylgeranylation facilitates proteasomal degradation of rho G-proteins in human trabecular meshwork cells." Invest Ophthalmol Vis Sci **52**(3): 1676-1683.
Wajant, H. (2002). "The Fas signaling pathway: more than a paradigm." Science **296**(5573): 1635-1636.
Wang, J., J. Y. Zhou, et al. (2007). "ERK-dependent MKP-1-mediated cisplatin resistance in human ovarian cancer cells." Cancer Res **67**(24): 11933-11941.
Wang, W., E. Collie-Duguid, et al. (2002). "Cerivastatin enhances the cytotoxicity of 5-fluorouracil on chemosensitive and resistant colorectal cancer cell lines." FEBS Lett **531**(3): 415-420.
Wang, X., W. R. Chen, et al. (2012). "A pathway from JNK through decreased ERK and Akt activities for FOXO3a nuclear translocation in response to UV irradiation." J Cell Physiol **227**(3): 1168-1178.
Wang, X., J. L. Martindale, et al. (2000). "Requirement for ERK activation in cisplatin-induced apoptosis." J Biol Chem **275**(50): 39435-39443.
Waris, G. and H. Ahsan (2006). "Reactive oxygen species: role in the development of cancer and various chronic conditions." J Carcinog **5**: 14.
Waugh, M. G. and J. J. Hsuan (2009). "Preparation of membrane rafts." Methods Mol Biol **462**: 403-414.
Weekes, U. Y. (1975). "Metabolism of dimethylnitrosamine to mutagenic intermediates by kidney microsomal enzymes and correlation with reported host susceptibility to kidney tumors." J Natl Cancer Inst **55**(5): 1199-1201.
Weiss, R. H., A. Ramirez, et al. (1999). "Short-term pravastatin mediates growth inhibition and apoptosis, independently of Ras, via the signaling proteins p27Kip1 and P13 kinase." J Am Soc Nephrol **10**(9): 1880-1890.
Werner, N., G. Nickenig, et al. (2002). "Pleiotropic effects of HMG-CoA reductase inhibitors." Basic Res Cardiol **97**(2): 105-116.
Weston, C. R. and R. J. Davis (2002). "The JNK signal transduction pathway." Curr Opin Genet Dev **12**(1): 14-21.
Weston, C. R. and R. J. Davis (2007). "The JNK signal transduction pathway." Curr Opin Cell Biol **19**(2): 142-149.
Weston, C. R., D. G. Lambright, et al. (2002). "Signal transduction. MAP kinase signaling specificity." Science **296**(5577): 2345-2347.

Weydert, C., B. Roling, et al. (2003). "Suppression of the malignant phenotype in human pancreatic cancer cells by the overexpression of manganese superoxide dismutase." Mol Cancer Ther **2**(4): 361-369.
Whitehead, I. P., S. Campbell, et al. (1997). "Dbl family proteins." Biochim Biophys Acta **1332**(1): F1-23.
Whitfield, J., S. J. Neame, et al. (2001). "Dominant-negative c-Jun promotes neuronal survival by reducing BIM expression and inhibiting mitochondrial cytochrome c release." Neuron **29**(3): 629-643.
Whitmarsh, A. J. and R. J. Davis (2007). "Role of mitogen-activated protein kinase kinase 4 in cancer." Oncogene **26**(22): 3172-3184.
Whitmarsh, A. J., P. Shore, et al. (1995). "Integration of MAP kinase signal transduction pathways at the serum response element." Science **269**(5222): 403-407.
Whyte, D. B., P. Kirschmeier, et al. (1997). "K- and N-Ras are geranylgeranylated in cells treated with farnesyl protein transferase inhibitors." J Biol Chem **272**(22): 14459-14464.
Wientjes, F. B., J. J. Hsuan, et al. (1993). "p40phox, a third cytosolic component of the activation complex of the NADPH oxidase to contain src homology 3 domains." Biochem J **296 (Pt 3)**: 557-561.
Wilson, K. P., J. A. Black, et al. (1994). "Structure and mechanism of interleukin-1 beta converting enzyme." Nature **370**(6487): 270-275.
Winter-Vann, A. M. and P. J. Casey (2005). "Post-prenylation-processing enzymes as new targets in oncogenesis." Nat Rev Cancer **5**(5): 405-412.
Wong, C. H., K. B. Iskandar, et al. (2010). "Simultaneous induction of non-canonical autophagy and apoptosis in cancer cells by ROS-dependent ERK and JNK activation." PLoS One **5**(4): e9996.
Wong, W. W., J. Dimitroulakos, et al. (2002). "HMG-CoA reductase inhibitors and the malignant cell: the statin family of drugs as triggers of tumor-specific apoptosis." Leukemia **16**(4): 508-519.
Wu, G. S. (2007). "Role of mitogen-activated protein kinase phosphatases (MKPs) in cancer." Cancer Metastasis Rev **26**(3-4): 579-585.
Wu, J., W. W. Wong, et al. (2004). "Blocking the Raf/MEK/ERK pathway sensitizes acute myelogenous leukemia cells to lovastatin-induced apoptosis." Cancer Res **64**(18): 6461-6468.
Wyllie, A. H., J. F. Kerr, et al. (1980). "Cell death: the significance of apoptosis." Int Rev Cytol **68**: 251-306.
Xia, Z., M. M. Tan, et al. (2001). "Blocking protein geranylgeranylation is essential for lovastatin-induced apoptosis of human acute myeloid leukemia cells." Leukemia **15**(9): 1398-1407.
Xin, W., K. J. Yun, et al. (2004). "MAP2K4/MKK4 expression in pancreatic cancer: genetic validation of immunohistochemistry and relationship to disease course." Clin Cancer Res **10**(24): 8516-8520.
Yakovlev, A. G., S. Di Giovanni, et al. (2004). "BOK and NOXA are essential mediators of p53-dependent apoptosis." J Biol Chem **279**(27): 28367-28374.
Yamada, S. D., J. A. Hickson, et al. (2002). "Mitogen-activated protein kinase kinase 4 (MKK4) acts as a metastasis suppressor gene in human ovarian carcinoma." Cancer Res **62**(22): 6717-6723.
Yang, D. D., C. Y. Kuan, et al. (1997). "Absence of excitotoxicity-induced apoptosis in the hippocampus of mice lacking the Jnk3 gene." Nature **389**(6653): 865-870.

Yeung, A. C. and P. Tsao (2002). "Statin therapy: beyond cholesterol lowering and antiinflammatory effects." Circulation **105**(25): 2937-2938.
Yin, X. M., Z. N. Oltvai, et al. (1994). "BH1 and BH2 domains of Bcl-2 are required for inhibition of apoptosis and heterodimerization with Bax." Nature **369**(6478): 321-323.
Yoshino, G., T. Kazumi, et al. (1986). "Effect of CS-514, an inhibitor of 3-hydroxy-3-methylglutaryl coenzyme A reductase, on lipoprotein and apolipoprotein in plasma of hypercholesterolemic diabetics." Diabetes Res Clin Pract **2**(3): 179-181.
Yu, J. and L. Zhang (2005). "The transcriptional targets of p53 in apoptosis control." Biochem Biophys Res Commun **331**(3): 851-858.
Yu, L., A. Alva, et al. (2004). "Regulation of an ATG7-beclin 1 program of autophagic cell death by caspase-8." Science **304**(5676): 1500-1502.
Yuan, J., S. Shaham, et al. (1993). "The C. elegans cell death gene ced-3 encodes a protein similar to mammalian interleukin-1 beta-converting enzyme." Cell **75**(4): 641-652.
Zalcman, G., V. Closson, et al. (1996). "RhoGDI-3 is a new GDP dissociation inhibitor (GDI). Identification of a non-cytosolic GDI protein interacting with the small GTP-binding proteins RhoB and RhoG." J Biol Chem **271**(48): 30366-30374.
Zhan, L., A. Rosenberg, et al. (2008). "Deregulation of scribble promotes mammary tumorigenesis and reveals a role for cell polarity in carcinoma." Cell **135**(5): 865-878.
Zhang, F. L. and P. J. Casey (1996). "Protein prenylation: molecular mechanisms and functional consequences." Annu Rev Biochem **65**: 241-269.
Zhang, S., J. Han, et al. (1995). "Rho family GTPases regulate p38 mitogen-activated protein kinase through the downstream mediator Pak1." J Biol Chem **270**(41): 23934-23936.
Zhang, S., X. L. Wang, et al. (2010). "Activation of c-Jun N-terminal kinase is required for mevastatin-induced apoptosis of salivary adenoid cystic carcinoma cells." Anticancer Drugs **21**(7): 678-686.
Zhao, Y., Y. Xue, et al. (2001). "Overexpression of manganese superoxide dismutase suppresses tumor formation by modulation of activator protein-1 signaling in a multistage skin carcinogenesis model." Cancer Res **61**(16): 6082-6088.
Zhong, W. B., C. Y. Wang, et al. (2003). "Lovastatin induces apoptosis of anaplastic thyroid cancer cells via inhibition of protein geranylgeranylation and de novo protein synthesis." Endocrinology **144**(9): 3852-3859.
Zhuang, L., J. Kim, et al. (2005). "Cholesterol targeting alters lipid raft composition and cell survival in prostate cancer cells and xenografts." J Clin Invest **115**(4): 959-968.
Zielonka, J., J. Vasquez-Vivar, et al. (2008). "Detection of 2-hydroxyethidium in cellular systems: a unique marker product of superoxide and hydroethidine." Nat Protoc **3**(1): 8-21.
Zornig, M., A. Hueber, et al. (2001). "Apoptosis regulators and their role in tumorigenesis." Biochim Biophys Acta **1551**(2): F1-37.

APPENDICES

A

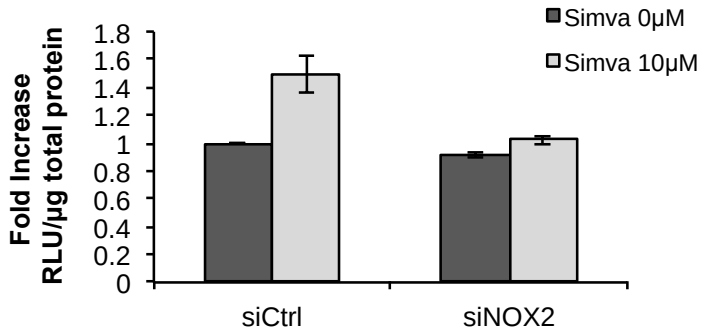

B

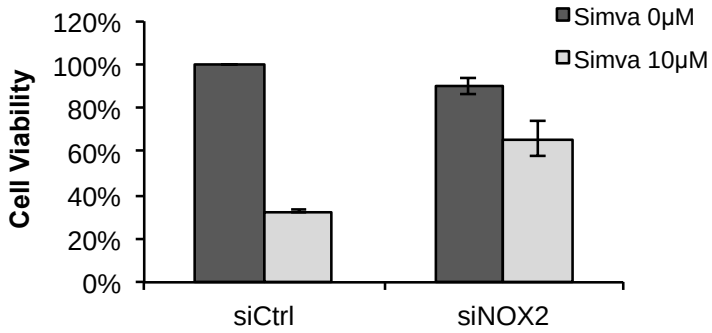

Appendix A: Knockdown of NOX2 reduces simvastatin-induced cell death.
In both panels, HCT116 cells were transfected with 100 nM of either control siRNA or NOX2 siRNA for 30 h before performing subsequent experiments. (A) Superoxide production after 10 μM simvastatin treatment for 24 h was measured by lucigenin chemiluminesence assay. (B) Cell viability after 48 h simvastatin treatment was measured by crystal violet assay. The bars represent means ± s.d. of two independent experiments.

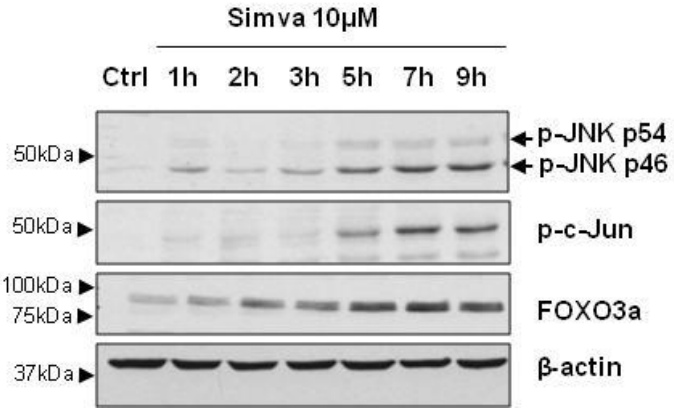

Appendix B: Simvastatin increases phosphorylation of c-Jun and FOXO3a expression.
HCT116 cells were treated with 10 μM simvastatin treatment for the indicated duration; protein expression of phospho-JNK, phospho-c-Jun and FOXO3a was measured by Western blot analysis. β-actin was included as a loading control.

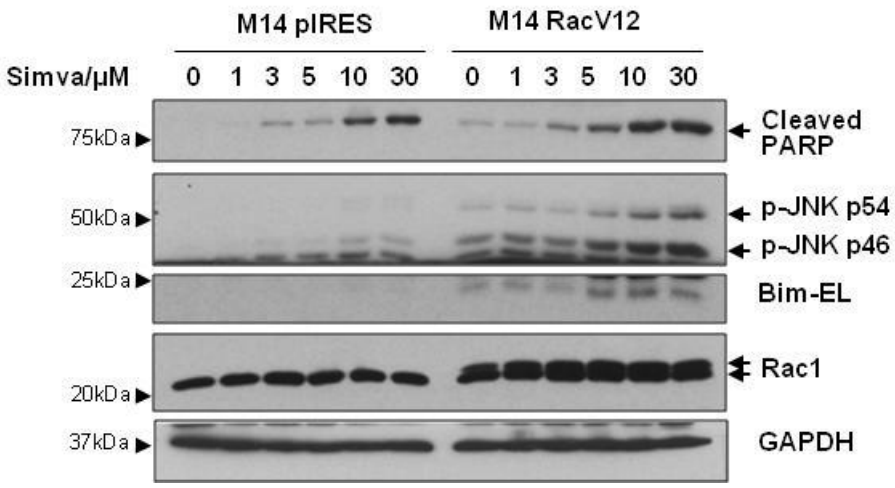

Appendix C: A more efficient Rac1-JNK-BIM-cell death signaling cascade is observed in M14RacV12 cells compared to M14pIRES cells.

M14 melanoma cells were stably transfected with parental pIREShyg vector (M14pIRES) or the pIREShyg vector encoding for a myc-tagged constitutively active mutant of Rac (M14RacV12). Both cell lines were treated with 10 μM simvastatin treatment for 48 h. Protein expression of cleaved-PARP, phospho-JNK, Bim-EL and Rac1 (the upper arrow is myc-tagged Rac1) was measured by Western blot analysis. GAPDH was included as a loading control.